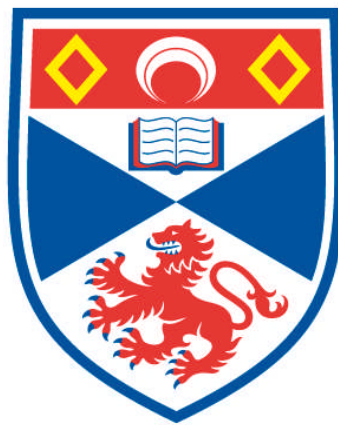


# **POLYCOMB PROTEINS AND BREAST CANCER**

**Vita Fedele**

**A Thesis Submitted for the Degree of PhD  
at the  
University of St Andrews**



**2013**

**Full metadata for this item is available in  
Research@StAndrews:FullText  
at:**

**<http://research-repository.st-andrews.ac.uk/>**

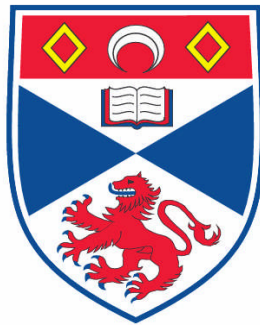
**Please use this identifier to cite or link to this item:**

**<http://hdl.handle.net/10023/3584>**

**This item is protected by original copyright**

# **Polycomb proteins and breast cancer**

Vita Fedele



This thesis is submitted in partial fulfilment for the degree of PhD at the

University of St Andrews

School of Medicine

November 2012



*“Keep away from people who try to belittle your ambitions. Small people always do that, but the really great make you feel that you, too, can become great”*

*Mark Twain*

## **ABSTRACT**

In the Western world, breast cancer is the most frequent malignancy in women and still the leading cause of cancer related deaths, therefore, a better understanding of the disease is needed. Adequate therapeutic targets for all breast cancer types have not been identified yet, and patients with the same type of cancer have often different outcomes. Polycomb proteins are emerging as important factors involved in breast cancer formation. Polycomb proteins play a crucial role in embryogenesis, early development, stem cell renewal and establishing and maintaining cell identity. Their alteration leads to mis-regulation of several important cellular factors including tumour suppressors, DNA repair factors, cell cycle regulation factors and cell-cell interaction factors.

In this thesis the importance of several polycomb proteins in breast cancer has been investigated. The effect of EZH2 knockdown has been tested in breast cancer cell lines expressing different level of the protein and with different features. The results obtained are in line with other studies and suggest that the effect of EZH2 down-regulation in breast cancer cells is dependent on cellular context. In vitro experiments, using both established breast cell lines and primary epithelial cells have been used for investigating the importance of CBX8 in breast cancer. The results obtained showed that the polycomb proteins CBX8 does not play a central role in malignant transformation of the mammary epithelial cells tested.

## **Abbreviations**

<b>ADH</b>	Atypical ductal hyperplasia
<b>AKR1C1</b>	aldo-keto reductase family 1, member C1
<b>AKT</b>	v-akt murine thymoma viral oncogene homolog 1
<b>ALH</b>	Atypical lobular hyperplasia
<b>ANXA8</b>	Annexin A8
<b>APS</b>	Ammonium persulfate
<b>AP1</b>	Jun proto-oncogene
<b>ARKS</b>	Ala, Arg, Lys, Ser
<b><math>\alpha</math>-SMA</b>	Alpha-smooth muscle actin
<b>ATCC</b>	America Type Culture Collection
<b>ATM/ATR</b>	Ataxia telangiectasia mutated/ ataxia telangiectasia and Rad3 related
<b>BARD1</b>	BRCA1 associated RING domain 1
<b>BCL2</b>	B-cell CLL/lymphoma 2
<b>Bim</b>	BCL2-like 11 (apoptosis facilitator)
<b>BM</b>	Basal membrane
<b>BMI1</b>	B lymphoma Mo-MLV insertion region 1
<b>BMP3</b>	Bone morphogenetic protein 3
<b>BPEC</b>	Breast Primary Epithelial cell
<b>BRCA1</b>	Breast cancer 1, early onset
<b>BRCT</b>	Breast cancer carboxyl terminal
<b>BRIT1</b>	Microcephalin 1
<b>BSA</b>	Bovine Serum Albumin
<b>CALLA</b>	Common leukocytic leukemia antigen
<b>CBX8</b>	Chromobox homologous protein 8
<b>CBX7</b>	Chromobox homologous protein 7
<b>CBX6</b>	Chromobox homologous protein 6
<b>Cdc2</b>	Cell division cycle 2
<b>CD-10</b>	CALLA/ common leukocytic leukemia antigen

<b>CD4</b>	CD4 molecule
<b>Cdk</b>	Cyclin dependent kinase
<b>Chk1</b>	Checkpoint homolog 1
<b>CK</b>	Cytokeratin
<b>c-MYC</b>	Cellular myelocytomatosis
<b>CRELD2</b>	Cysteine-rich with EGF-like domain
<b>CtIP</b>	Retinoblastoma binding protein 8
<b>CXCL12</b>	Chemokine (C-X-C motif) ligand 12
<b>BDS</b>	Double strand breaks
<b>DCIS</b>	Ductal carcinoma in situ
<b>DDT</b>	DL-dithiothreitol
<b>dHP1</b>	Su(var) 205 Suppressor of variegation 205
<b>DMEM</b>	Dulbecco's Modified Eagle Medium
<b>DMEM/F12</b>	Dulbecco's Modified Eagle Medium: Nutrient Mixture F-12
<b>DMSO</b>	Dimethyl sulfoxide
<b>DNase I</b>	Deoxyribonuclease I
<b>DNA</b>	Deoxyribonucleic acid
<b>DNMT</b>	DNA methyltransferases
<b>dPc</b>	<i>Drosophila</i> Polycomb
<b>E2F</b>	E2F transcription factor
<b>EB</b>	Elution buffer
<b>ECL</b>	Enhanced chemiluminescence
<b>EDTA</b>	Ethylenediaminetetraacetic Acid
<b>EED</b>	Embryonic ectoderm development
<b>EGF</b>	Epidermal Growth Factor
<b>EGFR</b>	Epidermal Growth Factor receptor
<b>EMT</b>	Epithelial mesenchymal transition
<b>EpCAM</b>	Epithelial cell adhesion molecule
<b>ER<math>\alpha</math></b>	Estrogen receptor $\alpha$

<b>ERE</b>	Estrogen receptor element
<b>ERM</b>	Ezrin-radixin-moesin
<b>ESC</b>	Embryonic stem cells
<b>EZH2</b>	Enhancer of zeste homolog 2
<b>FACL2</b>	acyl-CoA synthetase long-chain family member 1
<b>FACS</b>	Fluorescence Activated Cell Sorting
<b>FBS</b>	Fetal Bovine Serum
<b>GADPH</b>	Glyceraldehyde 3-phosphate dehydrogenase
<b>GAP</b>	GTPase-activating protein
<b>GATA3</b>	GATA binding protein 3
<b>GFP</b>	Green fluorescent protein
<b>GJB2/CX26</b>	Gap junction protein, beta 2
<b>GTP</b>	Glyceraldeide Tri-phosphate
<b>GRB7</b>	Growth factor receptor-bound protein 7
<b>HCC</b>	Hepatocellular carcinoma
<b>HCNE</b>	Highly conserved non-coding elements
<b>HDAC</b>	Histone deacetylase
<b>HEBS</b>	HEPES-buffered saline solution
<b>HEPES</b>	4-(2-hydroxyethyl)-1-piperazineethanesulfonic acid
<b>HER</b>	Human epidermal growth factor receptor
<b>HMEC</b>	Human mammary epithelial cells
<b>HMM</b>	Human Mammosphere Medium
<b>HNF3<math>\alpha</math></b>	Forkhead box A1
<b>HOXA9</b>	Homeo box A9
<b>HPC2</b>	Chromobox homolog 4 (Pc class homolog)
<b>HPH1</b>	Polyhomeotic homolog 1
<b>HR</b>	Homologous recombination
<b>H-RAS</b>	v-Ha-ras Harvey rat sarcoma viral oncogene homolog
<b>hTERT</b>	Human telomerase reverse transcriptase



<b>IGF-1</b>	Insulin growth factor-1
<b>INT</b>	p-iodonitro tetrazolium violet
<b>IRX3</b>	Iroquois homeobox 3
<b>LCIS</b>	Lobular carcinoma in situ
<b>LIF</b>	Leukemia inhibitory factor
<b>LIV</b>	LIV-1 protein, estrogen regulated
<b>MAP</b>	Mitogen-activated protein
<b>Mash1</b>	Achaete-scute complex homolog 1
<b>MBD4</b>	5-methyl-CpG binding domain protein 4
<b>MDF1</b>	Midgut Differentiation Factor 1
<b>MDM2</b>	Mdm2 p53 binding protein homolog
<b>MEPK</b>	Mitogen-activated protein kinase kinase 1
<b>MLH1</b>	MutL homolog 1, colon cancer, nonpolyposis type 2
<b>MMP</b>	Matrix metallo-proteinases
<b>MRE11</b>	Meiotic recombination 11
<b>MSH2</b>	MutS homolog 2, colon cancer, nonpolyposis type 1
<b>Msx1</b>	Homeobox protein Hox-7
<b>MTUS1</b>	Microtubule associated tumor suppressor 1
<b>MTT</b>	(3-(4,5-Dimethylthiazol-2-yl)-2,5-diphenyltetrazolium bromide, a yellow tetrazole
<b>MUC1</b>	Mucin 1, cell surface associated
<b>Myf5</b>	Myogenic factor 5
<b>NEB</b>	New England Biolabs
<b>NF-KB</b>	Nuclear factor of kappa light polypeptide gene enhancer in B-cells 1
<b>Nkx2-2</b>	NK2 homeobox 2
<b>NOTCH4</b>	Neurogenic locus notch homolog protein 4
<b>NP-40</b>	Nonyl phenoxyethoxyethanol-40
<b>NURF</b>	Nucleosome remodeling factor
<b>OLIG2</b>	Oligodendrocyte lineage transcription factor 2

<b>OPN</b>	Osteopontin/secreted phosphoprotein 1
<b>OPTIMEM</b>	Modified Eagle's Minimum Essential Media
<b>Pax3</b>	Paired box 3
<b>PBS</b>	Phosphate Buffered Saline
<b>PBS-T</b>	Phosphate Buffered Saline-Tween 20
<b>PcG</b>	Polycomb group protein
<b>PCR</b>	Polymerase chain reaction
<b>PDWA</b>	Proliferative disease without atypia
<b>PERP</b>	TP53 apoptosis effector
<b>PET</b>	Polyethylene terephthalate
<b>PGK</b>	Phosphoglycerate kinase
<b>PhoRC</b>	Pho (pleiohomeotic )-repressive complex
<b>PI3K/Akt-1</b>	Phosphoinositide 3-kinases/ v-akt murine thymoma viral oncogene homolog 1
<b>PKC</b>	Protein kinase C
<b>pS2</b>	Trefoil factor 1
<b>PR</b>	Progesterone receptor
<b>PRC1</b>	Polycomb Repressive Complex 1
<b>PRC2</b>	Polycomb Repressive Complex 2
<b>PTEN</b>	Phosphatase and tensin homolog
<b>PVDF</b>	Polyvinylidene fluoride
<b>RAD51</b>	RAD51 homolog
<b>RAF</b>	v-raf-1 murine leukemia viral oncogene homolog 1
<b>RAR</b>	Retinoic Acid Receptor
<b>RAS</b>	Rat sarcoma viral oncogene homolog
<b>RASSF1A</b>	Ras-associated domain family member 1 gene
<b>RB</b>	Retinoblastoma-family protein
<b>RMA</b>	Robust Multichip Avarage
<b>RNA</b>	Ribonucleic acid
<b>RNF8</b>	Ring finger protein 8

<b>RRE</b>	Rev-responsive element
<b>RSV</b>	Rous Sarcoma Virus
<b>SA-<math>\beta</math>-gal</b>	Senescence associated $\beta$ -galactosidase
<b>SAM</b>	S-adenosylmethionine
<b>SAPK</b>	Mitogen-activated protein kinase
<b>SCML</b>	Sex combs on midleg
<b>SDS</b>	Sodium dodecyl sulphate
<b>SDS-PAGE</b>	Sodium dodecyl sulfate polyacrylamide gel electrophoresis
<b>SEM</b>	Standard error of the mean
<b>SERM</b>	Selective estrogen receptor modulators
<b>sh-RNA</b>	Short harpin-RNA
<b>SNAIL</b>	Snail 1 homolog
<b>SNP</b>	Single nucleotide polymorphism
<b>SORBS1</b>	Sorbin and SH3 domain containing 1
<b>SOS</b>	Son of sevenless homolog
<b>SOX1</b>	SRY (sex determining region Y)-box 1
<b>SP1</b>	Sp1 transcription factor
<b>SUZ12</b>	Suppressor of zeste 12 homolog
<b>TEMED</b>	Tetramethylethylenediamine
<b>TBE</b>	Tris-Borate-EDTA
<b>TDLU</b>	Terminal duct lobular units
<b>TE</b>	Tris-EDTA
<b>TFF3</b>	Trefoil factor 3 (intestinal)
<b>THPO</b>	Thrombopoietin
<b>TIC</b>	Tumour initiating cells
<b>TNF<math>\alpha</math></b>	Tumour necrosis factor $\alpha$
<b>TRAP100</b>	Mediator complex subunit 24
<b>TRIM29</b>	Tripartite motif containing 29
<b>TrxG</b>	Trithorax group protein

<b>Ubc13</b>	Ubiquitin-conjugating enzyme E2N
<b>ULA</b>	Ultra Low Attachment
<b>VSV-G</b>	Vesicular stomatitis virus
<b>XPB1</b>	X-box binding protein 1

List of figures and tables

Chapter 1

**Figure 1.1:** Schematic representation of mature human mammary glands.....2

**Figure 1.2:** Schematic representation of the BRCA1 pathway.....16

**Figure 1.3:** Origin and related pathways of different types of triple-negative and basal-like breast tumours.....22

**Figure 1.4:** PRC1 and PRC2 induce transcriptional repression.....33

**Figure 1.5:** Schematic representation of EZH2 protein domains.....40

Chapter 2

**Figure 2.1:** Schematic representation of the Gateway cloning system.....56

**Table 2.1:** Transfection mixture components for lentivirus production.....64

**Table 2.2:** Basic WIT medium composition.....73

**Table 2.3:** SDS-PAGE resolving gel and stacking gel components.....75

**Table 2.4:** List of primary and secondary antibodies used for western blot analysis.....76

**Table 2.5:** List of primary and secondary antibodies used for immunofluorescence analysis.....80

Chapter 3

**Table 3.1:** EZH2 expression level in breast cancer cell lines.....84

**Figure 3.1:** EZH2 knockdown in T47D cells and CAMAI cells.....85

**Figure 3.2:** EZH2 expression level in MDA-MB-231 cells and HCC1937 cells....86

**Figure 3.3:** EZH2 knockdown in MDA-MB-231 cells.....87

**Figure 3.4:** The effect of EZH2 knockdown on the growth rate of MDA-MB-231 cells.....88

<b>Figure 3.5:</b> The effect of EZH2 knockdown on anchorage-independent growth of MDA-MB-231 cells.....	89
<b>Figure 3.6:</b> The effect of EZH2 knockdown on migration of MDA-MB-231 cells assessed by transwell Boyden chamber assay.....	91
<b>Figure 3.7:</b> The effect of EZH2 knockdown on migration of MDA-MB-231 cells assessed by a scratch assay.....	92
<b>Figure 3.8:</b> EZH2 knockdown in HCC1937 cells.....	94
<b>Figure 3.9:</b> The effect of EZH2 knockdown on the growth rate of HCC1937 cells .....	95
<b>Figure 3.10:</b> The effect of EZH2 knockdown on anchorage-independent growth of HCC1937 cells.....	96
<b>Figure 3.11:</b> The effect of EZH2 knockdown on HCC1937 migration as assessed by transwell Boyden chamber assay.....	98
<b>Figure 3.12:</b> The effect of EZH2 knockdown on HCC1937 migration as assessed by a scratch assay.....	100
 <u>Chapter 4</u>	
<b>Figure 4.1:</b> BRCA1 expression level in HCC1937EV28 cells and HCC1937BR69 cells.....	107
<b>Figure 4.2:</b> EZH2 knockdown in HCC1937EV28 cells and HCC1937BR69 cells.....	108
<b>Figure 4.3:</b> The effect of EZH2 knockdown on anchorage independent growth in HCC1937EV28 and HCC1937BR69 cells .....	109
<b>Figure 4.4:</b> The effect of EZH2 knockdown on HCC1937BR69 cell migration as assessed by a scratch assay.....	112
<b>Figure 4.5:</b> The effect of EZH2 knockdown on HCC1937EV28 cell migration as assessed by a scratch assay .....	114

<b>Figure 4.6:</b> The effect of EZH2 knockdown on HCC1937EV28 cells and HCC1937BR69 cells migration as assessed by transwell Boyden chamber assay.....	115
<b>Figure 4.7:</b> The effect of EZH2 knockdown on HCC1937EV28 cells and HCC1937BR69 cell growth rate .....	117
<b>Figure 4.8:</b> BRCA1 expression level in HCC1937EV28 cells and HCC1937BR69 cells after EZH2 knockdown .....	119
<b>Figure 4.9:</b> Schematic representation of possible interaction between BRCA1 and EZH2.....	125

## Chapter 5

<b>Figure 5.1:</b> An outline of the cloning method used to produce expression clones carrying the CBX genes tested.....	128
<b>Figure 5.2:</b> Analysis of Plasmid DNA by Restriction Digestion.....	130
<b>Figure 5.3:</b> Analysis of CBX6, CBX7 and CBX8 protein expression in MCF10A cells after lentiviral infection.....	131
<b>Figure 5.4:</b> Growth analysis of MCF10A cells over expressing CBX6, CBX7 or CBX8 protein.....	132
<b>Figure 5.5:</b> Analysis of CBX8 protein expression in MCF10A cells after lentiviral infection.....	133
<b>Figure 5.6:</b> Growth analysis of MCF10A cells over expressing CBX8 protein.....	134
<b>Figure 5.7:</b> The effect of over-expression of CBX8 on MCF10A cells as assessed by transwell Boyden chamber assay. ....	136
<b>Figure 5.8:</b> The effect of ectopic expression of CBX8 on anchorage-independent growth in MCF10A cells.....	137

## Chapter 6

<b>Figure 6.1:</b> Schematic representation of the experimental procedure used to study the effect of CBX protein ectopic expression in primary cells.....	145
--	-----

<b>Figure 6.2:</b> Images of Breast Primary Epithelial Cells (BPEC).....	146
<b>Figure 6.3:</b> Images of early passage BPECs and late passage BPEC.....	147
<b>Figure 6.4:</b> Expression of cytokeratins in non-infected BPEC assessed by Immunofluorescence.....	148
<b>Figure 6.5:</b> Images of BPEC after infection with GFP.....	151
<b>Figure 6.6:</b> Representative images of Breast Primary Epithelial Cells (BPEC) after infection with lentiviral particles carrying the appropriate expression construct....	151
<b>Figure 6.7:</b> Expression of cytokeratins in BPEC after infection with lentiviral particles carrying BMI1 and ER $\alpha$ , assessed by immunofluorescence.....	152
<b>Figure 6.8:</b> Expression of cytokeratins CK14 and CK18 in BPECs after infection with viral particles carrying BMI1/ER $\alpha$ / hTERT/HRAS assessed by Immunofluorescence.....	154
<b>Figure 6.9:</b> Expression of cytokeratins CK5 and CK19 in BPECs after infection with viral particles carrying BMI1/ER $\alpha$ / hTERT/HRAS assessed by Immunofluorescence .....	155
<b>Figure 6.10:</b> Analysis of BMI1, ER $\alpha$ and HRAS expression in BPEC. ....	157
<b>Figure 6.11:</b> Analysis of hTERT and $\alpha$ -SMA expression in BPEC. ....	158
<b>Figure 6.12:</b> Analysis of p16 expression in BPEC.....	160
<b>Figure 6.13:</b> Breast primary epithelial cell proliferation analysis upon BMI1 ectopic expression.....	162
<b>Figure 6.14:</b> The effect of polycomb protein BMI1 on BPEC anchorage independent growth.....	163
<b>Figure 6.15:</b> Representative images of BPEC after infection with lentiviral particles carrying CBX8, HRAS and ER $\alpha$ .....	166



<b>Figure 6.16:</b> Expression of cytokeratins in BPEC, after infection with lentiviral particles carrying CBX8 and ER $\alpha$ , assessed by Immunofluorescence.....	167
<b>Figure 6.17:</b> Expression of cytokeratins in BPEC, after infection with lentiviral particles carrying CBX8, hTERT and HRAS assessed by Immunofluorescence.....	167
<b>Figure 6.18:</b> Analysis of CBX8, ER $\alpha$ and HRAS expression in BPEC.....	169
<b>Figure 6.19:</b> Analysis of hTERT and $\alpha$ -SMA expression in BPEC after infection with lentiviral particle carrying CBX8, hTERT and HRAS.....	171
<b>Figure 6.20:</b> Analysis of p16 expression in BPEC after infection with lentiviral particles carrying either, CBX8, ER $\alpha$ , hTERT, HRAS.....	172
<b>Figure 6.21:</b> Breast primary epithelial cell proliferation analysis upon CBX8 ectopic expression.....	173
<b>Figure 6.22:</b> The effect of polycomb protein CBX8 on anchorage-independent growth in BPEC.....	175
<b>Figure 6.23:</b> Representative image of B42CP cells after infection with GFP.....	176
<b>Figure 6.24:</b> Representative images of B42CP cells after infection with lentiviral particles carrying the appropriate expression construct.....	176
<b>Figure 6.25:</b> Analysis of CBX8, ER $\alpha$ and HRAS expression in B42CP cells.....	177
<b>Figure 6.26:</b> B42CP cell proliferation analysis upon CBX8 ectopic expression.....	178
<b>Figure 6.27:</b> The effect of CBX8 ectopic expression on cell migration of B42CP cells as assessed by a scratch assay.....	180

**Figure 6.28:** The effect of CBX8 ectopioc expression on cells migration of B42CP cells as assessed by transwell Boyden chamber assay.....182

**Figure 6.29:** The effect of ectopic expression of CBX8 on anchorage-independent growth in B42CP cells.....184

**Figure 6.30:** Analysis of CBX8, ER $\alpha$  and HRAS expression in B42CP cells after invitro assays.....185

1	CHAPTER 1: INTRODUCTION.....	1
1.1	The basis of cancer.....	1
1.2	Breast cancer biology.....	2
1.2.1	Role of hormones and hormone receptors.....	5
1.2.2	Role of growth factors and growth factor receptors.....	9
1.2.3	Role of tumour-suppressor deregulation and oncogene activation.....	10
1.2.4	Role of susceptibility genes.....	13
1.3	Breast cancer is a heterogeneous disease.....	18
1.4	Epigenetic alterations in breast cancer.....	26
1.5	Post-translational modifications and gene expression: Trithorax and Polycomb protein.....	29
1.6	Polycomb proteins and stem cell renewal.....	35
1.7	Polycomb proteins and Breast cancer.....	37
1.7.1	BMI1.....	38
1.7.2	EZH2.....	40
1.7.3	CBX proteins.....	45
1.8	The use of different models for investigating breast cancer.....	49
1.9	Aim and scope of the thesis.....	52
2	CHAPTER 2: MATERIALS AND METHODS.....	54
2.1	Materials.....	54
2.2	Methods.....	55
2.2.1	Lentiviral vector production.....	55

2.2.1.1	PCR amplification of ORF .....	57
2.2.1.2	Agarose gel electrophoresis.....	58
2.2.1.3	PCR product purification.....	58
2.2.1.4	Constructing the entry clone – BP Reaction.....	59
2.2.1.5	Constructing the expression clone – LR reaction.....	59
2.2.1.6	Transformation of competent cells .....	59
2.2.1.7	Extraction of plasmid DNA.....	60
2.2.1.8	Restriction enzyme digestion of plasmid DNA.....	60
2.2.1.9	DNA Sequencing.....	61
2.2.2	Large scale plasmid DNA extraction – Maxiprep .....	62
2.2.3	Lentivirus production.....	63
2.2.4	Lentiviral infection .....	64
2.2.5	Lentiviral titration.....	65
2.2.6	Retrovirus production .....	65
2.2.7	Retroviral infection.....	66
2.2.8	Cell culture.....	67
2.2.8.1	Culture of cell lines .....	67
2.2.8.2	Cell freezing and thawing.....	67
2.2.8.3	Puromycin kill curve .....	68
2.2.8.4	Culture of primary mammary epithelial cells.....	68
2.2.9	Western blotting.....	73

2.2.9.1	SDS-Polyacrylamide gel electrophoresis (PAGE) .....	73
2.2.9.2	Transfer of proteins to nitrocellulose membrane.....	74
2.2.9.3	Western blot analysis.....	74
2.2.10	Determining antibody specificity using a blocking peptide .....	77
2.2.11	Analysing cell proliferation .....	77
2.2.12	Migration Assay.....	77
2.2.13	Colony formation in soft agar.....	78
2.2.14	Immunofluorescent Imaging.....	79
2.2.15	Analysis of cell viability – MTT assay.....	80
2.2.16	Scratch Assay.....	81
3	CHAPTER3: INVESTIGATING THE EFFECT OF ABROGATED EZH2 EXPRESSION IN BREAST CANCER .....	82
3.1	Introduction.....	82
3.2	EZH2 expression in breast cancer cell lines .....	83
3.3	EZH2 Knockdown in MDA-MB-231 breast cancer cells.....	86
3.3.1	Effect of EZH2 knockdown on MDA-MB-231 cell proliferation.....	88
3.3.2	Effect of EZH2 knockdown on MDA-MB-231 anchorage-independent growth .....	89
3.3.3	Effect of EZH2 knockdown on MDA-MB-231 cell migration .....	90
3.4	EZH2 Knockdown in HCC1937 breast cancer cells.....	93
3.4.1	Effect of EZH2 knockdown on HCC1937 cell proliferation.....	94

3.4.2	Effect of EZH2 knockdown on HCC1937 anchorage-independent growth .....	96
3.4.3	Effect of EZH2 knockdown on HCC1937 cell migration .....	97
3.5	Discussion .....	101
4	<b>CHAPTER 4: INVESTIGATING THE RELATIONSHIP BETWEEN EZH2 AND BRCA1 .....</b>	<b>105</b>
4.1	Introduction .....	105
4.2	EZH2 knockdown in HCC1937EV28 and HCC1937BR69 breast cancer cell lines .....	106
4.2.1	Effect of EZH2 knockdown on HCC1937EV28 and HCC1937BR69 cells anchorage independent growth .....	109
4.2.2	Effect of EZH2 knockdown on HCC1937EV28 and HCC1937BR69 cells migration .....	110
4.2.3	Effect of EZH2 knockdown on HCC1937EV28 and HCC1937BR69 cells proliferation.....	116
4.3	Evaluation of BRCA1 expression after EZH2 knockdown in late passage HCC1937EV28 and HCC1937BR69 .....	118
4.4	Discussion .....	120
5	<b>Chapter 5: THE EFFECT OF ECTOPIC EXPRESSION OF CBX POLYCOMB PROTEINS IN MCF10A CELLS.....</b>	<b>126</b>
5.1	Introduction .....	126
5.2	CBX proteins overexpression in MCF10A cells.....	127
5.2.1	Evaluating expression of ectopic CBX proteins .....	130

5.2.2	Evaluating the effect of CBX proteins over-expression on MCF10A cell proliferation .....	131
5.2.3	CBX8 over-expression has no effect on MCF10A cell migration.....	135
5.2.4	CBX8 over-expression has no effect on MCF10A anchorage-independent growth .....	136
5.3	Discussion .....	138
6	<b>CHAPTER 6: THE EFFECT OF ECTOPIC EXPRESSION OF CBX8 AND BMI1 IN BREAST PRIMARY EPITHELIAL CELLS .....</b>	<b>141</b>
6.1	Introduction .....	141
6.2	BPEC conditions allow growth of a mixed heterogeneous population of cells .....	143
6.3	Evaluating the effect of BMI/ER $\alpha$ expression in BPEC .....	148
6.3.1	Effect on morphology .....	150
6.3.2	Effect on cytokeratin expression.....	152
6.3.3	Evaluating expression of ectopic proteins .....	156
6.3.4	Evaluating the effect of BMI1/ER $\alpha$ on proliferation .....	161
6.3.5	Evaluating the effect of BMI1/ER $\alpha$ on anchorage independent growth .....	163
6.4	Evaluating the effect of CBX8/ER $\alpha$ in BPEC .....	164
6.4.1	Effect on morphology .....	164
6.4.2	Effect on cytokeratin expression.....	166
6.4.3	Evaluating expression of ectopic proteins .....	168

6.4.4	Evaluating the effect of CBX8/ER $\alpha$ on proliferation .....	173
6.4.5	Evaluating the effect of CBX8/ER $\alpha$ on anchorage independent growth .....	174
6.5	Effect of CBX8 expression on B42CP cells .....	175
6.5.1	Evaluating expression of ectopic protein.....	177
6.5.2	Evaluating the effect of CBX8 on proliferation of B42CP cells .....	178
6.5.3	Evaluating the effect of CBX8 on B42CP cell migration.....	178
6.5.4	Evaluating the effect of CBX8 on B42CP anchorage independent growth .....	183
6.5.5	Evaluating the expression of ectopic proteins after invtro assays .....	185
6.6	Discussion .....	186
7	CHAPTER 7: CONCLUSIONS AND FUTURE WORK .....	197
8	APPENDICES .....	225
8.1	Appendix A: Raw data and additional tables of chapter 3.....	225
8.2	Appendix B: Raw data and additional tables of chapter 4.....	230
8.3	Appendix C: Raw data and additional tables of chapter 5.....	233
8.4	Appendix D: Raw data and additional images of cultured primary cells of chapter 6.....	236
8.5	Appendix E: Ethical approval .....	249



# **1 CHAPTER 1: INTRODUCTION**

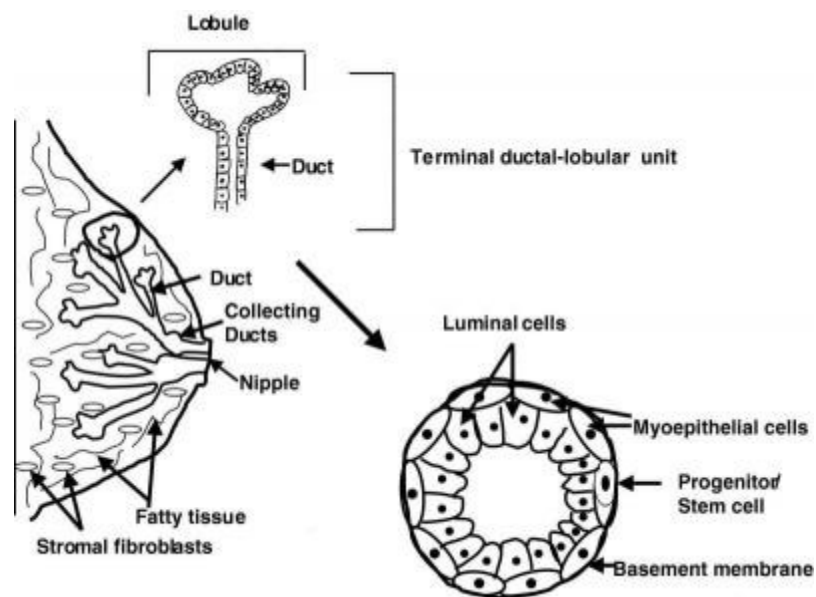
## **1.1 The basis of cancer**

The transformation of normal cells into neoplastic cells occurs through a multistep process, consisting of the accumulation of genetic and epigenetic alterations. Tumour cells are characterized by distinct properties, including, self-sufficiency in growth signals, unlimited replicative potential, abrogation of programmed cell death (apoptosis), insensitivity to growth-inhibitory signals, sustained angiogenesis, and tissue invasion and metastasis (Albini et al. 2007; Hanahan & Weinberg 2000; Hanahan & Weinberg 2011; Kufe 2003). In order for a cell to acquire these characteristics, several different cellular pathways must be altered. This can be achieved by a number of different mechanisms e.g. mutations, gene amplification, gene deletion and alteration of epigenetic pathways. Self-sufficiency in growth can be the result of alterations involving the extracellular growth signals and/or the intracellular circuits that translate the growth signals (i.e. alterations of HER family receptors, integrins and the SOS-Ras-Raf-MAP kinase pathway) (Aplin et al. 1998; Yarden et al. 1988). The insensitivity to growth signals and the consequent uncontrolled cell proliferation, is the result of alterations affecting pathways involved in the regulation of cell cycle progression (i.e. pRb/E2F pathway) (Weinberg 1995). As a consequence of de-regulation of cell cycle control, tumour cells also acquire the ability of unlimited replicative potential (the two major pathways are involved are p53 and/or pRb). Escape from apoptosis can be the result of alterations in a number of different pathways, including DNA damage sensors, pathways involved in the transmission of apoptotic signals and factors regulating the release of pro-apoptotic or anti-apoptotic effectors (Cotter et al. 1990). Lastly,

alterations affecting proteins involved in cell–cell interaction and cell to extracellular matrix component interactions are responsible for the ability of tumour cells to migrate and invade other organs.

## 1.2 Breast cancer biology

The human mammary gland consists of usually 15-20 lobes immersed in connective and adipose tissue. Each lobe is divided into lobules, connected to the nipples through lactiferous ducts (Figure 1.1). The development of the mammary gland occurs during puberty under the effect of oestrogens and growth hormones and will reach complete development only with pregnancy (Cowin & Wysolmerski 2010).



**Figure 1.1:** Schematic representation of mature human mammary glands. The mature human breast is composed of ducts diffusing from the nipple into the fat tissue. Each duct terminates into lobules. The distal ends of the ducts are called terminal duct lobular units (TDLU). A cross-section of the ducts reveals the presence of three different types of cells lining inside the basal membrane.

Breast cancer derives from the cells lining the terminal duct lobular units (TDLU) as a result of the accumulation of mutations and epigenetic changes leading to the activation of proto-oncogenes, the inactivation of tumour suppressor genes and alterations in DNA repair genes and cell cycle control genes (Huang et al. 1997; Koeffler et al. 1991; Weiss 2004). The entire process starts with abnormal proliferation in TDLU which leads to cystic structures that become highly proliferative without acquiring atypical characteristics. This stage is called proliferative disease without atypia (PDWA). PDWA may evolve into atypical hyperplasia that manifests as either ductal (ADH) or lobular (ALH) hyperplasia. The difference between ADH and ALH does not reflect differences in site or type of cell of origin, as it was originally proposed, but simply differences in cell morphology and immunohistochemistry of the lesions. The lobular subtypes stain negatively for E-cadherin (Gillett et al. 2001) and consist of small, non-polarized cells, while the ductal subtype consists of moderate to large and frequently polarized cells (Wellings et al. 1975). The atypical hyperplasia stages are the non-obligatory precursors of the pre-malignant non-invasive lesions, ductal carcinoma in situ (DCIS) and lobular carcinoma in situ (LCIS) respectively (Arpino et al. 2005; Cichon et al. 2010; Lopez-Garcia et al. 2010; Ma et al. 2003). About 15% to 30% of women diagnosed with pure DCIS develop invasive breast carcinoma within the first decade after treatment with lumpectomy (Kerlikowske et al. 2003). The transition from DCIS to invasive carcinoma involves disruption of the basement membrane (BM) and invasion of other tissue throughout the lymphatic system (Bombonati et al. 2011; Ma et al. 2009). The exact genetic and epigenetic changes characterizing every stage of the progression from atypical hyperplasia to invasive carcinoma remain poorly understood. What emerges from different expression analysis studies is the fact that

many alterations associated with the aggressive phenotype of invasive cancer are already present in the pre-malignant lesions (Ma et al. 2003; Yao et al. 2006). First of all, from the histo-morphological point of view, it has been shown that ADH and DCIS share many features (Tavassoli et al. 1990). In addition, Ma et al. have performed a comparison study in which patient-matched phenotypically normal breast tissue (N) from the TDLU and ADH, DCIS, and IDC were analysed. The gene-expression profile analysis revealed that the most alterations occur at the N to ADH transition and that the transcriptional alterations are maintained throughout DCIS and IDC (Ma et al. 2003). However the study conducted by Ma et al., failed to identify a clear defined gene expression signature for the progression from ADH to IDC.

Transcriptional profile studies have shown that the transition from DCIS to invasive carcinoma is the result of alterations affecting different component of the mammary gland, including epithelial cells, myoepithelial cells and fibroblasts. DCIS-associated myoepithelial cells have a different expression profile compared to normal myoepithelial cells, showing downregulation of genes involved in their normal function (thrombospondin, laminin, and oxytocin receptor) and upregulation of genes involved in increased proliferation, migration, invasion and angiogenesis (Allinen et al. 2004). Moreover, cancer-associated myoepithelial cells acquire the ability of producing matrix metalloproteinases (MMPs) and cathepsins that degrade the basement membrane, whereas normal myoepithelial cells secrete maspin and other proteinase inhibitors that suppress cancer cell proliferation and invasion (Barsky et al. 2005). Fibroblasts also have a key role in promoting progression from DCIS into invasive cancer (Hu et al. 2008). Studies using mouse models have shown that cancer-associated fibroblasts promote angiogenesis and increased cancer cell

proliferation through secretion of CXCL12 (chemokine (C-X-C motif) ligand 12 that interact with CXCR4, chemokine (C-X-C motif) receptor 4, expressed by tumour cells (Orimo et al. 2005).

Some of the well-known risk factors for breast cancer include family history, age of menopause, age of menarche, diet, parity, alcohol consumption and smoking (Alsaker et al. 2011). In a recent study, Tamimi et al. have evaluated the contribution of several risk factors to the cumulative risk of breast cancer (Tamimi et al. 2010). They reported that in women with a history of a benign breast disease the cumulative risk of breast cancer at age 70 was increased by 57%. In women who had used hormonal replacement therapy the cumulative risk increased by 23%, compared to women who had not used hormones. This study confirmed that of all the risk factors, hormones and susceptibility genes play a main role in breast carcinoma development. Some of the factors that play a crucial role in breast tumourigenesis, including steroid hormone receptors (ER, PR and RAR), peptide growth receptors (HER family), selected tumour suppressor genes and oncogenes (p53 and HRAS) and hereditary predisposition (susceptibility genes) (Clark 1995; Hulka et al. 2008; Keen et al. 2003) will be further discussed in the next sections.

### **1.2.1 Role of hormones and hormone receptors**

Progesterone and oestrogen are key regulators of normal development of the ovary, uterus and mammary gland; however they also play a crucial role in the neoplastic transformation of these tissues. One of the critical risk factor for developing breast cancer is the prolonged exposure to oestrogens. Several studies have shown that removal of endogenous oestrogen via oophorectomy decreases the

risk of the development of breast carcinoma, and the earlier the ovaries are removed, the greater the risk is reduced (Hulka & Moorman 2008; MacMahon et al. 1982). Oestrogens and progesterone exert their biological activity through binding to the intracellular receptors oestrogen receptor (ER) and progesterone receptor (PR). For both receptors (ER and PR) different isoforms exist: ER $\alpha$ /ER $\beta$  and PRA/PRB respectively. The oestrogen receptors and progesterone receptors belong to the nuclear hormone receptor superfamily which are normally present in an inactive form (in conjunction with HSP 90) and become active upon ligand binding. Upon ligand binding, ER and PR undergo a series of events, including dissociation from heat shock protein complexes, dimerization, phosphorylation, and translocation to the nuclear compartment (Lange et al. 2007).

The homology between ER $\alpha$  and ER $\beta$  is extremely high within the DNA binding domain (95%) and much lower within the ligand binding domain (59%) (Gustafsson 1999; Hall et al. 1999). The active form of the oestrogen receptors consists of phosphorylated dimers which will either bind directly to oestrogen response elements (EREs) present in the promoters of target genes (e.g. mammalian prolactin, pS2, cathepsin D, lactoferrin), or indirectly via other transcription factors such as AP1, SP1 or variant cyclic-AMP response elements (CRE) (Kushner et al. 2000a; Kushner et al. 2000b; McKenna et al. 1999; Saville et al. 2000). Many genes that are regulated by ER are involved in tissue remodelling and proliferation, including collagenase genes and other metalloproteinase genes, insulin growth factor-1 (IGF-1) gene (proliferation), cyclin-D gene (cell cycle control). In addition, ER is able to down-regulate target genes via the NF-KB transcription factor and examples are TNF $\alpha$  and cytokines IL-1 and IL-6 (An et al. 1999b). This effect of ER on anti-inflammatory factors is in line with the anti-inflammatory property of ER

(Pfeilschifter et al. 2002). The use of two separate promoters of a single gene produces the two progesterone receptor isoform, PR-A and PR-B (Richer et al. 2002). PR-A represents a truncated form of PR-B and their relative expression is dependent on cellular context, and physiological and hormonal status. As for ER, over-expression of PR is associated with cellular hyperplasia and breast cancer (Graham et al. 1996). The transcription control exerted by PRs is dependent on the presence and binding to coactivators and corepressors (Gao et al. 2002; McKenna et al. 1999). Alteration of coactivators and corepressors factors expression pattern is associated with alteration of normal development of the mammary gland (Brisken et al. 2010; Rowan et al. 2000).

Both ER and PR positivity are breast cancer markers for good prognosis (Gustafsson 1999). Approximately 70-80% of all breast cancers express ER $\alpha$  and about 65% of these cases also express PR (Caldarella et al. 2011). These tumours grow more slowly, are better differentiated and have a better prognosis compared to the ER $\alpha$  negative tumours. Patients with ER/PR-positive breast cancer have a better overall survival due to response to endocrine therapy (Elledge et al. 2000; Pritchard 2005; R. M. Elledge 2000). In contrast, ER-positive/PR-negative tumours are less responsive to endocrine therapy, suggesting that PR is required for the positive outcome with endocrine therapy (Graham et al. 1995). Endocrine therapy is based on the use of selective oestrogen receptor modulators, called SERM, which block the effects of oestrogen in the breast tissue (Pritchard 2005). The vast majority of oestrogen receptor modulators (SERMs developed in past few decades (i.e. Tamoxifen, Raloxifene, Arzoxifene and Idrxifene) have been proven to be effective against breast cancer and have beneficial effects on bones and the cardiovascular system (Bryant et al. 1999). Crystallography studies have shown that the ER

antagonist SERMs (specifically tamoxifen and raloxifene) induce conformational changes that block the interaction of ERs with coactivator proteins (Brzozowski et al. 1997). At the molecular level, SERMs cause down-regulation of cyclins D1 and E and inhibition of phosphorylation of retinoblastoma protein (Rb). As a result, SERM therapy induces tumour shrinkage, reduces the number of cells in S-phase and increases expression of apoptotic markers. However, most SERMs are associated with an increased risk of endometrial cancer (Jordan 2004), an effect that might be due to the fact that SERM-liganded ER $\alpha$  (specifically Tamoxifen) is recruited to different promoter genes in different tissues (Shang et al. 2002). Moreover, in many cases patients develop resistance to SERMs (Jiang et al. 1992). About 20-30% of all breast cancers do not express ER $\alpha$  and so do not respond to endocrine therapy. ER-negative breast cancers are more aggressive, less differentiated and more proliferative compared to ER-positive breast cancer (Hulka et al. 2001). For this group of breast cancers the treatment consists of chemotherapy and radiation therapy (Cristofanilli et al. 2004). Several studies have investigated the mechanism of loss of ER and PR expression and several hypotheses have been proposed including mutations, deletions, polymorphisms within the ER gene and epigenetic modifications such as histone deacetylation and DNA methylation (Ferguson et al. 1995; Lapidus et al. 1996; Ottaviano et al. 1994; Yang et al. 2001). However, the absence of ER does not account for all the negative features that distinguish ER-negative breast cancer. This will be further discussed in section 1.3. The identification of other pathways altered in ER-negative breast cancers and the exact mechanism by which ER-positive breast cancers lose the expression of the ER is essential in order to develop new therapeutic agents.



### **1.2.2 Role of growth factors and growth factor receptors**

Several growth factors and their receptors have been linked to breast tumourigenesis, including the epidermal growth factor (HER) family (Dickson et al. 1992; Rudland et al. 1995), tumour growth factor- $\beta$  (Drabsch et al. 2011) and Insulin-like growth factor family (Yerushalmi et al. 2010). The most studied and well characterized group is the receptor tyrosine kinase HER family. It comprises four different members: HER1, HER2, HER3 and HER4. The activation of HER, caused by ligand binding, results in the formation of homodimers or heterodimers with subsequent activation of the PI3K-Akt pathway or the MAPK pathway and phosphorylation of specific target genes playing crucial roles in apoptosis, cell cycle control, angiogenesis and proliferation (Muthuswamy et al. 2001; Press et al. 1990; Rudland et al. 1995; Zhou et al. 2000). Deregulation of epidermal growth factor receptors is associated with tumour formation and progression. Amplification of the genes coding for the receptors, over-expression of the protein and presence of mutation and/or SNP inducing constant activation of the receptor, are the alterations normally associated with the dysfunction of HER receptors (Benusiglio et al. 2005; Wenandy et al. 2009).

The HER-2 protein is overexpressed in 25% of breast cancers and its over-expression is associated with poor prognosis and poor overall survival (Press et al. 1990; Slamon et al. 1987; Thor et al. 2000). Similar to ER, HER-2 is a good target for developing new therapies. The most commonly used agents targeting HER-2 are the monoclonal antibodies raised against the ectodomain of HER-2, Trastuzumab (Kita et al. 1996; Kunisue et al. 2000) and Iressa (ZD1839) (Moasser et al. 2001; Moulder et al. 2001). Trastuzumab acts as inhibitor of both PI3K pathway and MAPK pathway, resulting in reduction of proliferation, accumulate of cells in G1

phase and increased apoptosis (De Lorenzo et al. 2005; Jahanzeb 2008; Mohsin et al. 2005). Iressa was initially developed as HER-1 inhibitor, but later it was found out to be also effective against HER-2. Some of the effects exerted by Iressa include inhibition of cell cycle progression, by down-regulation of cyclin D1, Cdk4, p27 and Cdk2, inhibition of proliferation and induction of apoptosis (Moasser et al. 2001; Moulder et al. 2001).

### **1.2.3 Role of tumour-suppressor deregulation and oncogene activation**

The neoplastic phenotype is the result of accumulation of genetic and epigenetic changes which normally cause activation of proto-oncogenes, inactivation of tumour suppressor genes, alterations of key regulators of DNA repair and cell cycle control. One of the tumour suppressors often mutated and deregulated in human cancer is the p53 tumour suppressor (also called the “guardian of the genome”). p53 is activated by phosphorylation (by kinases proteins including CHK2) in response to DNA damages and/or hypoxia (Okorokov et al. 2009). The active form of p53 forms tetrameric complexes which in turn induce the transcription of downstream targets such as p21 which inhibits Cyclin E and CDK2, leading to arrest at the G1-S cell cycle phase for either damage repair or apoptosis (Giaccia et al. 1998; Sherr et al. 1999). As a result of p53 mutations the cells are unable to activate the G1-S cell cycle checkpoint and its associated DNA repair or apoptosis, resulting in replication of damaged DNA and accumulation of genetic alterations. About 35% of invasive breast cancers carry mutated p53 and, as for many other human cancers, breast cancers with mutated p53 have a more aggressive behaviour, are highly invasive/metastatic, have a high grade and are poorly differentiated (Borresen-Dale 2003; Lee et al. 2010). There is a positive correlation between the presence of p53

and ER negativity in breast cancer, suggesting a possible interaction between the ER and p53. Indeed, a physical association between p53 the p53 regulator MDM2 and ER $\alpha$  has been shown. ER $\alpha$  protects p53 from the degradation activity of MDM2, therefore ER $\alpha$  might be responsible for the up-regulation and stabilization of p53. (Hurd et al. 1997; Liu et al. 2000; Moudgil et al. 2001; Yu et al. 1997). However, other evidence suggest that overexpression of ER $\alpha$  causes over-expression of MDM2 and consequent decreased p53 activity (Hori et al. 2002), suggesting another possible mechanism of tumourigenesis by loss of p53 function. p53 germline mutations are present in members of families with Li-Fraumeni syndrome, which is characterized by an increased risk of breast cancer, sarcomas, brain tumours, leukemias and adrenal tumours (Malkin et al. 1990). Fibroblasts derived from patients with Li-Fraumeni syndrome exhibit permanent loss of G1 or G2 cell cycle checkpoint control confirming that loss of p53 results in loss of cell cycle checkpoint control and, consequently, increased cellular proliferation (Boyle et al. 1998).

H-Ras belongs to the ras oncogene family. Ras is a monomeric membrane protein that has been defined as a “molecular switch” that converts signals from the cell membrane to the nucleus (Adjei 2001), via several effector pathways (P13K, PKC, MEK, SAPK, MAPK) with consequent regulation of cell survival, proliferation, and differentiation (Adjei 2001; DeNicola et al. 2009; Shaw et al. 2006; von Lintig et al. 2000). Oncogenic mutations of ras consist of point mutations affecting specific sites (amino acids 12, 13, 59, and 61) that result in abolishing the GAP-induced GTP hydrolysis of the Ras proteins and constitutive activation of the protein (DeNicola & Tuveson 2009). The aberration activity of Ras can be driven by deregulation/mutations of Ras interacting proteins. For instance, inactivation of RAS is regulated by GTPase activating proteins (GAPs). Neurofibromin1 (NF1) protein is

a tumour suppressor that belongs to the family of GAPs and its mutational inactivation leads to accumulation of activated RAS and then tumourigenesis (Shaw & Cantley 2006). In breast cancer, direct mutational activation of H-Ras is a rare event, but its hyperactivation caused by growth factor signalling (EGFR and HER2 overexpression) is more frequent (Clark et al. 1995; von Lintig et al. 2000). Recently, the presence of mutated H-Ras has been linked to BMI1 and its role in breast cancer formation (see section 1.8.1).

ER-negative and grade III breast cancers are associated with loss of RB1 (Retinoblastoma) protein expression (Berge et al. 2010; Chano et al. 2010). RB1 gene mutations were first identified as germline mutations in patients with retinoblastoma, a childhood eye tumour (Friend et al. 1986). Later, somatic mutations of RB1 were identified in different types of human cancers including osteosarcomas, small cell lung cancers and 10% of breast cancers (Lee et al. 1988; T'Ang et al. 1988). The retinoblastoma (RB) pathway play a crucial role in regulating the G1 to S-phase progression of the cell cycle (Genovese et al. 2006). During the G1 phase, upon mitogenic stimulation, the RB1 protein is phosphorylated by Cyclin D1 (with either CDK4 or CDK6 cyclin-dependent kinases) or Cyclin E/CDK2 complexes with subsequent release from the E2F transcription factor. E2F then becomes able to initiate E2F-dependent transcription of genes necessary for DNA replication and S-phase entry (Cam et al. 2003; Genovese et al. 2006). p16 protein inhibits the entire process, being responsible for inhibition of RB1 phosphorylation by the Cyclin D1/CDK complexes (Genovese et al. 2006). Loss of p16, loss of the RB1 tumour suppressors, or amplification and overexpression of Cyclin D1 or CDK4 are involved in human tumourigenesis (Sherr et al. 2002). Loss of p16 is present in about 30% of human breast cancers. While, in other tumours inactivation of p16

occurs through either deletions or point mutations (i.e. pancreatic cancers) (Caldas et al. 1994; Quesnel et al. 1995), in breast cancer inactivation occurs mainly through promoter hypermethylation (Quesnel et al. 1995; Silva et al. 2003). About 25% of all breast cancers have amplification or over-expression of Cyclin D1, which is associated with ER-positive breast cancers (Barbareschi et al. 1997; Bartkova et al. 1994), and about 15% have amplification of the CDK4 (An et al. 1999a).

#### **1.2.4 Role of susceptibility genes**

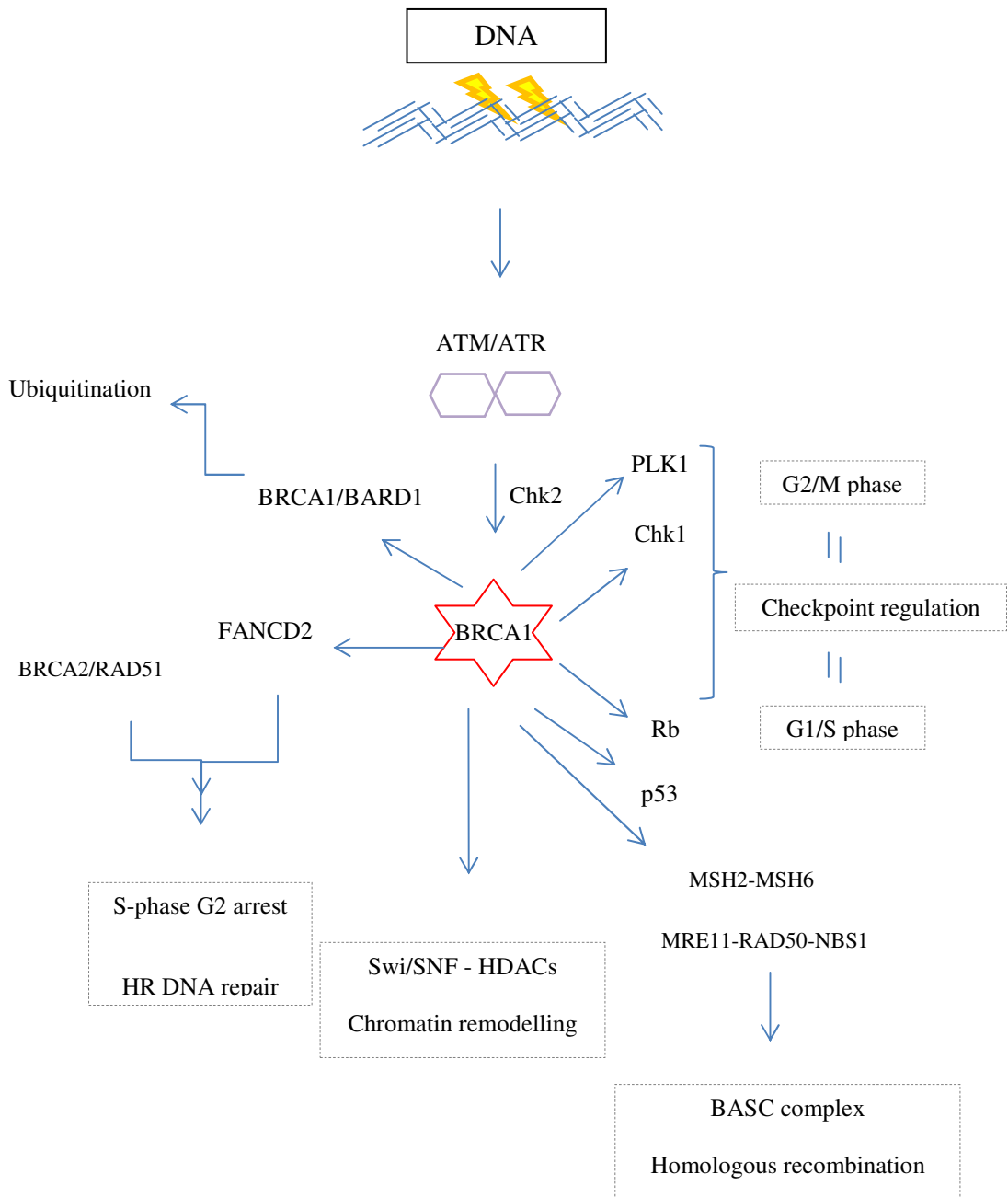
Hereditary breast cancers account only for a small proportion of all breast carcinomas. Women carrying germline mutations of the BRCA1 gene or BRCA2 gene have a high risk of developing breast cancer and ovarian cancer. It has been estimated that women carrying BRCA1 mutations have up to an 80% risk of developing breast cancer and up to a 50% risk of developing ovarian cancer, by the age of 70 (Antoniou et al. 2003; King et al. 2003; Petrucelli et al. 1993), whereas, men carrying germline mutations of BRCA1 and BRCA2 have a higher risk of developing prostate cancer compared to non-carriers (Gallagher et al. 2010). Tumour formation in individuals carrying germline BRCA1 or BRCA2 mutations is normally caused by the loss of the remaining wild type allele with consequent production of a non-functional protein, leading to loss of cell cycle control and loss of DNA repair mechanisms (Boyle et al. 1998). Both BRCA1 and BRCA2 mutant breast cancers have a higher frequency of p53 mutations and a high degree of aneuploidy (Crook et al. 1998; Marcus et al. 1996), confirming the role of the proteins in maintaining genome integrity. BRCA1 preserves genomic stability by playing a key role in a wide range of activities, including DNA repair, cell cycle control and DNA damage signalling (Mullan et al. 2006). Distinct domains of the protein interact with different

co-factors. The amino-terminal RING finger domain is important for the association of BRCA1 with several factors, including BARD1 (Baer et al. 2002). The two nuclear localization signals (NLSs) in the central region of the protein are responsible for the nuclear localization of BRCA1, and the two BRCA1 C-terminal (BRCT) domains, which are also present in other proteins involved in cell cycle control and DNA damage repair, are responsible for the high affinity of the protein for phosphoserine and phosphothreonine residues (Manke et al. 2003). BRCA1, together with RAD51, plays a crucial role in homologous recombination (HR) repair of the DNA during S and G2 phase of the cell cycle. Indeed, BRCA1 colocalizes with RAD51 at DNA repair foci and cells without BRCA1 display defects in HR (Bhattacharyya et al. 2000; Snouwaert et al. 1999). Several studies have shown the involvement of BRCA1 in other DNA repair mechanisms, including non-homologous end joining (NHEJ) mediated double strand break (DSB) repair pathway and nucleotide excision repair (NER) pathway (Wang et al. 2000; Zhong et al. 2002). Wang et al. have shown that BRCA1 is part of the BRCA1-associated genome-surveillance complex (BASC), which includes ATM, RAD50, MRE11 and NBS1 and the mismatch repair proteins MLH1, PMS2, MSH2 and MSH6 (Wang et al. 2000). BASC contains at least 15 units which also have a complex-independent function. MSH2 and MSH6 are required for transcription-coupled repair and their association with BRCA1 suggests that BRCA1 has a role in this pathway (Wang et al. 2000).

BRCA1 forms an E3 ubiquitin ligase complex with BARD1 (Boulton 2006). Starita et al. have shown that the BRCA1/BARD complex specifically ubiquitinates and degrades RNA Pol II stalled at DNA damage site, therefore allowing access for repair machinery (Starita et al. 2005). How the BRCA1/BARD complex is recruited

to DNA damage sites is not clear. Rpb1, the largest subunit of RNA Pol II is specifically targeted by BRCA1, therefore might be responsible for BRCA1 recruitment to DNA damage sites. The involvement of histone H3 and H2AX and RNF8 (ring finger protein 8) have also been proposed as a possible mechanism (Mailand et al. 2007). In summary, Mailand et al. have proposed that H3 and H2AX histones recruit BRCA1 to DNA damage sites through RNF8/Ubc13.

Due to the ability of BRCA1 to interact with RNA Pol II, (along with several co-activator and repressor factors) and proteins involved in chromatin remodelling, including histone deacetylases and components of SWI/SNF-related complexes, BRCA1 can participate in either transcription activation or transcription repression (Mullan et al. 2006; Yarden et al. 1999). In line with the role of BRCA1 in maintaining genome integrity, BRCA1 is involved in transcriptional regulation of transcription factors, including the p53 and retinoblastoma RB (Fabbro et al. 2004) (Figure 1.2). BRCA1 is involved in the regulation of several others factors involved in cell cycle regulation pathways in response to DNA damage, including Nbs1 and Smc1 (S-checkpoint arrest), CtIP and Chk1 (G2/M checkpoint), FANC proteins (S phase cell cycle arrest). BRCA1 also regulates the mitotic spindle checkpoint, a process that guarantees equal segregation of sister chromosomes through the action of the regulatory proteins responsible for metaphase/anaphase arrest, throughout transcriptional regulation of both BubR1 and Mad2 (Bae et al. 2005).



**Figure 1.2:** Schematic representation of the BRCA1 pathway. In response to DNA damage, ataxia telangiectasia mutated (ATM), CHK2 and other kinases are activated and, in turn, induce BRCA1 activation. Downstream targets of BRCA1 activation include p53 and the retinoblastoma protein (RB), important for checkpoint regulation. FANCD2 is also a target of activated BRCA1, and BRCA2/RAD51 complex that is believed to interact with FANCD2 and promotes S-phase or G2 arrest. BRCA1 forms a heterodimer with BARD1 to activate the ubiquitin-ligase function of BARD1. DNA repair by homologous recombination and transcription regulation are mediated by the BRCA1-associated surveillance complex (BASC) which comprises BLM, MSH2–MSH6 and MRE11–RAD50–NBS1. BRCA1 can form complexes with SW1/SNF to mediate chromatin remodelling and homologous recombination, while HDACs regulate the access of the SW1/SNF–BRCA1 complex to DNA. BRCA1 interacts with CHK1 and polo-like kinase 1 (PLK1) to regulate the G2/M and G1/S checkpoints (GADD45 might be involved, linking BRCA1 to the regulation of apoptosis).



The ER pathway is also regulated by BRCA1. Several studies have shown the ability of BRCA1 to repress both oestrogen dependent and independent signalling (Xu et al. 2005; Zheng et al. 2001). BRCA1 can exert its transcriptional repression activity on ER through interaction with several cofactors. The association between the N-terminal domain (aa 1-300) of the BRCA1 protein and the C-terminal activation domain of ER $\alpha$  seems to be responsible for the transcription repression activity of BRCA1 on ER $\alpha$  (Xu et al. 2005). This is confirmed by the fact that mutations occurring in the N-terminal domain of BRCA1 abolish or reduce the ability of BRCA1 to inhibit oestrogen dependent ER $\alpha$  signaling (Fan et al. 1999). However, some BRCA1 mutants with an intact N-terminal interaction domain show a reduced ability of inhibiting ER $\alpha$  transcription activity. This suggests that the C-terminus of BRCA1 might be involved in the ligand independent transcription repression activity of BRCA1 exerted on ER $\alpha$  signalling (Fan et al. 2001). It has been suggested that the oestrogen independent repression of ER $\alpha$  transcription involves histone deacetylase activity, since the repression activity is reversed by treatment with the deacetylase inhibitor trichostatin A (Zheng et al. 2001). Another mechanism through which BRCA1 could mediate ER $\alpha$  repression is through its ability to repress and compete with the co-activator p300 for binding to the activating domain AF-2 of ER $\alpha$  (Fan et al. 2001). In a similar manner, cyclin D1 has also been reported to compete with BRCA1 for ER- $\alpha$  binding. As a result of cyclin D1 binding to the ER $\alpha$  activation domain, the BRCA1-mediated ER $\alpha$  transcriptional repression is inhibited (Wang et al. 2005). BRCA1 can induce ER $\alpha$  repression via its co-factor COBRA1. COBRA1 is a subunit of the human-negative elongation factor (NELF) which induces transcriptional repression by stalling the RNA Pol II at the promoter region (Aiyar et al. 2004). However, BRCA1 might also induce transcription

activation of ER $\alpha$ . Hosey et al. have shown that BRCA1 can interact with the Oct-1 transcription activator factor and that both factors (BRCA1 and Oct-1) co-localize to the ER $\alpha$  promoter. Therefore they might act in concert to coactivate ER $\alpha$  (Hosey et al. 2007). This last property of BRCA1 is extremely relevant in the context of breast cancer aetiology. As discussed in section 1.2.1, ER status is a well-established prognosis marker for breast cancer. Breast cancers carrying a BRCA1 mutation and/or breast cancers with reduced expression of BRCA1 (sporadic breast cancers) are often associated with ER-negativity (Chen et al. 2009) and the link between the two pathways can be explained by the transcription activation activity of BRCA1 on ER $\alpha$ . The link between BRCA1 defect and ER $\alpha$ -negativity can also explain the resistance of BRCA1 mutated cancers to antioestrogen drugs. As for antioestrogen drugs, BRCA1 status might also be a predictive factor for response to new developed drugs. Recent studies have shown a possible interaction between BRCA1 and the polycomb protein EZH2 (Gonzalez et al. 2009). EZH2 plays a crucial role in breast carcinogenesis (see section 1.5 and 1.7.2) and it has been proposed to be a good therapeutic target. Understanding the interplay between BRCA1 and EZH2 might be useful in developing new therapeutic drugs and/or response predictors. The possible interaction between BRCA1 and EZH2 will be discussed in chapter 4.

### **1.3 Breast cancer is a heterogeneous disease**

According to the histological grading system, invasive ductal carcinomas (IDCs) are classified into three distinct groups: low (grade I), intermediate and high (grade III) (Elston et al. 1991). Grade I tumours are well differentiated, while grade III tumours are poorly differentiated and grade II are intermediate. Several groups, using aCGH analysis, have shown that specific tumour grades exhibit distinct

genomic aberrations (Roylance et al. 1999), and demonstrate that low grade tumours have less chromosomal aberrations compared to high-grade tumours. Grade I tumours, generally, display loss of 16q and gains of 1q, 16p, and 8q, while high-grade tumours display high-level amplifications of 17q12 and 11q13 along with losses of 8p, 11q, 13q, 1p, and 18q; and gains of 1q, 8q, 17q, 20q, and 16p (Buerger et al. 1999; Roylance et al. 1999). Intermediate-grade tumours share genomic alterations of both low-grade or high-grade carcinomas. The evidence that, in the vast majority of the cases, low grade tumours display loss of 16q while high grade tumours do not (Roylance et al. 1999), supports a proposed hypothesis, according to which the majority of grade I carcinomas may not evolve to grade III tumours, but an early divergence gives rise to distinct sub-types of tumours (Buerger et al. 1999). This idea is further supported by the observation that, similarly to IDC, DCIS can be sub-divided into low, intermediate and high grade and the genomic alterations associated with the three different DCIS subgroups are similar to the genomic alterations associated with the three IDC subgroups (Buerger et al. 1999; Ivshina et al. 2006; Ma et al. 2003; Sotiriou et al. 2003).

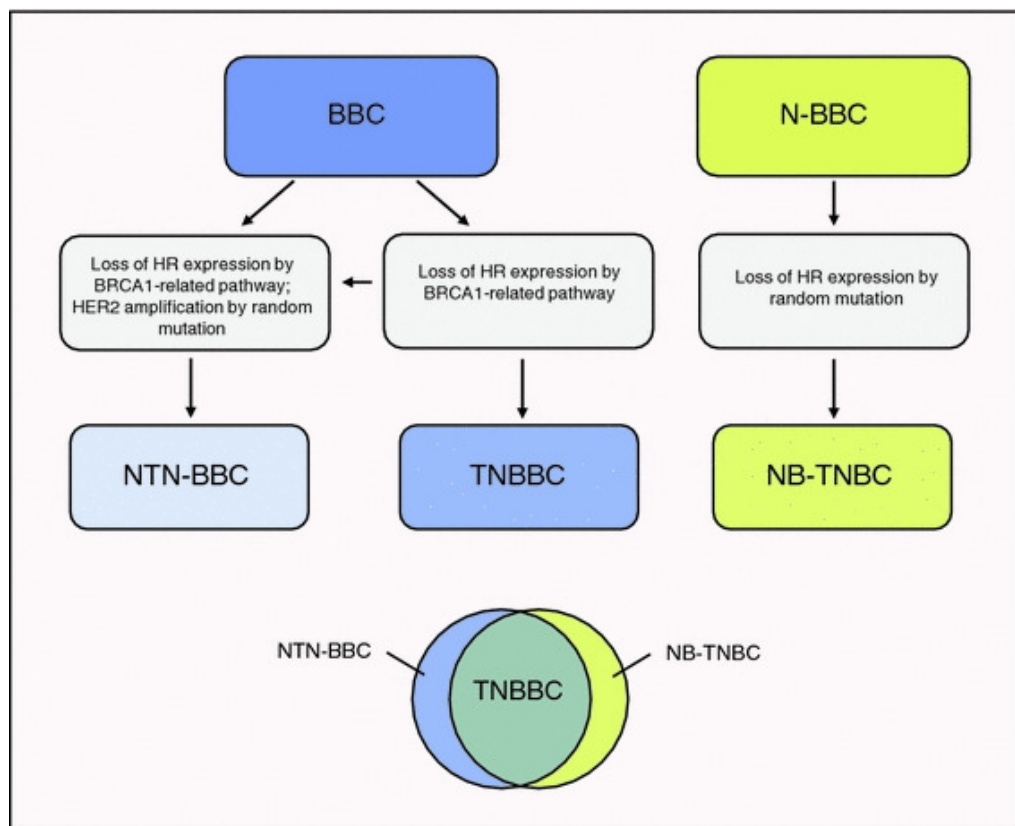
The use of gene expression profiling has allowed further characterization of IDCs and has revealed the existence of five sub-types of breast cancer (Sorlie et al. 2001; Sorlie et al. 2003). A decade ago, Sorlie et al. identified gene expression patterns that distinguish different breast tumour subclasses. Five different sub-types of IDCs have been identified: the luminal A and luminal B subtypes (both ER $\alpha$ -positive), basal-like subtypes (ER $\alpha$ -negative), the HER2-positive and the normal-like sub-group (Constantinidou et al. 2010; Gatzka et al.; Gluz et al. 2009; Haupt et al. 2010; Keller et al. 2010; Lopez-Garcia et al. 2010; Perou et al. 2000). Each group is characterized by the expression and/or repression of a distinct group of genes. In

their original paper Perou et al. described the normal-like subtype as a sub-group characterized by fewer alterations compared to the other sub-groups and displaying high expression of the adipose and non-epithelial gene cluster, including *FACL2*, *AKR1C1*, *PIK3R1* (Perou et al. 2000). Further studies, showed the existence of similarity between normal-like sub-type breast cancers and basal-like, consisting of low expression of genes such as *ER $\alpha$* , *GATA3*, *XBPI*, *TFF3*, *HNF3 $\alpha$*  and *LIV1* (luminal-like cluster). The immuno-histochemical analysis revealed that, similar to basal-like tumours, normal-like tumours are ER/PR/HER2 negative, but they lack expression of CK5/6 and EGFR typical of basal-like tumours. Moreover, these tumours have better prognosis compared to basal-like (Hu et al. 2006; Rakha et al. 2007a; Rakha et al. 2009b; Sorlie et al. 2001; Sorlie et al. 2003; Yu et al. 2004). The HER2-positive subtype comprises tumours with high expression of genes from the *ERBB2* amplicon at chromosome 17q, including *ERBB2*, *GRB7* and *TRAP100*. This group contains both ER positive and ER negative tumours. The HER2/ER negative are more similar to the basal-like, while the HER2/ER positive are similar to the luminal B (Raica et al. 2009). The luminal subtypes (subtype A and B) are both ER-positive and have high expression of genes including *GATA3*, *XBPI*, *TFF3*, *HNF3 $\alpha$*  and *LIV*. Both luminal A and B tumours express hormone receptors (oestrogen and progesterone), but the luminal B sub-type is characterized by proliferative signatures (Cheang et al. 2009). The specific gene expression signature associated with luminal B tumours is enriched in genes that drive the proliferation of cancer cells, including *CCNE1*, *MKI67* or *MYBL2* (Sorlie et al. 2001). Functional and clinic-pathological studies have shown that the risk of relapse in women treated with hormone therapy is higher in women with a luminal B tumour compared to women with a luminal A tumour and that the luminal B sub-type is associated with loss of RB1 (Cheang et al.

2009; Herschkowitz et al. 2008). In addition, luminal B tumours are associated with poor disease-specific survival when treated with chemotherapy (Cheang et al. 2009; Sotiriou et al. 2003). Both, luminal A and luminal B sub-types metastasized more frequently to bone and pleura (Rouzier et al. 2005; Smid et al. 2008; Sorlie et al. 2001; Sotiriou et al. 2003). The basal-like subtype was first identified as a ER-negative sub-group with high expression of genes including *CK14*, *ANXA8*, *CX3CL1* and *TRIM29*, laminin, fatty acid binding protein 7 and is characterized by high p53 mutation frequency (50% of basal-like breast cancer have p53 mutated) (Livasy et al. 2007) and high proliferation index (67% of basal-like breast cancer have high Ki67) (Livasy et al. 2007; Perou et al. 2000; Sorlie et al. 2001; Sorlie et al. 2003; Sotiriou et al. 2003). Basal-like breast cancers are characterized by the presence of CK5/6, CK14, CK17, vimentin and EGFR (Rakha et al. 2009b). Basal-like breast cancers are associated with worse clinical outcome (Sotiriou et al. 2003) and are more frequent in younger women (Bauer et al. 2007). Further clinical studies have also shown that basal-like (as well as HER2-positive subtypes) metastasized more frequently to the brain (Rouzier et al. 2005; Smid et al. 2008; Sorlie et al. 2001; Sotiriou et al. 2003).

Later evidence supports the idea that the basal-like group might represent a sub-group of triple negative breast cancers (ER-negative, PR-negative/HER2 negative) (de Ruijter et al. 2011; Rakha et al. 2007b). According to de Ruijter et al., only a proportion of basal like breast cancers are triple negative and the triple negative breast cancer can originate from either non-basal breast cancer (N-BBC) or basal-like breast cancer (BBC). This hypothesis is supported by several other studies (Bertucci et al. 2008; Morris et al. 2007; Rakha et al. 2009b). Triple negative basal-like breast cancers (TNBBCs) have high expression of Ki-67, vimentin, laminin and p53, and low expression of Bcl-2. This group of breast cancers also have higher

frequency of mutations affecting PTEN, the tumour suppressor retinoblastoma gene (*RBI*) and the *KRAS* oncogene (Hu et al. 2009; Rodriguez-Pinilla et al. 2007). Other features of TNBBCs include, high frequency of copy number alterations, high frequency of BRCA1 mutation/down-regulation and high expression of EGFR, CK5 and CK6 (Collins et al. 2009; Turner et al. 2007). Whereas, the non-basal-like triple negative breast cancers (NB-TNBC) are mostly characterized by the presence of random mutations causing loss of HR expression (de Ruijter et al. 2011) (Figure 1.3).



**Figure 1.3:** Origin and related pathways of different types of triple-negative and basal-like breast tumours. The non-basal-like triple-negative breast cancers (NB-TNBC) may originate from non-basal-like breast cancer (N-BBC), and the non-triple-negative basal-like breast cancer (NTN-BBC) as well as triple-negative basal-like breast cancers (TNBBC) may originate from basal-like breast cancers (BBC). Only the TNBBC subtype can be regarded as a homogeneous breast cancer subgroup. From (de Ruijter et al. 2011).

The origin and progression of the different sub-types of breast cancer is not known. To date, two possible hypotheses have been proposed to explain the heterogeneity of breast invasive carcinomas: the “cancer stem cell theory”, the “clonal evolution theory” (Campbell et al. 2007; Lindeman et al. 2010) . According to the “cancer stem cell theory”, a group of tumour cells with stem cell-like properties, called “cancer stem cells,” drive tumour initiation and progression. Due to their abilities of self-renewal and differentiation, cancer stem cells lead to the production of tumour cell types and generate tumour heterogeneity (Polyak 2007). According to the “clonal evolution theory”, tumour initiation occurs in one single random cell as a consequence of accumulated mutations that provide selective growth advantages (Nowell 1976). As the tumour progresses, genetic instability and uncontrolled proliferation allow the accumulation of additional mutations and the acquisition of new characteristics (Campbell & Polyak 2007). Polyak suggested that breast tumour heterogeneity is probably caused by a combination of the two theories. Tumour initiation may take place in a normal mammary stem or progenitor cell which can undergo a combination of differentiation and clonal selection, driven by the micro-environment and mutations. As a result, a variety of genetically and developmentally distinct tumour cells are formed. Some differentiated cells may have less proliferative potential, some mutated cells may acquire self-renewal capacity, some a higher proliferation rate and other cancer-promoting traits. Differences in microenvironment and/or specific mutations in cells with different molecular properties may drive different breast tumours (Polyak 2007).

Several different studies have tried to clarify the origin and the heterogeneity of breast cancer using cells derived from human reduction mammoplasty (both non-malignant and malignant). Lim et al., analysing the expression of the surface

markers CD49f (integrin alpha 6) and EpCAM (epithelial-specific antigen), have identified and characterized three different sub-populations of cells: the CD49f<sup>high</sup>EpCAM<sup>-</sup> population, CD49f<sup>+</sup>EpCAM<sup>+</sup> population and the CD49f<sup>-</sup>EpCAM<sup>+</sup> population. They have shown that the CD49f<sup>high</sup>EpCAM<sup>-</sup> population represents the myoepithelial/basal cells, the CD49f<sup>+</sup>EpCAM<sup>+</sup> population represents the luminal progenitor cells and the CD49f<sup>-</sup>EpCAM<sup>+</sup> population represent the mature luminal cells. A comparison with expression profile of the six tumour subtypes revealed that the mature luminal signature (CD49f<sup>-</sup>EpCAM<sup>+</sup>) was associated with the luminal A and luminal B subtypes, whereas the luminal progenitor signature (CD49f<sup>+</sup>EpCAM<sup>+</sup>) resembled the basal-like signature, which is in line with the bipotential progenitor theory (luminal progenitors giving rise to basal-like tumours). Lastly, the myoepithelial/basal cell signature (CD49f<sup>high</sup>EpCAM<sup>-</sup>) was associated with the claudin-low and normal-like subtypes (Lim et al. 2009). The claudin-low sub-group is characterized by low gene expression of the tight junction proteins claudin 3, 4 and 7 and E-cadherin, and enriched for tumour initiating cell (TIC) markers (i.e. CD44<sup>+</sup>/CD24<sup>-/low</sup>) (Herschkowitz et al. 2007; Prat et al. 2010).

Cells derived from human mammary glands can be cultured *in vitro* and characterized using several different methods. However, due to different culture conditions, different groups often report different results (Ethier 1996; Speirs et al. 1998; Stampfer et al. 2000; Taylor-Papadimitriou et al. 1993; Yaswen et al. 2002). Most studies report that cytokeratin 8 (CK8) and cytokeratin 18 (CK18) are luminal markers, while cytokeratin 5 (CK5) and cytokeratin 14 (CK14) are progenitor cell markers/myoepithelial cell markers. While CD10 has been described as specific progenitor myoepithelial cells, mucin 1 (MUC1) has been described as a marker of both luminal and progenitor cells (Stingl et al. 1998). Other markers, including the



epithelial cellular adhesion molecule (ESA), SMA, CK14, and integrin  $\alpha 6$  (ITGA6) shows contradictory results (Polyak 2007). A study conducted by Zhang et al. showed that some morphologically distinct myoepithelial cells fail to stain for the classical myoepithelial marker SMA, along with other myoepithelial markers (CD10, CK14, CK5 and CK17) (Zhang et al. 2003). The loss of myoepithelial markers might be due to a dynamic and reciprocal interaction between epithelial and myoepithelial cells. However further studies are need to identify the exact mechanism. A few other studies have also shown that some of the specific epithelial markers have been found expressed in basal cells and *vice versa* (Gusterson et al. 2005; Malzahn et al. 1998). More agreement exists among markers used to identify breast stem cells (CD44<sup>+</sup> / CD24<sup>-</sup> normally define a less differentiated phenotype typical of stem cells) (Al-Hajj et al. 2003; Polyak 2007). Markers that can be used for an accurate definition of stem cells, committed progenitors, and terminally differentiated luminal epithelial and myoepithelial cells are still not available. However, a subpopulation of cells situated in the basal layer of the TDLU has been defined as a stem cell population (Stingl et al. 2001). This population of cells comprises slowly dividing cells that have the ability of self-renewal and, in response to hormonal stimuli, give rise to transient populations that, following specific transcriptional programs, may differentiate into different epithelial lineages. Dontu et al. have shown that ER $\alpha$ -negative progenitors usually differentiate into myoepithelial cells, which form the basal layer of mammary ducts whereas other progenitors give rise to luminal epithelial cells, some of which appear are ER $\alpha$ -positive (Dontu et al. 2003a; Dontu et al. 2005; Pechoux et al. 1999). The stem/progenitor cell phenotype and the differentiation fate is maintained by a well-defined epigenetic program, whose deregulation may result in clonal

proliferation of transformed progenitor cells, also called tumour-initiating cells (TIC). (See section 1.6)

#### **1.4 Epigenetic alterations in breast cancer**

“An epigenetic trait is a stably heritable phenotype resulting from changes in a chromosome without alterations in the DNA sequence” (Berger et al. 2009). Epigenetic changes consist of conformational modifications of the chromatin, modifications that consist of DNA methylation of CpG dinucleotide sequences found at gene promoters and post-translational modifications of histone proteins (Jovanovic et al. 2010; Watanabe et al. 2010). Epigenetic changes are particularly important during development, being responsible for the correct expression of tissue specific sets of genes (Jovanovic et al. 2010; Watanabe & Maekawa 2010). The mammary gland represents a good model for studying these changes, due to the fact that complete development and differentiation occurs post-natally (puberty pregnancy and involution) (Cowin & Wysolmerski 2010). Different changes in chromatin conformation correlates with different stages of mammary gland development (Berger et al. 2009), however how these changes are regulated throughout the development remains not fully understood. Factors including hormone changes, growth factors and extracellular matrix (ECM) components play an important role. For instance, it has been suggested that the ECM component laminin-1 can mediate epigenetic changes at the E-Cadherin promoter in human breast cancer cells, via reduction of Dnmt1 levels (Benton et al. 2009). Other factors involved in the regulation of epigenetic changes characterizing mammary gland development include transcription factors and non-protein-coding RNA (ncRNA) (Khalil et al. 2009). Transcription factors such as YY1 and SNAIL are able to interact with

complexes involved in transcriptional repression, including the Polycomb repressive complex 2 (see section 1.5). These transcription factors target the repressive complex in certain sites of the genome and induce transcriptional repression. YY1 is known to be involved in  $\beta$ -casein gene repression and possibly other milk proteins, while SNAIL is known to be involved in E-cadherin gene repression and EMT processes (Herranz et al. 2008; Rosen et al. 1998; Thomas et al. 1999). ncRNAs also have been proposed to play a role in targeting chromatin modifying complexes to specific loci in the genome (Khalil et al. 2009).

Alterations of methylation of promoter CpG islands (either hypermethylation or hypomethylation) are associated with tumour initiation, progression, invasion and endocrine resistance (Cheng et al. 2008). CpG island methylation has been proposed to be the “second hit” of the Knudson two-hit hypothesis and BRCA1 is a good example (Pali et al. 2007). In BRCA1 mutation carriers, silencing of the second wild type allele is often observed and linked to development and progression of breast cancer. Several different genes have been found to be hypermethylated and silenced in breast cancer, including genes encoding for cell cycle regulation (i.e., *p16<sup>INK4a</sup>* and *p14<sup>ARF</sup>*), DNA repair (i.e., *MLH1* and *GST3*), tumour suppression (*BRCA1*), tissue remodeling (i.e., *E-cadherin*), and hormone receptor (i.e., *ESR1* and *ESR2*). (Birgisdottir et al. 2006; Reynolds et al. 2006; Tlsty et al. 2001). Interestingly, many of these genes are also hypermethylated in normal epithelium surrounding the tumour site (Dworkin et al. 2009). The observation that DNA hypermethylation has been reported in both pre-malignant lesions (atypical hyperplasia) and invasive breast carcinoma, suggests that it might be a potential marker for early detection and risk assessment. The Ras-associated domain family member 1 gene (*RASSF1A*) is another example of a gene often hypermethylated and associated with breast cancer

development (Dworkin et al. 2009). RASSF1A is involved in the regulation of apoptosis, cell growth and microtubule dynamics during mitotic progression. Knockout experiments in mice have shown that RASSF1A<sup>-/-</sup> mice are prone to develop breast cancer (Dworkin et al. 2009). Analysis of DNA methylation patterns in normal and breast cancer derived tissue has shown that the promoter of the gene encoding for RASSF1A is often hypermethylated in breast cancer tissue (75% of the cases) (Dworkin et al. 2009). As for other cases, an increase in RASSF1A promoter methylation has been reported also in areas surrounding the lesions (Dworkin et al. 2009; Visvanathan et al. 2006).

Hypomethylation of promoter CpG islands has also been proposed to be involved in breast cancer (Jovanovic et al. 2010). The hypomethylation associated with the cancer phenotype is due to deficiency of the production of S-adenosylmethionine (SAM), which is the methyl donor in the methylation reaction. The existence of an active demethylase has also been proposed and the T-G mismatch glycosylase, 5-methyl-CpG binding domain protein 4 (MBD4) is a good candidate. MBD4 has recently been found to induce active demethylation of methylated CpG sites (Kim et al. 2009). As a consequence of demethylation, genes that are normally silenced, i.e. oncogenes, get reactivated. Hypomethylation has also been observed in repeat elements (e.g., *Alu*, *LINE*, and  $\alpha$  satellites), contributing to reactivation of transposable elements, promotion of chromosomal translocation, deletion, and duplication and genomic instability (Ehrlich 2002).

Post-translational modifications of histone proteins has also been associated with several different human cancers including breast cancer, and with cancer stem cells (Widschwendter et al. 2007). Cancer stem cells have different gene activity, but the same DNA sequence, compared to normal stem cells and post-translational

histone modifications and DNA methylation could explain the different programming of these cells (Widschwendter et al. 2007). Following this general idea, Feinberg et al. have proposed an “epigenetic progenitor origin of human cancer” model (Feinberg et al. 2006). A polyclonal epigenetic disruption of stem/progenitor cells would be an early event in the non-malignant tissue. Later, other genetic and epigenetic lesions would lead to complete tumour formation (Feinberg et al. 2006). The epigenetic variation affecting progenitor cells would also be a good explanation for the plasticity and heterogeneity of human cancer and particularly breast cancer (Feinberg et al. 2006). Histone modifications and their relevance in breast cancer will be further discussed in the next sections.

## **1.5 Post-translational modifications and gene expression: Trithorax and Polycomb protein**

Chromatin is composed of a nucleosome core particle and a linker region in between nucleosomes (or inter-nucleosomal region) that joins adjacent cores. The core particle is highly conserved between species and is composed of 146 base pairs of DNA wrapped 1.7 turns around a protein octamer composed of one histone H3-H4 tetramer and two histones H2A-H2B (Campos et al. 2009). The core histones, H3, H4, H2A and H2B, are small, basic proteins highly conserved in evolution and the most conserved region of these histones is their central domain, while the N-terminal tails of each core histone are more variable and unstructured (Campos & Reinberg 2009). The tails, particularly rich in lysine and arginine residues, represent the site of numerous post-translational modifications, including acetylation, phosphorylation, ubiquitylation, and methylation (Korber et al. 2010). The best characterized, and most stable, modifications are acetylation and methylation of lysine residues. Both

modifications influence gene transcription by either enhancing or inhibiting the accessibility of transcription factors to target loci (Korber & Becker 2010). While generally, acetylation is associated with open chromatin structure and active transcription, methylation can be associated with either an active or repressive chromatin structural conformation (Wang et al. 2009).

The correct expression of genes involved in development and differentiation is maintained by the activity of two kinds of proteins: the Polycomb group (PcG) and the trithorax group (trxG). PcG and trxG proteins function in distinct multiprotein complexes that are believed to control transcription by changing the structure of chromatin, organizing it into either a 'closed' (PcG) or an 'open' (TrxG) conformation (McKeon et al. 1994; Pelegri et al. 1994; Pirrotta 1998). While methylation of histone H3 lysine 27, catalyzed by PcG is associated with transcriptional repression, methylation of histone H3 lysine 4, catalysed by the Trx proteins is associated with transcriptional activation (Pirrotta 1998; Whitcomb et al. 2007). Polycomb group (PcG) and trithorax group (trxG) proteins were discovered in *Drosophila melanogaster* as repressors and activators of Hox genes (Orlando et al. 1995; Pirrotta 1998). Different classes of TrxG proteins have been identified and they seem to be recruited to their targets in different ways (Orlando & Paro 1995). One class of TrxG binds specific sequences of DNA. A second class of trxG comprises SET domain factors like *Drosophila* Trx and Ash1 and vertebrate MLL. This class of proteins methylate lysine 4 of histone H3 (H3K4). A third class of trxG comprises protein components of ATP-dependent chromatin remodelling complexes like the SWI/SNF or the NURF complexes. Despite the fact that many TrxG proteins have been identified, the precise mechanisms by which these proteins regulate transcription remain unclear. Moreover, it has been suggested that, in addition to chromatin

conformation modification, trxG proteins are able to recruit factors necessary for transcription elongation, and noncoding RNAs involved in gene regulation (Caldas et al. 1999; Mahmoudi et al. 2001; Mazo et al. 2007).

In *Drosophila melanogaster*, polycomb proteins form 3 different complexes called Polycomb Repressive Complex 1 (PRC1) Polycomb Repressive Complex 2 (PRC2) and PhoRC complex (Levine et al. 2002; Orlando & Paro 1995). In vertebrates two major complexes have been identified, PRC1 and PRC2 (Levine et al. 2002). The two complexes cooperate to maintain long term gene silencing. PRC1 contains more than 10 subunits including the onco-protein BMI-1 and the heterochromatin associated (HPC) proteins (CBX2, CBX4, CBX7, and CBX8), HP1-3, RING1-2 and SCML; components of this complex possess H2A-K119 ubiquitin E3 ligase activity. PRC2 contains EZH2, EED, SUZ12 and RbAp48. EZH2 is the active component of the complex and exerts specific histone methyltransferase activity toward Lys 27 of H3 and Lys 26 of H1 (Hansen et al. 2008).

Trithorax and Polycomb proteins establish their role early during embryogenesis and are required for correct establishment of cell identity. In *Drosophila melanogaster* the two complexes work antagonistically via PRE/TRE (Polycomb responsive elements/ Trithorax responsive elements) to maintain active/silenced transcriptional states (Ringrose et al. 2007). No functional mammalian PREs/TREs have been identified yet. Lee et al., using genome-wide technique (ChIP arrays), have discovered that loci bound by one PcG protein (i.e. SUZ12) are highly conserved regions and they overlap with region of the vertebrate genome previously identified as highly conserved non-coding elements (HCNEs) (Lee et al. 2006). There are about 200 regions containing HCNEs, but their function is still unknown. Further studies will be required in order to prove and confirm that

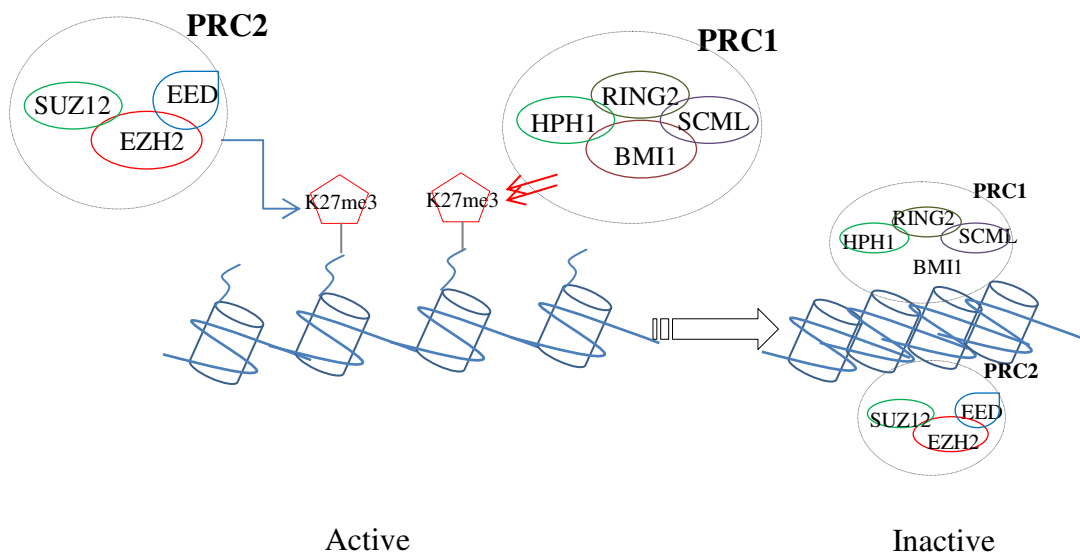
these HCNEs correspond to PRE/TRE. Bracken et al., (Bracken et al. 2006) using expression profiling studies and ChIP-on-chip experiments have identified 43 PcG target genes whose expression is dependent on the PcG proteins. These targets include some known markers of bone, cartilage, fat and neuronal differentiation, such as BMP3, CRELD2, MDF1, THPO, OLIG2, CD4 and NOTCH4. The identification of these target genes still does not help in understanding the mechanism by which PcGs repress transcription during development/differentiation (Bracken et al. 2006). Two alternative models have been proposed: according to the first model, the two complexes are bound to their target genes, and upon induction to differentiate, both PRC1 and PRC2 are displaced by undefined mechanisms, leading to their de-repression. A second model derives from the observation that Polycomb proteins, in some cases, are bound to their target genes in undifferentiated cells, despite the gene being actively expressed. According to this alternative model, specific developmental signals could trigger the PcG-repressive capacity (Kuzmichev et al. 2005; Martinez et al. 2006a).

PRC1 and PRC2 do not interact with each other but they are both required for transcriptional repression. The most accepted working model for PRC1/PRC2 in transcription repression is illustrated in figure 1.4. The PRC2 complex is responsible for specifically “marking” (histone trimethylation) target regions of the genome, which will be recognized by components of the PRC1 complex. It is not clear how the two complexes exactly mediate stable gene silencing, although a few hypotheses have been proposed, including direct inhibition of the transcriptional machinery by PRC1, PRC1-mediated ubiquitylation (Ub) of H2AK119, simply chromatin compaction which makes specific target region inaccessible to the transcription machinery and recruitment of DNA methyltransferases (DNMTs) by PRC2 to target



gene loci (Cao et al. 2005; Sparmann et al. 2006; Wang et al. 2004; Whitcomb et al. 2007).

The first step of the silencing process mediated by the two PRCs is the recruitment of PRC2 to target regions. The PRC2 complex is recruited to a specific chromatin domain through YY1, which is a transcription factor that binds a specific nucleotide sequences (CXGCCATXXXXGX); subsequently, DNMTs and HDACs are recruited to the complex to establish transcriptionally silenced states. Next, EZH2 trimethylates Lys 27 of histone H3, through its SET domain, a mark that is recognized by the chromodomain of sub-units belonging to PRC1 (Cao et al. 2002; Czermin et al. 2002; Min et al. 2003).



**Figure 1.4:** PRC1 and PRC2 induce transcriptional repression. PRC2 (Polycomb repressive complex 2) initiation complex binds to PcG targets and induces EZH2-mediated methylation of histone proteins, primarily at lysine 27 of histone H3 (K27me3). PRC1 is able to recognize the trimethylated K27 marks through the chromodomain of Polycomb proteins. Interaction between the two complexes induces gene silencing. See text for more details.

The role of PcG proteins is not limited to early differentiation in early development. Several lines of evidence suggest that PcG proteins are important for cellular memory (the maintenance of a defined transcriptional state over many cell divisions), and are also involved in the regulation of the cell cycle (Martinez et al. 2006b). The first evidence comes from a study involving Bmi1. The absence of Bmi1 in primary embryonic fibroblasts impairs their progression into S phase and induces premature senescence (possibly due to the fact that the locus INK4a/ARF is a downstream target of Bmi1 (Jacobs et al. 1999)). Similar results were obtained with SUZ12, another component of PRC2. SUZ12 knockdown induces abrogation of H3K27Me3 marks with consequent impaired S phase progression (Aoto et al. 2008). In this study, it was unclear whether or not this defect in S phase progression was due to de-repression of a critical cell cycle inhibitory factor. Evidence showing a specific transcriptional regulation of EZH2 and EED by the pRB/E2F pathway suggests that EZH2 and EED have a role in the regulation of normal cell proliferation (Bracken et al. 2003). Moreover, both pRB and its upstream regulator p16 suppress EZH2 and EED transcription in non-proliferating cells (Bracken et al. 2003). In human cancers, inactivation of the pRB/E2F pathway which leads to increased E2F activity and deregulation of E2F target genes is a frequent event (Pasini et al. 2004a). In line with this observation, both EZH2 and EED are highly expressed in a variety of human cancers. However, specific deregulation of other PcG proteins contribute to carcinogenesis (Bracken et al. 2003; Ding et al. 2006a; Pasini et al. 2004a; Pasini et al. 2004b).

In terms of regulation of cell cycle, not all the PcG proteins have that same regulatory effect. This can be explained, in part, by the ability of PcG complexes to change in composition and, consequently, in their target specificity (Kuzmichev et al.

2005). Indeed, in humans several PcGs orthologues are present and the PcG complex composition varies in relation to the type of tissue. For instance, CBX7 acts like BMI1 by inhibiting the transcription of INK4a/ARF. However, CBX7 does not interact or co-localize with BMI1 or HPC2, suggesting that the two proteins function independently from each other (Gil et al. 2004). Ectopic expression of BMI1 rescues CBX7 knockdown-induced premature senescence in mouse embryonic fibroblast; and ectopic CBX7 expression rescues premature senescence in BMI1<sup>-/-</sup> fibroblasts, suggesting that CBX7 and BMI1 might regulate the same loci (e.g. INK4a/ARF) as part of separate PRC1 complexes (Gil et al. 2004).

## **1.6 Polycomb proteins and stem cell renewal**

Embryonic stem cells (ESCs) are characterized by an unlimited potential for self-renewal and the ability to differentiate into all kinds of somatic cell types. Multiple factors are required for maintaining the pluripotency of ESCs, including ESC-selective transcription factors such as Oct4, Nanog, and Sox2 and extracellular signaling molecules such as leukaemia inhibitory factor (LIF) and bone morphogenic proteins (Boiani et al. 2005). Recent studies have suggested that maintenance of ESCs pluripotency and their ability to differentiate under appropriate stimuli, involve histone modification mechanisms (Azuara et al. 2006; Bernstein et al. 2006a). The first evidence of the PcG involvement in ESCs biology came from genome-wide location analysis in murine ES cells showing that the Polycomb repressive complexes PRC1 and PRC2 associate with genes encoding for transcription factors with important roles in development, including OCT4, SOX2, and NANOG (Boyer et al. 2006; Lee et al. 2006). PcG deficient mice show stem cell defects, including hematopoietic stem cells, neuronal stem cells, cerebellar progenitor and ESCs

(Molofsky et al. 2003; O'Carroll et al. 2001; Park et al. 2003) Lessard et al., have shown that in mice lacking *Rae28* and *Bmi1*, the self-renewal ability of hematopoietic stem cells is impaired. Interestingly, excessive proliferation was observed in *Eed*-deficient and in *Eed/Bmi1*-deficient primitive hematopoietic cells (Lessard et al. 1999) indicating that *Eed* is involved in the negative regulation of the pool size of lymphoid and myeloid progenitor cells.

It has been proposed that key lineage-control genes in ESCs are marked with a unique combination of activating and repressive histone modifications (Azuara et al. 2006). Data obtained from quantitative chromatin immunoprecipitation (ChIP) analysis have shown that in ESCs a number of critical transcription factors for cell lineage determination (i.e. *Sox1*, *Nkx2-2*, *Msx1*, *Irx3*, and *Pax3*) are not expressed and their promoters are associated with both activating (H3 Lys-9 acetylation and H3 Lys-4 methylation) and repressive (H3 Lys-27 methylation) histone modifications. This combination has been reported by several studies and has been called “bivalent” histone modifications (Azuara et al. 2006; Bernstein et al. 2006a). Bivalent histone modification patterns change during the differentiation from ESCs into a neuronal cell lineage: neuron-specific gene promoters will maintain H3 Lys-4 methylation, whereas H3 Lys-27 methylations will disappear. Promoters of other genes that remain silent in differentiated neurons lose H3 Lys-4 methylation and retain H3 Lys-27 methylation. In conclusion, when ESCs receive appropriate stimuli to differentiate into a particular lineage, the repressive histone modifications are removed from the required lineage-control gene loci, while the activating modifications are maintained. However, some promoters of multiple lineage-control genes do not show the bivalent histone modifications (i.e. *Myf5* and *Mash1*) (Williams et al. 2006). *Myf5* is a member of MyoD transcription factor family and regulates muscle lineage

determination (Pownall et al. 2002), Mash1 is a critical transcription factor for the production of neural precursor cells (Williams et al. 2006). In addition, some key developmental genes in ESCs appear to be marked only by H3 Lys-4 methylation, or they do possess neither H3 Lys-4 methylation nor H3 Lys-27 methylation (Williams et al. 2006). Therefore, it has been proposed that only a subset of key developmental genes and lineage-control genes in ESCs display the bivalent chromatin marks, while other lineage-control genes could be regulated by different mechanisms. However, it remains unclear why only a subset of lineage-control genes exhibit bivalent histone modification marks while others exhibit a different regulation mechanism (Pownall et al. 2002).

### **1.7 Polycomb proteins and Breast cancer**

Members of both polycomb repressive groups, PRC1 and PRC2, are often up-regulated in breast cancers and have been showed to play a crucial role in breast tumourigenesis and progression (Pasini et al. 2004a; Pasini et al. 2004b; Raaphorst 2005). Two classical examples of PcG proteins upregulated in breast cancer are BMI1 and EZH2. However, many other components of polycomb repressive complexes, including the CBX proteins, are emerging as key regulators of neoplastic transformation in several different human cancers.

### 1.7.1 BMI1

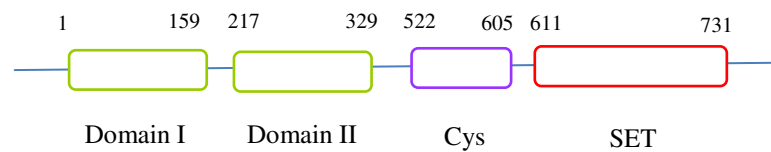
BMI1, the main component of PRC1, was first identified as a factor cooperating with the oncogene c-myc in inducing tumorigenesis (Haupt et al. 1993). Normal levels of BMI1 in normal cells prevent premature expression of the INK4a/Arf locus. It has been shown that BMI1 physically interacts and binds the INK4a locus both in vitro and in vivo (Bracken et al. 2009; Bracken et al. 2007). The repression of the INK4a locus by BMI1 is dependent on the continued association of the EZH2-containing PRC2 complex (Bracken & Helin 2009; Bracken et al. 2007; Kheradmand Kia et al. 2009). The levels of EZH2 are down-regulated in senescent and stressed cells, this causes loss of H3K27me3 followed by displacement of BMI1 and activation of INK4A transcription, resulting in senescence (Bracken et al. 2007). Over-expression of BMI1 can keep the INK4A/Arf locus silenced, causing alterations in cell cycle checkpoint control and apoptosis, leading to transformation (Shakhova et al. 2005). Studies conducted with breast cancer cell lines, along with transgenic mice, have shown a correlation between BMI1 over-expression and a highly aggressive phenotype, including increased metastasis to liver, spleen and brain (Hoenerhoff et al. 2009). The increase in metastasis due to over-expression of BMI1 has been reported in other human cancers, including gastric cancer, melanoma, non-Hodgkin B-cell lymphoma, oral squamous cell and nasopharyngeal cancers (Huang et al. 2007; Kang et al. 2007; Mihic-Probst et al. 2007). Hoenerhoff et al. have shown that BMI1 is able to contribute to breast cancer formation and progression via an INK4A-independent mechanism. According to their data, BMI1 collaborates with H-RAS to induce neoplastic transformation, through the deregulation of multiple growth regulatory pathways, including the AKT and MAPK/ERK pathways, and cell cycle mediators CDK4 and cyclin D (Datta et al.

2007; Hoenerhoff et al. 2009). In several human cancers, such as leukaemia and hepatocellular carcinomas, BMI1 over-expression is associated with a poor prognosis and reduced overall survival (Kang et al. 2007; Kim et al. 2004b). In breast cancer, however, a few studies have shown that over-expression of BMI1 is associated with good prognosis and increased overall survival (Choi et al. 2009). A possible explanation comes from the fact that BMI1 expression is associated with ER-positivity (Arnes et al. 2008; Choi et al. 2009). Pietersen et al. have shown that the level of BMI1 is particularly high in luminal A breast cancers compared with basal-like cancers and they proposed that ER-positive cells derive a selective advantage from BMI1 over-expression (Pietersen et al. 2008). In the normal mammary gland ER-positive cells undergo growth arrest. When cells derived from human mammary glands are grown in vitro, they normally lose the expression of ER and stop growing (Dontu et al. 2003a; Dontu et al. 2003b). However, Duss et al. have shown that over-expression of BMI1 in these cells prevents their growth arrest and allows for ER expression (Duss et al. 2007). In addition, when these cells (over-expressing BMI1 and ER-positive) were injected into immune-compromised mice they gave rise to tumours resembling human adenocarcinomas. However, the metastasis derived from these primary tumours showed a squamous phenotype, which is rare in human breast cancers.

It would be interesting to determine whether other components of the PRC1 have the same effect on normal mammary gland cells. This idea has been further investigated in this thesis and results will be presented in chapter 6.

### 1.7.2 EZH2

EZH2 is the catalytic component of PRC2 (Figure 1.5). EZH2 tri-methylates histone H3 lys 27 (H3K27), an activity that requires the presence of two additional members of PRC2, embryonic ectoderm development (EED) and suppressor of zeste 12 (SUZ12) (Kuzmichev et al. 2005).



**Figure 1.5:** Schematic representation of EZH2 protein domains. EZH2 contains 4 conserved regions: Domain I, Domain II, a cysteine-rich amino acid stretch and a carboxy-terminal SET domain. The SET domain is linked to HMTase activity. Domain I and Domain II are involved in interaction with several different factors (see text for details).

The H3 tri-methylation activity of EZH2 is also modulated by other interacting factors, including the jumonji AT rich interactive domain 2 (Jarid2), PHD finger protein 1 (PHF1), which specifically stimulates H3K27 trimethylation and sirtuin 1 (SIRT1) (Kuzmichev et al. 2005; Sarma et al. 2008). However, EZH2 also participates in transcription repression also *via* interaction with other factors (e.g. methyltransferases and deacetylases). EZH2 can bind DNA methyltransferases (DNMT1, DNMT3A, and DNMT3B) inducing promoter methylation and gene repression (Rush et al. 2009; Vire et al. 2006). EZH2 can also recruit histone deacetylases (HDAC) (van der Vlag et al. 1999). De-acetylation has been suggested to be an additional mechanism for the transcriptional repression function of PRC2. The  $\alpha$ -globin locus appears to be normally repressed, hypoacetylated and enriched in



H3K27me3 in non-erythroid cells. When these cells are treated with the HDAC inhibitor, trichostatin A, the  $\alpha$ -globin gene is re-expressed and PRC2 depleted (van der Vlag & Otte 1999), suggesting a possible role of acetylation in gene repression. Many genes can be re-activated by silencing H3K27me3 without interfering with the level of DNA methylation (Tan et al. 2007). Why some genes are regulated by histone methylation activity only while others require additional modifications, such as DNA methylation and de-acetylation is unknown. Understanding the multiple ways by which EZH2 is involved in epigenetic modification/gene silencing is important for clarifying how its de-regulation can induce tumourigenesis.

EZH2 is frequently over-expressed in many human cancers, including, breast cancer, prostate cancer, colon cancer, Lymphomas and hepatocellular carcinomas (Ding et al. 2006b; Dukers et al. 2004; Kleer et al. 2003; Raaphorst et al. 2000; Sudo et al. 2005). In clinically localized prostate cancer, as well as in breast cancer, EZH2 over-expression has been found to be a predictive marker for poor outcome (Kleer et al. 2003). In breast cancer an increase of the EZH2 mRNA transcript and protein level is already detected in DCIS and comparison analysis between normal breast and various stages of malignant breast lesions have shown that the level of over-expression is proportional to the malignant stage. In other words, the more advanced and aggressive the disease is, the higher the EZH2 expression (Kleer et al. 2003). The highest level of EZH2 protein is detected in high grade ER/PR-negative tumours. High EZH2 expression is associated with a shorter disease-free interval after initial surgical treatment, lower overall survival and high probability of disease-specific death (Kleer et al. 2003). EZH2 protein over-expression is already detectable in DCIS, suggesting that misregulation of EZH2 might be one of the first step towards neoplastic transformation (Ding et al. 2006a). This hypothesis is supported

by the fact that ectopic over-expression of EZH2 in normal mammary epithelial cells confers on them anchorage-independent growth capacity and cell invasion potential (Kleer et al. 2003). EZH2 de-regulation contributes to tumourigenesis via different mechanisms and influences several cellular pathways, including DNA repair, cell cycle control and proliferation (Cao et al. 2004; Kodach et al. 2010; Richter et al. 2009; Zeidler et al. 2006).

EZH2 (PRC2) can induce silencing of tumour suppressor genes (Kodach et al. 2010), either solely via tri-methylation of histone H3 or via a combination of activities, tri-methylation and DNA methylation. Suppression of tumour suppressor genes such as p16, CDKN1C (p57) and E-cadherin are good examples (Kotake et al. 2007; Yang et al. 2009; Zhao et al. 2005).

Several studies have reported that the over-expression of Ezh2 is associated with a more aggressive and undifferentiated tumour phenotype, not only in breast, but also in brain and bone (Crea et al. 2010; Puppe et al. 2009; Richter et al. 2009), supporting the idea that Ezh2 over-expression can enhance the development of undifferentiated highly proliferative tumours (Richter et al. 2009). As discussed in section 1.6, PcG protein play a crucial role in maintaining pluripotency and inhibiting differentiation of stem cells. Genome-wide studies have shown that the expression signature of poorly differentiated tumours is very similar to the expression signature of stem cells (Bracken et al. 2006). In mammary epithelial cells, HOXA9 is a positive regulator of terminal differentiation and it has been proposed to be also a tumour suppressor gene. The up-regulation of PcG proteins EZH2 and SUZ12 causes down-regulation of HOXA9 expression and therefore inhibits terminal differentiation and promotes the maintenance of a progenitor-like/undifferentiated phenotype (Reynolds et al. 2006).

EZH2 over-expression can impair the homologous recombination (HR) process. In breast cancer cells over-expression of EZH2 is accompanied by a significant decrease in the number of RAD51 repair nuclear foci after induction of DSBs (Zeidler & Kleer 2006). Zeidler et al. have shown that in normal spontaneous immortalized breast cells, EZH2 over-expression causes a reduction in expression of RAD1 (along with other RAD51 paralogues involved in HR repair) and consequent aneuploidy.

EZH2 over-expression can impair apoptosis. EZH2, as well as SUZ12 are downstream targets of Rb-E2F pathway (Cao & Zhang 2004), which is a pro-apoptotic pathway acting either via p53 or activation of other target genes, including the BCL2 family members (Bim, PUMA and Noxa) (Hallstrom et al. 2008). The pro-apoptotic activity of E2F can be altered in cancer in different ways: p53 deficiency, PI3K, MDM2 and HDAC defects (Zhao et al. 2005). Wu et al. showed that the activation of EZH2 by E2F1 inhibits E2F1-mediated apoptosis in cancer cells and this is achieved through epigenetic repression of Bim expression (Wu et al. 2010).

EZH2 has a dual function in transcription: activation and repression. While the SET domain of EZH2 is involved in its repression activity, domain I is involved in its gene activation ability. Data obtained from two independent studies provide the evidences that EZH2 transcription activation is involved in breast cancer formation (Li et al. 2009; Shi et al. 2007). Two major pathways are often deregulated in breast cancer, the Wnt/ $\beta$ -catenin signalling pathway, which plays an important role in regulating cell proliferation and differentiation at several stages during mammary gland development, and the ER pathway, which has been discussed in section 1.1.1. Alteration of the Wnt/ $\beta$ -catenin signalling pathway has been linked to several different types of human cancers, including breast. Disruption of the  $\beta$ -catenin

pathway induces mammary hyperplasia in mice (Li et al. 2009). Examples of genes often mis-regulated in breast cancer are c-myc and cyclin D and they are under the control of both ER and Wnt/ $\beta$ -catenin signalling (Li et al. 2009). Li et al., have shown that EZH2 physically interacts with  $\beta$ -catenin, inducing its nuclear accumulation in mammary epithelial cells and activation of the Wnt/ $\beta$ -catenin signal pathway. In line with these data, Shi et al. have proposed that EZH2 functions as a connector between the ER pathway and  $\beta$ -catenin pathway. EZH2 interacts with both ER and  $\beta$ -catenin enhancing the transcription and function of two common targets Cyclin D and c-myc. An additional connection between EZH2 and the Wnt/ $\beta$ -catenin signals derives from studies conducted in hepatocellular carcinoma. EZH2 has the ability to repress the expression of several antagonists of the Wnt/ $\beta$ -catenin (Cheng et al. 2010).

To date, the most common mechanism by which EZH2 induces tumourigenesis in breast cancer is over-expression. However, other factors or modification can influence EZH2 oncogenic potential. A recent study has shown the existence of acquired EZH2 heterozygous missense mutation at amino acid Y641 within the SET domain in lymphoma and myeloid neoplasms (Chase et al. 2011). Wild type EZH2 displays greatest catalytic activity for mono-methylation of H3K27 and a weaker efficiency for the subsequent (mono- to di- and di- to trimethylation) reactions. Y641 mutants have a weak catalytic activity for the first methylation and a much stronger catalytic activity for the subsequent methylation. Therefore, the heterozygous Y641mutation, together with wild type EZH2, could enhance the catalytic efficiency of EZH2 in histone methylation (Chase & Cross 2011; Sneeringer et al. 2010). In addition, Chen et.al have shown the phosphorylation of EZH2 at position 350 is essential for its oncogenic function in prostate cells (Chen et

al. 2010). Lastly, EZH2 also forms cytosolic complexes and regulates actin polymerization in different type of cells, suggesting its involvement in cell adhesion, migration and metastatic potential (Su et al. 2005). These data suggest that EZH2 is an excellent therapeutic target candidate.

In this thesis (Chapter 3 and 4), the effect of EZH2 knockdown, using shRNA, has been investigated in several different type of breast cancer cell, in order to clarify whether different type of cells respond differently to EZH2 silencing and to identify which factors might induce a different response.

### **1.7.3 CBX proteins**

CBX proteins are chromodomain-containing proteins, evolutionarily related to the *Drosophila* HP1 (*dHP1*) and Pc (*dPc*) proteins that are involved in regulation of heterochromatin, gene expression, and developmental programs (Kingston et al. 1996). Both heterochromatin protein (HP1) and polycomb protein (Pc) recognize repressive marks such as trimethylated Lys-9 and Lys-27 on histone H3, via their chromodomain. Eight homologous CBX proteins have been identified in Humans: three *dHP1* homologues (CBX1, CBX4 and CBX5) and five *dPc* homologues (CBX2/M33, CBX4/Pc2, CBX6, CBX7 and CBX8/Pc3). However, the binding specificity and function of the human homologues, CBX1–8 is not fully understood (Jacobs et al. 2002; Simon 2003; Simon et al. 2002; Whitcomb et al. 2007). Crystallography studies, conducted by Fischle et al., have shown that HP1 preferentially bind to methylated Lys9 on Histone H3, while Pc proteins preferentially bind to methylated Lys27 on histone H3 (Fischle et al. 2003). This is in line with fact that the five human homologues of Pc (CBX2, 4, 6, 7 and 8) belong to

the PRC1, which is the complex responsible for recognizing and binding H3K27me3 marks for transcription repression. A recent study conducted by Kaustov et al., showed that the human HP1 homologs CBX1, -3, and -5 preferentially recognize H3K9me3 in a manner similar to their *dHP1* counterpart and show strong affinity for the H3K9me3 markers. Chromodomains from the human Pc homologues showed a very low affinity for H3K9me3 and H3K27me3 peptides, and they do not seem to be able to distinguish well between the two marks. Kaustov et al. proposed the electrostatic surface of HP1 and Pc dictates the target specificity. CBX1, 3, and 5 have a large electronegative peptide binding surface complementing perfectly the basic histone peptides, while the CBX2, 4, 6, 7 and 8 have more hydrophobic surface, responsible for a less stable binding. The binding of CBX2 -8 to their targets may require other histone modification or modulators (Kaustov et al. 2011).

CBX proteins have two well conserved domains, a C-terminal domain called “C-box” involved in interaction with other members of PRC1 and a N-terminal domain called Chromo-domain (chromatin organization modifier domain) involved in the interaction with trimethylated Lys27 of histone H3 tail (Jacobs et al. 2001; Lachner et al. 2001). Three caging aromatic residues necessary for Lys methylation recognition have been identified within the Pc chromodomain (Jacobs & Khorasanizadeh 2002), and a consensus sequence, ARKS, surrounding lys 27 of Histone H3 (Jacobs et al. 2001). However, surrounding residues could also contribute to target selectivity and function (Fischle et al. 2003; Kaustov et al.; Vincenz et al. 2008). Moreover, some CBX proteins have been shown to recognize and bind other modifications in vitro, including H3K9me3 and non-coding RNA molecules (Bernstein et al. 2006b).

Alterations of CBX protein expression and/or mutations have been associated with developmental diseases and cancer. CBX2 (Pc1), known as M33 in mouse, is involved in neoplastic transformation, abnormality in sexual development and an inherited disease called campomelic syndrome (Biaison-Lauber et al. 2009; Core et al. 2004; Gecz et al. 1995). CBX4 (Pc2) mutations cause de-repression of the proto-oncogene *c-myc*, leading to neoplastic transformation (Satijn et al. 1997). CBX6 was first identified as a putative integral membrane protein interacting with neuronal pentraxin 1 and 2 and later classified as a Pc protein (Dodds et al. 1997; Gil et al. 2004; Vincenz & Kerppola 2008) but very little is known about its function and its possible involvement in cancer. Of all CBX proteins, CBX7 is the most studied. CBX7 mis-regulation has been shown to be associated with different types of cancer, including prostate, colon and gastric. CBX7 controls cellular lifespan through regulation of both the p16(*Ink4a*)/Rb and the Arf/p53 pathways (Gil et al. 2004), leading to tumorigenesis (Bernard et al. 2005; Gil et al. 2004; Maertens et al. 2009; Mohammad et al. 2009; Pallante et al. 2008). CBX8 also has been suggested as an important regulator of cell proliferation, acting through repression of p16<sup>Ink4a</sup> and p19<sup>Arf</sup> in mouse cells, enabling the cells to bypass senescence and apoptosis under stress and oncogenic stimuli (Bardos et al. 2000; Dietrich et al. 2007; Kirmizis et al. 2003). The role of CBX8 in both human and mouse fibroblasts has been investigated by Dietrich et al.. They showed that inhibition of CBX8 expression in mouse and human fibroblasts results in growth arrest, and ectopic expression of CBX8 bypasses stress-induced senescence in mice, suggesting a cell growth promoting function for CBX8. In addition, they showed that both CBX8 and BMI1 associate with the *INK4A-ARF* locus in human and mouse fibroblasts, and that BMI1 is dependent on CBX8 and *viceversa* for binding *INK4A-ARF*, suggesting that the chromodomain of

CBX8 alone is not sufficient for its binding to the *INK4A-ARF* locus, and that only when the two protein are bound together in a complex a correct conformation and stability is achieved. Upon the observation that downregulation of CBX8 leads to loss of proliferation and a decrease in cyclin A2 levels before a significant increase in p16<sup>INK4A</sup> levels, they suggested the possibility that CBX8 might regulate cell proliferation also through a pathway independent of *INK4A-ARF* (Dietrich et al. 2007). This hypothesis was confirmed by gene expression profiling. Of the 90 genes directly regulated by CBX8, at least 5 of them were candidate tumour suppressors (*INK4A*, *MTUS1*, *PERP*, *GJB2/CX26* and *SORBS1*) (Dietrich et al. 2007). *PERP* is a target of p53 involved in p53-induced apoptosis, suggesting that CBX8 in mouse cells, could work both up- and down-stream of p53 (Attardi et al. 2000). The *MTUS1* gene is a candidate tumour suppressor involved in control of cell proliferation (Dietrich et al. 2007; Seibold et al. 2003) *GJB2/CX26* belongs to the connexin family and a mediator of gap junctional intercellular communication (GJIC). *GJB2/CX26* is often silenced by CpG methylation in breast cancer (Miyamoto et al. 2005) and its loss is associated with uncontrolled proliferation and cancer progression. Lastly, *SORBS1* has been found to be downregulated in prostate cancer (Vanaja et al. 2006).

To date, the Dietrich et al. study is the only comprehensive CBX8 study conducted and it is based on experiments conducted in fibroblasts (both mouse and human). PRC1, as well as PRC2, is composed of several subunits and many other might be identified. It is likely that many combinations of subunits can associate with each other to form different functional complexes. Moreover, each subunit is expressed in a distinct set of cells and tissues, and the compositions of the complexes are therefore likely to vary depending on the cell type (Kerppola 2009). With this in mind, I have investigated the role of CBX8 in different types of human cells, two



immortalized non-tumorigenic breast epithelial cell lines and breast primary epithelial cells (chapter 5 and chapter 6).

### **1.8 The use of different models for investigating breast cancer**

The most used model for investigating breast cancer is represented by the use of established breast cancer cell lines. These cells have many advantages including easy propagation, easy genetic manipulation and reproduction of results. The cells can also be used for *in vivo* studies, since they can be grown as xenografts (Vargo-Gogola et al. 2007). However, due to that fact that most of them have been propagated for many years, there are multiple variants of the same cell line and some of them have acquired a different phenotype. Results from a comprehensive study, including 51 different breast cancer cell lines, which was based on a comparison of gene expression profile and genomic alterations between breast cancer cell lines and breast tumours have shown that in many cases breast cancer cell lines have many of the recurrent abnormalities found in breast cancers (Neve et al. 2006). However, some important differences in terms of expression profile were found. For instance the remarkably strong difference in gene copy numbers observed between luminal tumours and basal-like tumours is lost when luminal breast cancer cells and basal-like breast cancer cells are compared. Moreover, not all breast cancer sub-types were reflected in breast cancer cell lines classification. Neve et al., also described two new subtypes of basal-like cells, basal A and Basal B, referred only to established cell lines (Neve et al. 2006). The reason for the absence of a perfect match between breast cancer cell lines and tumours could be due to the fact that most established breast cancer cell lines do not derive from the primary tumour but from pleura effusion or an advanced breast cancer. One of the main limitations of the use of

breast cancer cell lines is the conditions used for growing the cells which is remarkably different from the breast microenvironment. The cells are grown on plastic and lack some of the important external factors, including stromal components which play a crucial role in tumour growth (Albini & Sporn 2007). Several culture methods have been developed in order to overcome some of these problems, including 3D culture (Dontu et al. 2003b; Dontu et al. 2005), non-adherent mammosphere culture (specific for propagation of self-renewal and progenitor cells) (Dontu et al. 2003b; Dontu et al. 2005) and co-culture with fibroblasts or macrophages (Tsutsui et al. 2005).

A good alternative to the long-term culture of established breast cancer cell lines is represented by the use of cells derived from primary human breast tissues. Normal cells derived from reduction mammoplasty represent a useful method to study the contribution of different type of genes towards the development of breast cancer, since primary cells have an unaltered genotype. Several different culture methods have been developed in the past years (Emerman et al. 1990). However, in most of the cases only a small number of the original population of cells continues to grow and growth is normally limited to a certain length of time (cells normally stop growing after 5 or 6 population doublings). The use of extracellular matrices, including endothelial cell extracellular matrix, or the use of dishes coated with collagen gel, improve the growth and the attachment of primary cells (Berthon et al. 1992; Ince et al. 2007). Another critical point is the manipulation of different types of cells will give different results and most growth media also induces the growth of fibroblast cells. A number of serum-free media have been developed in order to selectively grow mammary epithelial cells (Duss et al. 2007; Emerman & Wilkinson 1990; Hammond et al. 1984; Ince et al. 2007; Stampfer & Yaswen 2000).

Duss et al. have developed a culture system model that combines the use of defined serum free media and growing cells as floating mammospheres, in order to favour the growth of mammary gland progenitor cells and to eliminate fibroblasts. The mammosphere approach was first developed by Dontu et al. and was especially designed for the enrichment for bipotent progenitor cells that are capable of differentiating into myoepithelial and luminal cells, with production of milk proteins by the latter after treatment with prolactin in three-dimensional Matrigel culture (Dontu et al. 2003b).

Successfully growing and manipulating normal primary epithelial cells from reduction mammoplasty can be useful in shedding light on some controversies regarding the origin and the heterogeneity of breast cancers. While some ascribe the phenotypic heterogeneity of breast cancers to subtype-specific genetic and epigenetic alterations, others propose that breast cancer heterogeneity is also due to their derivation from a variety of distinct normal epithelial cell types (cell of origin theory) (Bocker et al. 2002; Dontu et al. 2003b; Keller et al. 2010; Welm et al. 2003). Ince et al. have shown that the use of chemically defined growth medium can enhance the growth ability of epithelial cells derived from reduction mammoplasties (Ince et al. 2007). Moreover, different growth media can give rise to different populations of cells (Ince et al. 2007). Indeed, they showed that these cells, injected into immunocompromised mice, gave rise to two tumour phenotypes with distinct morphology, tumorigenicity and metastatic behaviour. Their observations are therefore in support of the cell of origin theory.

Epithelial cells derived from reduction mammoplasty and cultured according to the Ince et al. protocol have been used in this thesis for the investigation of the involvement of CBX 8 polycomb protein in breast cancer (see chapter 6).

## **1.9 Aim and scope of the thesis**

The overall aim of this thesis was to investigate the importance of altering two polycomb proteins (EZH2 and CBX8) in breast cancer. For this purpose, breast cancer cell lines and breast primary epithelial cells derived from human reduction mammoplasty have been used.

EZH2 is over-expressed in many type of human cancer, including breast (Cao et al. 2002; Chase & Cross 2011; Ding & Kleer 2006b; Kamminga et al. 2006; Kleer et al. 2003; Pietersen et al. 2008; Sudo et al. 2005; Wu et al. 2010; Zeidler et al. 2005). In breast cancer, EZH2 is a good marker for aggressiveness and prognosis (Kleer et al. 2003) but its exact role in breast tumourigenesis and progression is not fully understood. EZH2 may represent a good therapeutic target candidate (Takawa et al. 2010), but the high heterogeneity of the disease has to be taken in account. It is possible that even within a group of breast cancers over-expressing EZH2, only a fraction might benefit from the use of a therapeutic agent specifically designed to target EZH2 (Puppe et al. 2009). In order to gain insight in to what factors might influence the response of cancer cells to therapeutic agents targeting EZH2, the effect of EZH2 knockdown has been carried out in cell lines with different characteristics, and some neoplastic features, including proliferation, invasion ability and migration have been evaluated (chapter 3 and 4).

CBX8 acts as a cell proliferation promoting gene in mouse and human fibroblasts, but its role in human epithelial cells and its role in breast cancer is unknown (Dietrich et al. 2007). In mouse and human fibroblasts, ectopic expression of CBX8 causes repression of the Ink4a-Arf locus and bypass of senescence. In addition, CBX8 regulates a number of other genes important for cell growth and survival, therefore CBX8 promotes immortalization, cell proliferation and survival

(Dietrich et al. 2007). According to Dietrich et al., CBX8 is an essential component of PRC1 complexes, and directly regulates the expression of numerous target genes, including the INK4A-ARF locus. In order to test whether CBX8 acts as a cell proliferation promoting gene in human epithelial cells and whether it is an important component of PRC1 in epithelial cells, CBX8 was ectopically expressed in MCF10A cells, normal human primary breast cells derived from reduction mammoplasty and B42CP cells. Several different in vitro assays were then used to evaluate the effect of CBX8 over-expression on specific cellular features (Chapter 5 and 6).

## **2 CHAPTER 2: MATERIALS AND METHODS**

### **2.1 Materials**

HsCD00045684, HsCD00079712, HsCD00079972, plasmids were obtained from the Harvard plasmID clone resource. Lentiviral vectors expressing shRNA-EZH2 (IDV2LHS\_17507) and the human GIPZ lentiviral shRNA control were obtained from Open Biosystems. pBABE puro HRas-V12 was obtained from Addgene. VSV-G (pVF11) construct, the packaging construct (pVF16), the lentiviral expression plasmid pSD69 were obtained from the Dr. R. Iggo group.

All virus work was performed in Class II biosafety cabinets with appropriate additional safety measures determined by local regulations. Both solid and liquid waste was autoclaved before final disposal.

MCF10A, MDA-MB-231, T47, 293T, PhoenixA, cells were obtained from ATCC. HCC1937-EV28 and HCC1937-BR69 cells were obtained from Dr. P. Harkin group. B42CP cells were obtained from Prof Riches. SNB19 cells were obtained from Prof Bredel group. Cell culture reagents were purchased from Invitrogen, Sigma and Lonza.

Custom oligonucleotides were purchased from Invitrogen. Gateway reagents were purchased from Invitrogen. Plasmid DNA extraction kits (miniprep and maxiprep) were purchased from Qiagen. PCR reagents were purchased from NEB. Enzymes, buffers and DNA markers were purchased from NEB. Chemically competent cells were purchased from Invitrogen. DNA purification and gel extraction kit were purchased from Qiagen. Rapid DNA ligation kit and complete protease inhibitor were purchased from Roche. Mirus TransIT®-LT1 transfection

reagent was purchased from Cambridge Bioscience. All chemicals were purchased from Sigma (unless stated otherwise). HeLa nuclear extract was purchased from Millipore. ECL and protein assay kit were purchased from Pierce. Protein marker and PVDF membrane were purchased from GE healthcare. 0.45 µm filter were purchased from Elkay UK Ltd. Regular plates for tissue culture were purchased from Nunc/Thermo Fisher scientific. Ultra Low Attachment plates were purchased from Fisher. Primaria plasticware were purchased from BD Biosciences. Polyethylene terephthalate (PET) membranes were purchased from VWR.

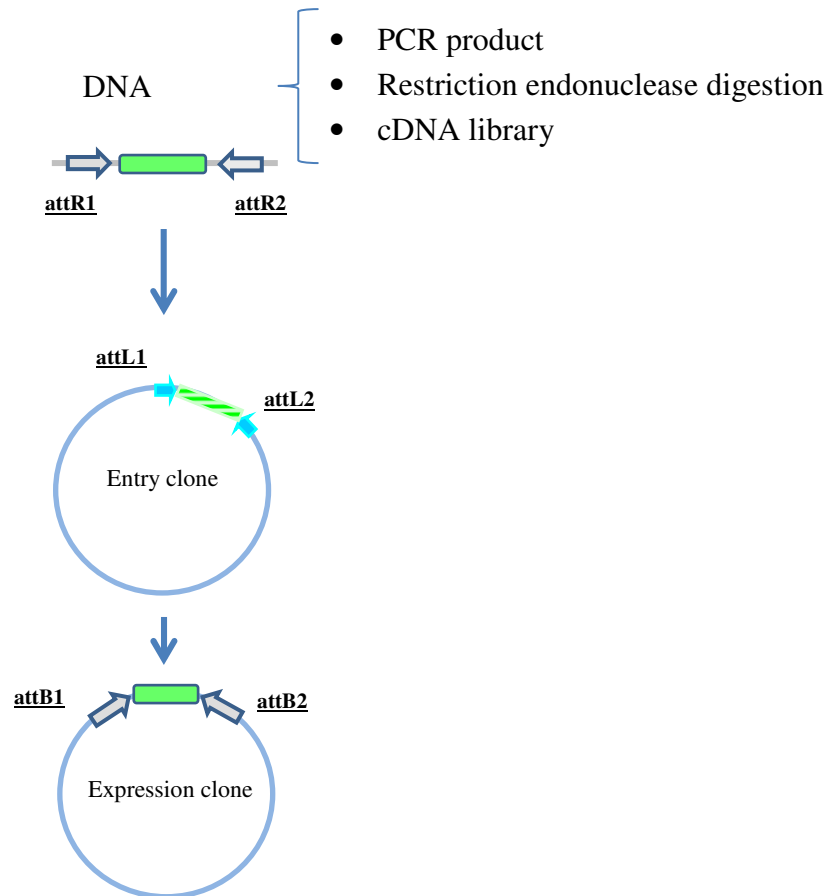
## **2.2 Methods**

### **2.2.1 Lentiviral vector production**

The gateway recombination cloning technique (Invitrogen) was used for lentiviral vector production (Figure 2.1). The technique relies on two major steps:

1. Constructing an entry clone
2. Constructing the expression clone.

Full length cDNA of CBX7 (reference sequence NM\_175709) and CBX8 (reference sequence BC009376) was used and derived from a HsCD00079712 and HsCD00079972 plasmid (from the Harvard plasmid clone resource) respectively.



**Figure 2.1** Schematic representation of the Gateway cloning system. This cloning technology is based on the nature of site-specific recombination. The recombination between *attR* and *attL* sites results in *attB* sites that flank the DNA integrated in the expression clone.



### 2.2.1.1 PCR amplification of ORF

Approximately 80 ng of plasmid DNA was used for each reaction; reactions were conducted in 50 µl total volume (1X PCR buffer, 0.25mM dNTPs, 2 µM Forward primer, 2 µM Reverse primer and 1.5 U of Taq DNA polymerase) in 0.2 ml thin wall PCR tubes (Axygen, cat # 321-02-051). The primer sequences were as follows:

- attB1-CBX7-Forward:

5'-GGGGACAAGTTTGTACAAAAAAGCAGGCTGCCACCATGGG  
CCAGACTGGGAAGAA-3'

- attB2-CBX7-Reverse:

5'-GGGGACCACTTTGTACAAGAAAGCTGGGTCAGGGATTTCCA  
TTTCTCTTTCG-3'

- attB1-CBX8-Forward:

5'-GGGGACAAGTTTGTACAAAAAAGCAAGCTGCAACCATGGAG  
CTTTCAGCGGTGGG-3'

- attB2-CBX8-Reverse:

5'-GGGGACCACTTTGTACAAGAAAGCTGGGTCATCTTTTCTCTT  
TAAAAAAGCC-3'

PCR was conducted on a BioRad thermocycler using the following condition:

- Pre-heat lid at 100 °C
- Initialize: 98 °C for 30 seconds
- Cycle of 25 repeats:
  - Denaturing: 98 °C for 15 second
  - Annealing: 54 °C for 15 seconds
  - Extending: 72 °C for 1 minute
- Final extension: 72 °C for 10 minutes

PCR products were stored at -20 °C.

### **2.2.1.2 Agarose gel electrophoresis**

A 0.8% agarose gel was made by adding 0.4 g agarose (Sigma, cat# A9539) to 50 ml TBE (Tris-Borate-EDTA) running buffer along with 1 $\mu$ L of 10 mg/mL ethidium bromide and heated in microwave. After 15-20 minutes gel was poured into mould; more buffer was added on top before samples were loaded. 0.8  $\mu$ L of 6X blue loading buffer (NEB, cat # N3232S) was added to each sample. 5  $\mu$ L of PCR products were loaded (together with) plus 5  $\mu$ L of 1 Kb ladder (NEB, cat # N3232S). The gel was run at 95-100 V for about one hour and then the DNA visualized under transilluminator light and digital image captured (Syngene Genetools software).

### **2.2.1.3 PCR product purification**

40  $\mu$ L of PCR products were loaded onto 0.8% low melting agarose gel and run at 90 V for about one hour. The correct products were visualized using a transilluminator and the products were then cut out of the gel using a clean scalpel and transferred into 1.5 ml eppendorf tubes. QIAquick Gel Extraction Kit (Qiagen, cat # 28704) was used to purify the PCR products. Briefly, 3 volumes of QG buffer was added to 1 volume of gel and incubated at 50 °C for 10 minutes (or until the gel was completely dissolved). One volume of isopropanol was subsequently added and the mixture was transferred to a QIAquick column. The column containing the mix was placed in a 1.5 ml eppendorf tube and centrifuged at 13000 rpm for 1 minute. Afterwards, the column was washed twice, once with QC buffer and once with PE buffer. The DNA was eluted using 35  $\mu$ L of EB buffer. 3  $\mu$ L of elution product was used for quantification of DNA using a spectrophotometer (Nanoview). 5  $\mu$ L was loaded onto 0.8% agarose gel to confirm the size of purified product.

#### **2.2.1.4 Constructing the entry clone – BP Reaction**

Entry clones were prepared following the BP reaction protocol (Invitrogen). 50 fmol of PCR product and 100 ng of donor vector (pDONR201) were used to carry out the BP reaction. 2 µl of BP Clonase™ II enzyme mix were added to the reaction mixture followed by incubation at 25 °C for 5 hours; the reaction was stopped by adding 1 µl of Proteinase K and incubation at 37 °C for 10 minutes. The BP reaction was either stored at -20 °C or used for transformation of competent cells.

#### **2.2.1.5 Constructing the expression clone – LR reaction**

Expression clones were prepared following the LR reaction protocol (Invitrogen). The destination vector used was the plasmid pSD69, a construct containing the human PGK promoter, the Gateway attR cassette, the mouse PGK promoter and the puromycin acetyltransferase gene. 120 ng of destination vector pSD69 was combined either with 154 ng of entry clone containing CBX6, or 200 ng of entry clone containing CBX7 or 219 ng of entry clone containing CBX8. The BP reaction was carried out in 10 µl total volume, containing 2 µl of LR Clonase™ II enzyme mix. The samples were incubated at 25 °C for 4 hours and the reaction was stopped by adding 1 µl of Proteinase K and incubation at 37 °C for 10 minutes. The LR reaction was either stored at -20 °C or used for transformation of competent cells.

#### **2.2.1.6 Transformation of competent cells**

1 µl of each BP or LR reaction was used to transform 50 µl of One Shot® chemically competent *E. coli*. Competent cells plus DNA were incubated on ice for 30 minutes, followed by heat-shock at 42°C for 30 seconds. 250 µl of S.O.C.

medium was then added and incubated at 37°C for 1 hour with shaking. 50 µl and 100 µl of each transformation were plated onto selective plates and grown overnight at 37 °C. 100ng of pUC19 DNA was used as a control for transformation efficiency. The following day plates were checked for colonies. An average of 12 colonies per plates were picked and grown overnight in LB broth containing the appropriate antibiotic for selection.

#### **2.2.1.7 Extraction of plasmid DNA**

Spin miniprep kit (Qiagen, cat # 27104) was used for plasmid DNA extraction which involves an alkaline/ SDS procedure and the use of silica membrane columns that bind plasmid DNA. 3 mL of overnight bacteria culture was centrifuged at 13000 rpm for 5 minutes using a microcentrifuge. The media was aspirated and the bacteria pellet resuspended in 250 µL of resuspension buffer, containing RNase A, followed by 250 µl of Lysis buffer and gently mixed. After 5 minutes incubation at room temperature 250 µl of precipitation buffer was added and the samples were centrifuged at 13000 rpm for 10 minutes. The supernatant, containing the plasmid DNA, was then transferred to the silica membrane column and centrifuged for 30-60 minutes. In order to remove contaminants, the column was washed twice with washing buffer and the DNA was eluted in 50 µl of elution buffer. 3 µl of elution product was used for quantification of DNA using a spectrophotometer (Nanoview).

#### **2.2.1.8 Restriction enzyme digestion of plasmid DNA**

In order to identify the plasmid containing the correct insert, a restriction enzyme analysis was performed. 250 ng of plasmid DNA was digested in 20 µl total

volume reaction, containing 1X buffer, 1X BSA (when required) and 0.5 µl of restriction enzyme. After 1.5 hours of incubation at 37 °C, 5 µl of reaction was loaded onto a 1% agarose gel and fragments were separated by electrophoresis. The DNA fragments were visualized under transilluminator light and a digital image was captured (Syngene Genetools software).

### **2.2.1.9 DNA Sequencing**

600ng of plasmid DNA along with 10 µl of 3.2 µM primer was sent for sequencing to the DNA sequencing Services, University of Dundee. Samples were processed/ sequenced using Applied Biosystems Big-Dye version 3.1 on an Applied Biosystems model 3730 automated capillary DNA sequencer.

The primers sequences were as follows:

#### For the entry clone

- OXS4\_pENTR201seq\_forward:

5'-TCGCGTTAACGCTAGCATGGATC-3'

- OXS5\_pENTR201seq\_reverse:

5'-GTAACATCAGAGATTTTGAGACAC-3'

#### For the expression clone

- OSD48seq:

5'-CTGTGACCGAATCAC-3'

- OSD49seq:

5'-GCGTAAAAGGAGCAACATAG-3'

### **2.2.2 Large scale plasmid DNA extraction – Maxiprep**

EndoFree Plasmid Maxi Kit (Qiagen, cat # 12362) was used for large scale plasmid DNA extraction. 100 mL of overnight bacteria culture was centrifuged at 6000 x g for 15 minutes at 4°C using a Beckman J2-MC centrifuge. The media was aspirated and the bacteria pellet resuspended in 10 mL of resuspension buffer, containing Rnase A, followed by 10 ml of Lysis buffer and gently mixed. After 5 minutes incubation at room temperature 10 mL of pre-chilled neutralization solution was added and gently mixed. The lysate was then cleared using QIA filter Maxi Cartridge: lysate was added to the cartridge and incubated at room temperature for 10 minutes. The cap from the cartridge outlet nozzle was then removed, the plunger was inserted and the lysate was filtered in a clean 50 ml tube. 2.5 ml of Endotoxin removal buffer was added followed by 30 minutes incubation on ice. Meanwhile 10 ml of equilibrating solution was used to equilibrate the Qiagen-Tip (anion-exchange column where plasmid DNA selectively binds under appropriate low-salt and pH conditions). The clear lysate was poured into the equilibrated Qiagen-Tip added and allowed to enter the resin by gravity flow. In order to remove contaminants, the column was washed twice with wash buffer and the DNA was eluted in 15 ml of high salt elution buffer. DNA was then concentrated and desalted by isopropanol precipitation and collected by centrifugation; 10.5 ml of room temperature isopropanol was added to the DNA and centrifuged at 15000 x g for 30 minutes at 4 °C. The supernatant was then gently removed and the DNA pellet was washed with 5 mL of 70% ethanol and centrifuged at 15000 x g for 10 minutes. Pellet was air dried at room temperature for 15 minutes and resuspended in either 120 µl of buffer TE or 120 µl dH<sub>2</sub>O. 3 µl of elution product was used for quantification of DNA using a spectrophotometer (Nanoview).

### **2.2.3 Lentivirus production**

24 hours prior to transfection,  $4.0 \times 10^6$  293T cells were seeded in 10 cm dishes; Mirus TransIT®-LT1 transfection reagent (Cambridge Bioscience, cat # MIR 2300) was used for transient transfection of the cells, at a ratio 1:3 (DNA:LT1). On the day of transfection the growth media (DMEM, 10%FBS) was changed and the transfection mix was prepared as follows (see also table 2.1): for each plate 2.1 µg of VSV-G (pVF11), construct providing the viral coat, 6.3 µg of packaging construct (pVF16), and 6 to 10 µg of viral expression construct (depending on the size of the plasmid) were mixed together. In a separate tube an appropriate amount of Mirus LT1 reagent was gently mixed with 1.5 ml of serum free OPTIMEM and incubated at room temperature for 20 minutes. The DNA transfection mix was then added to the OPTIMEM-LT1 solution and incubated for 30 minutes at room temperature; the OPTIMEM-LT1-DNA solution was then added dropwise to the cells. The media was changed 6 hours later. 24 hours post-transfection the media was removed and replaced with 4 ml, for each plate, of fresh DMEM, 2% FBS). Media containing newly produced virus was collected at 48 and 72 hours post-transfection, polybrene (SIGMA, cat # H9268) at 8 µg/ml final concentration was added and filtered with 0.45 µm filter (Elkay UK Ltd., cat # E25-PV45-50S). A small amount of virus was kept at 4 °C for titration, while the rest was aliquoted into cryovials and stored at -80°C.

<b>Expression clone (E.C.)</b>	<b>Plates</b>	<b>pSD11 (ul)</b>	<b>pSD16 (ul)</b>	<b>E.C. (ul)</b>	<b>Mirus LT1 (ul)</b>	<b>DMEM (ml)</b>
pSD82 (ESR1)	1	2.1	6.3	7.8	48.5	1.5
pSD83 (hTERT)	1	2.1	6.3	21.3	52.6	1.5
pSD84 (BMI1)	1	2.1	6.3	7.1	46.6	1.5
pSD69-EZH2	1	2.1	6.3	13.5	49.5	1.5
pSD69-CBX6	1	2.1	6.3	17.0	47.2	1.5
pSD69-CBX7	1	2.1	6.3	16.8	46.0	1.5
pSD69-CBX8	1	2.1	6.3	7.3	47.0	1.5
pSD3 (GFP)	1	2.1	6.3	6.0	43.1	1.5
pGIPZmirEZH2 (17507)	1	2.1	6.3	11.7	53.6	1.5
pGIPZmircontrol	1	2.1	6.3	9.5	53.6	1.5

**Table 2.1** Transfection mixture components for lentivirus production.

#### **2.2.4 Lentiviral infection**

24 hours prior to infection, an appropriate number of cells were seeded in 10 cm dishes, usually  $5 \times 10^5$  cells. Vials containing lentivirus, stored at  $-80\text{ }^{\circ}\text{C}$ , were thawed at  $37\text{ }^{\circ}\text{C}$  and the media aspirated from the plates containing the cells and replaced with the lentivirus solution. After 4 to 6 hours of incubation at  $37\text{ }^{\circ}\text{C}$  the lentiviral solution was aspirated and replaced with fresh media. 48 hours post-infection an appropriate amount of antibiotic (depending on cell type) was used to start antibiotic selection.



### **2.2.5 Lentiviral titration**

24 h prior to infection cells were seeded in 6 wells plate ( $3 \times 10^4$  cells per well):

1. Positive control (no lentivirus, no puromycin)
2. Negative control (no lentivirus, puromycin)
3.  $10^{-3}$  dilution
4.  $10^{-2}$  dilution
5.  $10^{-1}$  dilution
6. Undiluted

On the day of infection a series of dilutions (from  $1 \times 10^{-1}$  to  $1 \times 10^{-3}$ ) were prepared using fresh media with 1X polybrene. Media was aspirated from the wells and replaced either with fresh media (wells number 1 and 2) or lentivirus dilution. Media was changed after 6 hours. Puromycin selection was started 2 days post infection. 48 hours post-puro treatment the selection was checked and once it was established which lentivirus dilution killed 100% of the cells, the titre was calculated as follows.

Titre (infectious particles/ml) =

number of cells at infection (Cells/ml) X dilution factor

### **2.2.6 Retrovirus production**

24 h prior transfection  $2.5 \times 10^6$  Phoenix A cells were seeded in 10 cm dishes; Mirus TransIT®-LT1 transfection reagent (Cambridge Bioscience, cat # MIR 2300) was used for transient transfection of the cells, at a ratio 1:3 (DNA:LT1). On the day of transfection the growth media (DMEM, 10%FBS) was changed and the

transfection mix was prepared as follow: for each plate an appropriate amount of Mirus LT1 reagent (three times the amount of DNA) was gently mixed with 1.5 ml of serum free OPTIMEM and incubate at room temperature for 20 minutes. 6 to 10 µg of retroviral construct (pBABE puro HRas - V12) was then added and gently mixed, followed by 30 minutes incubation at room temperature. The OPTIMEM-LT1-DNA solution was then added dropwise to the cells. 24 hours post-transfection the media was removed and replaced with 4 ml, for each plate, of fresh DMEM, 10% FBS. Media containing newly produced virus was collected at 48 and 72 hours post-transfection, polybrene (SIGMA, cat # H9268) at 8 µg/ml final concentration was added and the virus solution was filtered with 0.45 µm filter (FISHER, cat # FDR050-400U). A small amount of virus was kept at 4 °C for titration, while the rest was aliquoted into cryovials and stored at -80 °C.

### **2.2.7 Retroviral infection**

24 hours prior to infection, an appropriate number of cells were seeded in 10 cm dishes, usually  $5 \times 10^5$  cells. Vials containing retrovirus, stored at -80 °C, were thawed at 37 °C and the media aspirated from the plates containing the cells and replaced with the retrovirus solution. After 8 hours of incubation at 37 °C the retroviral solution was aspirated and replaced with fresh media. 48 hours post-infection an appropriate amount of antibiotic (depending on cell type) was used to start antibiotic selection.

## **2.2.8 Cell culture**

### **2.2.8.1 Culture of cell lines**

Breast cancer cell lines MDA-MB-231, T47-D, the immortalized line MCF10A and packaging cell lines 293T and Phoenix A were grown in media according to ATCC instructions. MCF10A cells were grown in DMEM/F12 media (Invitrogen) supplemented with 5% Horse serum (Invitrogen), 20 ng/ml human recombinant EGF (Sigma), 0.5 µg/ml Hydrocortisone (Sigma), 100 ng/ml Cholera toxin (Sigma), 10 µg/ml Bovine Insulin (Sigma) and 1% Penicillin/ Streptomycin (Invitrogen). MDA-MB-231 and T47-D cells were grown in RPMI1640 media supplemented with 10% Fetal Bovine Serum (Invitrogen) and 1% Penicillin/ Streptomycin (Invitrogen). HCC1937 cells were grown in RPMI1640 media supplemented with 20% Fetal Bovine Serum (Invitrogen) and 1% Penicillin/ Streptomycin (Invitrogen). 293T and Phoenix A cells were grown in DMEM media containing 10% Fetal Bovine Serum and 1% Penicillin/ Streptomycin (Invitrogen). B-42CP cells were grown in MEGM (Lonza, cat. Number CC3150) containing growth supplements. SNB19 were grown in DMEM media containing 10% Fetal Bovine Serum. All cell lines were routinely maintained at 37 °C in a humidified atmosphere in 5% CO<sub>2</sub> and passaged using 0.25% Trypsin-EDTA every 2-3 days, depending on cell type growth rate. Cells were counted using a haemocytometer.

### **2.2.8.2 Cell freezing and thawing**

Freezing: cell were suspended in freeze medium (growth media containing 20% FBS + 10% FBS (Sigma, cat # D2650)) and frozen at -80 °C using an isopropanol-filled cryo-freezing container (Nalgene). After 3 or 4 days cells were transferred to liquid nitrogen. Thawing: cells were warmed in a waterbath at 37 °C and immediately resuspended in 5 ml of appropriate medium, centrifuged at 1200

rpm for 3 min then plated and grown at 37 °C in 5% CO<sub>2</sub>. Medium was changed 24 hours later.

### **2.2.8.3 Puromycin kill curve**

1x10<sup>5</sup> cells per well were seeded in 6 wells plate with the appropriate growth media. The following day media was replaced with fresh growth media containing a range of antibiotic concentration, normally from 1.5 µg/ml to 4.0 µg/ml. Cells were monitored for about a week during which selective media was replaced every 2 days. The minimum antibiotic concentration to use was determined as the lowest concentration that kills 100% of cells.

### **2.2.8.4 Culture of primary mammary epithelial cells**

Reduction mammoplasty tissue was obtained from Ninewells hospital, Dundee upon examination by a clinical pathologist and release, by them, for research use. Patients were free from observable disease, with no breast cancer family history and younger than 45 years of age. Ethical approval was gained from both the Tayside tissue bank and University of St Andrews (TBR83, MD4357).

Primary human mammary epithelial cells (HMECs) and breast primary epithelial cells (BPECs) were prepared following established protocols (Duss et al., 2007 and Ince et al., 2007). Briefly, the reduction mammoplasty samples were minced in a sterile biosafety cabinet using sterile scalpel blades and digested overnight at 37°C in DMEM/F12 media supplemented with Collagenase A (Roche cat. # 1088793) at 1mg/mL final concentration. The resulting multicellular structures were processed either following Duss et al. protocol to produce human mammary epithelial cells HMEC, or Ince et al. protocol to produce breast primary epithelial cells BPEC.

- **Culture HMEC**

Duss et al.: two different epithelial cell fractions and one fibroblast fraction were separated, first epithelial cell fraction was obtained after 4 min centrifugation at 1400 rpm; the supernatant was then centrifuged for 4 min at 1800 rpm in order to obtain the second epithelial cell fraction, which is thought to contain progenitor cells. The supernatant obtained was then centrifuged at 2400 rpm for 4 min in order to obtain the fibroblast fraction. Each epithelial cell fraction was washed twice with warm PBS 2% FBS (Biosera, cat # S1810-500). Pellets were either aliquoted and froze down or processed to obtain single cells. Organoids were frozen in cryotubes using freezing medium (10% DMSO, 90% FBS). In order to obtain single cells organoids were resuspended in 4 ml of warm HMM (Human Mammosphere Medium): Hepes-buffered DMEM/F12 without phenol red supplemented with 20 ng/mL EGF, 1x B-27 and 1 nM  $\beta$ -oestradiol and transferred to 15 ml falcon tube. After 2 min centrifugation at 500 rpm, cell pellet was resuspended in 3 ml of Trypsin and pipetted against the tube wall for 2 min using a 5 ml pipette. Trypsin was then neutralized using 5 mL of PBS + 2% FBS and the cell mixture was centrifuged at 1400 rpm for 3 min. 3 ml of warm filtered Dispase (GIBCO cat # 17105-041) and 200  $\mu$ l of DNase I (SIGMA, cat. # D-5025-15KU) was used to resuspend the cells; cell suspension was passed through a 40  $\mu$ m cell strainer (VWR cat. # 734-0002) and transfer in to a new 15 ml falcon tube. Cells were centrifuged at 1400 rpm for 3 min and then plated onto Corning ULA (Ultra Low Attachment) plates (Fisher, cat # TKT523070M). Cells were passaged every 7 days.

- **Passaging HMECs**

Cell suspension containing HMECs was transferred to a 15 ml falcon tube, using a 5 ml pipette. Cells were separated from the media by centrifugation at 500 rpm for 30 sec; 0.5 ml of Trypsin EDTA at room temperature was used to resuspend the cells followed by 2 minutes incubation at room temperature. Cell suspension was pipetted against the tube wall for about one minute in order to obtain single cells. Trypsin was neutralized using 1 ml of PBS-2% FBS; after 1 min incubation at room temperature, 4 ml of sterile PBS was added followed by a centrifugation at 1400 rpm for 1 min. Cell pellet was resuspended in 5 ml of sterile PBS and re-centrifuged at 1400 rpm for 2.5 minutes; the supernatant was removed and cells were plated onto Corning ULA plate either using HMM (Human Mammosphere Medium) or WIT medium.

- **Culture BPEC**

Ince et al: the organoids were separated by centrifugation at 800 rpm for 5 min. and either cultured in a chemically defined media WIT (table 1) on BD Biosciences Primaria plasticware (VWR, cat # 734-0072), or aliquoted in cryotubes using freezing medium (10% DMSO, 90% FBS) and frozen down. Within 4 to 5 days colonies of BPEC started to grow from the organoids. Cells were passaged every 4 to 5 days. BPEC were cultured in p-WIT medium (table 1) after lentiviral infection.

- **Passaging BPEC**

Medium was aspirated from the plates and cells were incubated with 3 ml of 0.15% Trypsin at 37°C; 20% serum containing medium was used to neutralize

trypsin. Cell suspension was then centrifuged at 800 rpm for 5 min; cells were resuspended using WIT medium and plated onto Primaria plasticware (BD Biosciences). Medium was changed after 12 hours.

<b>Additive</b>	<b>Source and Catalogue number</b>	<b>Final conc.</b>
F12 Ham, w L-glut. bicarb.	SIGMA N6658	1x
M199	SIGMA M4530	1x
HEPES pH 7.4	Invitrogen I5630-056	10 mM
Glutamine	SIGMA G7513	2 mM
Insulin solution	SIGMA I9278	10 µg/ml/ <b>20 µg/ml</b>
EGF	Invitrogen 132247-051	0.5 ng/ml/ <b>10 ng/ml</b>
Hydrocortisone	SIGMA H4001	0.5 ng/ml/ <b>0.5 µg/ml</b>
Apo-transferrin	SIGMA T2036	10 µg/ml
3,3',5-Triiodo-L-thyronine	SIGMA T6397	0.2 pg/ml
O-Phosphoethanolamine	SIGMA P0503	5 µg/ml
Selenious acid	SIGMA S9133	8 ng/ml
17-beta-estradiol	SIGMA E2758	0.5 ng/ml
Linoleic acid	SIGMA L1012	5 µg/ml
All-trans retinoic acid	SIGMA R2625	0.025 µg/ml
Hypoxanthine Na	SIGMA H9636	1.75 µg/ml
(+/-)-alpha-Lipoic Acid	SIGMA T1395	0.05 µg/ml
Cholesterol	SIGMA C3045	0.05 µg/ml
Glutathione	SIGMA G2140	0.012 µg/ml
Xanthine sodium	SIGMA X3627	0.085 µg/ml
L-Ascorbic Acid	SIGMA A4544	0.012 µg/ml
(+/-)-alpha-tocopherol phosphate	SIGMA T2020	0.003 µg/ml



Calciferol (Vit D <sub>2</sub> )/ Ergocalciferol	SIGMA E9007	0.025 µg/ml
Choline chloride	SIGMA C7527	3.5 µg/ml
Folic acid	SIGMA F8758	0.33 µg/ml
Vitamin B <sub>12</sub>	SIGMA V6629	0.35 µg/ml
Thiamine hydrochloride (Vitamin B <sub>1</sub> )	SIGMA T1270	0.08 µg/ml
myo-Inositol	SIGMA I7508	4.5 µg/ml
Uracil	SIGMA U1128	0.075 µg/ml
D(-)Ribose	SIGMA R9629	0.125 µg/ml
Para-aminobenzoic acid	SIGMA A9878	0.012 µg/ml
Bovine serum albumin	SIGMA A8412	1.25 mg/ml
Cholera toxin	SIGMA C8052	25 ng/ml/ <b>100 ng/ml</b>

**Table 2.2:** Basic WIT medium composition (Ince et al., Cancer Cell 2007 12, 160-170). Concentrations in bold are for primary BPEC culture-WIT (pWIT): basic WIT medium + insulin (20 µg/ml) + EGF (10 ng/ml) + hydrocortisone (0.5 µg/ml) + cholera toxin (100 ng/ml).

## 2.2.9 Western blotting

### 2.2.9.1 SDS-Polyacrylamide gel electrophoresis (PAGE)

Protein lysates were prepared from cells at 70-80% confluency. The cells were washed once with cold PBS and then extracted using lysis buffer containing 1% NP-40, 1% SDS, 1% Na Deoxycholate, 1 mM EDTA, 150 mM NaCl, 10 mM Tris pH 8.0 and 1X complete protease inhibitor (Roche, cat # 11697498001). Protein

concentrations were determined using the Pierce protein assay kit (Thermo Scientific, cat # 23225) and compared to a BSA standard. 30 µg of total lysates, 5 µl of protein marker (GE Healthcare, cat # RPN 800E) and a positive control, normally HeLa nuclear extract (Millipore, cat # 12-309), were loaded for each lane along with loading buffer (4% SDS, 40% glycerol, 0.05% bromophenol blue, 4 mM DDT, 0.05 M Tris pH 6.8). A 10 % SDS acrylamide resolving gel and a 3.4 % top stacking gel was prepared (table 2) and allowed to set at room temperature for about 20 minutes; samples were denatured at 100 °C for 5 minutes and loaded onto the gel. Electrophoresis was carried out using the Mini-PROTEAN Tetra Electrophoresis System (Bio-Rad laboratories, cat # 165-8003) in running buffer (0.25 M Tris-Base, 1.9 M Glycine and 1% SDS) at 100V for 10 minutes, then at 80V for 1.5 hours or until the dye front reached the bottom of the gel.

### **2.2.9.2 Transfer of proteins to nitrocellulose membrane**

The gel containing the resolved proteins was then transferred to a polyvinylidene difluoride membrane (PVDF) membrane, (GE healthcare cat. # RPN303-F) using a biorad Mini-PROTEAN trans blotting system (Bio-Rad laboratories, cat # 165-8003) in transfer buffer (0.25 M Tris-Base, 0.19 M Glycine, 0.05% SDS and 20% Methanol) at 90V for 45 minutes.

### **2.2.9.3 Western blot analysis**

Membranes were briefly washed in PBS-T (PBS containing 0.2 % Tween-20) then blocked in 5 % Milk in PBS-T (PBS-T + 5% w/v skimmed milk powder) for 1 hour at room temperature. Three washes in PBS-T of 5 minutes each were carried out before the overnight incubation with the appropriate primary antibody (Table 2.4). Membranes were subsequently washed 3 times with PBS-T for 5 minutes and probed with the appropriate secondary antibody (Table 2.4) for 1 hour. A chemiluminescent

method (ECL, Pierce cat. # 34080) was used for secondary antibodies detection and an Image Reader LAS-3000 system was used for acquiring digital images of blots. Densitometric analysis was carried out using ImageJ software.

10% SDS Resolving Gel (5 ml)		Stacking gel (2 ml)	
30% acrylamide/Bisacrylamide	1.6 ml	30% acrylamide/Bisacrylamide	0.825 ml
2 M Tris-HCl pH 8.8	0.9 ml	1 M Tris-HCl pH 6.8	0.625 ml
10% SDS	0.05 ml	10% SDS	0.05 ml
Water	2.4 ml	Water	0.445 ml
10% APS	50 $\mu$ l	10% APS	50 $\mu$ l
TEMED	5 $\mu$ l	TEMED	5 $\mu$ l

**Table 2.3:** SDS-PAGE resolving gel and stacking gel components. APS: Ammonium persulfate; TEMED: tetramethylethylenediamine.

<b>Primary Antibodies</b>			
<b>Name</b>	<b>Species</b>	<b>Concentration</b>	<b>Source ant cat. number</b>
Anti-EZH2	Rabbit	1:1000 (5% BSA in PBS-T)	NEB, 4905
Anti-CBX8	Rabbit	1:500 (5% Milk in PBS-T)	Abgent, AP2515b
Anti-CBX7	Mouse	1:500 (5% Milk in PBS-T)	Abnova, H00023492-B01P
Anti-CBX6	Rabbit	1:200 (5% Milk in PBS-T)	Aviva SystemBiology, ARP39074_T100
Anti-HRas	Rabbit	1:200 (5% Milk in PBS-T)	Santa Cruz, sc-520
Anti-BMI1	Mouse	1:1000 (5% Milk in PBS-T)	Millipore, 05-637
Anti-p16	Rabbit	1:500 (5% Milk in PBS-T)	Millipore, 04-239
Anti-BRCA1 (D9)	Mouse	1:100 (5% Milk in PBS-T)	Santa Cruz, sc-6954
Anti-BRCA1 (M13)	Mouse	1:100 (5% Milk in PBS-T)	Calbiochem, OP-93
Anti-BRCA1p	Rabbit	1:2500 (5% Milk in PBS-T)	AbCam, ab-2838
Anti-hTERT	Rabbit	1:500 (5% Milk in PBS-T)	Tebu Bio Ltd, 039600-401-252
Anti-ER	Rabbit	1:500 (5% Milk in PBS-T)	Thermo Fisher, RM-9101-SO
Anti- $\beta$ -Actin	Mouse	1:20000 (5% Milk in PBS-T)	Sigma, A1978
Anti-GAPDH	Mouse	1:20000 (5% Milk in PBS-T)	Sigma, G8795
<b>Secondary Antibodies</b>			
HRP anti-mouse	Goat	1:500 (5% Milk in PBS-T)	Jackson, 115035062
HRP anti rabbit	Goat	1:500 (5% Milk in PBS-T)	Jackson, 111035045

**Table 2.4:** List of primary and secondary antibodies used for western blot analysis.

### **2.2.10 Determining antibody specificity using a blocking peptide**

When non-specific signal was detected upon western blotting, a blocking peptide was used to determine antibody specificity. Two identical SDS-PAGE gels were run and transferred to 2 separate PVDF membranes. Then two different primary antibody solutions were prepared: one containing only the antibody at the established working dilution in 5% milk PBS-T; the second containing the antibody at the established working dilution plus the blocking peptide at a final concentration 4 to 10 times the antibody concentration in 5% milk PBS-T. The two solutions were incubated for 8 hours at 4°C before they were used for the overnight incubation of the membranes. The detection was carried out as usual. The signal which diminishes in the presence of the blocking peptide is the one specific to the antibody.

### **2.2.11 Analysing cell proliferation**

Cells were seeded either in 6 wells plates at  $7 \times 10^4$  cells per well or 10 cm dishes at  $5 \times 10^5$  cells per dish and counted every 24 hours for 6 days, using a haemocytometer or using the electronic Beckman Coulter Particles Counter Z1. The results were then plotted on a graph as the number of cells vs. time. Each data point was the average of 3 counts.

### **2.2.12 Migration Assay**

Cells were trypsinized, counted and resuspended in appropriate media: MCF10A cells were resuspended in serum free and EGF free growth media, other cell lines were resuspended in serum free growth media. Cell suspension was normally between  $5.0 \times 10^4$  and  $1.4 \times 10^5$ . Polyethylene terephthalate (PET)

membranes with 8  $\mu\text{m}$  pores (VWR, cat # 734-0038) were used for this experiment; 0.5 ml aliquots of cells suspension were added to the top chamber. The chamber was then put into 24 well plate, each well containing 0.5 ml regular growth media. After 18 – 24 hours, the top side of the insert membrane was cleaned several times using a cotton swab and 1X PBS washes. The bottom side of the chamber was stained by using 0.1% crystal violet solution in PBS, 20% ethanol. Cells were visualized and counted using a regular inverted microscope (Zeiss, Axiovert 40 CFL).

### **2.2.13 Colony formation in soft agar**

For the bottom agar layer, 1% Agarose in ddH<sub>2</sub>O was prepared and autoclaved; the solution was let cool down to 40 °C in a water bath, while a 2X growth media was being warmed up to 40 °C. Equal volumes of the two solutions were mixed together to give 0.5% agar + 1X DMEM/F12; 2 mL of mixture was pour into each well of a 6 wells plate and allowed to set. The plates were either stored at 4 °C for up to one week or used for the following step. For the top agar layer, 0.7% low melting Agarose in ddH<sub>2</sub>O was prepared and autoclaved; the solution was let cool down to 40 °C in a water bath, while a 2X growth media was being warmed up to 40 °C. Cells were trypsinized, counted and resuspended in specific media at  $2.0 \times 10^5$  cells per mL. 0.1 ml of cell suspension was then gently mixed with 3ml 2X growth media and 3ml 0.7% low melting agar, 1.5ml of the mixture was added to each replicate well (normally in triplicate) and allowed to set. 2 ml of growth media was added to each well and plates were transferred to a 37 °C incubator for 21 days, during which the media was changed every 2 days. After 21 days, plates were stained with 0.1% INT (Sigma cat # I7375). Colonies were visualized and counted using an

inverted microscope (Zeiss, Axiovert 40 CFL) and digital images were acquired using Axiovision imaging System.

#### **2.2.14 Immunofluorescent Imaging**

Cells were plated on 24 well Primaria plasticware plates (BD Biosciences) and grown for 24 hours at 37 °C in 5% CO<sub>2</sub>. After 24 hours cells were washed three times with cold PBS and then fixed for 10 minutes with neutral buffered formalin (NEB, 3.7% Formaldehyde, 1.5% MethylAlcohol, 1.0% Sodium phosphate). After 10 minutes, the cells were exposed to cold 0.5% Triton X in PBS over ice for 10 minute. Cells were then washed 3 times with PBS followed by block with 5% bovine serum albumin (BSA) in PBS at room temperature for 20 minutes. After the blocking stage, BSA was removed and cells were washed with PBS before incubation with primary antibody for two hours at room temperature. The primary antibodies used are listed in table 2.5. Cell were subsequently washed 5 times for 2 minute with PBS, and then incubated with the appropriate secondary antibody for 1 hour at room temperature, protected from the light. Cells were washed 4 times for two minutes with PBS, before adding Vectashield with DAPI (Vector Laboratories). Cells were viewed under 10 x magnification using a fluorescence microscope. Slides were visually analysed and classified either as positive (presence of stain) or negative (absense of stain).

Name	Concentration	Source and cat. number
CK5	1:50	Abcam, ab53121
CK14	1:50	ThermoScientific, MS-115-PO
CK18	1:50	ThermoScientific, MS-142-PO
CK19	1:50	ThermoScientific, MS-198-PO

**Table 2.5:** List of primary antibodies used for immunofluorescence analysis.

### 2.2.15 Analysis of cell viability – MTT assay

5000 cells were seeded in triplicate on 96 well Primaria plasticware plates (BD Biosciences) and grown at 37 °C in 5% CO<sub>2</sub>. 20µl of 5mg/ml MTT was added to each well every 24 hours and incubated at 37 °C for 3.5 hours. After incubation with MTT, the growth media was removed and 150µl of DMSO was added to each well. Plates were incubated at room temperature, protected from the light, for 15 minutes. The absorbance at 570, with a reference filter at 620, was then read using the Dynex MRX microplate reader (Dinex Technologies) and plotted on a graph as the absorbance vs. time.



### 2.2.16 Scratch Assay

Cells were seeded on 10 cm plates and allowed to reach confluency. Using a p500 or a p200 pipet tip, the cell monolayer was scraped in a straight line to create a scratch. Cells were washed twice with 1 ml of sterile PBS to remove debris. The wound edges were imaged using Axiovision imaging System (day 0). The area of the scratch imaged was marked on the outer bottom of the dish with an ultrafine marker. The cells were then incubated at 37 °C for 24 hours. Cells were periodically checked during the 24 hours. After 24 hours a second image of the marked area of the scratch was acquired using Axiovision imaging System (day 1). The size of the scratch was evaluated using the software ImageJ (<http://rsbweb.nih.gov/ij>), as described elsewhere ([www.le.ac.uk/biochem/microscopy/wound-healing-assay.html](http://www.le.ac.uk/biochem/microscopy/wound-healing-assay.html)). Briefly, the images acquired (day 0 and day 1) were converted in 8-bit mode and opened with imagej program. The image scale was setup to pixel and the size values were set up 0 -1.0 (in a scale between  $1 \times 10^5$  and  $5 \times 10^7$ ). The area measurements were made using “analyze particle” mode of the software. The measurements obtained were then exported into excel file. Cell migration was calculated using the following formula: **(Pre-migration area – Migration area)/Pre-migration area X 100** and represented in a graph as percent of cell migration. The “pre-migration area” is the area free of cells at time zero, while the “migration area” is the area free of cells at day one or at 14 hours.

### **3 CHAPTER3: INVESTIGATING THE EFFECT OF ABROGATED EZH2 EXPRESSION IN BREAST CANCER**

#### **3.1 Introduction**

The polycomb group protein EZH2 is the catalytically active component of Polycomb Repressive Complex 2 (PRC2) (Cao et al. 2002; Czermin et al. 2002; Schneider et al. 2002; Simon et al. 2008) and it is over-expressed in several types of human cancers, including pancreatic (Toll et al. 2010), prostate (Varambally et al. 2002), bladder (Arisan et al. 2005; Weikert et al. 2005), gastric (Matsukawa et al. 2006), lung (Watanabe et al. 2008), liver (Sudo et al. 2005) and breast (Kleer et al. 2003). Abnormal levels of EZH2 are already present in precancerous breast lesions and EZH2 expression levels progressively increase from DCIS to metastatic breast tumours (Kleer et al. 2003) making EZH2 a good marker of aggressiveness in breast cancer and a good candidate for a therapeutic target. In breast cancer EZH2 overexpression correlates positively with aggressiveness, bad prognosis, metastasis, resistance to Paclitaxel and ER-negativity (Bachmann et al. 2006; Collett et al. 2006; Gonzalez et al. 2009; Kleer et al. 2003; Reijm et al. 2010). ER status is one of the most important prognostic factors in breast cancer (Knight et al. 1977; Rakha et al. 2007a; Swain et al. 2004) and patients with ER negative breast cancers have poor outcome and lower overall survival compared to patients with ER positive breast cancer. EZH2 over-expression might be one of the factors contributing to the poor outcome and prognosis of ER negative breast cancer patients. In addition, it might represent a good target for the development of a novel strategy for basal breast cancer treatment.

The aim of this chapter was to investigate the effect of EZH2 down regulation in breast cancer cell lines. EZH2 was knocked down in two breast cancer cell lines,

HCC1937 (Coene et al. 2011; Gazdar et al. 1998; Tomlinson et al. 1998) and MDA-MB-231 (Cailleau et al. 1974; Mladkova et al. 2010). Both cell lines are highly aggressive and ER $\alpha$  negative but they have different level of expression of EZH2 (Neve et al. 2006). The effect of EZH2 knockdown on cell proliferation, migration and anchorage-independent growth was then tested in both breast cancer cell lines.

### **3.2 EZH2 expression in breast cancer cell lines**

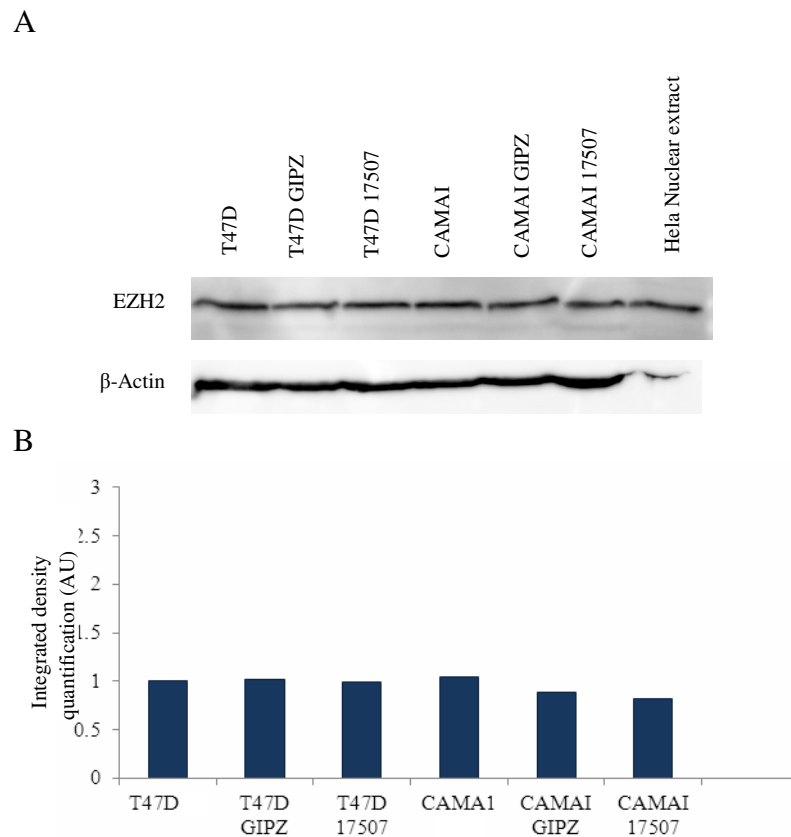
In order to identify breast cancer cell lines over-expressing EZH2, the transcription profiles of a collection of breast cancer cell lines analysed by Neve et al. were used (<http://www.cell.com/cancer-cell/supplemental/S1535-6108%2806%2900314-X>). See also appendix A). The probe ID associated with EZH2 “203358\_s\_at” was identified and the expression value of each cell line was annotated. The relative expression of EZH2 was calculated relative to the cell line with the lowest expression level of EZH2, SUM52PE (Table 3.1).

Cell lines with high level of EZH2 were called “EZH2-High” and cell lines with low level of EZH2 were called “EZH2-low”. T47D and HCC1937 (ER positive and ER negative respectively) were selected within the “EZH2-low” group (first 15 in table 3.1) and MDA-MB-231 and CAMA1 (ER negative and ER positive respectively) were selected within the “EZH2-High” group (last 15 in table 3.1).

Cell line	203358_s_at	Relative expression	Cell line	203358_s_at	Relative expression
SUM52PE	4.5082	1	HCC1008	6.4767	1.43664877
SUM185PE	5.1597	1.14451444	SUM190PT	6.5029	1.44246041
UACC812	5.1968	1.15274389	SUM1315	6.526	1.4475844
HCC38	5.6466	1.25251763	MDAMB415	6.5436	1.4514884
MDAMB435	5.7264	1.27021871	SUM159PT	6.5655	1.45634621
ZR751	5.7307	1.27117253	MCF7	6.5875	1.46122621
HCC1007	5.7875	1.28377179	LY2	6.5997	1.46393239
HCC1500	5.8376	1.29488488	HCC1143	6.636	1.47198438
SUM149PT	5.9101	1.31096668	HCC202	6.6486	1.47477929
MDAMB157	5.9424	1.3181314	AU565	6.6713	1.47981456
<b>T47D</b>	5.9634	<b>1.32278958</b>	BT20	6.6773	1.48114547
ZR7530	5.9984	1.33055321	BT483	6.7528	1.49789273
SKBR3	6.0059	1.33221685	HCC1599	6.808	1.51013708
SUM44PE	6.0907	1.35102702	HCC2185	6.8098	1.51053636
<b>HCC1937</b>	6.0917	<b>1.35124884</b>	BT474	6.8147	1.51162326
MDAMB175	6.1376	1.36143028	MCF12A	6.9434	1.54017124
MDAMB361	6.188	1.37260991	HCC3153	6.9493	1.54147997
600MPE	6.1922	1.37354155	MCF10A	6.9494	1.54150215
HCC1428	6.1947	1.37409609	MDAMB134	6.9647	1.54489597
HCC1954	6.2031	1.37595936	ZR75B	7.0262	1.55853778
SUM225CWN	6.2155	1.37870991	HCC1569	7.0909	1.5728894
HS578T	6.3218	1.40228916	DU4475	7.1831	1.59334102
BT549	6.4114	1.42216406	<b>CAMA1</b>	7.4147	<b>1.64471408</b>
HCC2157	6.42	1.42407169	HCC70	7.4838	1.6600417
MDAMB436	6.4424	1.42904042	MDAMB468	7.5411	1.67275187
MDAMB453	6.4659	1.43425314	<b>MDAMB231</b>	7.6266	<b>1.69171732</b>
HBL100	6.4747	1.43620514	HCC1187	8.1892	1.81651213

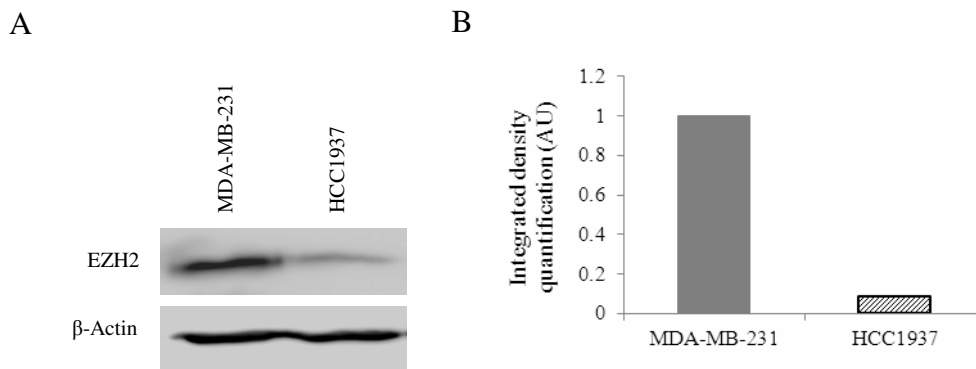
**Table 3.1:** EZH2 expression level in breast cancer cell lines used in Neve et al. study (2006). “203358\_s\_at” represents the Affymetrix probe set associated with EZH2 mRNA and values are represented in Log2 after Robust Multichip Average (RMA). EZH2 relative expression was calculated relative to SUM52PE cell line. Cells lines in bold were used in the experiments in this chapter.

Short hairpin RNA (shRNA) targeting human EZH2 and a second generation lentiviral system was used to knockdown EZH2 (section 2.2.3 and 2.2.4). EZH2 expression was not significantly reduced in both ER positive cell lines, T47D and CAMAI (Figure 3.1), while it was significantly reduced in both ER negative cell lines (Figure 3.3 and 3.8). Therefore further experiments were performed only on HCC1937 and MDA-MB-231 cells.



**Figure 3.1:** EZH2 knockdown in T47D cells and CAMAI cells. Cells were infected using lentiviral particles carrying either the shRNA oligo targeting EZH2 or the GIPZ shRNA control. The HeLa nuclear extract was used as a positive control. Representative image and graph of western blot analysis performed three times. **A.** Infected cells were harvested five days after puromycin selection. Extracted proteins were resolved by 10% SDS-PAGE and membrane was probed with the indicated antibodies.  $\beta$ -Actin was used as a loading control. **B.** Results obtained after integrated density quantification of A using ImageJ software (measurements expressed in arbitrary units). All values were normalized against  $\beta$ -Actin.

In order to confirm and compare the level of EZH2 expression in HCC1937 and MDA-MB-231 cell lines, western blot analysis was performed. This confirmed that the level of protein expression of EZH2 in MDA-MB-231 cells is higher compared to the level of expression of EZH2 in HCC1937 cells (Figure 3.2).



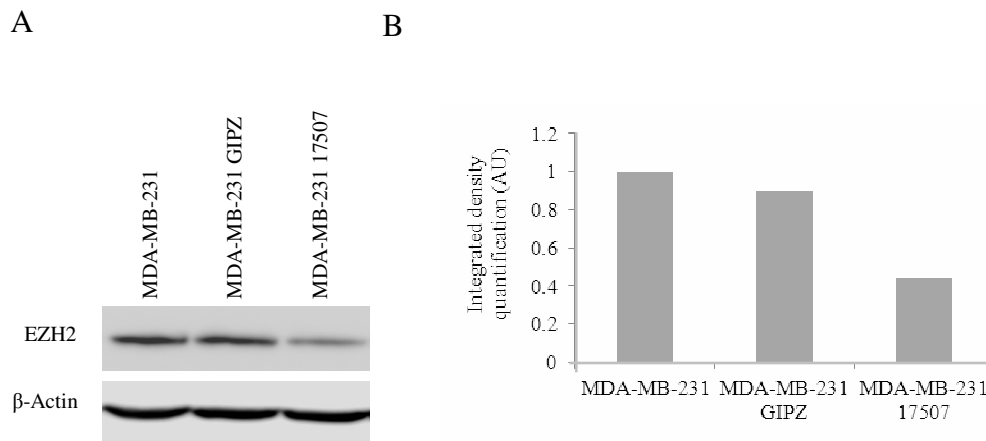
**Figure 3.2:** EZH2 expression level in MDA-MB-231 cells and HCC1937 cells. Representative image and graph of western blot analysis. **A.** Extracted proteins were resolved by 10% SDS-PAGE and membrane was probed with the indicated antibodies.  $\beta$ -Actin was used as a loading control. **B.** Results obtained after integrated density quantification of A using ImageJ software (measurements expressed in arbitrary units). All values have been normalized against  $\beta$ -Actin.

### 3.3 EZH2 Knockdown in MDA-MB-231 breast cancer cells

EZH2 knockdown in MDA-MB-231 cells was performed using shRNA and a second generation lentiviral system (section 2.2.3 and 2.2.4). Briefly, 293T packaging cells were used for production of lentivirus particles. Cells were transfected with the required amount of packaging constructs and viral expression construct (V2LHS\_17507 targeting EZH2) using Mirus *TransIT*<sup>®</sup>-LT1 transfection reagent. GIPZ scrambled shRNA was used as negative control for lentiviral infection. Only batches containing infectious particles between  $10^7$  and  $10^8$  per ml were used for MDA-MB-231 infection, which was carried out as described in materials and methods (section 2.2.4). Four days after infection, MDA-MB-231 cells were selected using 4.5 $\mu$ g/ml of puromycin (determined by puromycin killing curve,

see Section 2.2.8.3). Cells infected with lentivirus containing V2LHS-17507 shRNA targeting EZH2 were called MDA-MB-231 17507, while cells infected with lentivirus containing GIPZ control were called MDA-MB-231 GIPZ.

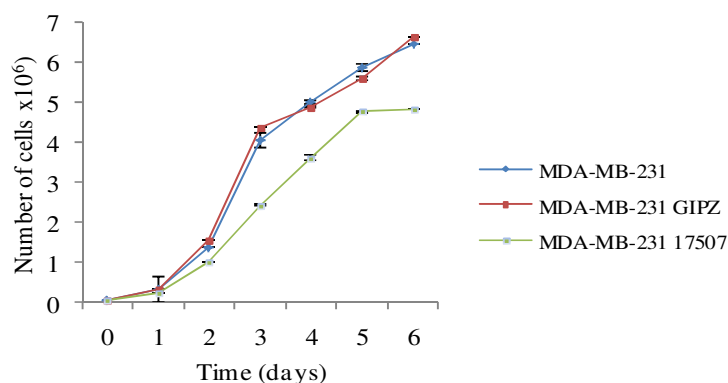
To confirm the reduced expression of EZH2 protein in MDA-MB-231 17507, western blot analysis was performed (Figure 3.3). Total protein extracted from non-infected MDA-MB-231 cells, MDA-MB-231 17507 cells and MDA-MB-231 GIPZ cells were analyzed. For each sample, 30  $\mu$ g of proteins were loaded onto a 10% SDS acrylamide resolving gel and western blot analysis was performed as described in materials and methods (section 2.2.9.1 – 2.2.9.3). Western blot analysis showed a significant decrease of EZH2 protein expression in MDA-MB-231 17507 cells compared to non-infected MDA-MB-231 cells and MDA-MB-231 GIPZ cells (Figure 3.3).



**Figure 3.3:** EZH2 knockdown in MDA-MB-231 cells. Cells were infected using lentiviral particles carrying either the shRNA oligo targeting EZH2 or the GIPZ shRNA control. Representative image and graph of western blot analysis. **A.** Infected cells were harvested five days after puromycin selection. Extracted proteins were resolved by 10% SDS-PAGE and membrane was probed with the indicated antibodies.  $\beta$ -Actin was used as a loading control. **B.** Results obtained after integrated density quantification of A using the software ImageJ (measurements expressed in arbitrary units). All values were normalized against  $\beta$ -Actin.

### 3.3.1 Effect of EZH2 knockdown on MDA-MB-231 cell proliferation

Growth curve analysis was performed in order to test whether EZH2 knockdown in MDA-MB-231 cells has any effect on cell proliferation (Figure 3.4). Non-infected MDA-MB-231 cells, MDA-MB-231 GIPZ and MDA-MB-231 17507 cells were seeded in 10 cm plates, starting with  $4.0 \times 10^4$  cells. Cells were trypsinized and counted, using Beckman Coulter Particles Counter Z1, every 48 hours. MDA-MB-231 17507 cells showed a much slower proliferation rate compared to non-infected cells and MDA-MB-231 GIPZ cells. EZH2 knockdown resulted in a doubling time increase of about 12 hours. Cells with reduced EZH2 expression, in fact, showed a doubling time of 36 hours while non-infected cells and the negative control showed a doubling time of less than 24 hours (Figure 3.4 Day 2 to day 3 interval). A clear difference in proliferation between MDA-MB-231 17507 cells and, either, non-infected MDA-MB-231 cells or MDA-MB-231 GIPZ cells was observed over the six days. These results agree with those reported by Gonzalez et al. 2009, that EZH2 knockdown decreases MDA-MB-231 cell proliferation.

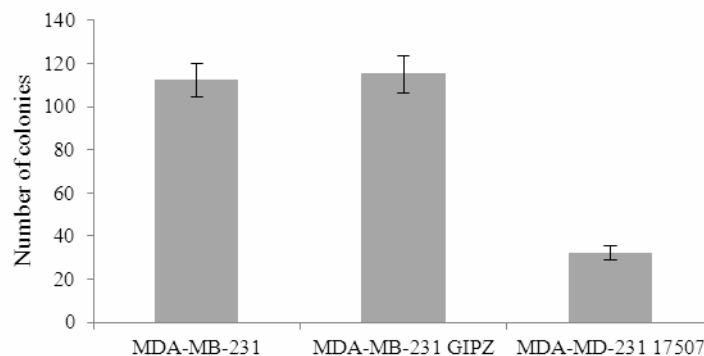


**Figure 3.4:** The effect of EZH2 knockdown on the growth rate of MDA-MB-231 cells. Representative graph of MDA-MB-231 cells growth rate. Cells were infected using lentiviral particles carrying either the shRNA oligo targeting EZH2 or the GIPZ shRNA control. Five days after puromycin selection,  $4.0 \times 10^4$  cells were plated in 10 cm plates. Cells were counted every 48 hours. The experiment was performed three times in triplicate ( $n=9$ ; error bars  $\pm$ SEM). See appendix A for raw data.



### 3.3.2 Effect of EZH2 knockdown on MDA-MB-231 anchorage-independent growth

To determine whether EZH2 knockdown reduces anchorage-independent growth of the highly malignant MDA-MB-231 cells, a colony formation in soft agar assay was performed (Figure 3.5). MDA-MB-231 cells, MDA-MB-231 GIPZ cells and MDA-MB-231 17507 cells were tested in triplicate (section 2.2.13). For each replicate, 5000 cells were used and the cells were grown at 37 °C for 21 days. After 21 days, colonies were counted. Non-infected MDA-MB-231 cells, as well as MDA-MB-231 GIPZ cells and MDA-MB-231 17507 cells formed colonies in soft agar (Figure 3.5).



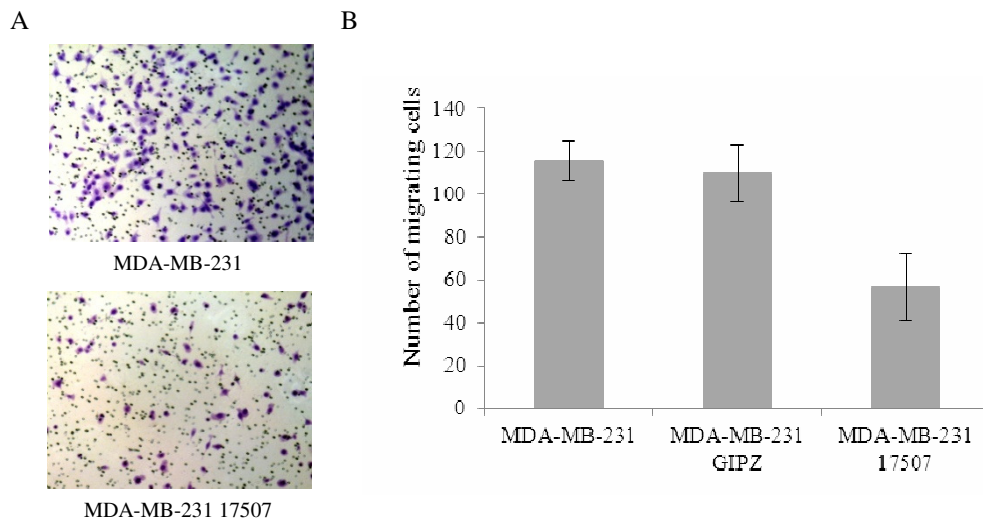
**Figure 3.5:** The effect of EZH2 knockdown on anchorage-independent growth of MDA-MB-231 cells. Cells were infected using lentiviral particles carrying either the shRNA oligo targeting EZH2 or the GIPZ shRNA control. Cells were grown for 21 days and colonies were stained with INT. The graph is representative of an experiment performed three times in triplicate (n=9; error bars  $\pm$ SEM). See appendix A for raw data.

The number of colonies formed by MDA-MB-231 17507 was significantly lower compared to non-infected cells and MDA-MB-231 GIPZ cells (an average of 25 colonies for MDA-MB-231 17507 cells vs an average of 110 colonies for both non-infected and MDA-MB-231 GIPZ cells). The results obtained showed that EZH2 knockdown in MDA-MB-231 breast cancer cells reduces their anchorage-independent growth.

### **3.3.3 Effect of EZH2 knockdown on MDA-MB-231 cell migration**

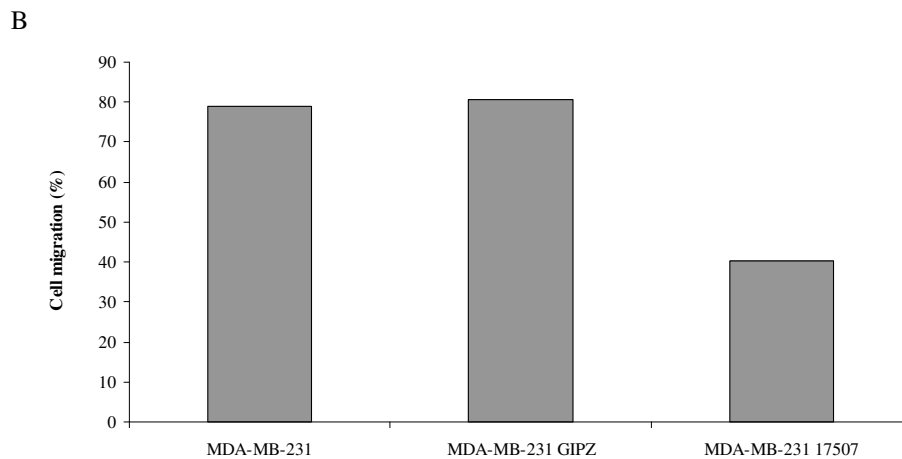
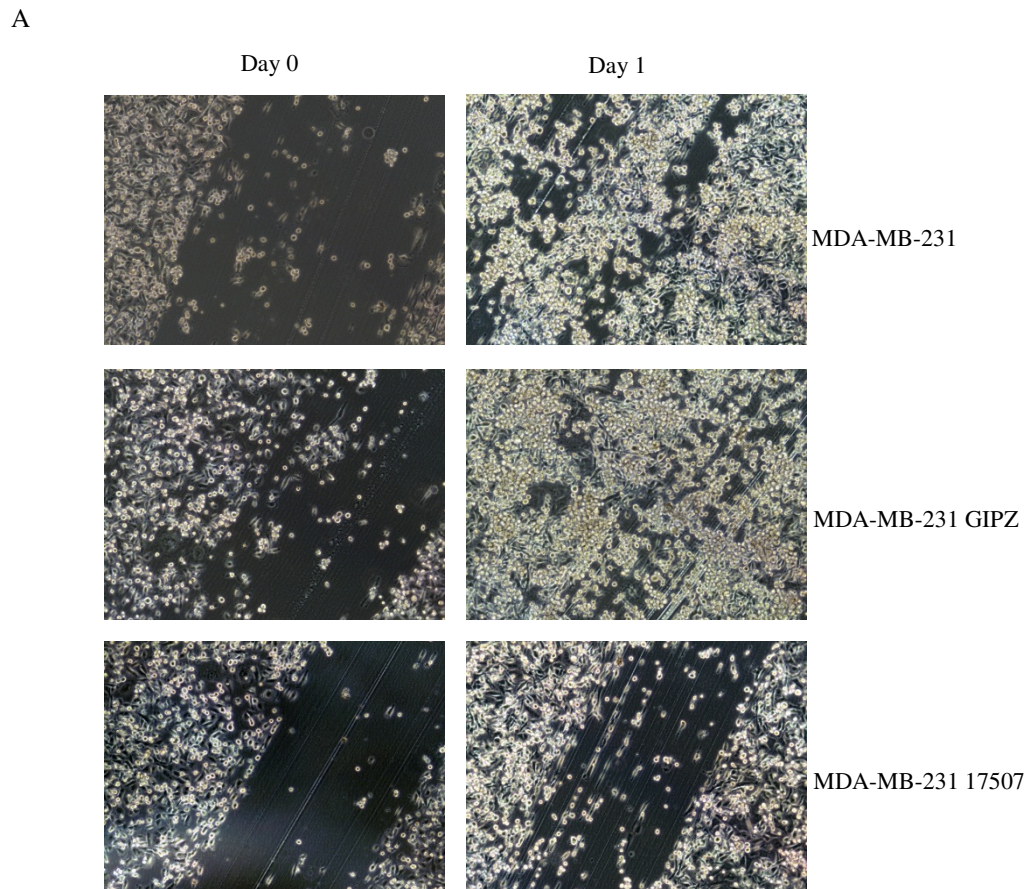
MDA-MB-231 cells are highly migratory cells (Mladkova et al. 2010; Neve et al. 2006; Wang et al. 2007), The ability of EZH2 knockdown to reduce MDA-MB-231 cell migration was tested using two different assays: the transwell Boyden chamber assay (Chen 2005; Li et al. 1999) and the scratch assay (Liang et al. 2007) (Section 2.2.12 and 2.2.16).

For the transwell Boyden chamber assay, non-infected MDA-MB-231 cells, MDA-MB-231 GIPZ cells and MDA-MB-231 17507 cells were trypsinised and separately re-suspended in serum free growth media.  $2.5 \times 10^4$  cells were added to the top of each PET membrane (section 2.2.12). After 18-24 hours, three randomly selected fields in the central part of the chamber were chosen and the number of migrating cells was counted. The stained cells which were often observed in the peripheral area of the chamber were considered to be background noise and only the central part of the chamber was taken into consideration (Figure 3.6A). For each cell type the experiment was performed in triplicate and a total of 9 counts were made (3 counts for each chamber) which were then averaged in order to give an estimation of the number of migrating cells. The number of migratory cells for non-infected MDA-MB-231 and MDA-MB-231 GIPZ was significantly higher compared to the number of migratory cells for MDA-MB-231 17507 (Figure 3.6 B). An average of 110 migrated cells was counted for non-infected MDA-MB-231 and MDA-MB-231 GIPZ cells *vs.* an average of 50 migrating cells for MDA-MB-231 17507. The results obtained showed that EZH2 knockdown reduces MDA-MB-231 migration using the Boyden chamber assay.



**Figure 3.6:** The effect of EZH2 knockdown on migration of MDA-MB-231 cells assessed by transwell Boyden chamber assay. Cells were infected using lentiviral particles carrying either the shRNA oligo targeting EZH2 or the GIPZ shRNA control.  $2.5 \times 10^3$  cells were resuspended in serum deprived media and added to the top of a Boyden chamber. The Boyden chambers were placed in 24 well plates containing complete grow media. After 24 hours, migrating cells were stained and counted under a microscope. **A.** Representative fields showing reduced migration caused by EZH2 knockdown. **B.** The graph is representative of an experiment performed three times in triplicate (n=9; error bars  $\pm$ SEM). See appendix A for raw data.

The scratch assay was performed as described in section 2.2.16. Non-infected MDA-MB-231 cells, MDA-MB-231 GIPZ cells and MDA-MB-231 17507 cells were seeded in 10 cm plates and allowed to reach confluency. At day 0 a scratch was created in the monolayer of cells using a sterile 500  $\mu$ l pipette and the cells were observed for 24 hours. The area of a marked scratch was measured at day 0 and at day 1 using the software imagej. Cell migration was calculated using the following formula: “(Pre-migration area – Migration area)/Pre-migration area X 100” and represented in a graph as percent of cell migration (Figure 3.7 A and B). Compare to non-infected MDA-MB-231 and to MDA-MB-231 GIPZ cells, MDA-MB-231 17507 cells showed a significant reduction of the migrating area.

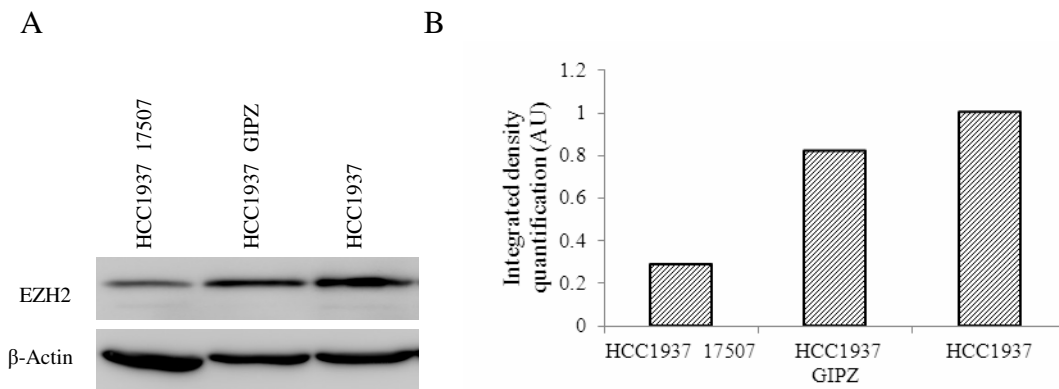


**Figure 3.7:** The effect of EZH2 knockdown on migration of MDA-MB-231 cells assessed by scratch assay. Migration is reduced in MDA-MB-231 17507 compared to non-infected MDA-MB-231 and MDA-MB-231 GIPZ. **A:** Representative images showing difference in migration between non-infected MDA-MB-231 cells, MDA-MB-231 GIPZ cells and MDA-MB-231 17507 cells. Photographs of the cells were taken at day 0 and day 1 at 10X magnification. **B:** The graph is representative of a single experiment and single marked scratches. The size of the scratch was measured at day 0 and at day 1, using the software imageJ. Cell migration was expressed in percentage and was calculated using the formula: “(Pre-migration area – Migration area)/Pre-migration area X 100”. (see section 2.2.16 for more details)

### **3.4 EZH2 Knockdown in HCC1937 breast cancer cells**

EZH2 knockdown in HCC1937 cells was performed using shRNA and a second generation lentiviral system (section 2.2.3 and 2.2.4; see also section 3.3). V2LHS\_17507 targeting EZH2 was used for EZH2 knockdown and GIPZ scrambled shRNA was used as negative control for lentiviral infection. Cells infected with lentivirus containing V2LHS-17507 shRNA targeting EZH2 were called HCC1937 17507, while cells infected with lentivirus containing GIPZ control were called HCC1937 GIPZ.

To confirm the reduced expression of EZH2 protein in HCC1937 17507, western blot analysis was performed (Figure 3.8). Total protein extracted from non-infected HCC1937 cells, HCC1937 17507 cells and HCC1937 GIPZ cells were analyzed. For each sample, 30 µg of proteins were loaded onto a 10% SDS acrylamide resolving gel and western blot analysis was performed as described in materials and methods (section 2.2.9.1 – 2.2.9.3). Western blot analysis showed a significant decrease of EZH2 protein expression in HCC1937 17507 cells compared to non-infected HCC1937 cells and HCC1937 GIPZ (Figure 3.8).

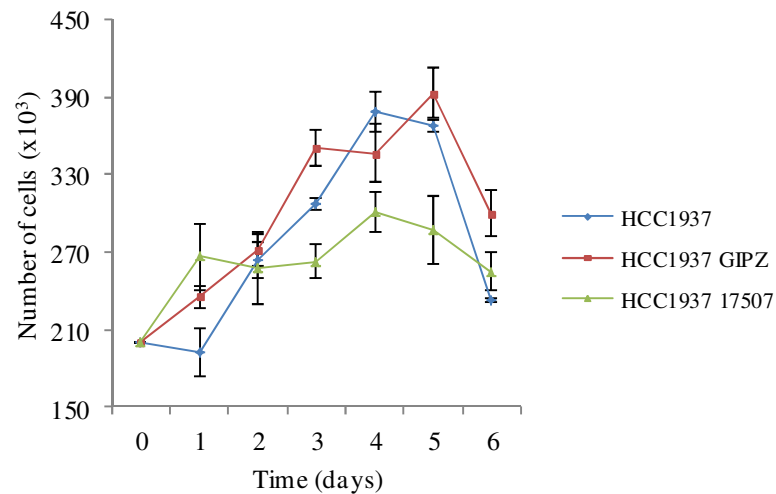


**Figure 3.8:** EZH2 knockdown in HCC1937 cells. Non-infected cells, cells infected using lentiviral particles carrying either the shRNA oligo targeting EZH2 or the GIPZ shRNA control are shown. Representative image and graph of western blot analysis. **A.** Infected cells were harvested five days after puromycin selection. Extracted proteins were resolved by 10% SDS-PAGE and membrane was probed with the indicated antibodies.  $\beta$ -Actin was used as a loading control. **B.** Results obtained after integrated density quantification of A using ImageJ software (measurements expressed in arbitrary unit). All values were normalized against  $\beta$ -Actin.

### 3.4.1 Effect of EZH2 knockdown on HCC1937 cell proliferation

In order to test whether EZH2 knockdown affects HCC1937 cell proliferation, a growth curve analysis was performed (Figure 3.9). Non-infected HCC1937 cells, HCC1937 GIPZ cells and HCC1937 17507 cells were seeded in 6 cm plates, starting with  $2.0 \times 10^5$  cells. Cells were trypsinized and counted, using Beckman Coulter Particles Counter Z1, every 24 hours for 6 days. An accurate estimation of doubling time for the HCC1937 cells was not possible due to the high death rate of the cells. The high mortality rate of the cells confounded the results and caused some problems in quantification of proliferation rate. Focusing on the interval between day 2 and day 3 non-infected HCC1937 and HCC1937 GIPZ cells showed an increase in cell number of 44000 and 78000 respectively, while the HCC1937

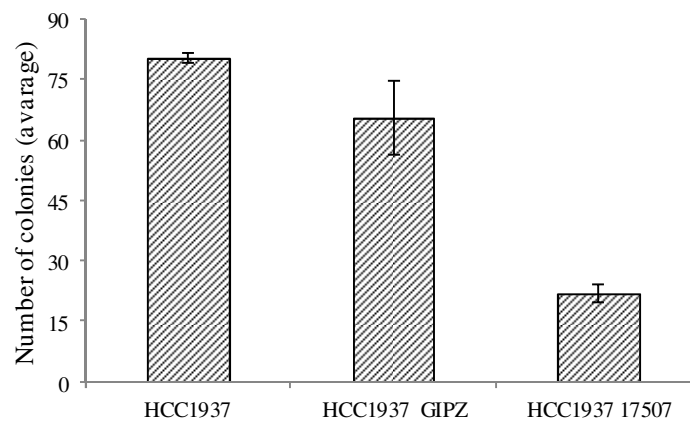
17507 showed an increase in cell number of only 4700 cells. These results suggested that reduced expression of EZH2 in HCC1937 cells inhibits cell proliferation.



**Figure 3.9:** The effect of EZH2 knockdown on the growth rate of HCC1937 cell. Representative graph of HCC1937 cell growth rate. Cells were infected using lentiviral particles carrying either the shRNA oligo targeting EZH2 or the GIPZ shRNA control and. Five days after puromycin selection, cells were plated in 6cm plates. Cells were counted every 24 hours. The experiment was performed three times in triplicate (n=9; error bars  $\pm$ SEM). See appendix A for raw data.

### 3.4.2 Effect of EZH2 knockdown on HCC1937 anchorage-independent growth

To assess whether EZH2 knockdown influences the anchorage-independent growth of the HCC1937 cells, a colony formation in soft agar assay was performed (Figure 3.10). HCC1937 cells, HCC1937 GIPZ cells and HCC1937 17507 cells were tested in triplicate (section 2.2.13). For each replicate 5000 cells were used and the cells were grown at 37 °C for 21 days. After 21 days, colonies were counted. Both, non-infected HCC1937 and HCC1937 GIPZ cells formed a higher number of colonies compared to HCC1937 17507 cells (Figure 3.10). An average of 20 colonies were counted for HCC1937 17507 cells, while an average of 70 and 75 colonies was counted for non-infected HCC1937 cells and HCC1937 GIPZ cells. The results obtained showed that EZH2 knockdown in HCC1937 breast cancer cells reduces their anchorage-independent growth.



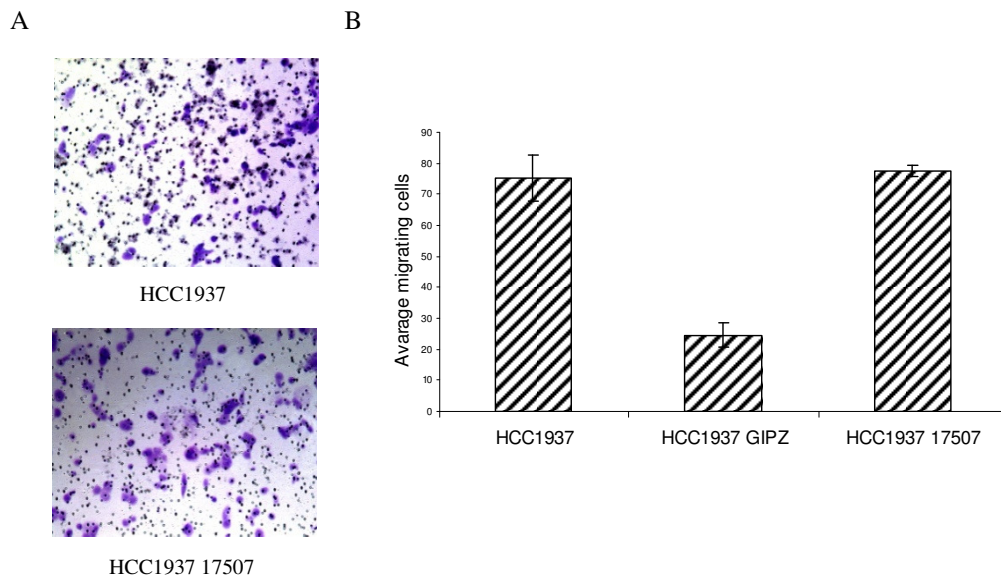
**Figure 3.10:** The effect of EZH2 knockdown on anchorage-independent growth of HCC1937 cells. Cells were infected using lentiviral particles carrying either the shRNA oligo targeting EZH2 or the GIPZ shRNA control. Cells were grown for 21 days and colonies were stained with INT. The graph is representative of an experiment performed three times in triplicate (n=9; error bars  $\pm$ SEM). See appendix A for raw data.



### **3.4.3 Effect of EZH2 knockdown on HCC1937 cell migration**

HCC1937 cells are also highly motile aggressive cells (Coene et al. 2011). Two different assays, the trans-well Boyden chamber assay (Chen 2005; Li & Zhu 1999) and the scratch assay (Liang et al. 2007) (Section 2.2.12 and 2.2.16), were used in order to test whether EZH2 knockdown reduce HCC1937 cell migration.

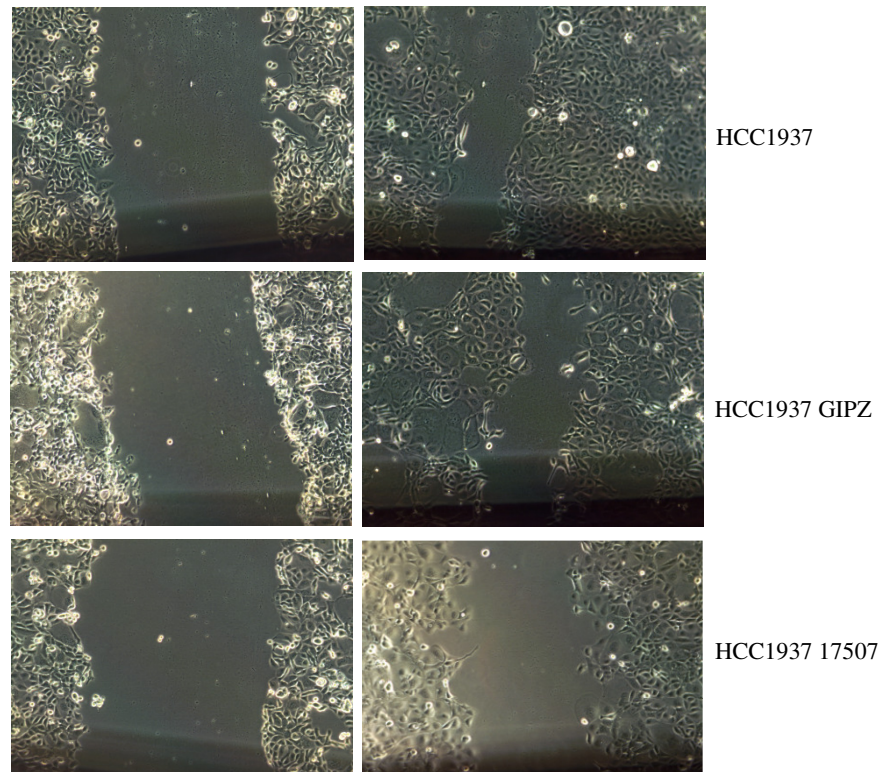
The transwell Boyden chamber assay was performed as described in materials and methods (section 2.2.12). Non-infected HCC1937 cells, HCC1937 GIPZ cells and HCC1937 17507 cells were trypsinised and separately re-suspended in serum free growth media.  $2.5 \times 10^4$  cells were added to the top of each PET membrane. After 18-24 hours, three randomly selected fields in the central part of the chamber were chosen and the number of migrating cells was counted. Representative images of randomly selected field are shown in figure 3.11A. For each cell type the experiment was performed in triplicate and a total of 9 counts were made (3 counts for each chamber) which were then averaged in order to give an estimation of the number of migrating cells per field. The number of migratory cells for non-infected HCC1937 was similar to the number of migrating cells for HCC1937 17507 (about 70 migrating cells), suggesting that EZH2 knockdown did not influence cell migration using the transwell Boyden chamber assay. Surprisingly, the number of migratory cells for HCC1937 GIPZ control was significantly lower compared to the number of migratory cells for non-infected HCC1937. The unexpected result could be due to either experimental error or to the fact that the GIPZ control had an effect on the migration ability of HCC1937 cells. In order to clarify this point, and to test whether a different assay would give the same results, a scratch assay was performed.



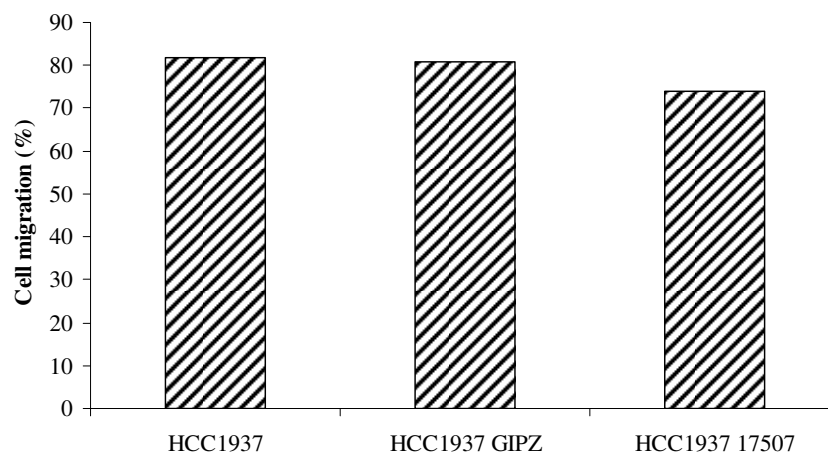
**Figure 3.11:** The effect of EZH2 knockdown on HCC1937 migration as assessed by transwell Boyden chamber assay. Migration is not significantly reduced in HCC1937 17507 compared to non-infected HCC1937. Cells were infected using lentiviral particles carrying either the shRNA oligo targeting EZH2 or the GIPZ shRNA control.  $2.5 \times 10^3$  cells were resuspended in serum deprived media and added to the top of a Boyden chamber. After 24 hours migrating cells were stained and counted under a microscope. **A.** Representative fields of two Boyden chambers after staining. **B.** The graph is representative of an experiment performed three times in triplicate ( $n=9$ ; error bars  $\pm$ SEM). See appendix A for raw data.

The scratch assay was performed as described in section 2.2.16. Non-infected HCC1937 cells, HCC1937 GIPZ cells and HCC1937 17507 cells were seeded in 10 cm plates and allowed to reach confluency. At day 0 a scratch was created in the monolayer of cells using a sterile 500  $\mu$ l pipette and the cells were observed for 24 hours. The area of a marked scratch was measured at day 0 and at day 1 using the software imageJ. Cell migration was calculated using the following formula: “(Pre-migration area – Migration area)/Pre-migration area X 100” and represented in a graph as percent of cell migration (Figure 3.12 A and B). No significant difference in terms of migration area was observed when non-infected HCC1937 cells, HCC1937 GIPZ cells and HCC1937 17507 cells were compared (Figure 3.12 B and Table A.11 Appendix A). Cell migration for non infected HCC1937 and HCC1937 GIPZ was 81,9% and 80,92% respectively and cell migration for HCC1937 17507 73,94% (see Table A.11). Moreover, using this assay, the GIPZ control did not have any effect on cell migration.

A



B



**Figure 3.12:** The effect of EZH2 knockdown on HCC1937 migration as assessed by a scratch assay. Migration is not significantly reduced in HCC1937 17507 compared to non-infected HCC1937 and HCC1937 GIPZ control. **A:** Representative images showing difference in migration between non-infected HCC1937 cells, HCC1937 GIPZ cells and HCC1937 17507 cells. Photographs of the cells were taken at day 0 and day 1 at 10X magnification. **B:** The graph is representative of a single experiment and single marked scratches. The size of the scratch was measured at day 0 and at day 1, using the software imageJ. Cell migration was expressed in percentage and was calculated using the formula “(Pre-migration area – Migration area)/Pre-migration area X 100” (see section 2.2.16 for more details).

### 3.5 Discussion

In this chapter I sought to investigate the effect of knocking down EZH2 in breast cancer cell lines expressing different levels of EZH2. Two breast cancer cell lines were used MDA-MB-231 and HCC1937 (See also table A.1, appendix A). They derive from different breast cancer subtypes and from different sources (adenocarcinoma/pleural effusion for MDA-MB-231 and infiltrating ductal carcinoma/primary breast for HCC1937) but they have some features in common *i.e.* they are both highly aggressive, ER/PR and HER2 negative (Neve et al. 2006). MDA-MB-231 is a cell line with a very high level of EZH2, while HCC1937 is a cell line with a lower level of EZH2 (Table 3.1). This was confirmed also at the protein level (Figure 3.2).

shRNA-mediated knockdown of EZH2 induced inhibition of cell proliferation in both cell lines with a stronger effect on MDA-MB-231 cells compared to HCC1937 cells (Figure 3.4 and 3.9). The fact that EZH2 knockdown had a more drastic effect on MDA-MB-231 (high EZH2) cells proliferation compared to HCC1937 (low EZH2), suggests that the level of EZH2 overexpression might influence the behaviour of the cells. The differences observed was not due to the amount of EZH2 knockdown *i.e.* the higher the amount of knockdown the more drastic effect on cell proliferation. In fact, when the amounts of EZH2 knockdown was compared, HCC1937 cells actually showed higher amount of knockdown compared to MDA-MB-231 cells (70% and 50% respectively) (Figure 3.3 and 3.8). The two cell lines are both ER $\alpha$  negative therefore the implication of the oestrogen receptor status can be excluded. Repression of EZH2 causes inhibition of cell proliferation and induces G2/M arrest (Gonzalez et al. 2009; Sharif et al.; Tang et al. 2004). Tang et al. have shown that activated p53 suppresses EZH2 and they

proposed that repression of EZH2 by p53 is one of the pathway by which p53 mediates G2/M checkpoint arrest (Tang et al. 2004). The MDA-MB-231 cell line has high level of a mutant p53 (Hui et al. 2006; Olivier et al. 2002), EZH2 knockdown in these cells might compensate for the lack of wild type p53. However, HCC1937 also have mutated p53 suggesting that the different effect of EZH2 knockdown in the two cell lines is not linked to p53 status. The inhibition of cell proliferation, upon EZH2 knockdown, supports and confirms data reported by others (Bryant et al. 2007; Francis et al. 2001; Gonzalez et al. 2009; Zhang et al. 2011). In fact, it has been suggested that different EZH2 levels can be used to identifying patients with breast cancer of a more aggressive phenotype (Kleer et al. 2003; Li et al. 2009).

In both cell lines EZH2 knockdown significantly reduced their ability of forming colonies in soft agar (Figure 3.5 and 3.10). However, EZH2 knockdown had different effect on cell migration when the two cell lines were compared and two different invitro assays were performed. Using the trans-well Boyden chamber assay a significant reduction in cell migration was observed in MDA-MB-231 cells upon EZH2 knockdown (Figure 3.6), while no effect was observed in HCC1937 cells upon EZH2 knockdown (Figure 3.11). The results obtained using the Boyden chamber assay in HCC1937 cells suggest that the control transfection GIPZ had an effect on cell migration (Figure 3.11). In order to verify this hypothesis, the Boyden chamber assay should have been repeated using a different infection control vector. However, Neve et al. have classified HCC1937 as Basal A subtype of cell. They have reported that Basal A cells are normally less invasive in Boyden chamber assay (Neve et al. 2006). Since, the outcome of an *in vitro* assay to test specific features correlated to neoplastic transformation is often influenced by the cell type used, the use of an

alternative assay might be more suitable for testing migration of HCC1937 cells. The alternative assay was also chosen in order to test whether the GIPZ control would still show an effect on cell migration. In MDA-MB-231 cells the results obtained using Boyden chamber assay were also confirmed by the scratch assay results, the migration ability of MDA-MB-231 was reduced by 50% upon knockdown of EZH2 (Figure 3.7). In HCC1937 cells the results obtained using Boyden chamber assay were confirmed by the scratch assay results, the migration ability of HCC1937 cells was not significantly influenced by knockdown of EZH2, in fact only a 10% reduction in cell migration was observed upon EZH2 knockdown (Figure 3.12). In addition, using the scratch assay the control GIPZ did not show any effect on cell migration. Both cell lines showed reduction of anchorage-independent growth and cell proliferation, upon EZH2 knockdown. The identification of genes involved in these processes represent an important instrument for identifying more aggressive tumours (Bozzuto et al. 2010; Mori et al. 2009).

The more aggressive breast cancers are normally the ER negative tumours. Compared to patients with ER positive tumours, patients with ER negative tumours have worse outcome and prognosis. There is a proportion of ER positive breast cancer, even though small, that over-expresses EZH2. It would be interesting to test whether knocking down EZH2 in ER $\alpha$  positive breast cancer cell lines have the same effect as EZH2 knockdown in ER $\alpha$  negative cell lines. For this purpose CAMA1 and T47D cell lines were selected (table 3.1). CAMA1 cells are ER positive cells with high level of EZH2 while T47D cells are ER positive with a lower level of EZH2 (Table 3.1). The unsuccessful EZH2 knockdown in ER $\alpha$  positive CAMA1 cells and T47D cells (Figure 3.1) was probably due to technical problems, i.e. low infection of lentiviral particles, even though the cells were successfully selected with puromycin.

The idea of ER $\alpha$  positive cells resistant to EZH2 knockdown can be excluded, since EZH2 knockdown has been successfully performed in other ER $\alpha$  positive breast cancer cell lines (Reijm et al. 2010). Additional experiments and troubleshooting will be necessary in order to further investigate the effect of EZH2 knockdown in ER $\alpha$  positive breast cancer cells.

A distinct characteristic of HCC1937 cells is the presence of mutated BRCA1 (5382insC mutation in one allele and a deletion of the second allele) (Foray et al. 2002; Tomlinson et al. 1998). BRCA1 plays a crucial role in S and G2/M checkpoints during DNA damage response (Cortez et al. 1999; Venkitaraman 2002; Xu et al. 2001; Yan et al. 2005). A link between EZH2 mis-regulation and BRCA1 has been previously reported with contrasting conclusions. Puppe et al reported that EZH2 knockdown has an effect only in BRCA1deficient tumours (Puppe et al. 2009), while Gonzalez et al. reported wild type BRCA1 is required in order to observe effect on cell proliferation upon EZH2 knockdown (Gonzalez et al. 2009). The presence of mutated BRCA1 in HCC1937 might explain the observed less significant effect of EZH2 knockdown on cell proliferation and cell migration. This will be further investigated in chapter 4.



## **4 CHAPTER 4: INVESTIGATING THE RELATIONSHIP BETWEEN EZH2 AND BRCA1**

### **4.1 Introduction**

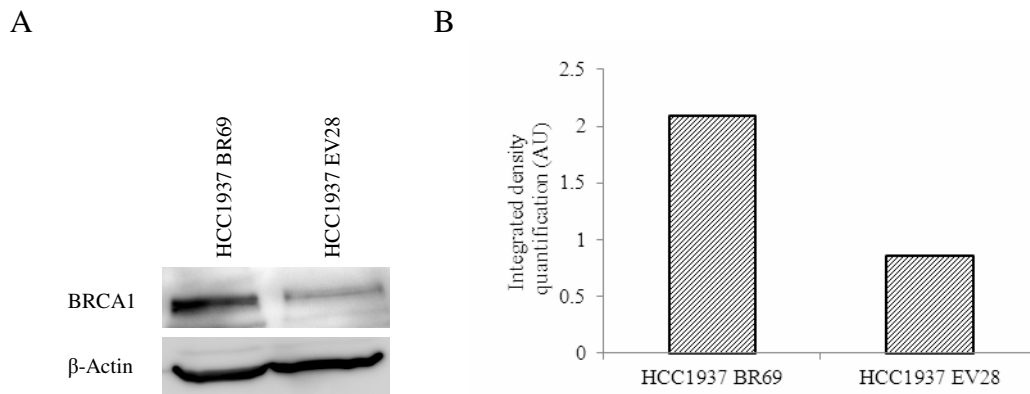
Basal-like breast carcinomas consist of a morphologically heterogeneous subgroup of aggressive breast cancers exhibiting distinct features, such as hormone receptors negativity, HER2 negativity (i.e. triple negative), expression of high-molecular-weight cytokeratin, BRCA1 mutations/down regulation and EZH2 over-expression. This group of cancers could be further subdivided. For example, within the basal-like group not all tumours are triple negative (ER/PR/HER2), and, even though the basal-like phenotype has been associated to BRCA1 mutation and EZH2 mis-regulation, not all basal cancers have mutated BRCA1 or over-express EZH2 (Gluz et al. 2009; Rakha et al. 2009a; Sorlie et al. 2001; Tischkowitz et al. 2006; Venkitaraman 2002; Xu et al. 2001; Yoshida et al. 2004). The tumour suppressor BRCA1 plays a central role in maintaining genome stability acting through different pathways involved in regulation of cell cycle, DNA repair, apoptosis and transcriptional regulation (Harkin 2009; Rosen et al. 2003; Savage 2009; Venkitaraman 2002; Yoshida & Miki 2004). EZH2 is an important regulator of cell development, differentiation and proliferation (Aoki et al. 2010; Bracken et al. 2003; Cao et al. 2002; Collett et al. 2006; Li et al. 2009; Matsukawa et al. 2006; Tonini et al. 2008). BRCA1, as well as EZH2 are involved in the regulations of the G2/M phase of the cell cycle (Gonzalez et al. 2009; Xu et al. 2001). Two recent studies have reported contrasting data on the interplay between BRCA1 and EZH2. Gonzalez et al. suggested that EZH2 is a regulator of BRCA1 and proposed that in breast cancer the over-expression of EZH2 caused a decrease of BRCA1

(accompanied by high levels of Cdc2-CyclinB1 complex) and consequently uncontrolled proliferation and cell cycle which contributes to breast cancer formation. In their model the effect of EZH2 knockdown on cell proliferation is dependent on the presence of wild type BRCA1. Puppe et al. have suggested that the effect of EZH2 knockdown on cell proliferation is more apparent in the absence of BRCA1 (Puppe et al. 2009). However, the two studies followed different experimental procedures: Gonzalez et al study used human breast cancer cells while Puppe et al. used mouse tumour cell lines. The aim of this chapter was the further investigation of the relationship between BRCA1 status and the effect of EZH2 knockdown in breast cancer cells. In order to do so, the effect of EZH2 knockdown on cell proliferation, migration and anchorage independent growth was tested in the context of HCC1937 breast cancer cell line that carries a mutated BRCA1. Two cell lines were compared, a derivative (HCC1937 BR69) expressing ectopic wild type BRCA1 and a derivative expressing an empty vector (HCC1937 EV28).

#### **4.2 EZH2 knockdown in HCC1937EV28 and HCC1937BR69 breast cancer cell lines**

Two cell lines, HCC1937EV28 and HCC1937BR69, were obtained from Dr Harkin's group. HCC1937EV28 cells are homozygous for the BRCA1 5382insC mutation, resulting in the formation of a truncated protein of 1829 aa (compared to a full length BRCA1 with 1863 aa) (Foray et al. 2002; Tomlinson et al. 1998) transfected with a control empty construct, while HCC1937BR69 cells are cells stably transfected with a construct containing wild type BRCA1(Quinn et al. 2003). Cells were grown according to instructions (see section 2.2.8.1).

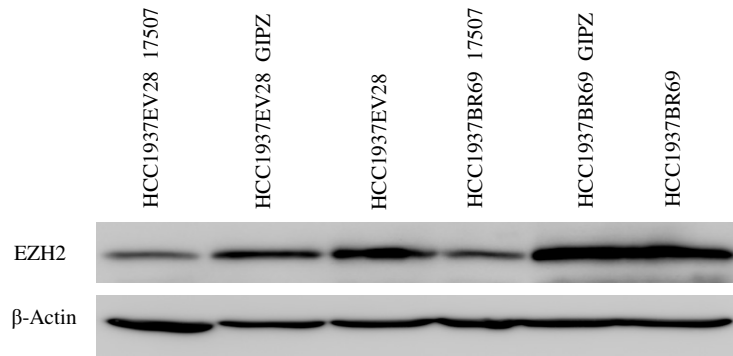
The expression of BRCA1 protein in HCC1937BR69 was confirmed by western blot analysis and compared to the expression in HCC1937EV28 cells (Figure 4.1). The level of expression of BRCA1 in HCC1937BR69 was 2 fold higher compared to the level of expression of BRCA1 in HCC1937EV28.



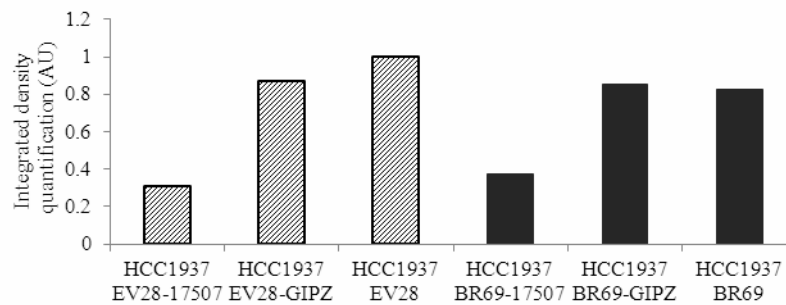
**Figure 4.1:** BRCA1 expression level in HCC1937EV28 cells and HCC1937BR69 cells. Representative image and graph of western blot analysis performed three times. **A.** Extracted proteins were resolved by 8 % SDS-PAGE and membranes were probed with the indicated antibodies.  $\beta$ -Actin was used as a loading control. **B.** Results obtained after integrated density quantification of A using ImageJ software (measurements expressed in arbitrary units).

EZH2 knockdown in HCC1937EV28 and HCC1937BR69 cells was performed using shRNA and a second generation lentiviral system (section 2.2.3 and 2.2.4; see also section 3.4). V2LHS\_17507 targeting EZH2 was used for EZH2 knockdown and GIPZ scrambled shRNA was used as negative control for lentiviral infection. Cells infected with lentivirus containing V2LHS-17507 shRNA targeting EZH2 were called HCC1937EV28 17507 and HCC1937BR69 17507, while cells infected with lentivirus containing GIPZ control were called HCC1937EV28 GIPZ and HCC1937BR69 GIPZ. To confirm the reduced expression of EZH2 protein in HCC1937BR69 17507 cells and HCC1937EV28 17507 cells, western blot analysis was performed (Figure 4.2).

A



B



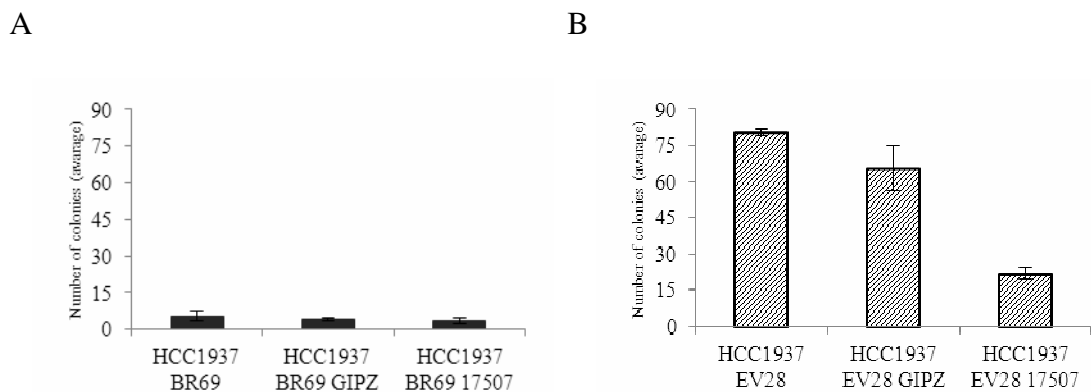
**Figure 4.2:** EZH2 knockdown in HCC1937EV28 cells and HCC1937BR69 cells. Cells were infected using lentiviral particles carrying either the shRNA oligo targeting EZH2 or the GIPZ shRNA control. Infected cells were harvested 5 days after puromycin selection. Representative image and graph of western blot analysis performed three times. **A.** Extracted proteins were resolved by 10 % SDS-PAGE and membranes were probed with the indicated antibodies.  $\beta$ -Actin was used as a loading control. **B.** Results obtained after integrated density quantification of A using ImageJ software (measurements expressed in arbitrary units).

Total protein extracted from non-infected HCC1937BR69 cells, HCC1937BR69 17507 cells, HCC1937BR69 GIPZ cells, non-infected HCC1937EV28 cells, HCC1937EV28 17507 cells and HCC1937EV28 GIPZ cells were analyzed. For each sample, 30  $\mu$ g of proteins were loaded onto a 10% SDS acrylamide resolving gel and western blot analysis was performed as described in materials and methods (section 2.2.9.1 – 2.2.9.3). In both cell lines western blot analysis showed about 60% reduction of EZH2 protein expression in cells infected

with lentiviral particles carrying shRNA targeting EZH2 compared to non-infected cells and GIPZ control (Figure 4.2).

#### 4.2.1 Effect of EZH2 knockdown on HCC1937EV28 and HCC1937BR69 cells anchorage independent growth

To assess whether the presence of wild type BRCA1 has any effect on the anchorage-independent growth of the HCC1937 cells in relation to EZH2 knockdown, a colony formation in soft agar assay, using HCC1937BR69 cell line, was performed and results were compared to those obtained for HCC1937EV28 cells (Figure 4.3) (see section 3.4.2). Non-infected HCC1937BR69 cells, HCC1937BR69 GIPZ cells and HCC1937BR69 17507 cells were tested three times in triplicate (section 2.2.13). For each replicate 5000 cells were used and the cells were grown at 37 °C for 21 days. After 21 days, colonies were stained and counted.



**Figure 4.3:** The effect of EZH2 knockdown on anchorage independent growth in HCC1937EV28 and HCC1937BR69 cells. Cells were infected using lentiviral particles carrying either the shRNA oligo targeting EZH2 or the GIPZ shRNA control. 5 days after puromycin selection cells were seeded in 3.5 % low melting agarose containing RPMI1640 media plus supplements. Colonies were stained with INT and counted after 21 days. The graph is representative of an experiment performed three times in triplicate (n=9; error bars  $\pm$ SEM). **A.** EZH2 knockdown in HCC1937BR69 cells. **B.** EZH2 knockdown in HCC1937EV28 cells. See appendix B for raw data.

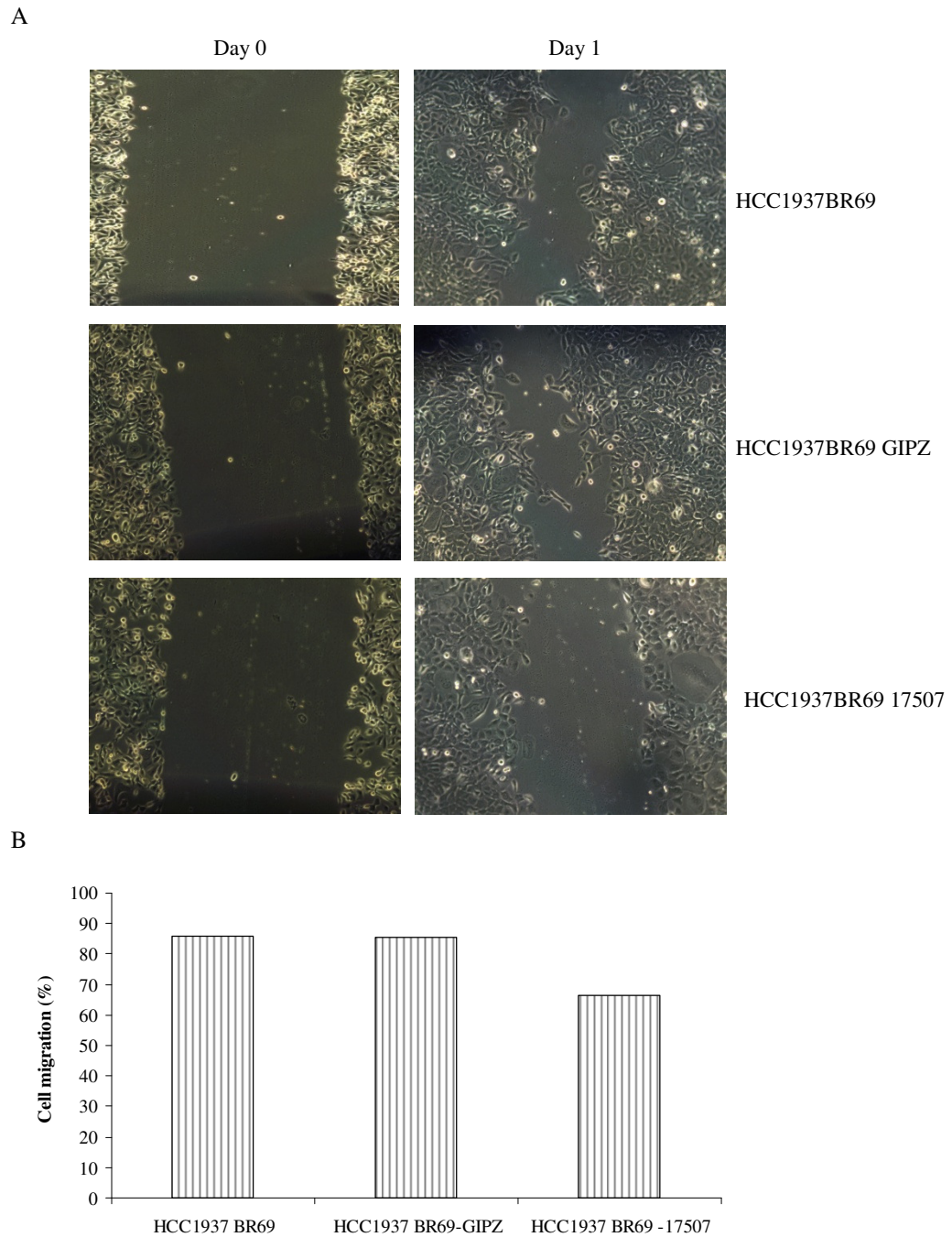
The number of colonies formed by HCC1937BR69 17507 cells was not significant different compared the number of colonies formed by non-infected cells and HCC1937BR69 GIPZ cells (Figure 4.3 A and Table B.3 Appendix B). The number of colonies formed by HCC1937EV28 17507 cells was significantly lower compared to the number of colonies formed by non-infected cells and HCC1937EV28 GIPZ cells (Figure 4.3 B and Table B.4 Appendix B). Non-infected HCC1937EV28 cells and HCC1937EV28 GIPZ cells formed an average of 80 and 66 colonies respectively, while HCC1937 EV28-17507 cells formed an average of 20 colonies. Moreover, the number of colonies formed by HCC1937BR69 cells was lower compared to the number of colonies formed by HCC1937EV28 cells (5 and 80 colonies respectively) and no difference in size of colonies was observed. These results suggest that the inhibition of anchorage-independent growth upon down-regulation of EZH2 is not dependent on the presence of wild type BRCA1.

#### **4.2.2 Effect of EZH2 knockdown on HCC1937EV28 and HCC1937BR69 cells migration**

To test whether the migration ability of HCC1937 cells after EZH2 knockdown is affected by the presence of wild type BRCA1, a comparison between HCC1937BR69 and HCC1937EV28 cells was performed. As in the previous chapter, two different assays were used, the trans-well Boyden chamber assay (Chen 2005; Li & Zhu 1999) and the scratch assay (Liang et al. 2007) (Section 2.2.22 and 2.2.23).

The scratch assay was performed as described in section 2.2.16. Non-infected HCC1937BR69 cells, HCC1937BR69 GIPZ cells and HCC1937BR69 17507 cells

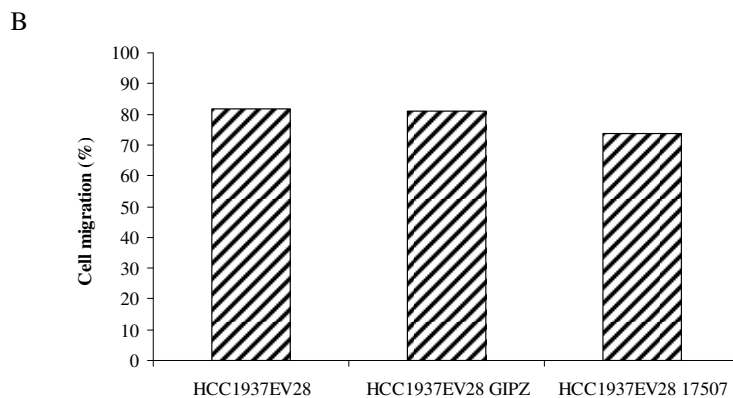
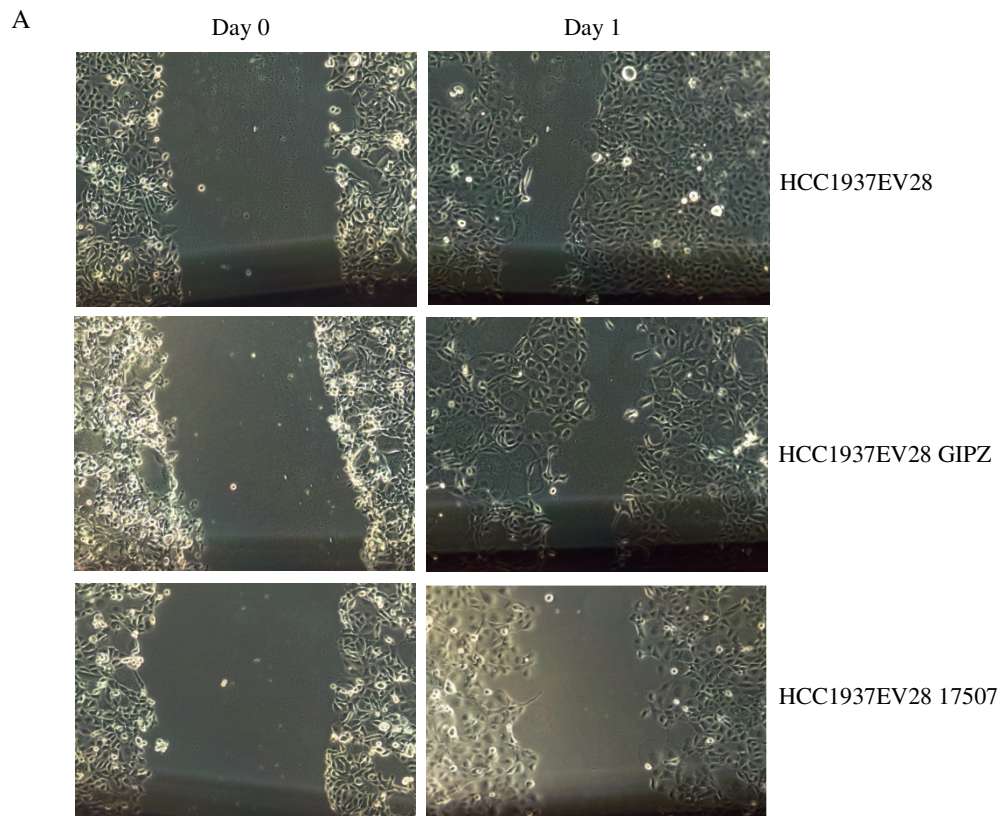
were seeded in 10 cm plates and allowed to reach confluency. At day 0 a scratch was created in the monolayer of cells using a sterile 500 µl pipette and the cells were observed for 24 hours. The area of a marked scratch was measured at day 0 and at day 1 using the software imageJ. Cell migration was calculated using the following formula: “(Pre-migration area – Migration area)/Pre-migration area X 100” and represented in a graph as percent of cell migration (Figure 4.4 A and B). When compared to non-infected HCC1937BR69 cells and to HCC1937BR69 GIPZ cells, HCC1937BR69 17507 cells showed a reduction of cell migration of 22% (Figure 4.4 and Table B.7 Appendix B). Cell migration for non infected HCC1937BR69 cells and HCC1937BR69 GIPZ cells was 85,92% and 85,54% respectively, while cell migration for HCC1937BR69 17507 cells was 66,56% (Table B.7 Appendix B).



**Figure 4.4:** The effect of EZH2 knockdown on HCC1937BR69 cell migration as assessed by a scratch assay. Migration is reduced in HCC1937BR69 17507 compared to non-infected HCC1937BR69 and HCC1937BR69 GIPZ. **A:** Representative images showing difference in migration between non-infected HCC1937BR69, HCC1937BR69 GIPZ and HCC1937BR69 17507 cells. Photographs of the cells were taken at day 0 and day 1 at 10X magnification. **B:** The graph is representative of a single experiment and single marked scratches. The size of the scratch was measured at day 0 and at day 1, using the software imageJ. Cell migration was expressed in percentage and was calculated using the formula: “(Pre-migration area – Migration area)/Pre-migration area X 100”. (see section 2.2.16 for more details)

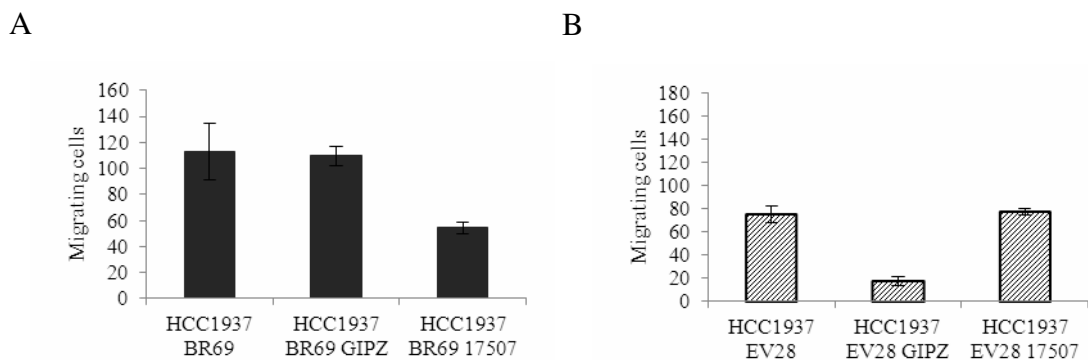


These results were different from results obtained with HCC1937EV28 cells (Figure 4.5, see also section 2.4.3). When compared to non-infected HCC1937EV28 and to HCC1937EV28 GIPZ cells, HCC1937EV28 17507 cells showed a reduction of cell migration of 10%. Cell migration for non infected HCC1937EV28 and HCC1937EV28 GIPZ was 81,9% and 80,92% respectively and cell migration for HCC1937EV28 17507 was 73,94% (see Table A.11). The results obtained using the scratch assay, suggest that EZH2 knockdown has a more pronounced effect in reducing migration of HCC1937 cells in the presence of wild type BRCA1. In order to confirm these data, additional experiments should have been performed using measurements taken from multiple scratches. The experiment was not repeated due to the fact that the HCC1937BR69 cells available had lost the expression of BRCA1 during passaging (see section 4.3 and 4.4).



**Figure 4.5:** The effect of EZH2 knockdown on HCC1937EV28 migration as assessed by a scratch assay. Migration is not significantly reduced in HCC1937EV28 17507 cells compared to non-infected HCC1937EV28 and HCC1937EV28 GIPZ cells. **A:** Representative images showing difference in migration between non-infected HCC1937EV28, HCC1937 EV28 GIPZ and HCC1937EV28 17507. Photographs of the cells were taken at day 0 and day 1 at 10X magnification. **B:** The graph is representative of a single experiment and single marked scratches. The size of the scratch was measured at day 0 and at day 1, using the software imageJ. Cell migration was expressed in percentage and was calculated using the formula: “(Pre-migration area – Migration area)/Pre-migration area X 100”. (see section 2.2.16 for more details)

In order to confirm data obtained with the scratch assay, a transwell Boyden chamber assay was also performed (section 2.2.12). Non-infected HCC1937BR69 cells, HCC1937BR69 GIPZ cells and HCC1937BR69 17507 cells were trypsinized and separately re-suspended in serum free growth media.  $2.5 \times 10^4$  cells were added to the top of each PET membrane. After 18-24 hours, three randomly selected fields in the central part of the chamber were chosen and the number of migrating cells was counted. For each cell type the experiments was performed in triplicate and a total of 9 counts were made (3 counts for each chamber) which were then averaged in order to give an estimation of the number of migrating cells per field.



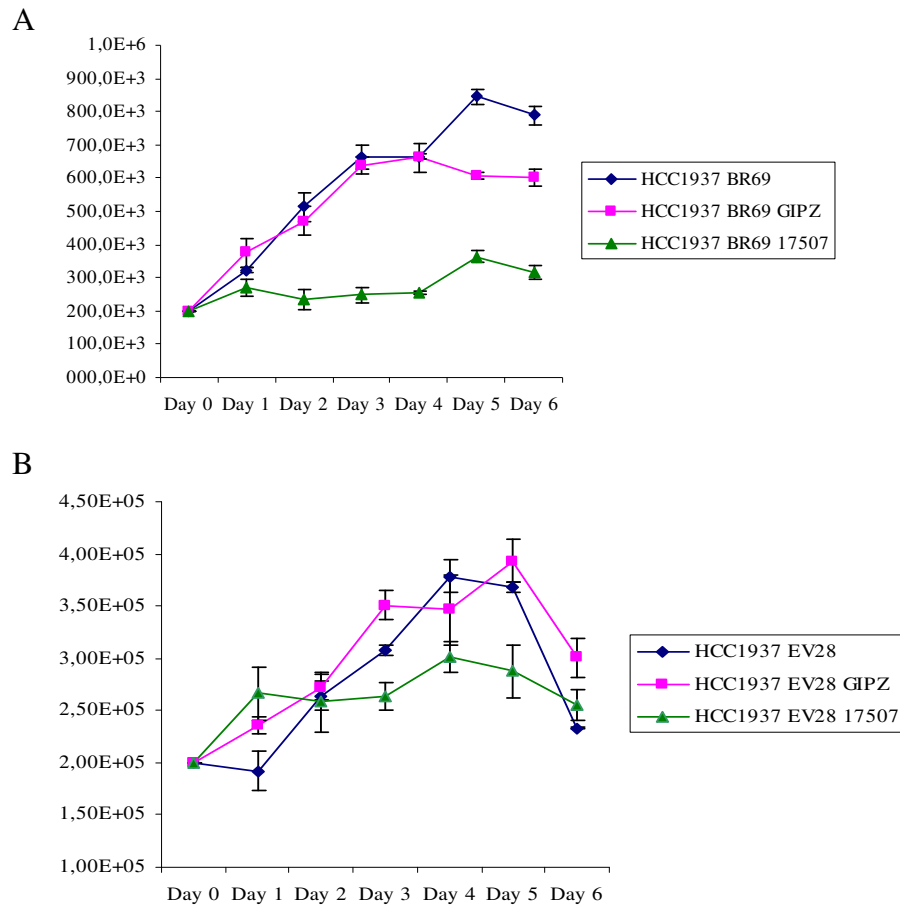
**Figure 4.6:** The effect of EZH2 knockdown on HCC1937EV28 cells and HCC1937BR69 cells migration ability as assessed by transwell Boyden chamber assay. Cells were infected using lentiviral particles carrying either the shRNA oligo targeting EZH2 or the GIPZ shRNA control. 5 days after puromycin selection  $2.5 \times 10^3$  cells were resuspended in serum deprived media and added to the top of a Boyden chamber; after 24 hours migrating cells were stained with crystal violet and counted under microscope. The graphs are representative of experiments performed in triplicate (n=9; error bars  $\pm$ SEM). **A.** EZH2 knockdown in HCC1937 BR69 cells. **B.** EZH2 knockdown in HCC1937EV28 cells. (See appendix B for raw data)

Using the transwell Boyden chamber assay, migration of HCC1937BR69 cells was reduced by 50% upon EZH2 knockdown (Figure 4.6.A). About 110 migrating cells were counted for non-infected cells and cells infected with GIPZ control, while only 50 migrating cells were counted for HCC1937BR69 17507 cells.

In contrast, using the transwell Boyden chamber assay, migration of HCC1937EV28 cells was not influenced by EZH2 knockdown (Figure 4.6 right). The number of migratory cells for non-infected HCC1937EV28 was similar to the number of migrating cells for HCC1937EV28 17507 (about 80 in both cases). However, the number of migratory cells for HCC1937EV28 GIPZ was significantly lower compared to the number of migratory cells for non-infected HCC1937EV28, suggesting that the vector GIPZ control could have had an effect on cell migration (discussed in section 3.5). In addition, the data presented here show that HCC1937BR69 cells migrate faster than HCC1937EV28, suggesting that re-expression of BRCA1 increases the migratory ability of HCC1937 cells, which is in clear disagreement with previously reported data (Coene et al. 2011). These unexpected results could be due to the fact that the HCC1937BR69 cells had lost BRCA1 expression during passaging (see section 4.3).

#### **4.2.3 Effect of EZH2 knockdown on HCC1937EV28 and HCC1937BR69 cells proliferation**

In order to test whether EZH2 knockdown effects on HCC1937 cell proliferation is dependent on the presence of wild type BRCA1, growth curve analysis of HCC1937BR69 cells was performed and compared to growth curve analysis of HCC1937EV28 cells (Figure 4.7). Non-infected HCC1937BR69 cells, HCC1937BR69 GIPZ cells and HCC1937BR69 17507 cells were seeded in 6 cm plates, starting with  $2.0 \times 10^5$  cells. Cells were trypsinized and counted, using Beckman Coulter Particles Counter Z1, every 24 hours for 6 days (section 2.2.11).



**Figure 4.7:** The effect of EZH2 knockdown on HCC1937EV28 cells and HCC1937BR69 cell growth rate. Cells were infected using lentiviral particles carrying either the shRNA oligo targeting EZH2 or the GIPZ shRNA control. Five days after puromycin selection,  $2.0 \times 10^5$  cells were plated in 6cm plates. Cells were trypsinized and counted every 24 hours using the Beckman Coulter Particles Counter Z1. The graph is representative of an experiment performed three times in triplicate ( $n=9$ ; error bars  $\pm$ SEM). **A.** EZH2 knockdown in HCC1937BR69 cells. **B.** EZH2 knockdown in HCC1937 EV28 cells. See appendix B for raw data.

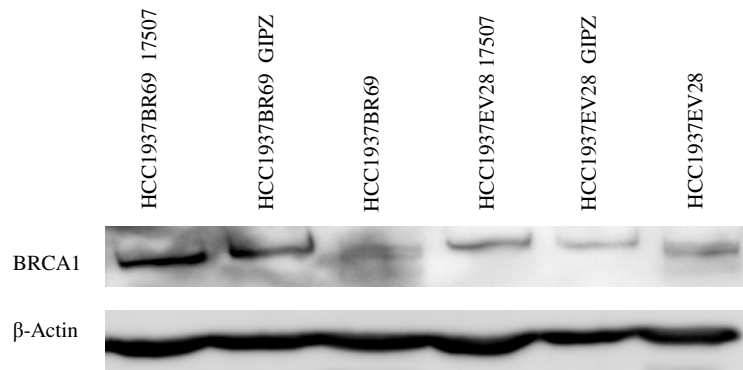
The doubling time for the non-infected HCC1937BR69 and HCC1937BR69 GIPZ cells was about 48 hours, while the HCC1937BR69 17507 cells did not show any growth. As discussed in previous chapter (section 3.4.1) an accurate estimation of doubling time for the HCC1937EV28 cells was not possible due to the high death rate of the cells. The data obtained suggest that EZH2 knockdown in HCC937EV28 cells reduces their growth rate, but the inhibition effect is much stronger in HCC1937BR69. However, these data show that the HCC1937BR69 cells have higher proliferation rate compared to HCC1937EV28 cells. These results strongly

disagree with previously reported data (Promkan et al. 2009) and suggest that the HCC1937BR69 cells might have lost BRCA1 expression with passaging (see section 4.3).

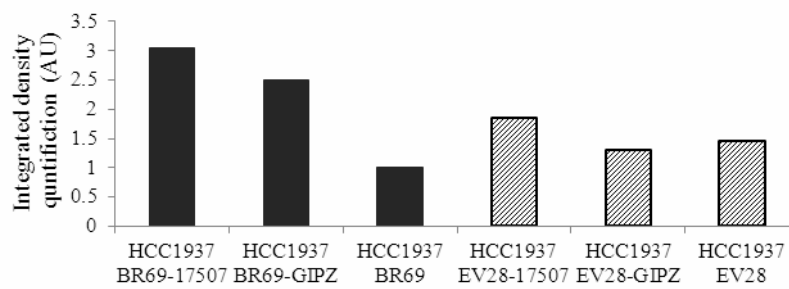
### **4.3 Evaluation of BRCA1 expression after EZH2 knockdown in late passage HCC1937EV28 and HCC1937BR69**

In order to test whether the HCC1937BR69 cells have lost the expression of BRCA1 with passaging, western blot analysis was performed. Total protein extracted from non-infected HCC1937BR69, HCC1937BR69 GIPZ, HCC1937BR69 17507, non-infected HCC1937EV28, HCC1937EV28 GIPZ and HCC1937EV28 17507 cells was analyzed (Figure 4.8). For each sample, 30 µg of proteins were loaded onto a 8% SDS acrylamide resolving gel and western blot analysis was performed as described in materials and methods (section 2.2.9.1 – 2.2.9.3). The BRCA1 antibody D9 from Santa Cruz (against the C-terminal domain of the protein) was used for the analysis. The expression of BRCA1 protein was higher in HCC1937BR69 17507 and HCC1937BR69 GIPZ cells compared to non infected HCC1937EV28, HCC1937EV28 17507 and HCC1937EV28 GIPZ cells. However, no increase in BRCA1 expression was detected when the non-infected HCC1937BR69 cells were compared to the non-infected HCC1937EV28 cells (Figure 4.8). The difference in the expression of BRCA1 between HCC1937BR69 cells and HCC1937EV28 cells initially observed (Figure 4.1) was no longer detected. These results suggest that the HCC1937BR69 cells have lost the expression of BRCA1 during passaging and shed light on the unexpected results obtained when Boyden chamber migration assay and proliferation assay were performed (Figure 4.6 and 4.7).

A



B



**Figure 4.8:** BRCA1 expression level in HCC1937EV28 cells and HCC1937BR69 cells after EZH2 knockdown. Representative image and graph of western blot analysis performed three times. **A.** Extracted proteins were resolved by 8 % SDS-PAGE and membranes were probed with the indicated antibodies.  $\beta$ -Actin was used as a loading control. **B.** Results obtained after integrated density quantification of A using the software ImageJ (measurements expressed in arbitrary units).

#### 4.4 Discussion

Many lines of evidence support the idea that EZH2 might represent a good target for the development of a novel strategy for breast cancer treatment (Gonzalez et al. 2009; Kunju et al. 2011; Li et al. 2009; Puppe et al. 2009; Sun et al. 2009; Wicha 2009; Xiao 2011). Knowing the exact role of EZH2 in tumorigenesis and its potential interaction with other pathways is crucial in order to develop a selected therapy and identify what group of tumours might benefit from it. Recently the idea of a possible interaction between EZH2 and BRCA1 has emerged, suggesting that the beneficial effect of EZH2 down-regulation in breast cancer might be dependent on BRCA1 status (Gonzalez et al. 2009; Puppe et al. 2009; Wicha 2009).

The over-expression of EZH2 is associated with several tumour characteristics, i.e. high proliferation, aggressiveness and metastatic behaviour. In this thesis no experiments were performed in order to test whether these tumour characteristics would be modified by down-regulation of EZH2 in cells grown *in vivo* in whole organisms. However, some features of neoplastic cells were tested, such as proliferation rate, anchorage independent growth and migration.

EZH2 knockdown significantly reduced the ability of anchorage-independent growth in cells carrying mutated/non-functional BRCA1 but not in cells carrying wild type BRCA1 (Figure 4.3). When the number of colonies formed by the two cell lines HCC1937EV28 and HCC1937BR69 (mutated BRCA1 and wild type BRCA1 respectively) were compared, a significant difference was observed: HCC1937EV28 cells form a higher number of colonies compared to HCC1937BR69. Therefore, the difference observed, upon EZH2 knockdown, may simply be due to the fact that re-expression of wild type BRCA1 causes loss of the ability of anchorage independent growth. Indeed several studies have reported that expression of wild type BRCA1



inhibits the malignant behaviour of cancer cell lines, including the ability of cancer cells of growing in an anchorage-independent manner (El-Tanani et al. 2006; Promkan et al. 2009; Tassone et al. 2003). The exact mechanism through which BRCA1 inhibits malignant behaviour is not fully understood. It might act through several different regulators i.e. by maintaining a correct level of cyclin-dependent kinase inhibitor p21/Waf1 and p27 (Promkan et al. 2009), or by maintaining correct expression pattern of P-cadherin, Caveolin-1 and E-cadherin (Yasmeen et al. 2008). It has also been shown that in rats, BRCA1 represses neoplastic transformation by repression of the adhesive glycoprophosphoprotein, OPN (El-Tanani et al. 2004; Oates et al. 1996). However, some cell lines, even though expressing wild type BRCA1, retain the ability of growing in anchorage-independent manner. MDA-MB-231 cells are a good example (see previous chapter), they have a wild type BRCA1, but they maintain the ability of forming colonies in soft agar, suggesting that expression of wild type BRCA1 might not be the only regulator of anchorage-independent growth.

Results obtained with HCC1937EV28 cells and HCC1937BR69 cells were contradictory across different assays (migration and proliferation assays) and, in some cases, in disagreement with data reported in other studies (Coene et al. 2011; Promkan et al. 2009). Using the scratch assay, a 22% reduction in cell migration upon EZH2 knockdown was observed in cells carrying the wild type BRCA1, whereas a 10% reduction in cell migration upon EZH2 knockdown was observed in cells with mutated BRCA1 (Figure 4.4 and 4.5). Using the transwell assay, a reduction of cell migration upon EZH2 knockdown was observed only in cells with wild type BRCA1 (Figure 4.6). In addition, migration appeared to be drastically reduced in HCC1937EV28 GIPZ cells (Figure 4.6 B), suggesting that the infection control vector GIPZ had an effect on cell migration and that a different vector control

should have been tested (see discussion chapter 3). The highly mortality rate observed for HCC1937EV28 cells could have caused some errors when migrating cells were counted (see section 3.4.1). In order to clarify whether the results obtained were due to experimental error or were due to the infection control vector GIPZ, further experiments using a different control vector would be required. In addition, data obtained with the transwell Boyden chamber assay showed that the migratory ability of HCC1937BR69 cells was higher than migratory ability of HCC1937EV28 cells (Figure 4.6), suggesting that reconstitution of BRCA1 increases migration of HCC1937 cells. This is in contrast with data recently reported (Promkan et al. 2009). A recent study has shown that re-expression of wild type BRCA1 in HCC1937 cells significantly reduces their migration, suggesting a new role for BRCA1 in regulation of motility of breast cancer cells (Coene et al. 2011). According to this study, wild type BRCA1 exerts its tumour suppression activity through the interaction between its N-terminal domain BRCT (Glover 2006) and the ezrin-radixin-moesin (ERM) complex which plays a role in cell motility regulation (Ou-Yang et al. 2011).

Data presented in this thesis show that EZH2 knockdown drastically reduces the proliferation rate of HCC1937 breast cancer cells in the presence of wild type BRCA1 while it has less stronger effect in the presence of mutated BRCA1 (Figure 4.7). However, the HCC1937EV28 cells appeared to grow more slowly than the HCC1937BR69 cells. These data are also in disagreement with data previously reported (Coene et al. 2011; Promkan et al. 2009)

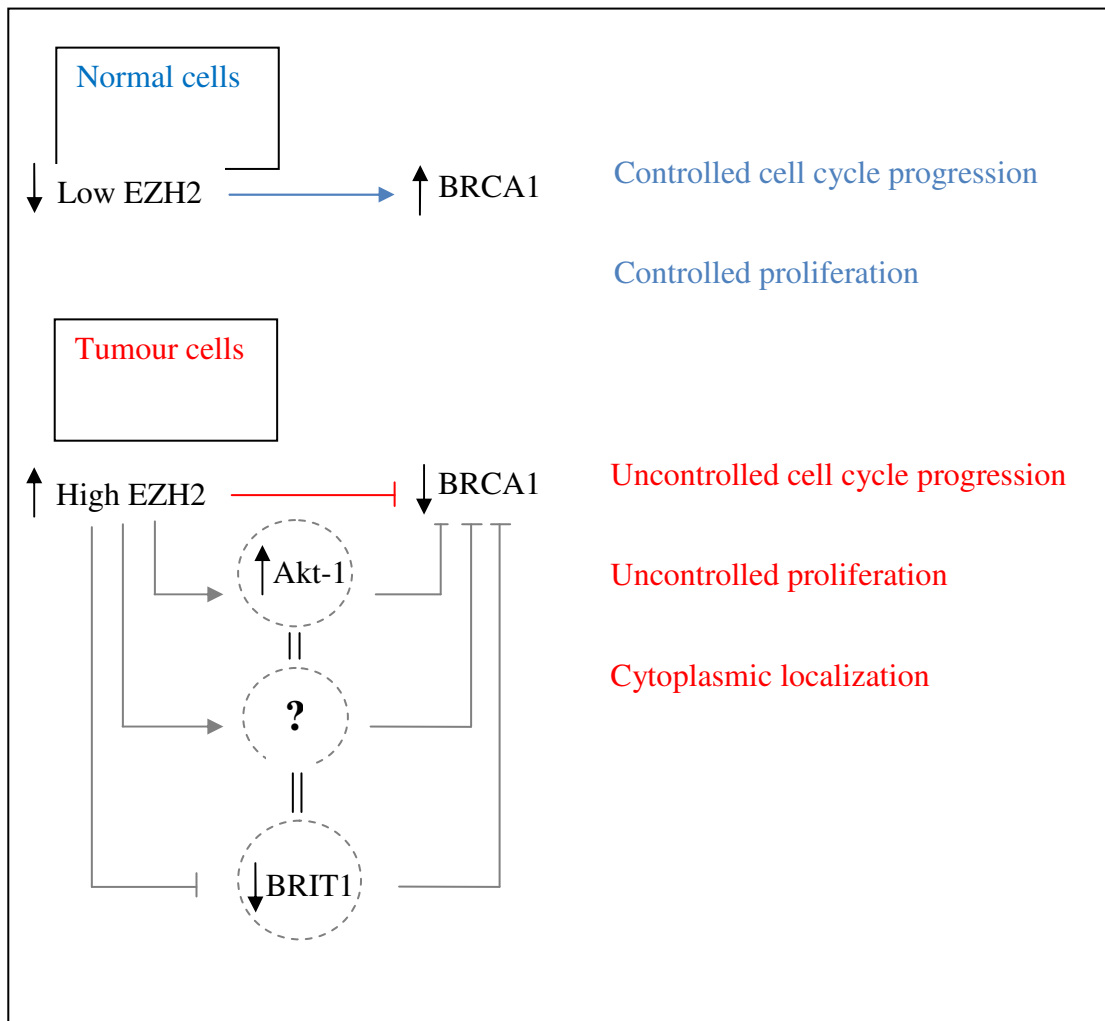
The contradictory results obtained using the transwell assay and the proliferation assay strongly suggests that the HCC1937BR69 cells had reverted back to their original phenotype (i.e. they have lost BRCA1 expression during passaging). Indeed, an expression analysis of later passage cell showed no difference in BRCA1

expression between HCC1937BR69 and HCC1937EV28 cells (Figure 4.8), confirming that HCC1937BR69 cells had lost the expression of BRCA1 during passaging.

The loss of BRCA1 expression in HCC1937BR69 cells and the contradictory results obtained are not sufficient to further clarify the relationship between EZH2 and BRCA1 status. Due to the lack of HCC1937 cells expressing BRCA1 and to the fact that a new study investigating the relationship between EZH2 and BRCA1 was published, no further experiments were performed. Gonzalez et al. proposed that EZH2 knockdown acts through BRCA1 and pBRCA1 in regulating cell proliferation and G2/M phase (Gonzalez et al. 2009). In normal mammary cells the low level of EZH2 regulates cell proliferation via modulation of BRCA1 and pBRCA1 s1423 level and consequently Cdc2-Cyclin B1 complex level. EZH2 over-expression induces inhibition of BRCA1 and pBRCA1 s1423 level which leads to upregulation of Cdc2-Cyclin B1 complex and uncontrolled cell proliferation. These data, together with the observation that a direct physical interaction between EZH2 and BRCA1 has not been reported suggests that other factors are involved. One of the major roles assigned to BRCA1 is linked to DNA damage response, therefore maintenance of genome stability. A followup study suggested that activation of the PI3K/Akt-1 signalling pathway could be the link between EZH2 and BRCA1 (Gonzalez et al. 2011). They showed that up-regulation of EZH2 in non-tumourigenic cells promotes aneuploidy, genomic instability and translocation of BRCA1 from nucleus to the cytoplasm and that down-regulation of EZH2 exerts opposite effects, and they proposed that Akt-1 functions as an intermediate in this process. In fact, Akt activation has been shown to induce BRCA1 cytoplasmic localization (Plo et al.

2008) and over-expression of EZH2 induces activation of Akt-1 (Gonzalez et al. 2011) with a consequent influence on the intracellular localization of BRCA1.

It would be interesting to investigate the possible role of other factors. Recently, BRIT1/MCPH has been identified as new regulator of the DNA damage response, via the ATM/ATR pathway (Chaplet et al. 2006; Peng et al. 2009). BRIT1 binds to SWI/SNF, a complex involved in chromosomal relaxation which is also an antagonist of polycomb complexes (Wilson et al. 2010). In addition, BRIT1-deficient cells show premature chromosome condensation (Jeffers et al. 2008; Wood et al. 2008). Interestingly, it has been shown that BRIT1 regulates the expression of BRCA1 and Chk1 (Lin et al. 2005) and it is required for regulation of G2/M cell cycle in response to ionizing radiation. Reduced levels of BRIT1 cause a reduction of BRCA1 and Chk1 expression levels and consequently loss of G2/M checkpoint control. The connection between BRIT1 and G2/M cell cycle control, DNA damage response, and chromatin status, together with high density array comparative genomic hybridization data showing a reduced level of BRIT1 in several human cancers, including ovarian, and in breast cancer cell lines (Lin et al. 2010; Rai et al. 2006), suggests that BRIT1 might be an alternative mechanistic link between EZH2 and BRCA1 (Figure 4.10). One of the mechanisms through which EZH2 has been proposed to be involved in tumourigenesis and cancer progression is silencing of tumour suppressor genes and BRIT1 might be one of the possible tumour suppressors down-regulated by EZH2.



**Figure 4.9:** Schematic representation of possible interaction between BRCA1 and EZH2. In normal breast epithelial cells low levels of EZH2 regulates the level of BRCA1 resulting in controlled proliferation and cell cycle progression. In tumour cells over-expression of EZH2 causes down-regulation of BRCA1 resulting in uncontrolled and cell cycle progression. A direct interaction between EZH2 and BRCA1 has not been reported, therefore other factors might be involved. The PI3K/Akt-1 signalling pathway has been proposed as the link between EZH2 and BRCA1 (Gonzalez et al. 2011). However, other factors, *i.e.* BRIT1, might be involved (see text for details).

## **5 Chapter 5: THE EFFECT OF ECTOPIC EXPRESSION OF CBX POLYCOMB PROTEINS IN MCF10A CELLS**

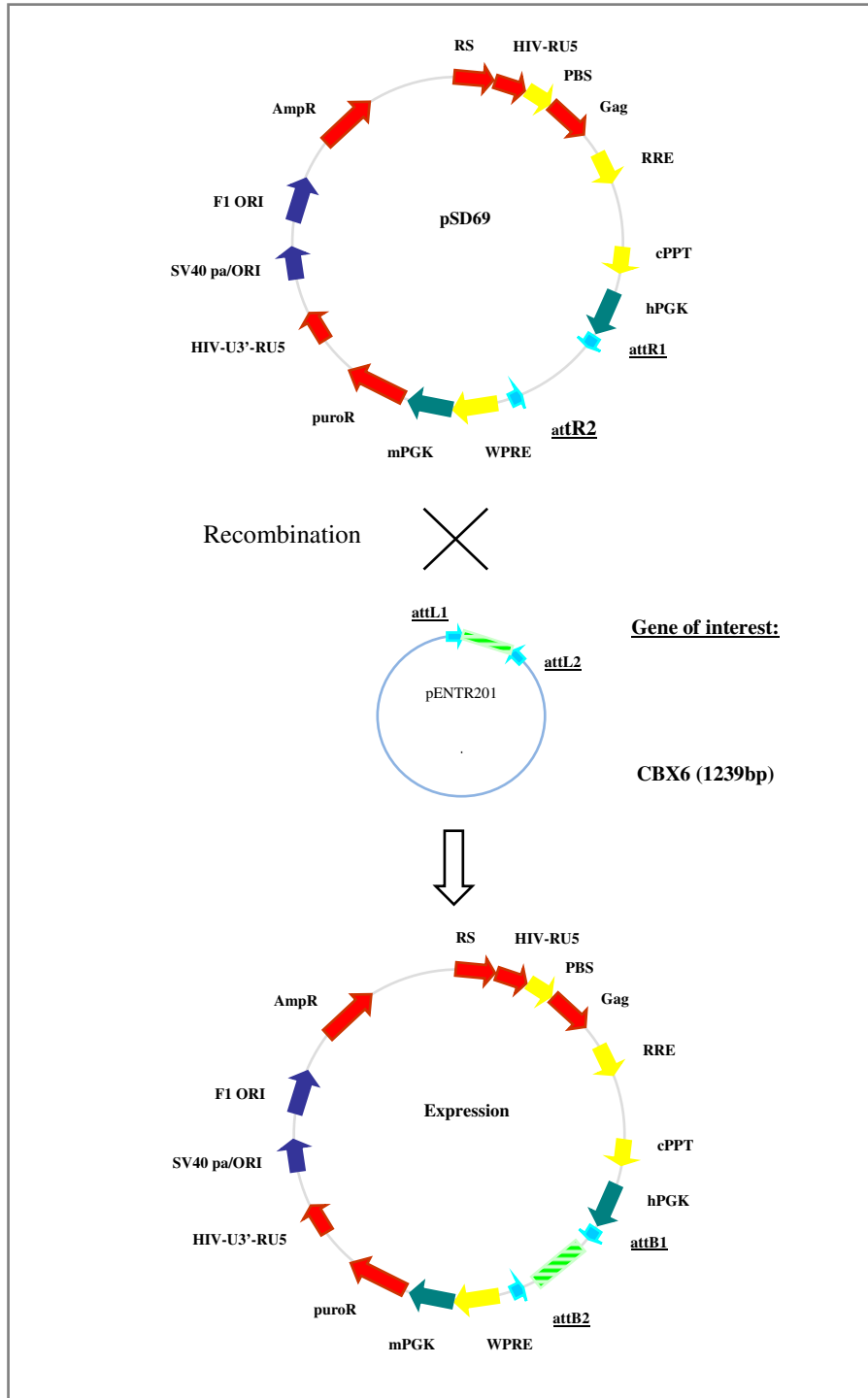
### **5.1 Introduction**

The human chromodomain-containing protein, CBX8 (also known as PC3, RC1, HPC3) has been identified a decade ago as part of the polycomb repressive complex 1 (PRC1); its well conserved C-terminal domain (14 aa) binds to other components of PRC1, such as RING1 and BMI1 and it has been shown to be involved in repression of transcriptional activity (Bardos et al. 2000). CBX8 and its 4 homologues, CBX2, CBX4, CBX6 and CBX7, have not been completely characterized and very little is known about their role in normal and transformed cells.

This chapter describes the effect of expressing various chromobox-containing proteins (CBX) in immortalized breast epithelial cells MCF10A. In order to assess whether and to what extent CBX proteins are involved in breast cancer initiation three different CBX proteins (CBX6, CBX7 and CBX8) were ectopically expressed in MCF10A cells, and their ability to alter cell growth was tested. Out of the three CBX proteins tested, CBX8 significantly altered cell growth of MCF10A cells, and therefore was chosen for further analysis. The ability of CBX8 to alter cell migration and anchorage-independent growth was also assessed. MCF10A cells are considered to be similar to normal cells having a near-diploid karyotype, few genetic changes typical of culture-adapted breast epithelial cells and loss of the p16 locus but normal p53 expression. MCF10A cells do not form colonies in soft agar, and they do not grow in immuno-compromised mice (Imbalzano et al. 2009).

## 5.2 CBX proteins overexpression in MCF10A cells

MCF10A cells were obtained from ATCC and grown in media according to ATCC instructions (section 2.2.8.1) and were passaged every 2 or 3 days. CBX protein ectopic expression was carried out using a second generation lentiviral system. Three different CBX lentiviral constructs were prepared as described below (see also section 2.2.1). Plasmids containing CBX6 (HsCD00045684), CBX7 (HsCD00079712) and CBX8 (HsCD00079972), were obtained from Harvard plasmID clone resource (<http://plasmid.med.harvard.edu/PLASMID/>). Each plasmid consist of the recombinant Gateway donor clone pDONR221 containing respectively CBX6 cDNA (<http://www.ncbi.nlm.nih.gov/gene/23466>) or CBX7 cDNA (<http://www.ncbi.nlm.nih.gov/gene/23492>) or CBX8 cDNA (<http://www.ncbi.nlm.nih.gov/gene/57332>). CBX7 and CBX8-containing plasmids did not contain a STOP codon and so one was created by PCR amplification from the pDONR221-CBX template, and a purified cDNA was inserted into the pDONR201 donor vector using the Gateway cloning system (section 2.2.1.1 – 2.2.1.5). Since the CBX6 ORF contained a STOP codon, it was used directly in the Gateway cloning system. The destination vector used for constructing the expression clone was pSD69, a lentiviral vector obtained from Prof. R. Iggo (Figure 5.1). The resulting expression clones were named pSD69-CBX6, pSD69-CBX7 and pSD69-CBX8 (Figure 5.1). pSD3 was the lentiviral vector used as a control (obtained from Prof. Iggo).

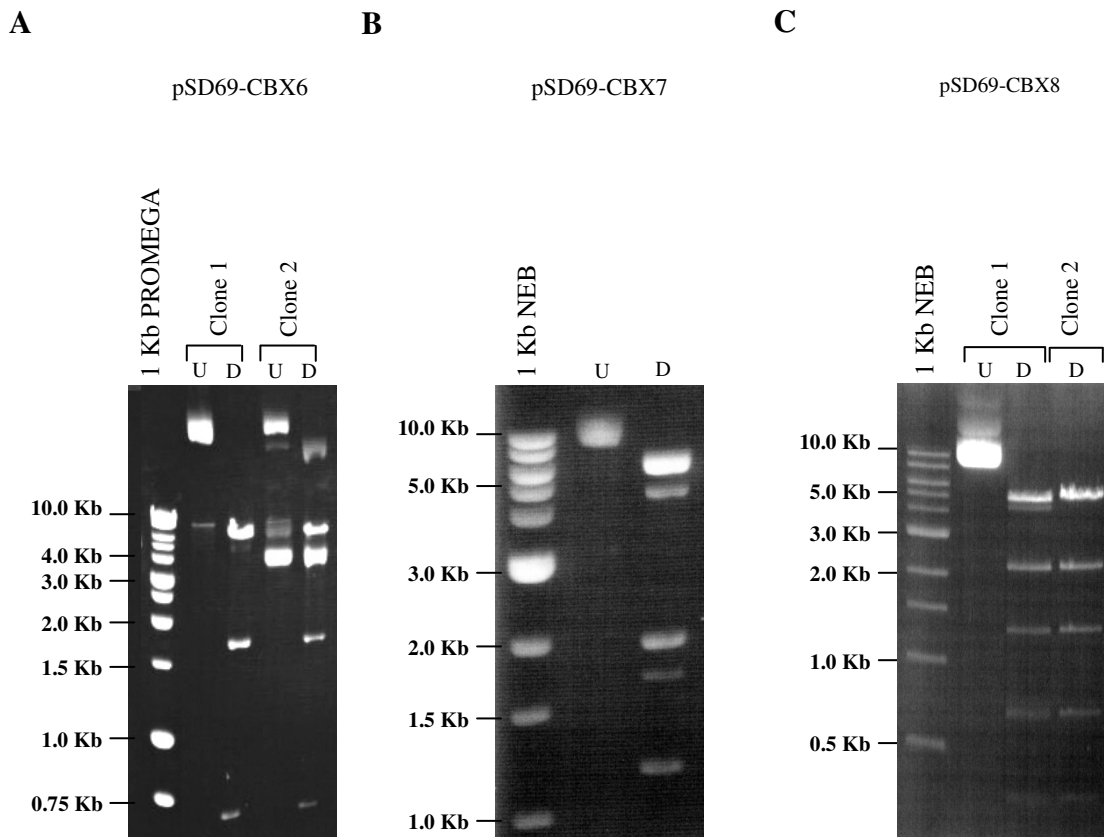


**Figure 5.1:** An outline of the cloning method used to produce expression clones carrying the CBX genes tested (see also materials and methods paragraph 2.2). The 9535bp pSD69 plasmid contains Rous Sarcoma Virus (RSV) enhancer/promoter, HIV-RU5, Rev-responsive element (RRE), the human phosphoglycerokinase gene (PGK) promoter, and Mouse PGK promoter, HIV-U3'RU5, the SV40 pA/ORI, the F1 ORI, the puromycin resistance gene, the ampicillin resistance gene and the Gateway attB cassette. The entry plasmid (pENTR201 clone) contains the Gateway attL cassette and carries the gene of interest (CBX6, CBX7 or CBX8). The expression clone is the result of recombination between the empty expression clone pSD69 and the entry clone pENTR201 via the gateway cassettes (attL x attR).



Inserts size were verified by restriction enzyme digestion (Figure 5.2) and DNA was sent to the DNA sequencing Services, University of Dundee and sequenced using the primers OSD48 and OSD49 (section 2.2.1.9). pSD69-CBX6 (9089bp) plasmid DNA was digested using the EcoRI restriction enzyme producing three fragments of 697 bp, 1714 bp and 6678 bp respectively. pSD69-CBX7 (8636bp) plasmid was digested using two restriction enzymes, BglIII and EcoRI, producing four fragments of 3773 bp, 1946 bp, 1706 bp, and 1192 bp respectively. pSD69-CBX8 (9020) was digested using two restriction enzymes BamHI and PstI, producing four fragments of 4822 bp, 2198 bp, 1252 bp and 848 bp respectively (Figure 5.2).

293T packaging cells were used for production of lentivirus particles. Cells were transfected with the required amount of packaging constructs providing the viral coat (pVF11 and pVF16) and viral expression constructs using Mirus *TransIT®-LT1* transfection reagent (section 2.2.3). A small amount of packaged lentiviruses was used for titration (section 2.2.5) and only batches containing between  $10^8$  and  $10^7$  infectious particles per ml were used for MCF10A infection, which was carried out as described in materials and methods (section 2.2.4). At four days post infection, MCF10A cells were treated with an amount of puromycin previously found to be sufficient to kill non-infected cells (Debnath et al. 2003). MCF10A cells over-expressing CBX proteins were subsequently grown in the appropriate growth media (section 2.2.8.1) containing the selective antibiotic puromycin.

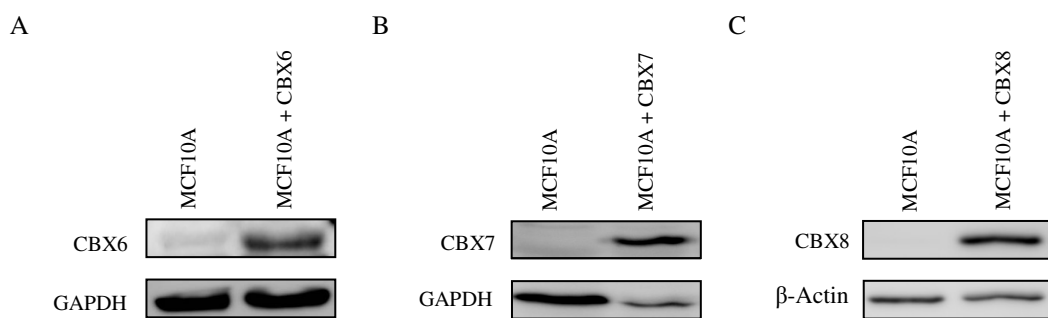


**Figure 5.2:** Analysis of Plasmid DNA by Restriction Digestion. The presence of CBX genes within the pSD69 expression clone was verified by restriction enzymes digestion. **A.** pSD69-CBX6 digested with EcoRI; two different clones are shown. The uncut (U) plasmid is 9089 bp and three fragments are expected (697, 1714 and 6678 bp respectively) after restriction enzyme digestion (D). **B.** pSD69-CBX7 digested with BglII and EcoRI. The uncut (U) plasmid is 8636 bp and four fragments are expected (3773, 1946, 1706, and 1192 bp respectively) after restriction enzyme digestion (D). **C.** pSD69-CBX8 digested with BamHI and PstI. The uncut (U) plasmid is 9020 bp and four fragments are expected (4822, 2198, 1252 and 848bp respectively); after restriction enzyme digestion (D). Two digested clones are shown.

### 5.2.1 Evaluating expression of ectopic CBX proteins

To confirm the ectopic expression of CBX proteins, western blot analysis was performed on several samples derived from independent batches of infections of MCF10A cells (Figure 5.3). Total protein extracted from different aliquots of MCF10A cells infected either with CBX6 or CBX7 or CBX8 expressing vectors were analyzed. For each sample, 30  $\mu$ g of proteins were loaded onto a 10% SDS acrylamide resolving gel and western blot analysis was performed as described in

materials and methods (section 2.2.9.1 – 2.2.9.3). Western blot analysis showed a significant increase of CBX6 protein expression in cells infected with CBX6 containing lentivirus compared to non-infected MCF10A cells (Figure 5.3 A). Similarly, a significant increase of CBX7 protein expression in cells infected with CBX7 containing lentivirus was detected by western blot analysis when compared to non-infected MCF10A cells (Figure 5.3B). MCF10A cells infected with CBX8 containing lentivirus also showed a robust increase of CBX8 protein expression when compared to non-infected MCF10A cells, as shown by western analysis (Figure 5.3C). The batches of cells over-expressing the three different CBX proteins were used for growth curve analysis.

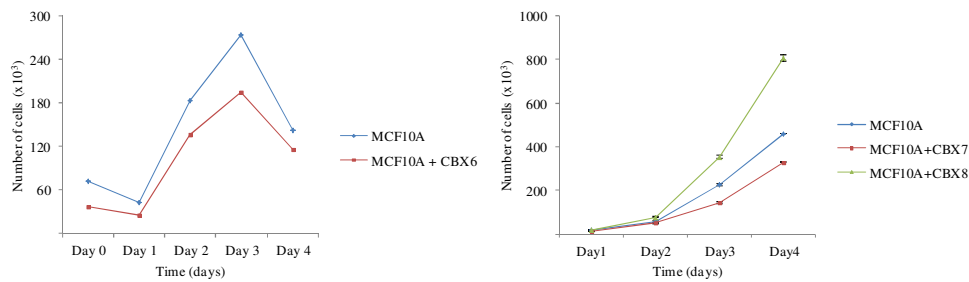


**Figure 5.3:** Analysis of CBX6, CBX7 and CBX8 protein expression in MCF10A cells after lentiviral infection. MCF10A cells were infected using lentiviral particles carrying CBX6 (A), CBX7 (B) or CBX8 (C) cDNA. Infected cells were harvested 5 days after puro selection and extracted proteins were resolved by 10 % SDS-PAGE and membranes were probed with the indicated antibodies.  $\beta$ -Actin or GAPDH antibodies were used as loading controls. Images are representative of western blot analysis performed three times.

## 5.2.2 Evaluating the effect of CBX proteins over-expression on MCF10A cell proliferation

To test whether ectopic expression of CBX proteins have any impact on immortalized epithelial breast cells proliferation, a series of growth curve experiments were performed (section 2.2.11). Non-infected MCF10A cells,

MCF10A cells infected either with CBX6, or CBX7 or CBX8 were seeded in 6-wells plates, starting with either  $3.0 \times 10^4$  cells for CBX6 or  $1.5 \times 10^4$  for CBX7 and CBX8. Cells were trypsinized and counted, using Beckman Coulter Particles Counter Z1, every 48 hours (Figure 5.4).

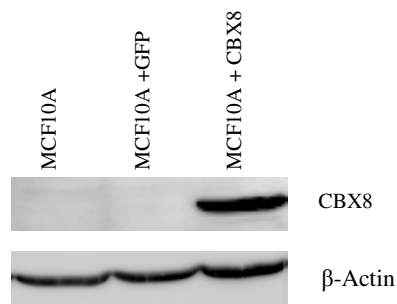


**Figure 5.4:** Growth analysis of MCF10A cells overexpressing CBX6, CBX7 or CBX8 protein. A. The growth rate of MCF10A overexpressing CBX6 is compared to the growth rate of parental cell line. B. The growth rate of MCF10A overexpressing either CBX7 or CBX8 is compared with the growth rate of parental cell line. Cells were infected using lentiviral particles carrying either CBX8 cDNA, CBX7 cDNA or CBX8 cDNA and, 5 days after puro selection, cells were plated in 6 wells plates. Cells were trypsinized and counted every 48 hours using the Beckman Coulter Particles Counter Z1. The experiments were performed in triplicate and each replica was counted three times. The graph is representative of one experiment performed three times in triplicate (n=9; error bars $\pm$ SEM). See appendix C for raw data.

The cell proliferation rate of non-infected MCF10A cells varied between experiments, ranging from 24 hours to 48 hours. The cell proliferation rate of MCF10A cells over-expressing CBX6 was similar to the cell proliferation rate of uninfected MCF10A cells (Figure 5.4A). The doubling time was about 24 hours for both MCF10A over-expressing CBX6 and non-infected MCF10A cells. A similar scenario was observed for MCF10A overexpressing CBX7. The doubling time was about 48 hours for both MCF10A over-expressing CBX7 and non-infected MCF10A cells (Figure 5.4B). However, the cell proliferation rate of MCF10A cells over-expressing CBX8 was higher compared to non infected MCF10A cells (Figure 5.4B). The doubling time for MCF10A cells overexpressing CBX8 was about 35 hours, ten hours shorter than non-infected MCF10A or MCF10A over-expressing CBX7. Of the

three CBX proteins analyzed, only CBX8 showed ability to alter proliferation rate of MCF10A cells, therefore, it was chosen for further experiments. However, the fact that the experiment was carried out without using a vector control represents an issue, and in all the subsequent experiments performed a vector control containing GFP was used.

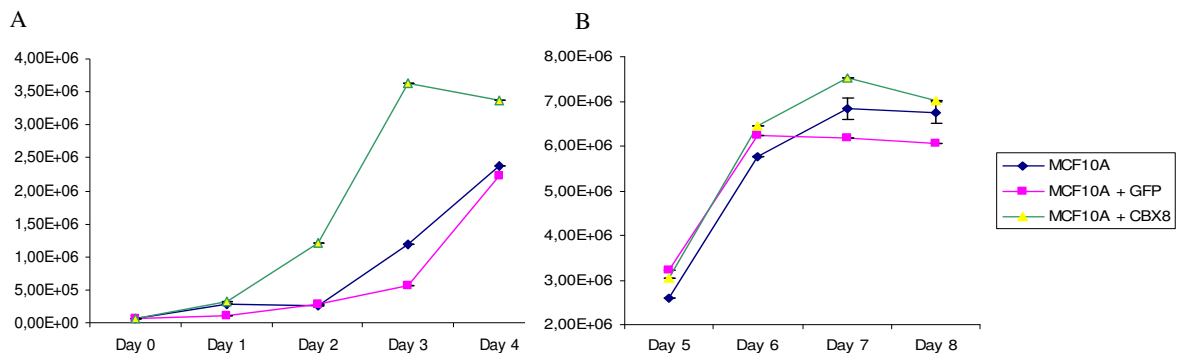
To test whether CBX8 acts as cell growth promoting gene in normal epithelial breast cells and whether it has a long term effect or a more temporary effect, additional growth curve analysis experiments were performed. The experiments were performed using non infected MCF10A cells, MCF10A cells over-expressing CBX8 and MCF10A cells expressing GFP as a control. The over-expression of CBX8 was confirmed by western blot analysis (Figure 5.5).



**Figure 5.5** Analysis of CBX8 protein expression in MCF10A cells after lentiviral infection. MCF10A cells were infected using lentiviral particles carrying CBX8 cDNA. Infected cells were harvested 5 days after puro selection and extracted proteins were resolved by 10 % SDS-PAGE. Membranes were probed with the indicated antibodies.  $\beta$ -Actin antibody was used as loading controls.

The ability of CBX8 to increase MCF10A cells growth rate was clearly visible between day one and day three, supporting first set of experiments. The doubling time of MCF10A over-expressing CBX8 was about 12 hours, while the doubling time of non-infected MCF10A and MCF10A expressing GFP was about 30

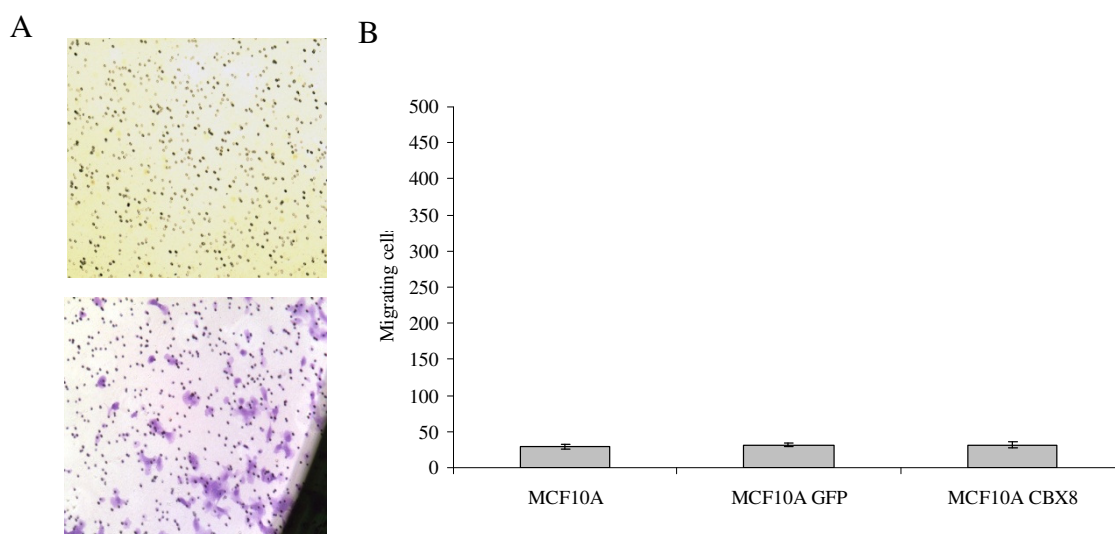
hours (Figure 5.6 A). At day five, however, MCF10A cells over-expressing CBX8 proliferation rate was significantly reduced and the growth rates of the three cells type were similar. This was probably due to the fact that MCF10A over-expressing CBX8 cells had reached confluency and had stopped growing. Cells were then transferred to larger plates and their growth rate measured (Figure 5.6 B) from day five on the growth rate of MCF10A over-expressing CBX8 was similar to growth rate of non-infected MCF10A cells or MCF10A expressing GFP. These data suggest that CBX8 initially increases the proliferation rate of MCF10A cells, but this is only a transient or temporary effect. Other genetic and/or epigenetic changes might be required for the high proliferative phenotype to become stable.



**Figure 5.6:** Growth analysis of MCF10A cells overexpressing CBX8 protein. The growth rate of MCF10A cells overexpressing CBX8 was compared to growth rate of non infected MCF10A cells and MCF10A cells expressing GFP. **A.** Cells were infected using lentiviral particles carrying either CBX8 cDNA or GFP cDNA control and, 5 days after puro selection, cells were plated in 6cm plates. Cells were trypsinized and counted every 24 hours using the Beckman Coulter Particles Counter Z1. **B.** Cells were trypsinized and transferred to larger plates. Cells were coated every 24 hours using the Beckman Coulter Particles Counter Z1. The graphs are representative of one experiment performed three times in triplicate (n=9; error bars±SEM). See appendix C for raw data.

### **5.2.3 CBX8 over-expression has no effect on MCF10A cell migration**

As normal cells transform into tumour cells, they acquire new characteristics and properties. One new property tumour cells exhibit is their ability to migrate from one site to another, generally in response to chemical signal. To test whether CBX8 ectopic expression affects the ability of MCF10A cells to migrate, a transwell (Boyden chamber) assay was carried out (section 2.2.12). Non infected MCF10A cells, MCF10A cells expressing GFP and MCF10A cells expressing CBX8 were trypsinised and separately resuspended in serum free and EGF free growth media.  $2.5 \times 10^4$  cells were added to the top of each chamber. After 18-24 hours, three randomly selected fields in the central part of the chamber were chosen and number of migrating cells was counted. For each cell type the experiment was performed in triplicate a total of 9 counts were made (3 counts for each chamber) which were then averaged in order to give an estimation of the number of migrating cells. The stained cells which were often observed in the peripheral area of the chamber were considered to be background noise and only the central part of the chamber was taken into consideration (Figure 5.7). Non infected MCF10A cells and MCF10A cells infected with GFP control did not migrate across the PET membrane, as expected. MCF10A cells over-expressing CBX8 did not show any difference compared to the uninfected and control cells. Ectopic expression of CBX8 did not affect MCF10A migratory behavior using modified Boyden chamber assay.



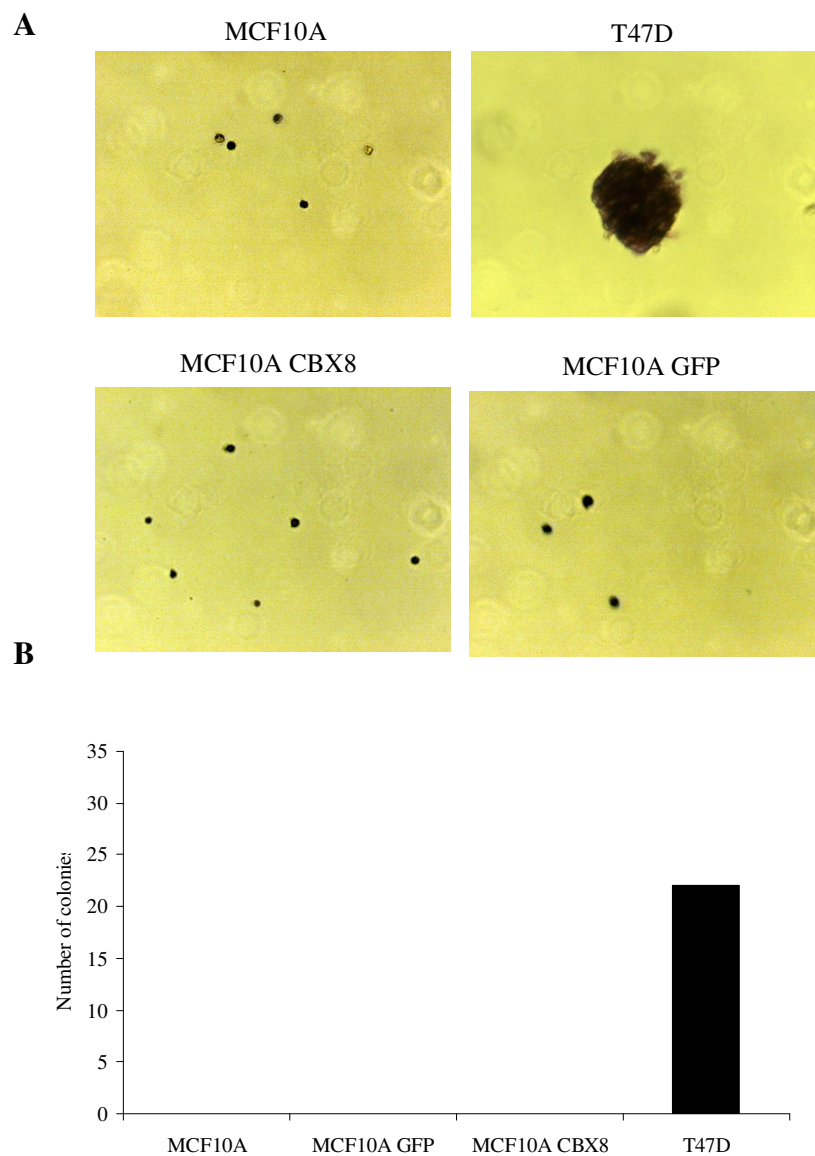
**Figure 5.7:** The effect of over-expression of CBX8 on MCF10A cells as assessed by transwell Boyden chamber assay. Cells were infected using lentiviral particles carrying either CBX8 cDNA or the GFP control control. 5 days after puromycin selection  $2.5 \times 10^4$  cells were resuspended in serum free and EGF free media and added to the top of a Boyden chamber. After 24 hours migrating cells were stained with crystal violet and counted under microscope. **A.** Image showing the difference between the peripheral and central area of the chamber. **B.** The graphs are representative of single experiments performed three times in triplicate (n=9; error bars  $\pm$ SEM).

#### 5.2.4 CBX8 over-expression has no effect on MCF10A anchorage-independent growth

To determine whether the immortalized epithelial breast cells MCF10A acquire the ability of anchorage independent growth due to ectopic expression of CBX8, a colony formation in soft agar assay was performed. Non infected MCF10A cells, MCF10A cells expressing GFP, MCF10A cells expressing CBX8 and T47D cells (positive control) were tested in triplicate (section 2.2.13). For each replicate 5000 cells were used and the cells were grown at 37 °C for 21 days. After 21 days, colonies were counted. MCF10A cells did not form colonies in soft agar, as expected, while the positive control T47D breast cancer cells did form colonies (Figure 5.8 A and B) as previously reported (Kuppumbatti et al. 2001). Both,



MCF10A cells infected with CBX8 and MCF10A cells infected with the GFP control, did not form colonies in soft agar, in each of the three wells analyzed. The ectopic expression of CBX8 alone is not sufficient to confer the ability to form colonies in soft agar to MCF10A cells .



**Figure 5.8:** The effect of ectopic expression of CBX8 on anchorage-independent growth in MCF10A cells. Cells were infected using lentiviral particles carrying either CBX8 or the GFP control. Five days after puro selection cells were seeded in 3.5% low melting agarose containing growth media plus additives. **A.** After 21 days colonies were stained with INT and counted. **B.** The graph is representative of an experiment performed three times in triplicate. T47D cells were used as positive control.

### 5.3 Discussion

Several studies have shown the involvement of two major polycomb proteins in breast cancer. Over-expression of EZH2, the main component of PRC2, has been related to breast cancer as well as over-expression on BMI1, the main component of PRC1 (Bezsonova et al. 2009; Elsheikh et al. 2009; Feinberg et al. 2006; Kerppola 2009; Kingston et al. 1996; Kirmizis et al. 2003; Kleer et al. 2003; Raaphorst et al. 2000; Ren et al. 2008; Schumacher et al. 1997; Simon 2003; van Kemenade et al. 2001; Varambally et al. 2002; Whitcomb et al. 2007). It is not clear whether altered expression of other polycomb proteins plays any role in breast cancer. CBX protein mis-regulation can alter the expression pattern of key regulator genes, such as genes encoding for factors involved in cell cycle regulation, DNA repair or development. Therefore, they might have a role in tumorigenesis. A clear association between CBX proteins and neoplastic transformation in various tissue has been already shown in several studies (Bernard et al. 2005; Dietrich et al. 2007; Federico et al. 2009; Gil et al. 2004; Kaustov et al.; Kerppola 2009; Kingston et al. 1996; Leeb et al.; Li et al. 2007; Maertens et al. 2009; Min et al. 2003; Mohammad et al. 2009; Pallante et al. 2008; Scott et al. 2007; Simon & Tamkun 2002; Vincenz & Kerppola 2008), but very little is known about the role of CBX proteins in breast cancer. In this chapter, the effect of ectopic expression of CBX8 in human immortalized epithelial cells was investigated. A preliminary analysis of three CBX proteins was first performed. The CBX proteins chosen were CBX6, CBX7 and CBX8. There is no evidence supporting the role of CBX6 in cancer (Dodds et al. 1997; Gil et al. 2004; Vincenz & Kerppola 2008). More information about CBX7 and CBX8 is available, they both alter cell proliferation, acting through repression of p16(Ink4a)/Rb and the Arf/p53 pathways, causing abnormal proliferation and neoplastic transformation in different

type of cells such as prostate cells, gastric cells, lymphocytes and fibroblasts (Bernard et al. 2005; Bracken & Helin 2009; Dietrich et al. 2007; Gil et al. 2004; Kirmizis et al. 2003; Maertens et al. 2009; Mohammad et al. 2009; Pallante et al. 2008; Scott et al. 2007; Vincenz & Kerppola 2008; Zhang et al.) .

The preliminary results obtained with ectopic expression of CBX6, CBX7 and CBX8 have shown that CBX proteins have different effects on MCF10A cell proliferation (Figure 5.4). The three CBX proteins were successfully ectopically expressed in MCF10A cells as shown by western blot analysis (Figure 5.3), but only CBX8 over-expression significantly increased the proliferation rate of MCF10A cells (Figure 5.4 - 5.5), therefore only CBX8 protein was chosen for further experiments. As already mentioned in section 5.2.2, this first set of experimentst lacks the presence of a control vector. It would have been appropriate to use a control vector in order to confirm that the increase of proliferation rate of MCF10A cells was specifically caused by the ectopic expression of CBX8. In the later experiments carried out to investigate the effect of CBX8, a GFP containing vector was used as a control (Figure 5.5). The growth curve experiments showed that ectopic expression of CBX8 significantly increased the proliferation rate of MCF10A cells, suggesting that CBX8 might act as a cell growth promoting gene in MCF10A cells (Figure 5.5) and it might contribute to cancer initiation. However, when the effect of CBX8 over-expression on cell migration and anchorage independent growth was tested, no significant changes were observed (Figure 4.6 and 4.7). CBX8 alone is not sufficient to confer anchorage-independent growth, neither it is sufficient to influence the ability of MCF10A cells to migrate. One of the reasons why these results were observed might be due to the fact that MCF10A cells infected with CBX8, after a short period of time tend to revert back to their wild type phenotype. Late passage MCF10A cells

could have lost CBX8 expression which could be the reason why CBX8 did not show any effect when anchorage-independent growth and migration ability was tested. However, other possibilities must be considered, it is unlikely that the over-expression of one single gene could cause transformation..

CBX8 over-expression might be just enough to increase the proliferation rate of MCF10A cells but it is not sufficient to completely transform the cells. MCF10A cells are immortalized cells which exhibit few abnormalities, altered karyotype and loss of both copies of the p16. However, these abnormalities and the introduction of a single potential oncogene are not enough to transform the cells. A similar scenario was observed when the potential oncogenic activity of BMI1 in epithelial breast cells was tested (Datta et al. 2007). The study showed that over-expression of BMI1 alone does not have any effect on proliferation activity and ability to form colonies in soft agar of immortalized breast epithelial cells. However when a second oncogene, HRAS, was introduced the cells became highly proliferative and were able to form colonies in soft agar. Moreover, when the BMI1/HRAS over-expressing cells were injected into nude mice, they were able to form tumors. In this chapter the ability of CBX8 to transform MCF10A cells was tested and the results obtained showed that CBX8 promotes transient cell proliferation when over-expressed in MCF10A cells, but its over-expression alone is not sufficient to transform the cells. Neoplastic transformation is a multistage process, a series of genetic and epigenetic changes, with or without exposure to carcinogens, is required for a cell to become malignant (Boehm et al. 2005; Loeb et al. 2003).

Other oncogenic stimuli and genetic/epigenetic changes, along with CBX8 de-regulation, may be required in order to observe more definitive switch towards the cancerous phenotype. This hypothesis will be further investigated in chapter six.

## **6 CHAPTER 6: THE EFFECT OF ECTOPIC EXPRESSION OF CBX8 AND BMI1 IN BREAST PRIMARY EPITHELIAL CELLS**

### **6.1 Introduction**

In this chapter the effect of ectopic expression of CBX8 in two different types of breast epithelial cells was investigated: BPEC (breast primary epithelial cells) (Ince et al. 2007) and B42CP cells (Unger et al. 2010). The aim of the experiments performed with BPEC was to analyse the effect of ectopic expression of CBX8 and compare it to the effect of ectopic expression of BMI1. The aim of the experiments performed with B42CP cells was to better clarify the effect of ectopic expression of CBX8 in immortalized breast epithelial cells. CBX8 belong to PRC1 and its key component is BMI1 (Sparmann & van Lohuizen 2006). BMI1 is an oncogene frequently over-expressed in many different types of cancer, including breast cancer (Bea et al. 2001; Duss et al. 2007; Kim et al. 2004a; Kim et al. 2004b; van Kemenade et al. 2001; Vonlanthen et al. 2001). Previous studies have shown that BMI1 binds and down-regulates the INK4A/ARF locus and its over-expression prevents senescence in human fibroblasts, rodent fibroblasts and human mammary epithelial cells (Dimri et al. 2002; Itahana et al. 2003; Jacobs et al. 1999). BMI1, however, can also lead to neoplastic transformation via INK4a/ARF-independent mechanism (Dimri et al. 2002). In MCF10A immortalized non tumourigenic breast cells lacking both p16 and p19, for instance, BMI1 over-expression, along with G12V mutant of H-Ras, is sufficient for oncogenic transformation (Datta et al. 2007).

Previous studies have investigated the role of CBX8 over-expression in human and mouse fibroblasts, showing that CBX8 promotes abnormal proliferation and leads to neoplastic transformation through direct binding and repression of INK4A/ARF locus, and through regulation of other genes important for cell growth

and survival (Dietrich et al. 2007). In the previous chapter, the effect of CBX8 ectopic expression in MCF10A immortalized non tumorigenic breast epithelial cells was investigated. When over-expressed in MCF10A cells, CBX8 promotes transient cell proliferation, but it does not promote neoplastic transformation (see chapter 5). MCF10A cells lack expression of both p16 and p19 and to explore the possibility that CBX8 acts through the INK4A/ARF locus in breast epithelial cells, cells with an intact INK4A/ARF locus may be required. However, most tumour cell lines have altered p16 expression. A good alternative system is the use of primary epithelial cells. Breast primary epithelial cells (BPEC) derived from reduction mammoplasty of healthy women (see section 2.2.8.4) were used for the first set of experiments performed in this chapter. Using lentiviral and retroviral particles, BPEC were infected with different combination of genes, including BMI1 and CBX8. BPEC expressing GFP and BPEC over-expressing human telomerase reverse transcriptase (hTERT) and Harvey rat sarcoma viral oncogene homolog (HRAS), called respectively BPEC plus GFP and BPEC plus hTERT/HRAS were used as controls. The different sets of genes chosen were: BMI1 along with ER $\alpha$  (BPEC plus BMI1/ER $\alpha$ ), BMI1 along with ER $\alpha$ , hTERT and HRAS (BPEC plus BMI1/ER $\alpha$ /hTERT/HRAS), CBX8 either alone or with ER $\alpha$  (BPEC plus CBX8 and BPEC plus CBX8/ER $\alpha$  respectively), CBX8 along with hTERT and HRAS (BPEC plus CBX8/hTERT/HRAS) and CBX8 along with ER $\alpha$ , hTERT and HRAS (BPEC plus CBX8/ER $\alpha$ /hTERT/HRAS).

Infected and non-infected breast mammary epithelial cells were observed every day and morphological changes were annotated (see appendix D). Protein expression analysis was performed by western blot and, where enough cells were

available, they were characterised by immunofluorescence assay, proliferation assay and soft agar assay.

Due to the high variability of the system used for growing BPEC, and several technical difficulties, it was not possible to fully evaluate to effect of CBX8 ectopic expression in BPEC and compare it to the effect of BMI1 ectopic expression. Therefore, the attention was focused only on CBX8, using the well characterised human mammary epithelial cell line B42CP. B42CP cells are cells isolated from tumour free breast tissue that have been immortalized by transduction with hTERT (Unger et al., 2010). Since B42CP is a well established and characterized cell line, there was no limitation in terms of number of cells available for invitro assays. The different sets of genes chosen to infect B42CP cells were HRAS alone, HRAS/CBX8 and HRAS/CBX8/ER $\alpha$ . After ectopic expression of the appropriate transgenes, the following assays were performed: proliferation assay, soft agar assay and migration assay.

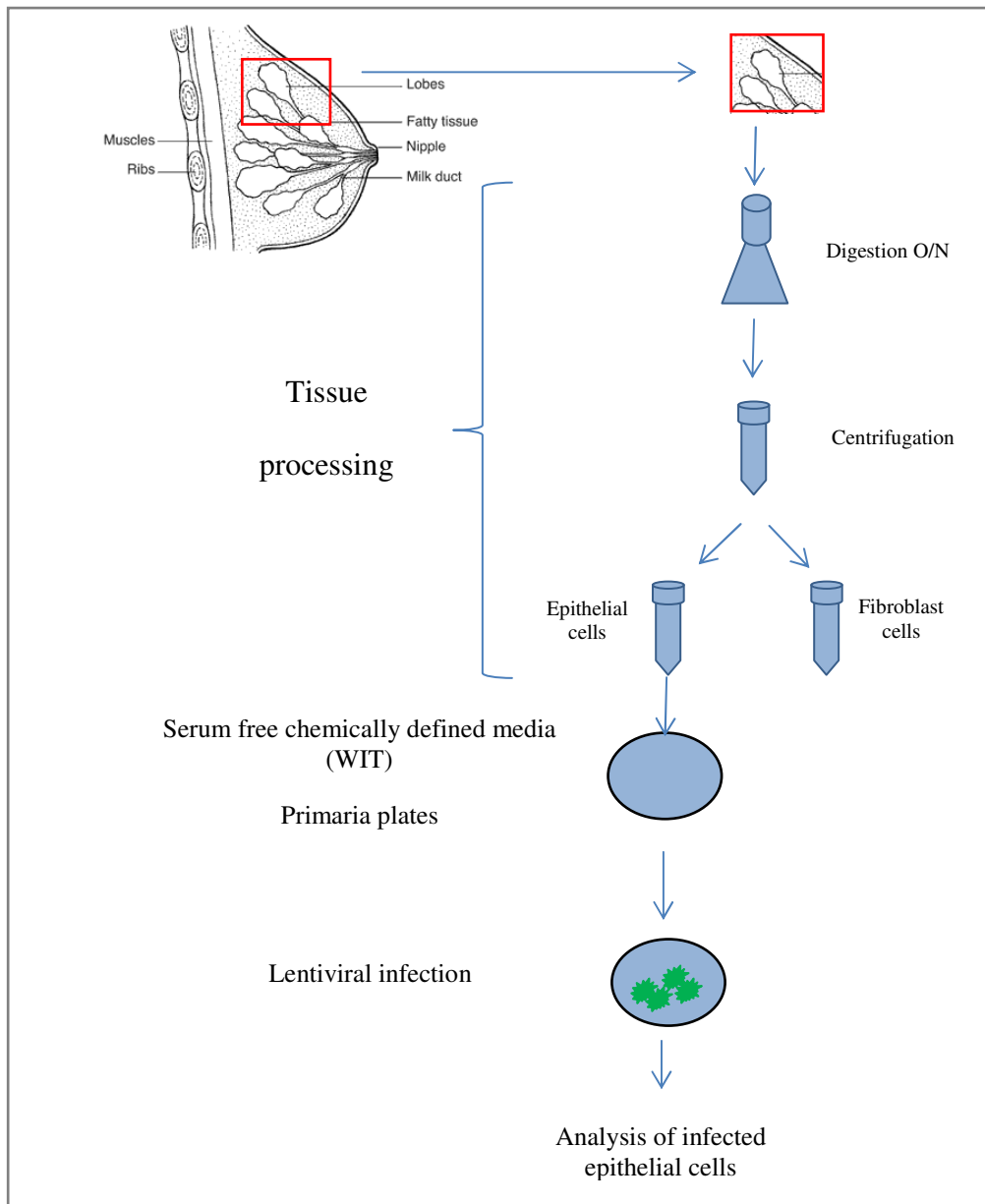
## **6.2 BPEC conditions allow growth of a mixed heterogeneous population of cells**

Reduction mammoplasty tissue obtained from Ninewells hospital, Dundee was processed and digested overnight (see section 2.2.8.4 and Figure 6.1). The resulting multicellular structures, organoids, were then cultured using 2 different protocols: Duss et al. protocol or Ince et al. protocol (Duss et al. 2007; Ince et al. 2007). The human mammary epithelial cells (HMEC), obtained and cultured according to the Duss et al. protocol, had a very short survival time. Cells were passaged once and medium was changed every two days, but after one week the

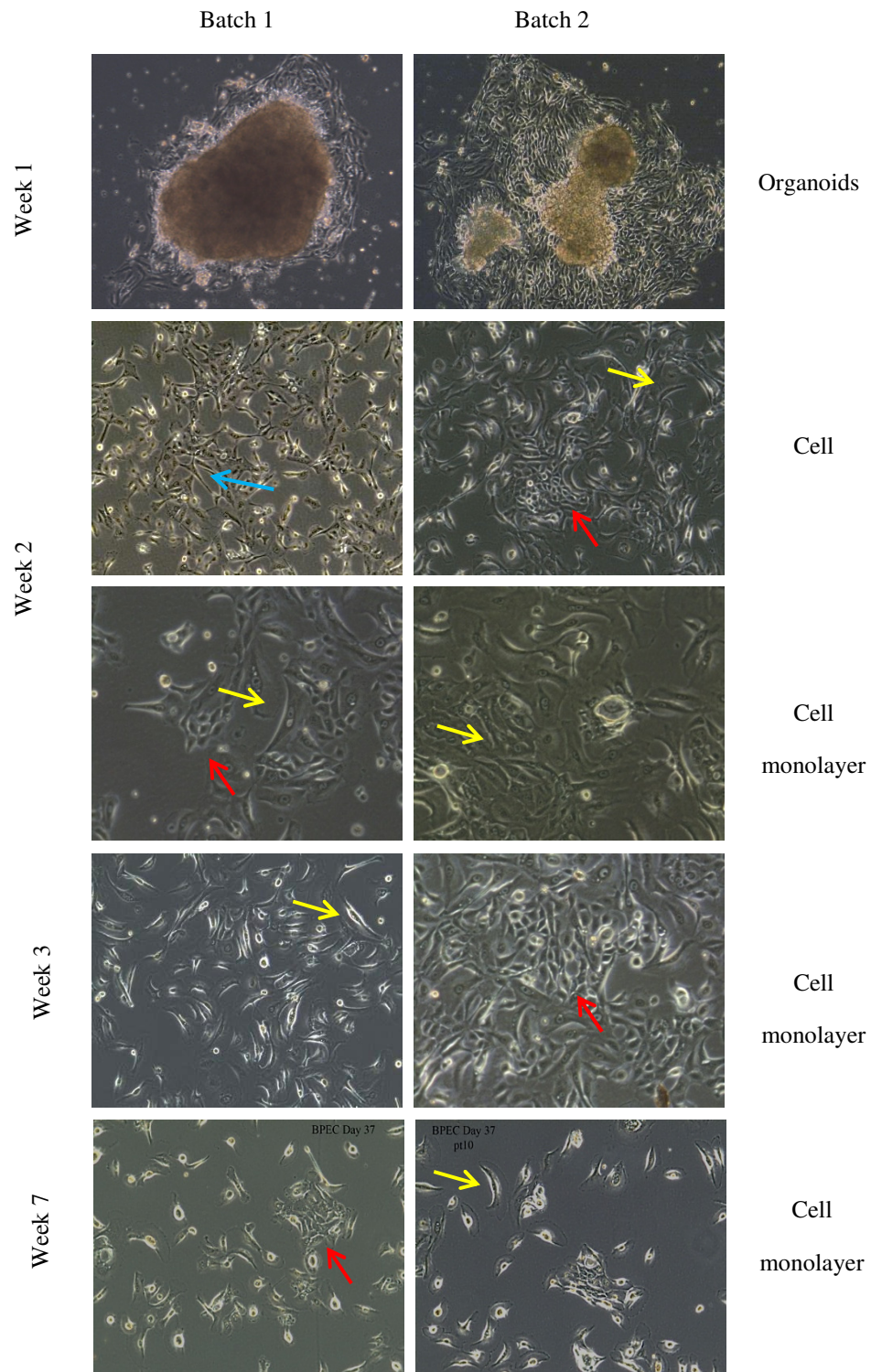
HMEC stopped proliferating and insufficient cells were available to carry out lentiviral infection (see appendix D).

The Ince et al. protocol produced a greater number of cells. Breast Primary Epithelial Cells (BPEC), obtained and cultured according to the Ince et al. protocol were cultured in the chemically defined serum free WIT media, passaged every four or five days and observed at regular intervals (see section 2.2.8.4). Organoids of different sizes were visible for the first 5 or 6 days and a monolayer of cells started to clearly appear at day 4 (Figure 6.2). The organoids cultured in WIT media produced a heterogeneous population of cells. At day 10 at least three morphologically distinct types of cell were present, which were defined as: “stellate cells”, “epithelial-like cells” and “elongated cells” (Figure 6.2). “Stellate cells” represented a very small proportion of the mixed population of cells and presented morphological features resembling neuronal cells i.e. very small and characterised by the presence of two or three protrusion (Kadar et al. 2009). The “epithelial-like cells” had a defined regular shape and their morphology resembles MCF10A morphology. The “elongated cells” were generally irregular larger cells and their shape resembled the myo-epithelial cells. The mixed population of cells were kept in culture for 7 weeks. (See appendix D for more images).

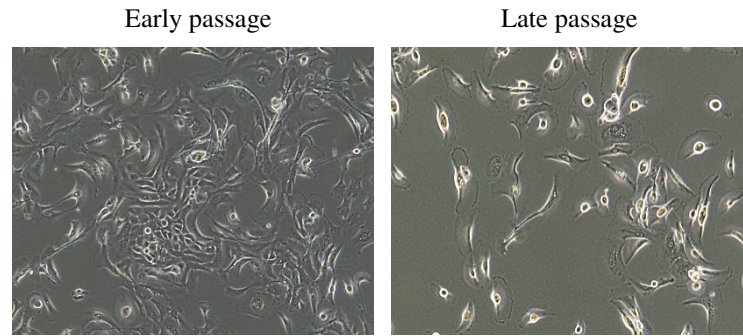




**Figure 6.1:** Schematic representation of the experimental procedure used to study the effect of CBX8 ectopic expression in normal epithelial breast cells. Reduction mammoplasty tissue from healthy women was processed overnight, the resulting multicellular structures were separated by centrifugation and cultured in a chemically defined media (WIT) on Primaria plates. The monolayer of cells obtained was then infected with lentiviral particles carrying the appropriate expression construct.

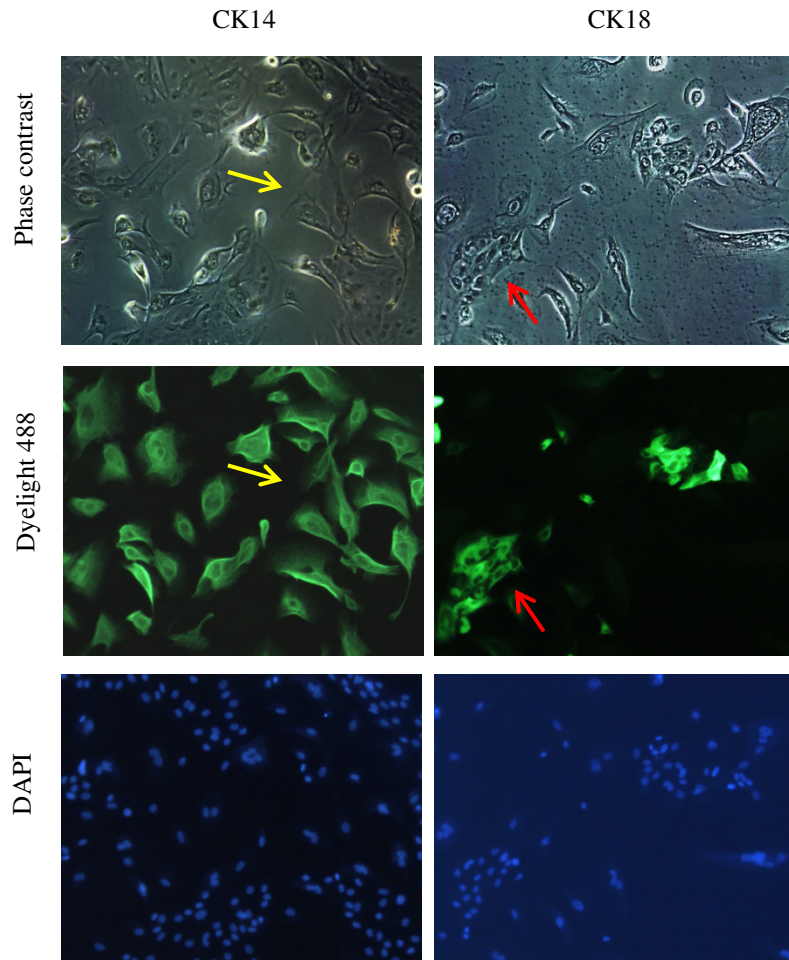


**Figure 6.2:** Images of Breast Primary Epithelial Cells (BPEC). Multicellular structures derived from reduction mammoplasty were cultured with WIT media on Primaria plates. At day four organoids of different sizes are visible and monolayer of cells starts to appear (top two images). At day ten a monolayer of morphologically heterogeneous cells is visible. Three morphologically distinct types of cells are visible: “stellate cells” which are very small and have two or three protrusions (blue arrow). “Epithelial-like” cells which are also small and have defined regular shape (red arrow). “Elongated cells” which are larger cells characterized by more irregular shape (yellow arrow). Photos were taken every 4 or 6 days using the Axiovision imaging System. Objective magnification 10X.



**Figure 6.3:** Images of early passage BPEC and late passage BPEC. Cells were grown in WIT media on primaria plates. Early passages BPEC are defined as cells grown for less than two weeks. Late passages BPEC are defined as cells grown for more than two weeks. Photos were taken every 4 or 6 days using the Axiovision imaging System. Objective magnification 10X.

In order to confirm the heterogeneity of the cell population, the expression of two cytokeratins was tested by immunofluorescence: cytokeratin 14 (CK14), a basal marker, and cytokeratin 18 (CK18), a luminal marker. The immunofluorescence analysis showed that different cell morphology corresponded to a distinct expression of cytokeratins. The “epithelial-like cells” were all CK18 positive (Figure 6.4 right panel), while the “elongated cells” were all CK14 positive (Figure 6.4, left panel) suggesting heterogeneity and the presence of a mixed population of cells. The “stellate cells” fraction was present only for the first two weeks and it was not possible to further characterize them, while the remaining two types of cells, “epithelial-like and elongated” were still distinguishable for all 7 weeks. From now on the “epithelial-like” cells will be referred to as CK18+ cells and the “elongated” cells as CK14+ cells.



**Figure 6.4:** Expression of cytokeratins in non-infected BPEC assessed by Immunofluorescence. At least two morphologically distinct cells are visible: small cells with a more regular shape resembling epithelial cells are CK18-positive (red arrow) and larger cells with an elongated shape resembling myoepithelial cells are CK14-positive (yellow arrow). No double labelling was performed. Cells were visualized using an inverted microscope (Zeiss, Axiovert 40 CFL) and digital images were acquired using Axiovision imaging System. Objective magnification 10X. See appendix D for a representative image of secondary antibody only control.

### 6.3 Evaluating the effect of BMI/ER $\alpha$ expression in BPEC

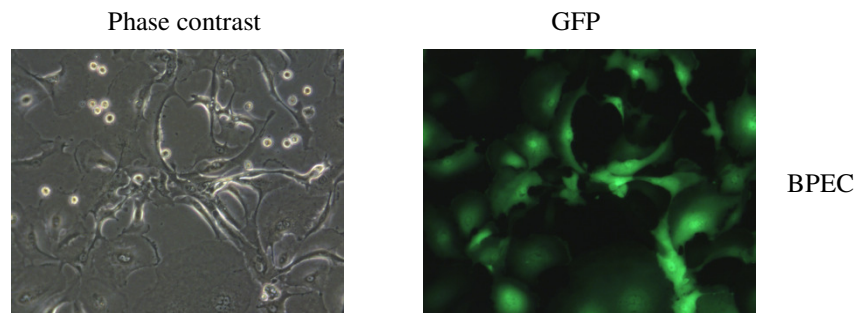
BPEC were infected with three different lentiviral particles carrying three different cDNA (the polycomb proteins BMI1, Oestrogen receptor alpha and human telomerase reverse transcriptase) and retroviral particles carrying the Harvey rat sarcoma viral oncogene homolog HRAS-G12V (see section 2.2.3, 2.2.4, 2.2.6 and 2.2.7). Two rounds of infections were performed and different batches of BPEC were infected with different combination of genes. The first round of infections consisted

of polycomb protein BMI1 along with ER $\alpha$ . Seven days later, the cells were infected with lentiviral particles containing hTERT and retroviral particles containing HRAS. BPEC infected with lentiviral particles containing GFP and BPEC infected with hTERT/HRAS were used as controls (called respectively BPEC plus GFP and BPEC plus hTERT/HRAS). Changes in morphology and cytokeratin expression were evaluated (sections 6.3.1 and 6.3.2).

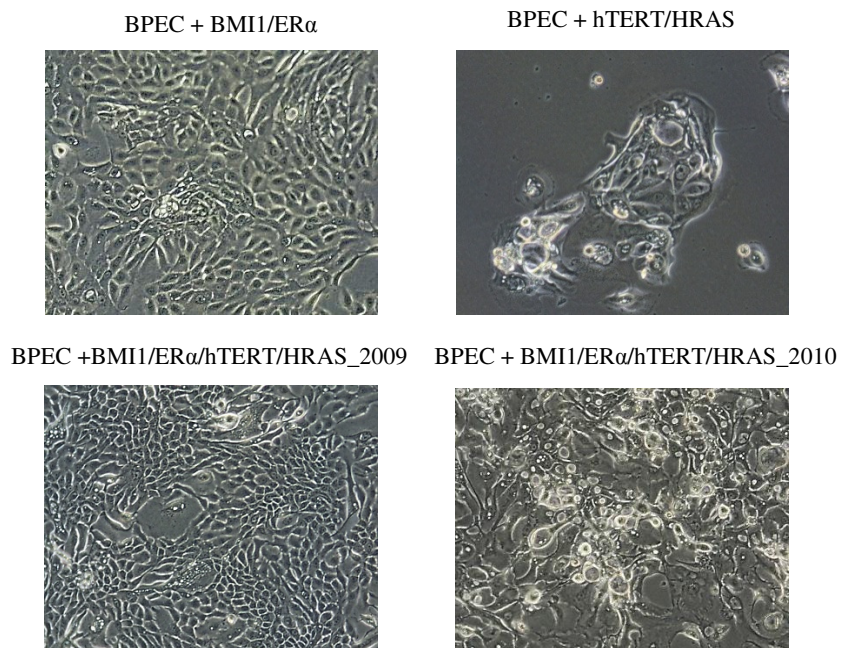
### 6.3.1 Effect on morphology

When BPEC plus GFP were analyzed no changes in cell morphology were observed, cells kept their original shape and heterogeneity (Figure 6.5), confirming that lentiviral infection *per se* did not affect cell morphology. All viral particles, lentiviral and retroviral, carry the puromycin resistance gene. Infected BPEC were selected using 2.5 µg/ml of puromycin. BPEC infected with lentiviral particles containing BMI1 and ER $\alpha$  and selected using the appropriate amount of puromycin were called BPEC plus BMI1/ER $\alpha$ . BPEC infected with lentiviral particles carrying hTERT and retroviral particles carrying HRAS and selected with the appropriate amount of puromycin were called BPEC plus hTERT/HRAS. BPEC infected with lentiviral particles containing BMI1, ER $\alpha$ , hTERT and retroviral particles carrying HRAS and selected using the appropriate amount of puromycin were called BPEC plus BMI1/ER $\alpha$ /hTERT/HRAS.

BPEC plus BMI1/ER $\alpha$  grew as a homogeneous sheet of cells (Figure 6.6). The second round of infections (hTERT and HRAS) led to contradictory results: in some cases, the cells kept their epithelial-like morphology and homogeneity, while in other cases some changes were observed. Large vacuoles started to appear inside the cells, most cells lost their regular original shape and appear similar to BPEC plus hTERT/HRAS (Figure 6.6). The BPEC that kept their original epithelial like morphology appeared to be growing faster than the BPEC that showed morphological changes. In order to distinguish between the two, they were called BPEC plus BMI1/ER $\alpha$ /hTERT/HRAS<sub>2009</sub> and BPEC plus BMI1/ER $\alpha$ /hTERT/HRAS<sub>2010</sub> respectively. The differences observed might reflect differences in the level of expression of each ectopic protein and this was investigated further in section 6.3.3.



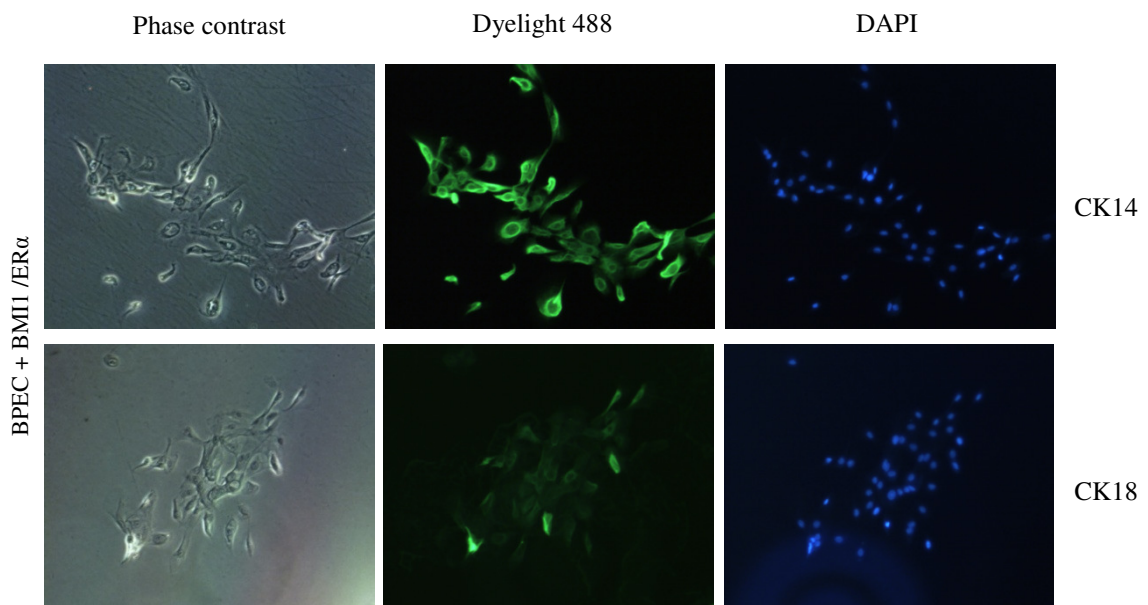
**Figure 6.5** Images of BPEC after infection with GFP. GFP expression was used as a control. The figure shows a representative image of BPEC infected with lentiviral particles containing GFP. Photos were taken 6 days after infection using the Axiovision imaging System. Objective magnification 10X.



**Figure 6.6:** Representative images of Breast Primary Epithelial Cells (BPEC) after infection with lentiviral particles carrying the appropriate expression construct (see text for details). Photos were taken using the Axiovision imaging System. Objective magnification 10X.

### 6.3.2 Effect on cytokeratin expression

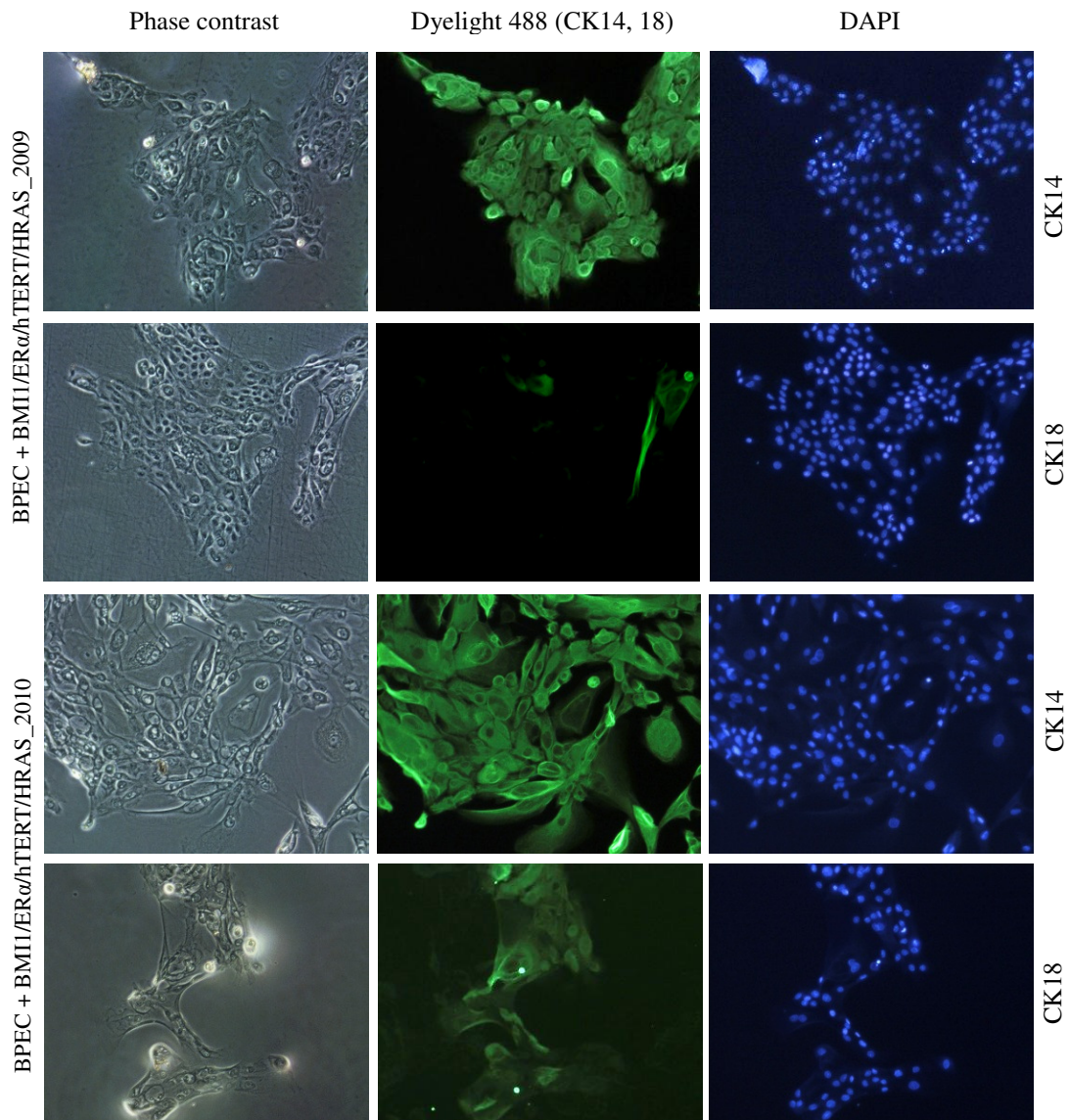
To test whether the infection of BPEC with different combination of lentiviral particles induced any change in the expression of specific basal and luminal markers, the expression of CK14 and CK18 was measured by immunofluorescence (Figure 6.7, 6.8 and 6.9). BPEC, after infection with lentiviral particles carrying BMI1 and ER $\alpha$  were analysed and they were positively stained for CK14 but not for CK18 (Figure 6.7). These cells, did lose their original heterogeneity and grew as a homogeneous epithelial-like sheet of cells.



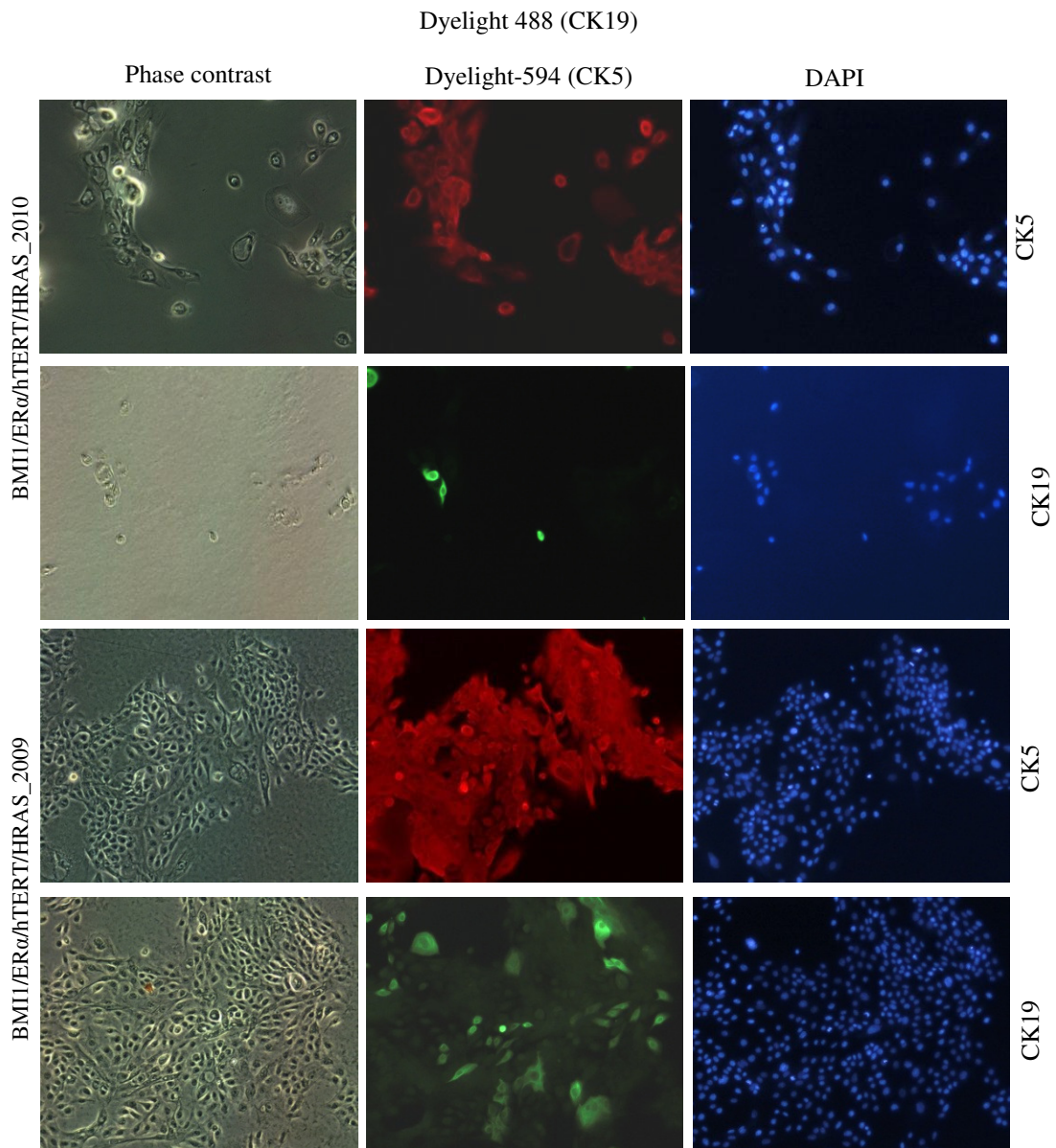
**Figure 6.7:** Expression of cytokeratins in BPEC, after infection with lentiviral particles carrying BMI1 and ER $\alpha$ , assessed by Immunofluorescence. BPEC, after infection with lentiviral particles carrying BMI1 and ER $\alpha$ , displays CK14 but not CK18 expression. Cells were visualized using an inverted microscope (Zeiss, Axiovert 40 CFL) and digital images were acquired using Axiovision imaging System. Objective magnification 10X.



Both batches of BPEC infected with viral particles carrying BMI1/ER $\alpha$ /hTERT/HRAS showed positive staining for CK14 but showed an inconsistent staining for CK18 (Figure 6.8). BPEC plus BMI1/ER $\alpha$ /hTERT/HRAS\_2010 showed positive staining for CK18 (Figure 6.8 lower panel) BPEC plus BMI1/ER $\alpha$ /hTERT/HRAS\_2009 showed no staining for CK18 (Figure 6.8 upper panel). Therefore, two additional markers were tested, CK5, a basal/myoepithelial maker and CK19, a luminal/epithelial marker. Both batches of BPEC infected with viral particles carrying BMI1/ER $\alpha$ /hTERT/HRAS showed positive staining for CK5 but showed an inconsistent staining for CK19 (Figure 6.9). BPEC plus BMI1/ER $\alpha$ /hTERT/HRAS\_2009 showed positive staining for CK19 (Figure 6.9 lower panel), while BPEC plus BMI1/ER $\alpha$ /hTERT/HRAS\_2010 showed no staining for CK19 (Figure 6.9 upper panel). These results confirmed the heterogeneity of the cells and suggested that the inconsistent results of cytokeratin analysis could be due to the fact that expression of ectopic proteins varied between the different batches of cells (see section 6.3.3).



**Figure 6.8:** Expression of cytokeratins CK14 and CK18 in BPEC after infection with viral particles carrying BMI1/ER $\alpha$ / hTERT/HRAS assessed by Immunofluorescence. Cells were infected with viral particles containing BMI1, ER $\alpha$ , hTERT and HRAS. BPECs, after infection with lentiviral particles carrying BMI1, ER $\alpha$  hTERT and HRAS, display CK14 expression. The expression of CK18 was not observed in all batches of BPECs. Single labelling only was performed. Cells were visualized using an inverted microscope (Zeiss, Axiovert 40 CFL) and digital images were acquired using Axiovision imaging System. Objective magnification 10X.

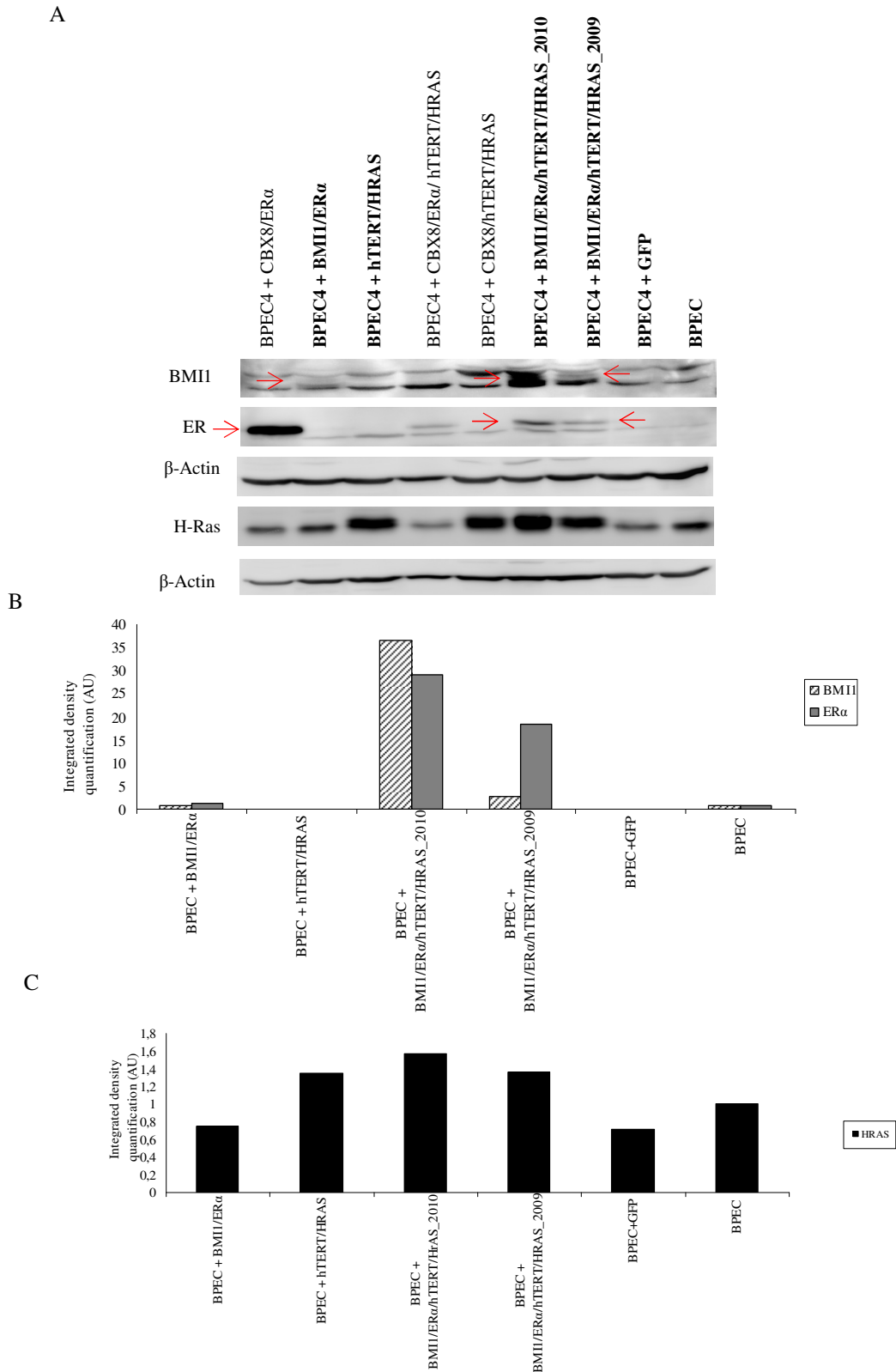


**Figure 6.9:** Expression of cytokeratins CK5 and CK19 in BPEC after infection with viral particles carrying BMI1/ER $\alpha$ / hTERT/HRAS assessed by Immunofluorescence. Cells were infected with viral particles containing BMI1, ER $\alpha$ , hTERT and HRAS. BPEC, after infection with lentiviral particles carrying BMI1, ER $\alpha$  hTERT and HRAS displays CK5 expression. The expression of CK19 was low and not observed in all batches of BPECs. Only single labelling was performed. Cells were visualized using an inverted microscope (Zeiss, Axiovert 40 CFL) and digital images were acquired using Axiovision imaging System. Objective magnification 10X.

### 6.3.3 Evaluating expression of ectopic proteins

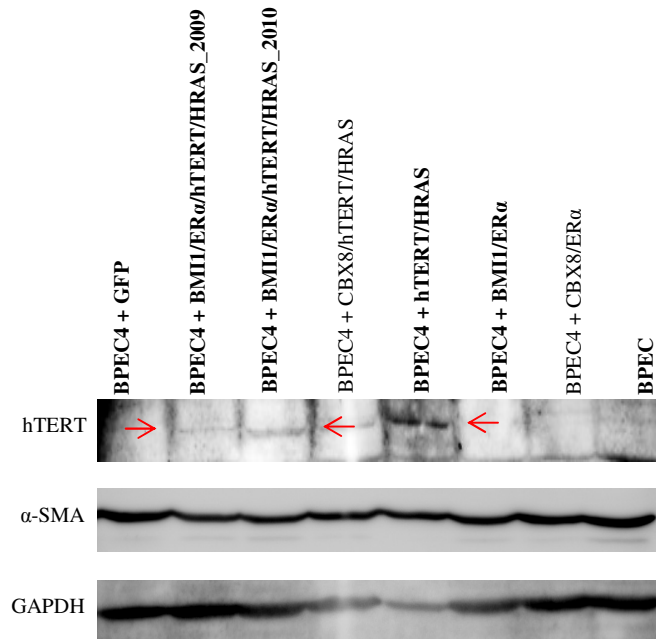
To confirm the ectopic expression of the different proteins, western blot analysis (section 2.2.9.1 – 2.2.9.3) was performed on samples derived from independent batches of infected BPECs (Figure 6.10, 6.11 and 6.12). The level of expression of BMI1, ER $\alpha$ , HRAS and hTERT varied between different batches of BPEC analyzed. Infection of BPEC with lentiviral particles containing BMI1 was carried out in three independent batches of cells (Figure 6.10A, lanes 2, 6 and 7 marked in bold). Red arrows in the figure indicate the appropriate band for BMI1. A significant increase of BMI1 protein expression was detected by western blot analysis in one (Figure 6.10.A, lane 6 and Figure 6.10.B) of the three independent batches of BPEC, corresponding to BPEC plus BMI1/ER $\alpha$ /hTERT/HRAS\_2010. The level of expression of BMI1 detected in the other two batches of BPECs was very low or absent (Figure 6.10.A, lanes 2 and 7 and Figure 6.10.B). An increase of ER $\alpha$  protein expression was detected by western blot analysis in both batches of BPEC infected with viral particles carrying BMI1/ER $\alpha$ /hTERT/HRAS (Figure 6.10.A lane 6 and 7, and Figure 6.10.B). In contrast no increase of ER $\alpha$  expression in BPEC plus BMI1/ER was detected by western blot (Figure 6.10.A lane 2, and Figure 6.10.B). A significant increase of HRAS expression was detected in both batches of BPEC plus BMI1/ER $\alpha$ /hTERT/HRAS (Figure 6.10.A lanes 6 and 7 and Figure 6.10.C). HRAS expression level in BPEC infected with lentiviral particles carrying BMI1/ER $\alpha$  was similar to endogenous level (non-infected BPEC) (Figure 6.10.A lanes 2, 8 and 9 and Figure 6.10 C).

Western blot analysis showed a very low hTERT level of expression in both batches of BPEC plus BMI1/ER $\alpha$ /hTERT/HRAS (Figure 6.11.A lanes 2 and 3, and Figure 6.11.B).

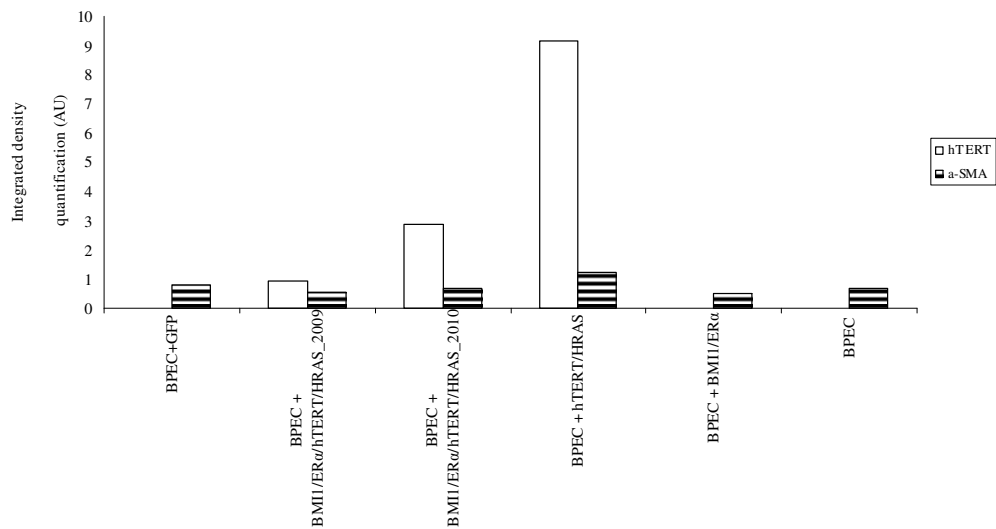


**Figure 6.10:** Analysis of BMI1, ER $\alpha$  and HRAS expression in BPEC. Representative images and graph of western blot analysis. **A.** Protein extracted from BPEC were resolved by 10% SDS-PAGE. Membranes were probed with the indicated antibodies.  $\beta$ -Actin was used as a loading control. Red arrows indicate the appropriate band for BMI1 and ER $\alpha$ . **B.** and **C.** Results obtained after integrated density quantification of **A** using the software ImageJ (measurements expressed in arbitrary units refer to cell type in bold in **A**). All values have been normalized against  $\beta$ -Actin.

A



B

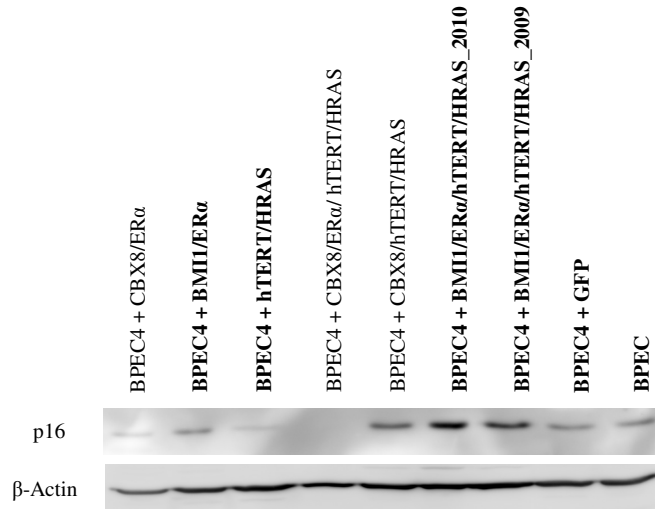


**Figure 6.11:** Analysis of hTERT and  $\alpha$ -SMA expression in BPEC. BPEC were infected using lentiviral particles carrying either hTERT or  $\alpha$ -SMA. Representative images and graph of western blot analysis performed twice. **A.** Infected cells were harvested and the extracted proteins were resolved by 10% SDS-PAGE. Membranes were probed with the indicated antibodies. Red arrows indicate the appropriate band for hTERT. GAPDH was used as a loading control. **B.** Results obtained after integrated density quantification of A using the software ImageJ (measurements expressed in arbitrary units refer to cell type in bold in A). All values have been normalized against GAPDH.

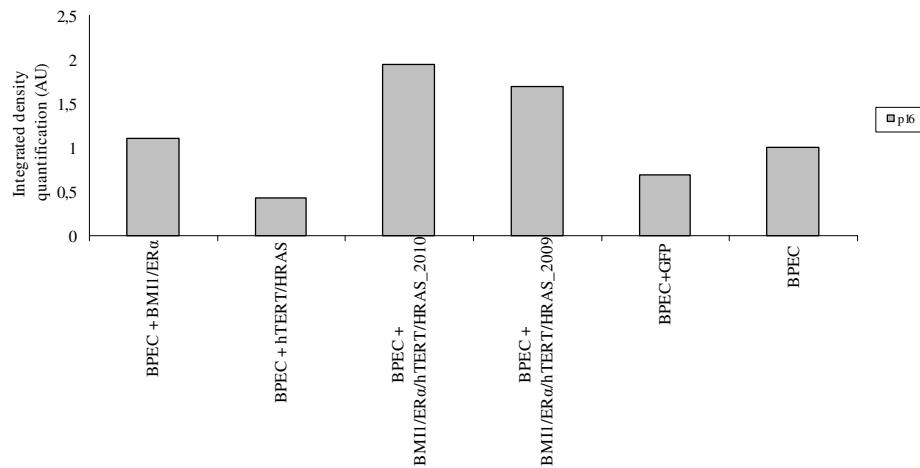
BPEC plus BMI1/ER $\alpha$ /hTERT/HRAS\_2010 showed ectopic expression of the polycomb protein BMI1. To test whether the cells obtained upon ectopic expression of BMI1 represent a distinct subtype of cell, expressing specific markers, the expression of the basal marker  $\alpha$ -smooth muscle actin ( $\alpha$ -sma) was tested. There was no difference in the level of  $\alpha$ -SMA protein expression across the different batches of BPEC (Figure 6.11.A and 6.11.B).

In order to test whether BMI1 regulates the INK4A/ARF locus in BPEC, expression of p16 was measured by western blot. A low/moderate expression of p16 protein was detected in non infected BPEC, BPEC infected with GFP, BPEC infected with HRAS/hTERT and BPEC infected with BMI1/ER $\alpha$  (Figure 6.12.A lane 2, 3, 8, 9, and Figure 6.12.B). A moderate increase in the expression of p16 protein was detected in both batches of BPECs infected with BMI1/ER $\alpha$ /hTERT/HRAS (Figure 6.12.A lane 6, 7 and Figure 6.12.B). Only BPEC plus BMI1/ER $\alpha$ /hTERT/HRAS\_2010 showed expression of BMI1, however the level of p16 expression in this batch of BPEC was similar to the level of p16 expression detected in BPEC plus BMI1/ER $\alpha$ /hTERT/HRAS\_2009, which showed a very low level of BMI1 (Figure 6.10). These data suggest that the level of p16 expression in BPEC was not affected by BMI1 expression.

A



B

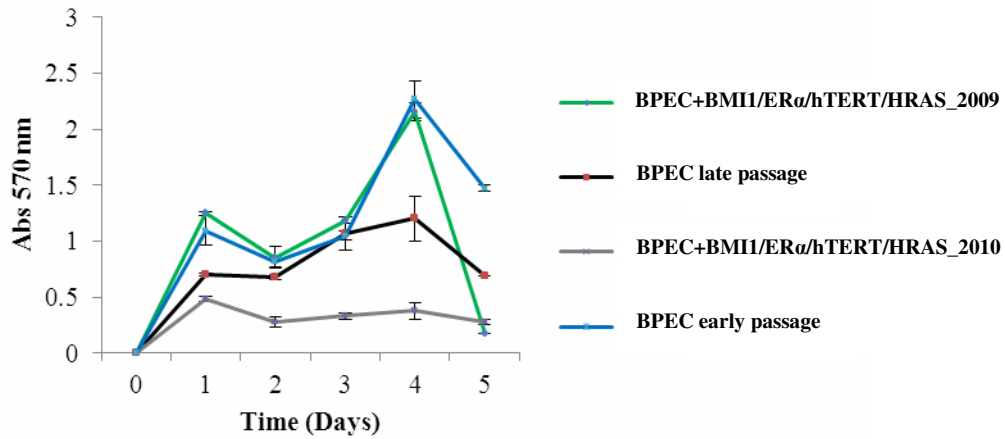


**Figure 6.12:** Analysis of p16 expression in BPEC. BPEC were infected using lentiviral particles carrying either, BMI1, ER $\alpha$ , hTERT, HRAS. Representative images and graph of western blot analysis performed twice. **A.** Infected cells were harvested and the extracted proteins were resolved by 10% SDS-PAGE. Membranes were probed with the indicated antibodies.  $\beta$ -Actin was used as a loading control. **B.** Results obtained after integrated density quantification of A using the software ImageJ (measurements expressed in arbitrary units refer to cell type in bold in A). All values have been normalized against  $\beta$ -Actin.



#### **6.3.4 Evaluating the effect of BMI1/ER on proliferation**

To test the effect of ectopic expression of BMI1 on BPEC cell proliferation, the calorimetric MTT proliferation assay was performed (section 2.2.15). Results are represented in Figure 6.13. The assay measures cell viability and is based on the activity of the mitochondrial enzyme, succinate dehydrogenase, which reduces the yellow tetrazolium (MTT) into insoluble purple formazan crystals. The crystals can be solubilized, using either isopropanol or DMSO and the purple solution can be spectrophotometrically read at 570 nm. An increase in absorbance is a reflection of an increase of MTT formation due to an increase in cell number. BMI1/ER $\alpha$ /hTERT/HRAS\_2010 showed expression of BMI1, HRAS and low moderate expression of ER $\alpha$  and hTERT (see section 6.3.3). The proliferation rate of BPEC plus BMI1/ER $\alpha$ /hTERT/HRAS\_2010 was analysed and compared to BPEC plus BMI1/ER $\alpha$ /hTERT/HRAS\_2009, which did not show an increase in BMI1 expression and a very low ER $\alpha$  and hTERT expression. BPEC infected with lentiviral particles carrying BMI1 and ER $\alpha$  were not analysed because they did not show any expression of ER $\alpha$  and BMI1. Two batches of non infected BPEC were used as a control, BPEC early passage (less than two weeks in culture) and BPEC late passage (more than two weeks in culture) were analysed and compared to early passage (less than two weeks in culture) (Figure 6.13).



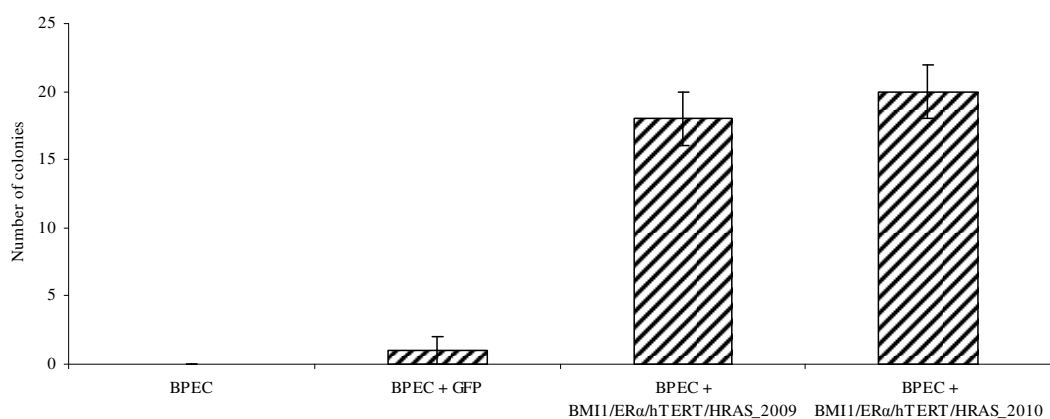
**Figure 6.13:** Breast primary epithelial cell proliferation analysis upon BMI1 ectopic expression. Cells were infected using lentiviral particles carrying the appropriate cDNA (BMI1, ER $\alpha$ , hTERT, HRAS). Infected cells were plated in 24 well primary plates. Cells were treated with MTT and DMSO before reading absorbance at a wavelength of 570nm with background subtraction at 650nm. The graph is representative of one experiment performed in triplicate. (n=3; error bars $\pm$ SEM).

Focusing on the interval between day 2 and day 4 (Figure 6.13), the cells that had a highest proliferation rate were BPEC plus BMI1/ER $\alpha$ /hTERT/HRAS\_2009, which were late passage cells, and non infected BPEC early passage. While BPEC plus BMI1/ER $\alpha$ /hTERT/HRAS\_2010 and non infected BPEC late passage had the lowest growth rate. The batch of BPEC showing higher expression of the transgenes were the BPEC plus BMI1/ER $\alpha$ /hTERT/HRAS\_2010, which are the cells that showed the lowest proliferation rate (Figure 6.13). Even though there was a high variability in the data, the fact that BPEC with an higher expression of the single transgene had a lower proliferation rate compared to non infected BPEC, suggested that the over-expression of BMI1/ER $\alpha$ /hTERT/HRAS does not increase the proliferation rate of BPEC. However, the results obtained do not explain why the BPEC plus BMI1/ER $\alpha$ /hTERT/HRAS\_2009 (with lower expression of the transgenes) showed an higher proliferation rate compared to the BPEC plus BMI1/ER $\alpha$ /hTERT/HRAS\_2010 and to BPEC late passage, and if cells were

available additional experiments should be performed in order to clarify these results.

### 6.3.5 Evaluating the effect of BMI1/ER $\alpha$ on anchorage independent growth

To determine whether breast primary epithelial cells acquire the ability of anchorage independent growth due to ectopic expression of BMI1/ER $\alpha$ , a colony formation in soft agar assay was performed. Non-infected BPEC, BPEC plus GFP, BPEC plus BMI1/ER $\alpha$ /hTERT/HRAS\_2009, BPEC plus BMI1/ER $\alpha$ /hTERT/HRAS\_2010 were tested in triplicate (section 2.2.13, T47D cells were used as positive control). For each replicate 5000 cells were used and the cells were grown at 37 °C for 21 days. After 21 days, colonies were counted. Non-infected BPEC and BPEC plus GFP did not form colonies, while BPEC plus BMI1/ER $\alpha$ /hTERT/HRAS\_2010 did form colonies (Figure 6.14). However, BPEC plus BMI1/ER $\alpha$ /hTERT/HRAS\_2009, which did not show an adequate expression of the transgenes used, also showed the ability of forming colonies. It was not possible to repeat the assay, due to lack of cells.



**Figure 6.14:** The effect of polycomb protein BMI1 on BPEC anchorage-independent growth. Representative graph of one experiment performed in duplicate. Cells were infected using lentiviral particles carrying the appropriate cDNA (BMI1, ER $\alpha$ , hTERT, HRAS). Infected cells were seeded in 3.5 % low melting agarose containing WIT media. Colonies were stained with INT and counted after 21 days. The graph is representative of an experiment performed twice in duplicate (n=4; error bars $\pm$ SEM).

## **6.4 Evaluating the effect of CBX8/ER $\alpha$ in BPEC**

Ectopic expression of polycomb proteins CBX8, Oestrogen Receptor alpha (ER $\alpha$ ) and human telomerase reverse transcriptase (hTERT) was carried out using a second generation lentiviral system (see section 2.2.4). Ectopic expression of Harvey rat sarcoma viral oncogene homolog (HRAS-G12V) was carried out using a retroviral system (see section 2.2.7). Two rounds of infection were performed and different batches of BPEC were infected with different combination of genes. The first round consisted of CBX8 with or without ER $\alpha$ . Seven days after the first round of infection, the cells were infected with viral particles containing hTERT and HRAS.

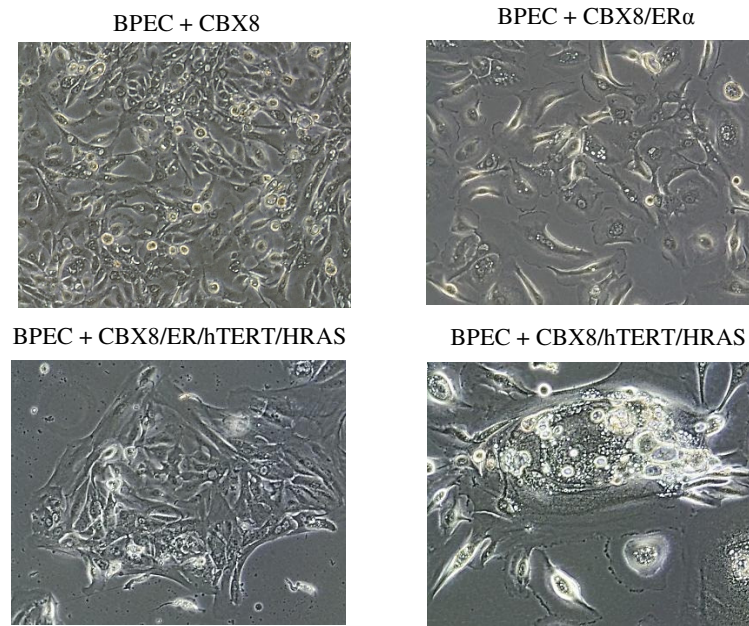
### **6.4.1 Effect on morphology**

When BPEC plus GFP were analyzed no changes in cell morphology were observed, cells kept their original shape and heterogeneity (Figure 6.5), confirming that lentiviral infection *per se* did not affect cell morphology. All viral particles, lentiviral and retroviral, carry the puromycin resistance gene. Infected BPEC were selected using 2.5  $\mu$ g/ml of puromycin. BPEC infected with lentiviral particles containing CBX8 and selected using the appropriate amount of puromycin were called BPEC plus CBX8. BPEC infected with lentiviral particles containing CBX8 and ER $\alpha$  and selected using the appropriate amount of puromycin were called BPEC plus CBX8/ER $\alpha$ . After the second round of infection with lentiviral particles carrying hTERT and retroviral particles carrying HRAS, the cells were selected using the appropriate amount of puromycin and called BPEC plus CBX8/ER $\alpha$ /hTERT/HRAS and BPEC plus CBX8/hTERT/HRAS.

BPEC plus CBX8 and BPEC plus CBX8/ER $\alpha$  maintained their original morphological heterogeneity and grew as a mixed population of cells (Figure 6.15).

However in the BPEC plus CBX8/ER $\alpha$  the “epithelial like cells” defined in section 6.2, started to disappear and some cells acquired a different morphology, they appeared to be much larger than the rest, irregular in shape and characterized by large nuclei and large cytoplasmic portion (See appendix D for more images).

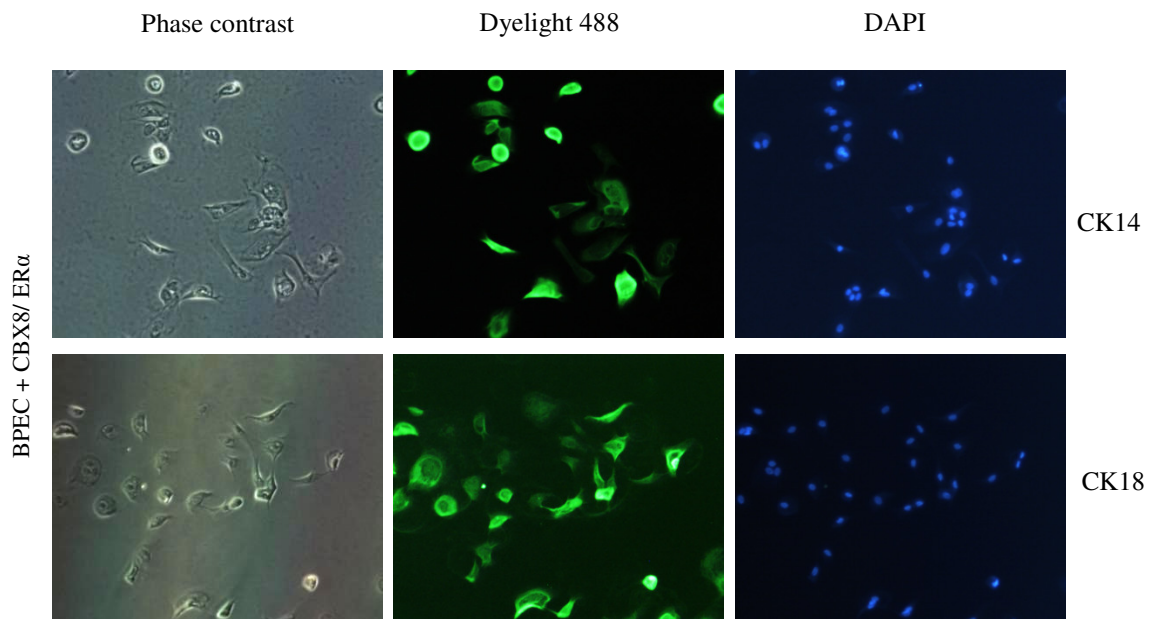
When BPEC plus CBX8/ER $\alpha$  and BPEC plus CBX8 were infected with lentiviruses and retroviruses containing hTERT and HRAS respectively, the vast majority of cells lost their original shape (Figure 6.15). The cells appeared to be much larger with irregular shape, and much flattened compared to other cells. These cells also did have small nuclei, large cytoplasmic portion, and multi-vacuoles started to appear in many of them. The morphology of BPEC plus CBX8/ER $\alpha$ /hTERT/HRAS and BPEC plus CBX8/hTERT/HRAS appear to be very similar to the morphology of BPEC plus HRAS/hTERT (see Figure 6.6). Fifteen days after infection, undefined structures were visible, along with cells containing large vacuoles. The cells gradually became bigger, started to lose their original shape and stopped growing.



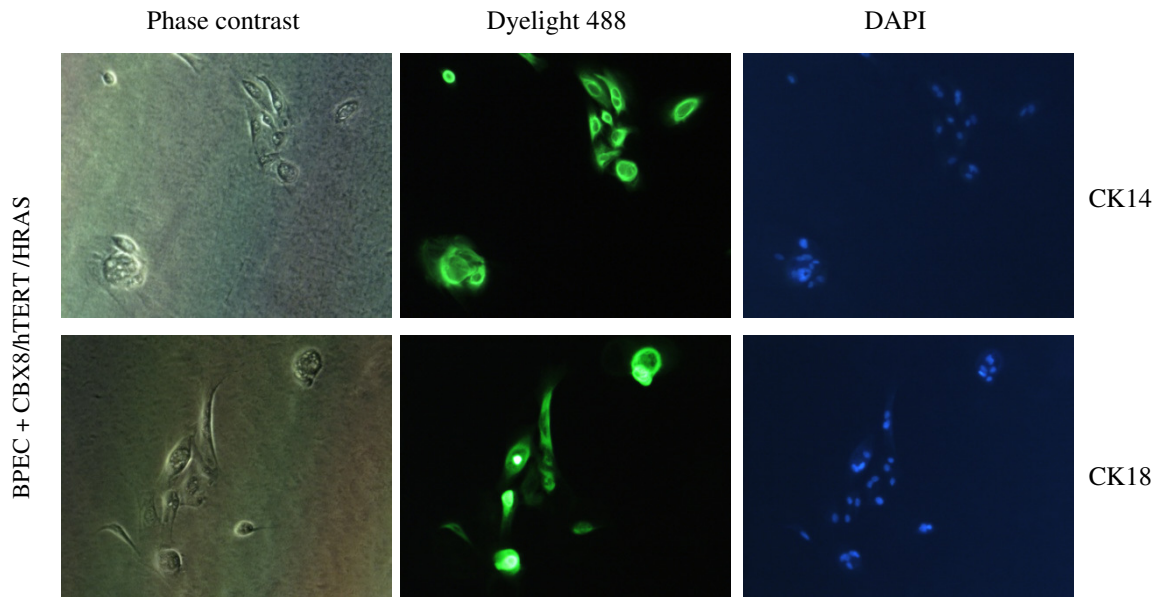
**Figure 6.15:** Representative images of BPEC after infection with lentiviral particles carrying CBX8, HRAS and ER $\alpha$  (see text for more details). Photos were taken using the Axiovision imaging System. Objective magnification 10X.

#### 6.4.2 Effect on cytokeratin expression

Upon infection of BPEC with CBX8, the cells formed a very heterogeneous and disorganized layer of slow growing cells with undefined shape (Figure 6.15). To test whether these differences in shape also reflect differential expression of specific basal and luminal markers, the expression of two cytokeratins, CK14 and CK18, was measured by immunofluorescence (section 2.2.14). Only single labelling was performed. BPEC infected with lentiviral particles carrying CBX8 and ER $\alpha$  stained positively for both markers CK14 and CK18 (Figure 6.16), as well as BPEC plus CBX8/hTERT/HRAS (Figure 6.16). The expression of cytokeratins in BPEC infected with CBX8/ER $\alpha$ /hTERT/HRAS and BPEC infected with CBX8 alone was not performed as cells were no longer available.



**Figure 6.16:** Expression of cytokeratins in BPEC after infection with lentiviral particles carrying CBX8 and ER $\alpha$ , assessed by Immunofluorescence. Cells were infected with lentiviral particles containing CBX8, and ER $\alpha$ . BPEC, after infection with lentiviral particles carrying CBX8 and ER $\alpha$  displays CK14 and CK18 expression. No double labelling was performed. Cells were visualized using an inverted microscope (Zeiss, Axiovert 40 CFL) and digital images were acquired using Axiovision imaging System. Objective magnification 10X.



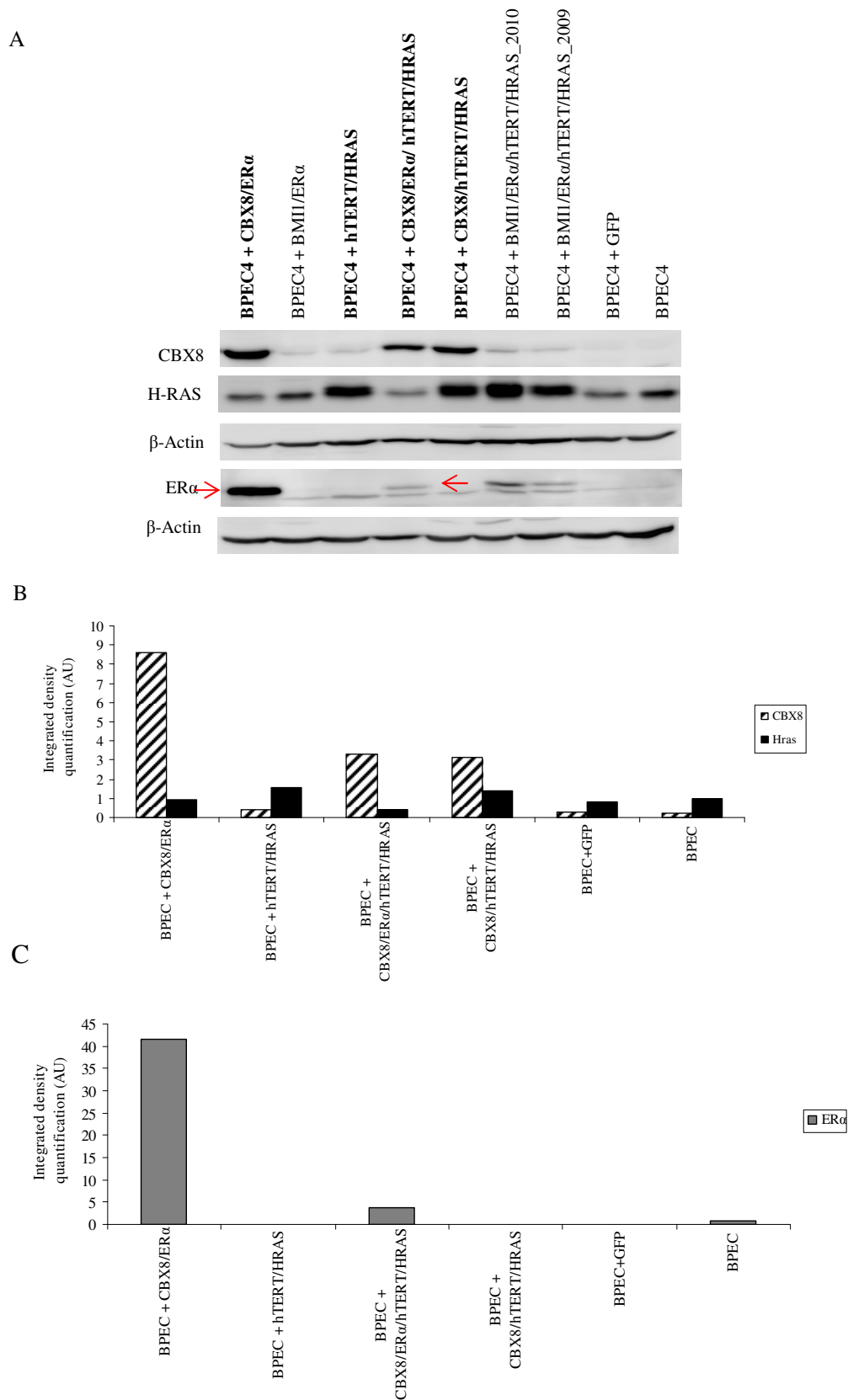
**Figure 6.17:** Expression of cytokeratins in BPEC after infection with lentiviral particles carrying CBX8, hTERT and HRAS assessed by Immunofluorescence. Cells were infected with lentiviral particles containing CBX8, hTERT and HRAS. BPEC, after infection with lentiviral particles carrying CBX8, hTERT and HRAS displays both CK14 and CK18 expression. No double labelling was performed. Cells were visualized using an inverted microscope (Zeiss, Axiovert 40 CFL) and digital images were acquired using Axiovision imaging System. Objective magnification 10X.

### 6.4.3 Evaluating expression of ectopic proteins

To confirm the ectopic expression of the different proteins, western blot analysis (section 2.2.9.1 – 2.2.9.3) was performed on samples derived from independent batches of infected BPECs (Figure 6.18, 6.19 and 6.20). Western blot analysis showed a significant increase of CBX8 protein expression in cells infected with CBX8-containing lentivirus compared to non-infected BPEC (Figure 6.18.A, lanes 1, 4 and 5). A robust increase of ER $\alpha$  protein expression was detected by western blot analysis in BPEC plus CBX8/ER $\alpha$  (lane 1, Figure 6.18.A), while a lower level of ER expression was detected in a separate batch of BPEC plus CBX8/ER $\alpha$ /hTERT/HRAS (lanes 4, Figure 6.18.A). In BPEC plus CBX8/ER $\alpha$  expression of ER $\alpha$  was 13.5 fold higher compared to BPEC plus CBX8/ER $\alpha$ /hTERT/HRAS (Figure 6.18C and Table D.3 AppendixD). Western blot analysis showed a significant increase of HRAS expression in BPEC plus CBX8/hTERT/HRAS, while a level of HRAS similar to endogenous level was detected in BPEC plus CBX8/ER $\alpha$ /hTERT/HRAS and BPEC plus CBX8/ER $\alpha$  (lane 1, 4, 8 and 9 Figure 6.18.A and Figure 6.18.B).

No expression of hTERT was detected in non infected BPEC, BPEC plus GFP and BPEC plus CBX8/ER $\alpha$  (Figure 6.19.A lane 1, 7, 8 and Figure 6.19.B). BPEC infected with viral particles carrying CBX8, hTERT and HRAS showed a very low expression of hTERT compared to BPEC infected with viral particles carrying hTERT and HRAS (Figure 6.19.A lane 4, 5 and Figure 6.19.B).

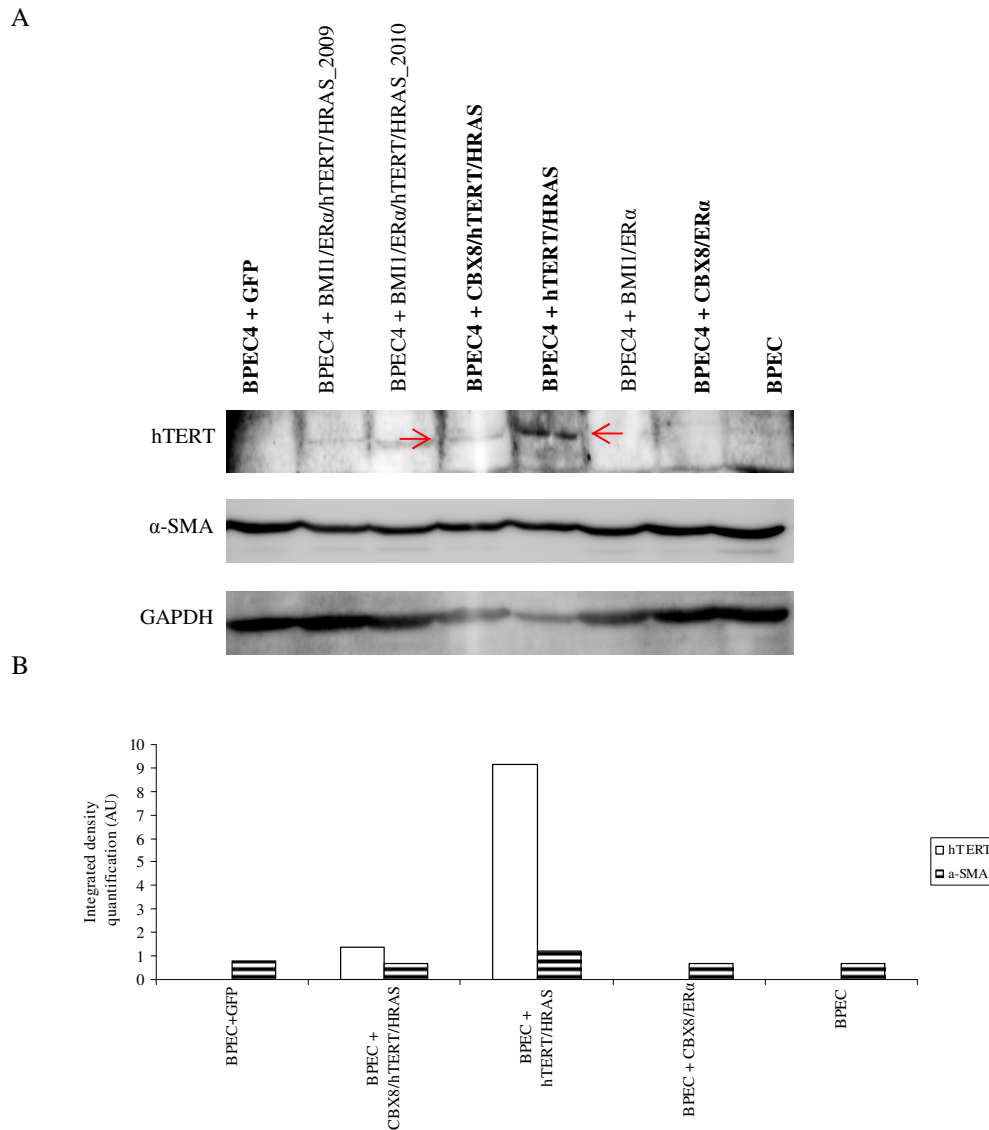




**Figure 6.18:** Analysis of CBX8, ER $\alpha$  and HRAS expression in BPEC. Representative images and graph of western blot analysis. **A.** Protein extracted from BPEC were resolved by 10% SDS-PAGE. Membranes were probed with the indicated antibodies.  $\beta$ -Actin was used as a loading control. Red arrows indicate the appropriate band for ER $\alpha$ . **B.** and **C.** Results obtained after integrated density quantification of **A** using the software ImageJ (measurements expressed in arbitrary units refer to cell type in bold in **A**). All values have been normalized against  $\beta$ -Actin.

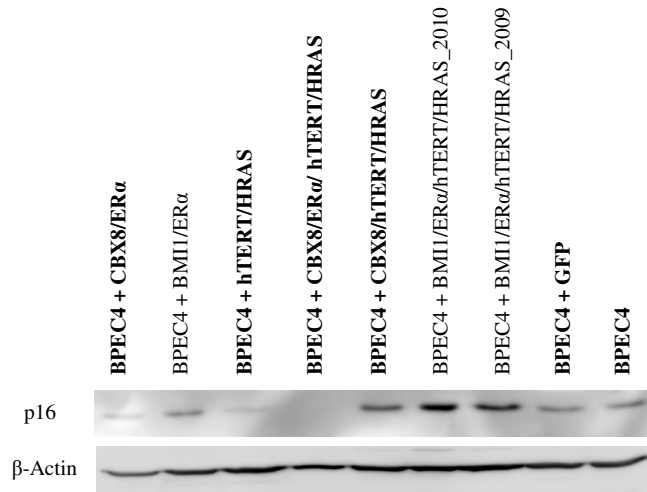
The expression of the basal marker  $\alpha$ -smooth muscle actin ( $\alpha$ -sma) was also tested and compared to non-infected BPEC. Western blot analysis showed the same level of  $\alpha$ -SMA protein expression across the different batches of BPEC over-expressing CBX8 and the level of  $\alpha$ -sma expression was similar to non-infected BPEC (Figure 6.19.A and 6.19.B).

In order to test whether CBX8 regulates the INK4A-ARF locus in BPEC, the level of expression of p16 was measured by western blot (Figure 6.20). BPECs plus CBX8/hTERT/HRAS showed a small increase on p16 expression compared to non infected BPEC and BPEC plus GFP (Figure 6.20.A lanes 5, 8, 9 and Figure 6.20). A weak expression of p16 was also detected in BPEC expression CBX8/ER $\alpha$  and BPEC expressing hTERT/HRAS (Figure 6.20.A lanes 1,3 and Figure 6.20.B). BPEC plus CBX8/ER $\alpha$ /hTERT/HRAS, showed no expression of p16 protein (Figure 6.20.A lane 4 and Figure 6.20.B). The level of p16 in BPEC expressing the highest level of CBX8 was not significant different from the level of p16 in BPEC not expressing CBX8. Based on the data presented here, it is not possible to establish whether CBX8 has an effect on the expression of p16.

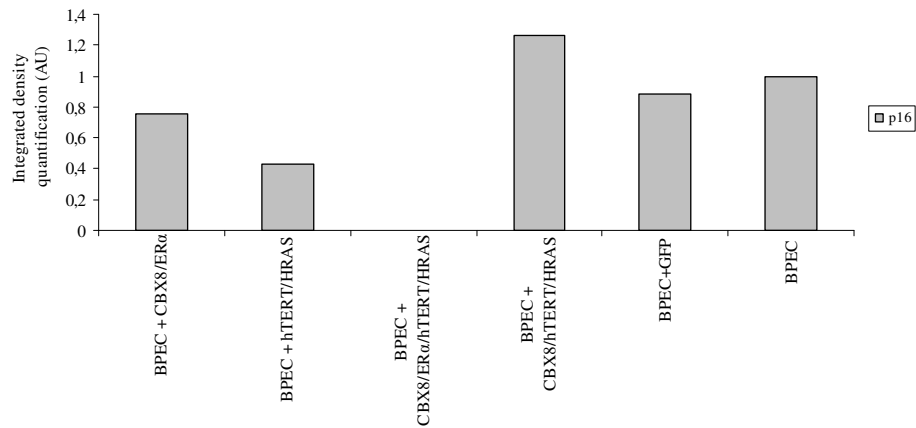


**Figure 6.19:** Analysis of hTERT and  $\alpha$ -SMA expression in BPEC after infection with lentiviral particle carrying CBX8, hTERT and HRAS. BPEC were infected using lentiviral particles carrying CBX8, ER $\alpha$ , hTERT and HRAS. Representative images and graph of western blot analysis performed twice. **A.** Infected cells were harvested and the extracted proteins were resolved by 10% SDS-PAGE. Membranes were probed with the indicated antibodies. Red arrows indicate the appropriate band for hTERT. GAPDH was used as a loading control. **B.** Results obtained after integrated density quantification of A using the softwareImageJ (measurements expressed in arbitrary units refer to cell type in bold in A). All values have been normalized against GAPDH.

A



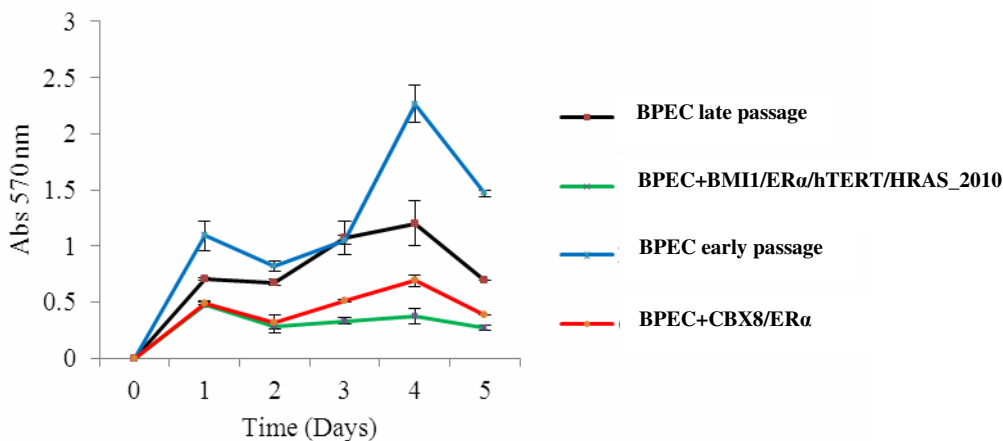
B



**Figure 6.20:** Analysis of p16 expression in BPEC after infection with lentiviral particles carrying either, CBX8, ER $\alpha$ , hTERT, HRAS. Representative images and graph of western blot analysis performed twice. **A.** Infected cells were harvested and the extracted proteins were resolved by 10% SDS-PAGE. Membranes were probed with the indicated antibodies.  $\beta$ -Actin was used as a loading control. **B.** Results obtained after integrated density quantification of A using the software ImageJ (measurements expressed in arbitrary units refer to cell type in bold in A). All values have been normalized against  $\beta$ -Actin.

#### 6.4.4 Evaluating the effect of CBX8/ER $\alpha$ on proliferation

To test the effect of ectopic expression of CBX8 on BPEC cell proliferation, the colorimetric MTT proliferation assay was performed (section 2.2.15 and section 6.3.3). Results are represented in Figure 6.13. Due to the low number of cells available, only late passage BPECs over-expressing CBX8/ER $\alpha$  were analysed and compared to non-infected BPEC (early and late passage) and BPEC plus BMI1/ER $\alpha$ /hTERT/HRAS\_2010 (Figure 6.21). Focusing on the interval between day 2 and day 4, the proliferation rate of BPEC over-expressing CBX8/ER $\alpha$  was slightly higher compared to the proliferation rate of BPEC plus BMI1/ER $\alpha$ /hTERT/HRAS\_2010, but similar to the proliferation rate of non infected BPEC late passage (Figure 6.21) (see also appendix). As expected, late passage non-infected BPEC had a lower proliferation rate compared to early passage non-infected BPEC.

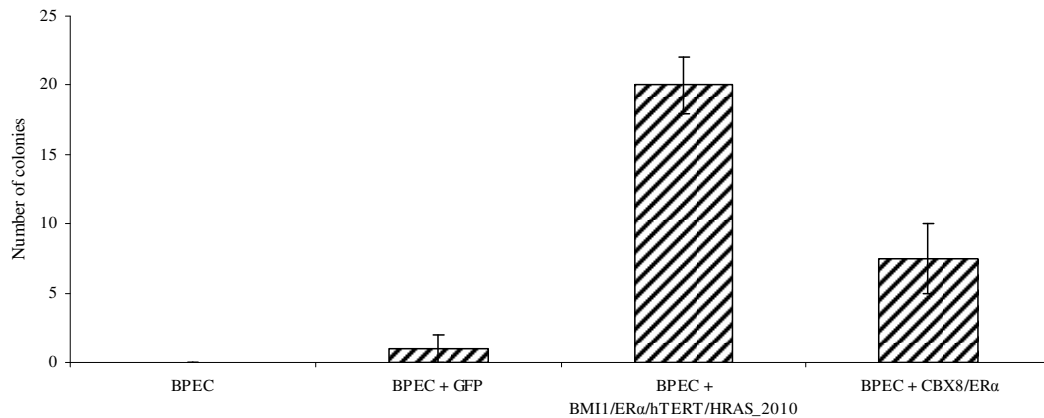


**Figure 6.21:** Breast primary epithelial cell proliferation analysis upon CBX8 ectopic expression. Cells were infected using lentiviral particles carrying the appropriate cDNA (CBX8, BMI1, ER $\alpha$ , hTERT, HRAS). Infected cells were plated in 96well primary plates. Cells were treated with MTT and DMSO before reading absorbance at a wavelength of 570nm with background subtraction at 650nm. The graph is representative of one experiment performed in triplicate. (n=3; error bars $\pm$ SEM).

The results obtained suggested that the over-expression of CBX8/ER $\alpha$  in late passage BPEC does not increase the proliferation rate of non infected late passage BPEC. However the BPEC plus CBX8/ER $\alpha$  showed an higher proliferation rate compared to BPEC plus BMI1/ER $\alpha$ /hTERT/HRAS\_2010. It was not possible to repeat the experiment in order to confirm these data as cells were no longer available.

#### **6.4.5 Evaluating the effect of CBX8/ER $\alpha$ on anchorage independent growth**

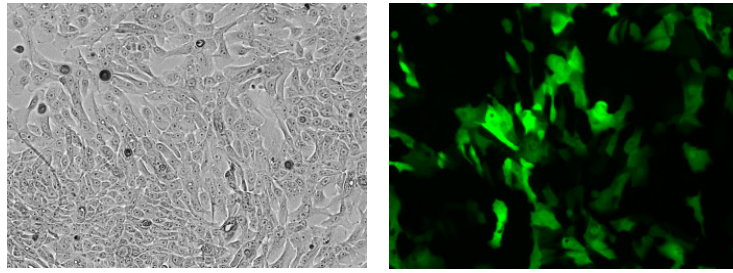
To determine whether breast primary epithelial cells acquire the ability of anchorage independent growth due to ectopic expression of CBX8, a colony formation assay was performed. Non-infected BPEC, BPEC plus GFP, BPEC plus CBX8/ER $\alpha$ , were tested in triplicate (section 2.2.13, T47D cells were used as positive control). For each replicate 5000 cells were used and the cells were grown at 37 °C for 21 days. After 21 days, colonies were counted. Non-infected BPEC and BPEC plus GFP did not form colonies, while BPEC over-expressing CBX8/ER $\alpha$  did form colonies (Figure 6.22). However the number of colonies was low compared to the number of colonies formed by BPEC plus BMI1/ER $\alpha$ /hTERT/HRAS\_2010 and this might be due to the fact that the additional over-expression of hTERT/HRAS is required. It was not possible to test this hypothesis due to the lack of available cells.



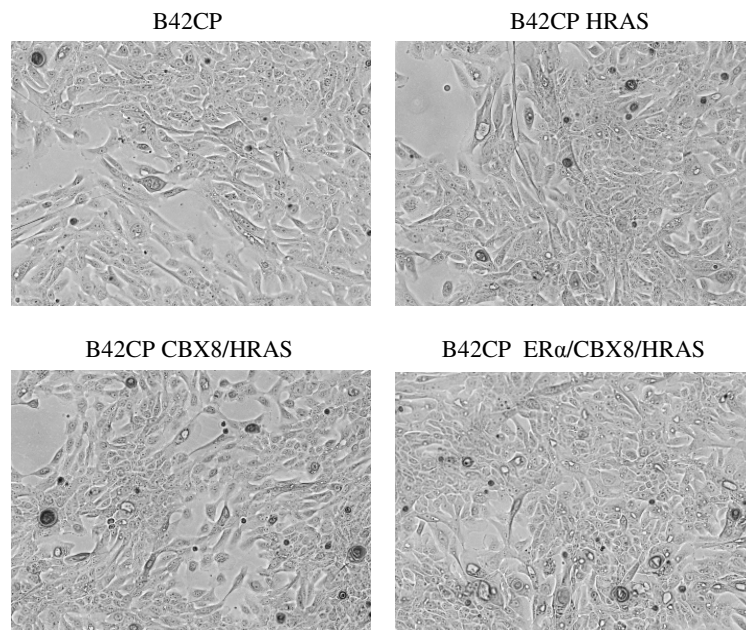
**Figure 6.22:** The effect of polycomb protein CBX8 on anchorage-independent growth in BPEC. Representative graph of one experiment performed in triplicate. Cells were infected using lentiviral particles carrying the appropriate cDNA (CBX8, BMI1, ER $\alpha$ , hTERT, HRAS). Infected cells were seeded in 3.5 % low melting agarose containing WIT media. Colonies were stained with INT and counted after 21 days. The graph is representative of an experiment performed in triplicate (n=3, error bars $\pm$ SEM).

## 6.5 Effect of CBX8 expression on B42CP cells

B42CP cells are mammary epithelial cells immortalized with the human telomerase reverse transcriptase (hTERT) (Unger et al., 2010). B42CP cells were infected with two different lentiviral particles carrying two different cDNA (the polycomb proteins CBX8 and the Oestrogen receptor alpha) and retroviral particles carrying the Harvey rat sarcoma viral oncogene homolog HRAS-G12V (see section 2.2.3, 2.2.4, 2.2.6 and 2.2.7). Two rounds of infections were performed and different batches of BPEC were infected with different combination of genes. The first round consisted of polycomb protein CBX8 along with ER $\alpha$ . Seven days after the first round of infection, the cells were infected with retroviral particles containing HRAS. B42CP cells infected with lentiviral particles containing GFP (Figure 6.23) and B42CP cells infected with HRAS only were used as controls. Cells were selected using 2.4  $\mu$ g/ml of puromycin. After 7 days of puro selection no change in terms of morphology was observed (figure 6.24).



**Figure 6.23:** Representative image of B42CP cells after infection with GFP. GFP expression was used as a control. The figure shows a representative image of B42CP cells infected with lentiviral particles containing GFP. Photos were taken six days after infection using the Axiovision imaging System. Objective magnification 10X.

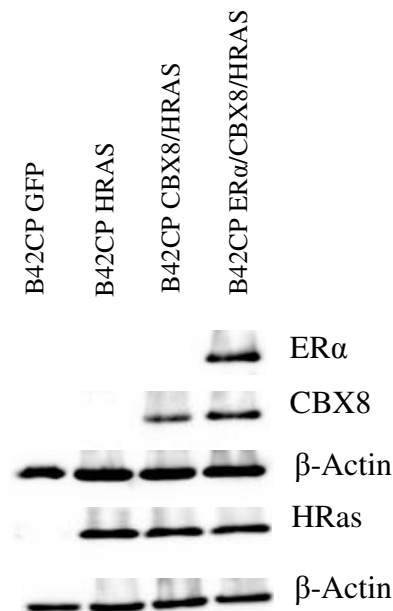


**Figure 6.24:** Representative images of B42CP cells after infection with lentiviral particles carrying the appropriate expression construct. Lentiviral particles containing cDNA encoding CBX8, ER $\alpha$  and HRAS were used for infection of B42CP cells. The figure shows representative images of non infected B42CP, B42CP infected with HRAS, B42CP infected with CBX8/HRAS and B42CP infected with ER $\alpha$ /HRAS/CBX8. Photos were taken using the Axiovision imaging System. Objective magnification 10X.



### 6.5.1 Evaluating expression of ectopic protein

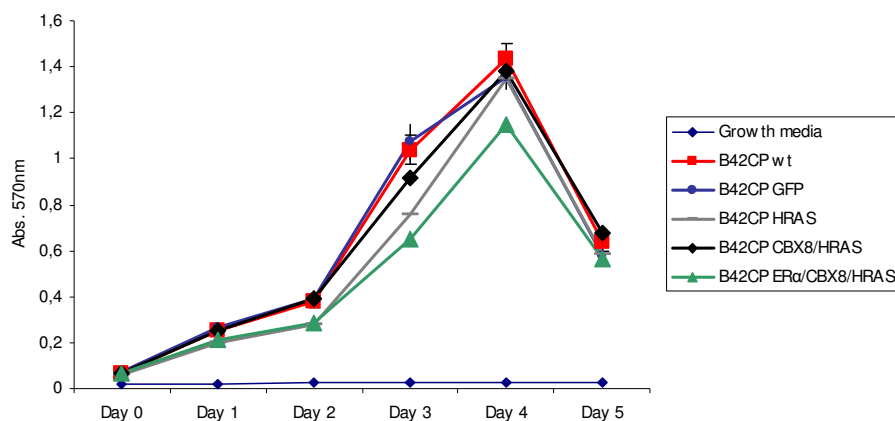
To confirm the ectopic expression of the different proteins, western blot analysis (section 2.2.9.1 – 2.2.9.3) was performed on samples derived from independent batches of infected B42CP cells (Figure 6.25). A robust increase of ER $\alpha$  protein expression was detected by western blot analysis in B42CP cells plus ER $\alpha$ /CBX8/HRAS (Figure 6.25, lane 4). Western blot analysis showed a significant increase of CBX8 protein expression in cells infected with CBX8-containing lentivirus compared to B42CP control GFP, B42CP infected with HRAS only (Figure 6.25, lanes 3 and 4). Western blot analysis showed a significant increase of HRAS expression in B42CP cells infected with lentiviral particles carrying HRAS only, HRAS/CBX8 and HRAS/ER $\alpha$ /CBX8 respectively (Figure 6.25 lanes 2, 3 and 4).



**Figure 6.25:** Analysis of CBX8, ER $\alpha$  and HRAS expression in B42CP cells. Representative images of western blot analysis. Protein extracted from B42CP cells was resolved by 10% SDS-PAGE. Membranes were probed with the indicated antibodies.  $\beta$ -Actin was used as a loading control.

### 6.5.2 Evaluating the effect of CBX8 on proliferation of B42CP cells

To test the effect of ectopic expression of CBX8 on B42CP cells proliferation, the colorimetric MTT proliferation assay was performed (section 2.2.15). Focusing on the exponential phase of the growth curve (interval between day 2 and day 4), the proliferation rate of B42CP cells overexpressing CBX8, along with HRAS and with or without ER $\alpha$ , is similar to the proliferation rate of non infected B42CP cells and B42CP GFP control (Figure 6.26). The results obtained suggested that the over-expression of CBX8 in B42CP cells does not increase the proliferation rate of B42CP cells.

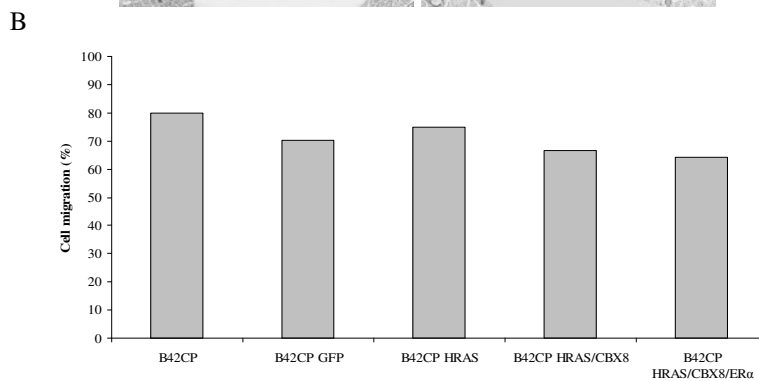
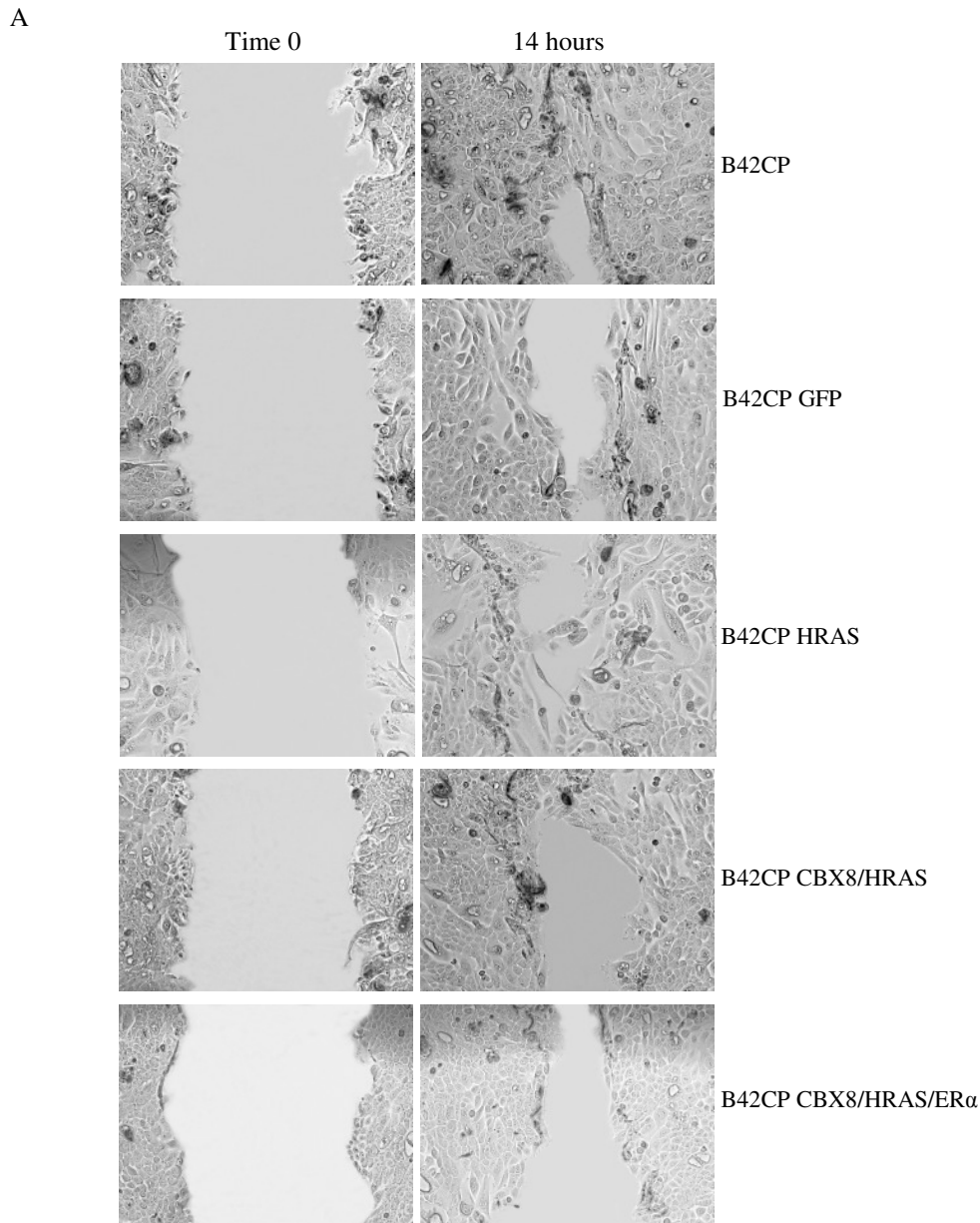


**Figure 6.26:** B42CP cell proliferation analysis upon CBX8 ectopic expression. Cells were infected using lentiviral particles carrying the appropriate cDNA (CBX8, ER $\alpha$  and HRAS). Infected cells were plated in 24 well plates, 12 replica for each cell type. Cells were treated with MTT and DMSO before reading absorbance at a wavelength of 570nm with background subtraction at 650nm. The graph is representative of one experiment conducted with 12 replicates (n=12; error bars $\pm$ SEM).

### 6.5.3 Evaluating the effect of CBX8 on B42CP cell migration

To test whether the migration ability of B42CP cells was affected by the over-expression of the polycomb protein CBX8, two different assays were performed, the trans-well Boyden chamber assay (Chen 2005; Li & Zhu 1999) and the scratch assay (Liang et al. 2007) (Section 2.2.22 and 2.2.23).

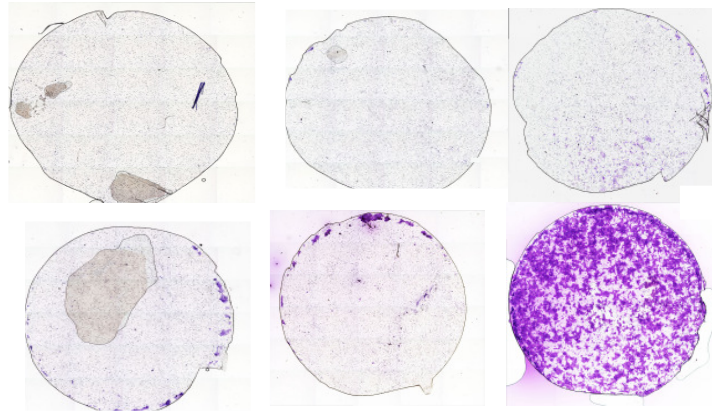
The scratch assay was performed as described in section 2.2.16. Non-infected B42CP cells, B42CP plus GFP, B42CP plus HRAS, B42CP plus HRAS/CBX8 and B42CP plus CBX8/HRAS/ER $\alpha$  cells were seeded in 10 cm plates and allowed to reach confluency. At time 0 a scratch was created in the monolayer of cells using a sterile 200  $\mu$ l pipette and the cells were observed for 24 hours. The area of a marked scratch was measured at time 0 and every 4 hours afterwards using the software imageJ. Cell migration was calculated using the following formula: “(Pre-migration area – Migration area)/Pre-migration area X 100” and represented in a graph as percent of cell migration (Figure 6.27 A and B). The results obtained using the scratch assay suggest that the ectopic expression of CBX8 did not effect the migration ability of B42CP cells (see Figure D.1 and table D.7 appendix D for measurements performed on additional scratches).



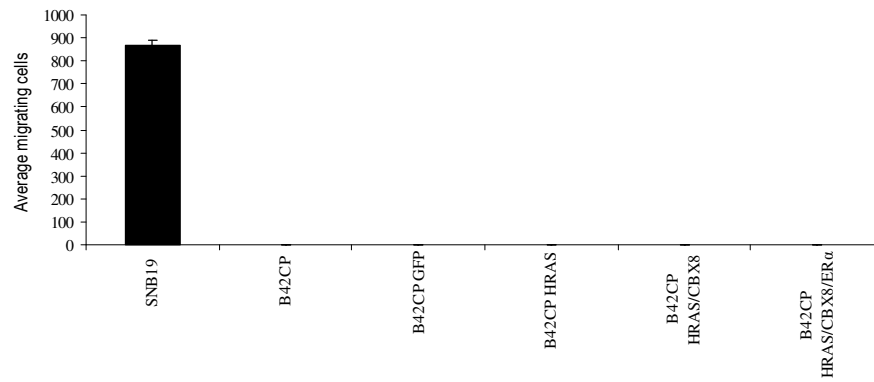
**Figure 6.27:** The effect of CBX8 ectopic expression on cell migration of B42CP cells as assessed by a scratch assay. Migration of B42CP cells is not affected by ectopic expression of CBX8 protein. **A:** Representative images showing migration of non infected B42CP, B42CP GFP control, B42CP HRAS, B42CP HRAS/CBX8 and B42CP HRAS/CBX8/ER $\alpha$  in 14 hours. Photographs of the cells were taken at time 0 and 14 hours later at 10X magnification. **B:** The graph is representative of a single experiment and single marked scratches. The size of the scratch was measured at time 0 and at 14 hours, using the software imageJ. Cell migration was expressed in percent and was calculated using the formula: “(Pre-migration area – Migration area)/Pre-migration area X 100”. (see section 2.2.16 for more details)

In order to confirm data obtained with the scratch assay, a transwell Boyden chamber assay was also performed (Figure 6.28 and section 2.2.12). Non infected B42CP cells, B42CP plus GFP, B42CP plus HRAS, B42CP plus HRAS/CBX8 and B42CP plus HRAS/CBX8/ER $\alpha$  cells were trypsinized and separately re-suspended in serum free growth media.  $2.5 \times 10^4$  cells were added to the top of each PET membrane. The whole chamber was examined for migrating cells (Figure 6.28). For each cell type the experiment was performed in triplicate. Migration of B42CP cells was not effected by ectopic expression of CBX8 (Figure 6.28).

A



B



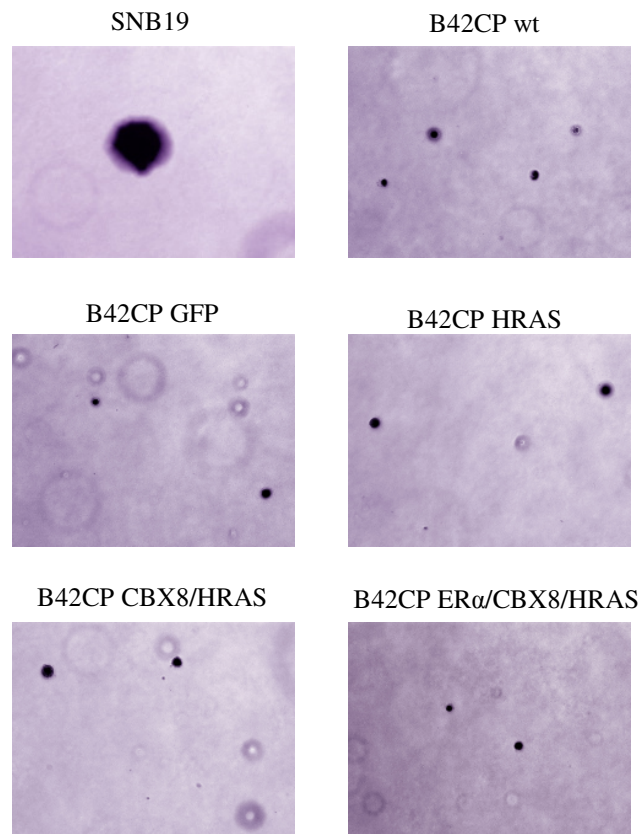
**Figure 6.28:** The effect of CBX8 ectopic expression on B42CP cells migration ability as assessed by transwell Boyden chamber assay. Cells were infected using lentiviral particles carrying either the GFP control, HRAS, HRAS/CBX8 and HRAS/CBX8/ER $\alpha$ . 5 days after puromycin selection  $2.5 \times 10^3$  cells were added to the top of a Boyden chamber and placed in serum deprived media; after 24 hours migrating cells were stained with crystal violet and counted under microscope. **A.** Representative images of Boyden chamber membranes after staining. **B.** The graph is representative of two experiments performed in triplicate (n=6; error bars  $\pm$ SEM).

#### **6.5.4 Evaluating the effect of CBX8 on B42CP anchorage independent growth**

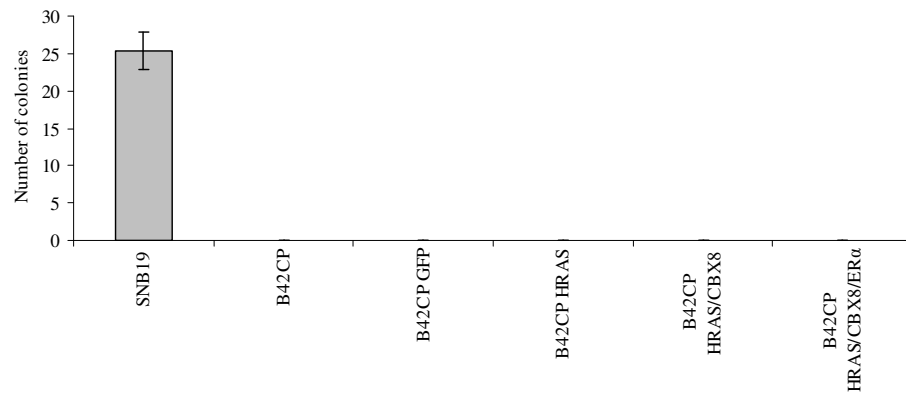
To determine whether B42CP cells acquire the ability of anchorage independent growth due to ectopic expression of CBX8, a colony formation in soft agar assay was performed. Non-infected B42CP, B42CP plus GFP, B42CP plus HRAS, B42CP plus HRAS/CBX8 and B42CP plus HRAS/CBX8/ER $\alpha$  cells were tested in triplicate (section 2.2.13, SNB19 cells were used as positive control). For each replicate 5000 cells were used and the cells were grown at 37 °C for 21 days

After 21 days, colonies were counted. Non infected B42CP cells, B42CP plus GFP cells and B42CP plus HRAS cells did not form colonies in soft agar, while the positive control SNB19 cells did form colonies (Figure 6.29 A and B) as previously reported (Kuppumbatti et al. 2001). Both, B42CP cells infected with CBX8, with or without ER $\alpha$ , did not form colonies in soft agar, in each of the three wells analyzed. B42CP cells do not acquire the ability of forming colonies in soft agar upon ectopic expression of CBX8.

A



B

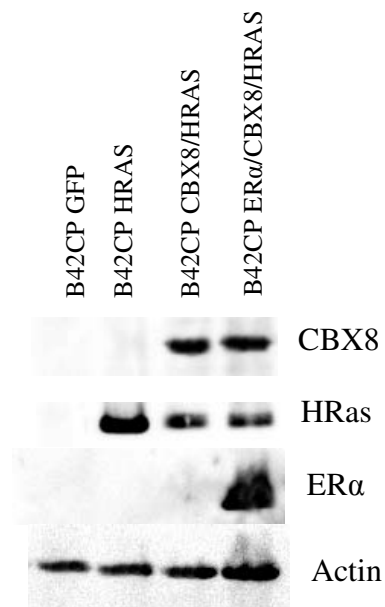


**Figure 6.29:** The effect of ectopic expression of CBX8 on anchorage-independent growth in B42CP cells. Cells were infected using lentiviral particles carrying respectively, GFP, HRAS, HRAS/CBX8 and HRAS/CBX8/ER $\alpha$ . Seven days after puro selection cells were seeded in 3.5% low melting agarose containing growth media plus additives. **A.** After 21 days colonies were stained with INT and counted. **B.** The graph is representative of an experiment performed in triplicate showing total number of colonies in all wells. (SNB19 cells were used as positive control).



### 6.5.5 Evaluating the expression of ectopic proteins after invitro assays

To confirm the ectopic expression of the different proteins after the invitro assays were performed, western blot analysis (section 2.2.9.1 – 2.2.9.3) was carried out on samples derived from independent batches of infected B42CP cells (Figure 6.30). The results from western blot analysis showed that the cells maintained the expression of the appropriate proteins.



**Figure 6.30:** Analysis of CBX8, ER $\alpha$  and HRAS expression in B42CP cells after invitro assays. Representative images of western blot analysis. Protein extracted from B42CP cells was resolved by 10% SDS-PAGE. Membranes were probed with the indicated antibodies.  $\beta$ -Actin was used as a loading control.

## 6.6 Discussion

The use of mammary primary epithelial cells derived from reduction mammoplasty for studying the process of malignant transformation has many advantages compared to traditional approaches (Dimri et al. 2005; Garbe et al. 2009; Gudjonsson et al. 2005; Ince et al. 2007; Kendrick et al. 2008; Nardone et al.; Pechoux et al. 1999; Petersen et al. 2001; Stampfer & Yaswen 2000; Stampfer et al. 2003; Stingl et al. 2001; Tlsty et al. 2004; Veneziani et al. 2007). The traditional approach consists of using established breast cancer cell lines which often have an altered genetic background, including abnormal DNA content and mutations or altered expression of oncogenes and/or tumour suppressor genes (Burdall et al. 2003). Primary cells derived from healthy donors are more likely to have a normal genetic background, therefore representing a good alternative to the traditional approach. Several different methods have been developed for culturing primary cells (Duss et al. 2007; Garbe et al. 2009; Ince et al. 2007). The protocol followed for experiments in this chapter was the Ince protocol, which involves the use of WIT media, a chemically defined serum-free medium, and the use of modified plastic surface plates, called primaria plates (section 2.2.18.6). Compared to others, this protocol claims the advantage of overcoming the growth arrest, termed M0, normally observed in the first 2 weeks of culturing primary cells (Romanov et al. 2001; Stampfer & Yaswen 2000; Stampfer & Yaswen 2003). Ince et al., have shown that BPEC can be grown in WIT media for up to 150 days (and 40 population doublings) without significantly inducing p16. Moreover, this homogeneous population of cells has a gene signature similar to epithelial cells (i.e. high epithelial marker claudin and low myoepithelial marker CD-10). They also showed that transformed BPEC

implanted in nude mice gave rise to tumours resembling those naturally occurring in humans.

Despite the fact that WIT media and primaria plates were used, the results obtained in this thesis did not recapitulate those reported by Ince et al., in terms of the propagation time and type of cells grown. After fifty days BPEC stopped growing (see appendix), suggesting that cells were not able to overcome the M0 growth arrest (Ethier et al. 1991; Ratsch et al. 2001; Yaswen & Stampfer 2002). The different result might be due the size of the biopsy used, which is related to the number of potential different type of cells presents.

Unlike reported by Ince et al., the organoids derived from a healthy donor, grown in WIT media, gave rise to a heterogeneous population of cells (Figure 6.2). Two of the three morphologically distinct types of cells initially visible, “epithelial-like” cells and “elongated” cells, were characterized by immunofluorescence analysis which showed that they were CK18 positive and CK14 positive respectively (Figure 6.4). The presence of a mixed population of cells might be expected, since the mammary gland is not composed of one type of cell. The terminal ducts of the mammary gland consist of an inner single layer of epithelial cells and an outer layer of a mixed population of cells consisting in myoepithelial cells and progenitor stem cells (Dimri et al. 2005; Smalley et al. 2003). The presence of three distinct types of cells in short-term cultures of normal human breast cells have been previously reported (Stingl et al. 1998; Stingl et al. 2001): epithelial cells, expressing luminal specific markers, myoepithelial cells, expressing basal marker and a third fraction of cells expressing both epithelial and myoepithelial markers which are suggested to be bipotent progenitor cells. This last fraction of cells, under appropriate stimuli, can differentiate into epithelial or myoepithelial cells (Stingl et al. 2001). Based on the

limited number of experiments performed, the three different types of cells initially distinguishable in the present system might represent the same mixed population reported by Stingl et al. However, further analysis would be necessary in order to confirm this possibility, i.e. FACS sorting using specific markers for epithelial/luminal (MUC1+, CK19+ and EpCAM+), myoepithelial/basal (CALLA+ and  $\alpha 6$  integrin+) and bipotent cells ( $\alpha 6$  integrin+/EpCAM+).

Normal breast primary epithelial cells when put in culture loose ER $\alpha$  expression, do not proliferate and rapidly stop growing (Anderson 2002; Clarke et al. 1997). Duss et al. showed that ectopic expression of polycomb protein BMI1 in breast primary epithelial cells is able to overcome this growth arrest. Their model showed for the first time that ectopic expressions of BMI1/ER $\alpha$  allowed the cells to grow in response to Estradiol and maintain ER $\alpha$  expression, as well as the ability of anchorage independent growth. In this chapter I sought to verify whether ectopic expression of CBX8/ER $\alpha$  in BPEC would have the same effect of ectopic expression of BMI1/ER $\alpha$  and recapitulate what was reported by Duss et al..

CBX8 belongs to a mammalian family of chromobox-containing proteins (Flanagan et al. 2005; Nielsen et al. 2002) and is part of the Polycomb Repressive Complex 1 (PRC1) (Bardos et al. 2000). Several different studies have shown the importance of deregulated polycomb protein expression in cancer initiation and progression, but their exact role is not completely understood. Since polycomb complex compositions may vary depending on cell type (Gunster et al. 2001; Kerppola 2009; Maertens et al. 2009), deregulation of individual components could have effects that are cell type dependent. It has been shown that CBX8 can bypass senescence, acting through the INK4A/ARF locus, in human and mouse fibroblasts, but its effect in human mammary epithelial cells has not been investigated. One of

the unsolved questions is whether deregulation of any component within a polycomb repressive complex has the same effect. BMI1 is the main component of PRC1 and was first identified as oncogene cooperating with cMYC to induce lymphomas in mice (van Lohuizen et al. 1991). It has been shown that BMI1 is able to transform MCF10A cells in presence of HRAS alone (Datta et al. 2007) and it is also able to transform normal primary epithelial mammary cells in presence of ER $\alpha$ , hTERT and cMYC (Duss et al. 2007). It has not been tested whether breast primary epithelial cells would become cancerous cells upon ectopic expression of BMI1, in the absence of cMYC. In order to answer some of these questions I planned to overexpress BMI1 (without cMYC) and CBX8 in BPEC and compare the effects that the two polycomb proteins would have on BPECs. The cells were infected with lentiviral particles carrying either BMI1 or CBX8, along with a different combination of genes, including ER $\alpha$ , hTERT and HRAS. The rationale behind the choice of this combination of genes relies on their importance in breast cancer: HRAS is an important prognostic factor in breast cancer (Watson et al. 1991) (Clark & Der 1995; Miyakis et al. 1998) and evidence suggests that HRAS alterations are some of the earliest events involved in breast cancer formation. It is well known that Oestrogen Receptor  $\alpha$  over-expression plays a major role in breast cancer and it is one of the first alterations detected in pre-cancerous lesions (Fowler et al. 2007; Hartmann et al. 2005; Holst et al. 2007). Finally, the immortalization of cells is required for neoplastic transformation (Hahn 2002; Hahn 2005; Hahn et al. 1999), hence the ectopic expression of hTERT.

After BPEC were infected with lentiviral particles carrying different combination of genes, cells were checked for changes in morphology and expression of specific basal/myoepithelial and luminal/epithelial cytokeratins, in order to verify

whether the two polycomb proteins would affect differently the morphology of the cells and the cytokeratins expression. According to Duss et al. paper primary epithelial breast cells, upon ectopic expression of the full set of genes BMI1, ER $\alpha$ , hTERT and cMYC, become tumourigenic cells expressing initially only CK18 and later on both CK14 and CK18. The use of Ince et al. protocol and the transformation of primary cells with a different set of genes, gave contradictory and inconsistent results. In addition, due to a lack of available BPECs it was not possible to repeat the experiments, which made it not possible to draw any conclusion. Two batches of BPEC, infected with viral particles carrying BMI1, ER $\alpha$ , hTERT and HRAS were compared and they clearly behaved differently in terms of morphology, CKs expression and growth rates (Figures 6.6, 6.7, 6.8, 6.9 and 6.13). One of two batches consisted of very homogeneous, morphologically well-defined cells with higher proliferation rate compared to the second batch of cells consisting of a very heterogeneous group of cells, with a not well defined morphology and containing multiple vacuoles. These cells also appear to be similar to BPEC infected with HRAS/hTERT (Figure 6.6). The two batches were named 2009 and 2010, indicating higher proliferating regular cells and lower proliferating irregular cells respectively. The 2009 batch expresses basal/myoepithelial cytokeratins (CK14 and CK5) and showed a very low expression of epithelial/luminal marker (CK18 and CK19), while the 2010 batch showed unclear results in terms of epithelial/myoepithelial cytokeratin expression (Figure 6.7, 6.8 and 6.9). These results underline the variability of the system and put an emphasis on some of the issues associated with the use of cytokeratins expression for characterizing and distinguishing epithelial/luminal cells vs. myoepithelial/basal cells. The 2010 batch also showed signs resembling senescence (Figure 6.6) which may be caused by a higher level of

HRAS expression. However, cells were not tested for markers for senescence. HRAS is an oncogene that requires either the presence of a cooperating oncogene or mutated tumour suppressor genes in order to exert its oncogenic activity (DeNicola & Tuveson 2009; Hahn et al. 1999; Ince et al. 2007; Serrano et al. 1997). In primary rodent and human primary cells it causes growth arrest and senescence (Serrano et al. 1997). The growth arrest observed upon ectopic expression of HRAS in primary cells is also known as oncogene-induced senescence, which is characterized by morphological changes such as flattened cells, large nucleus with a prominent nucleolus, along with other changes including chromatin reorganisation and activation of the p53 and p16<sup>INK4a</sup> pathways. HRAS ectopic expression in primary cells does not always cause senescence though. When the level of HRAS expression is similar to the level of expression driven by endogenous promoter HRAS can act as an oncogene and does not cause senescence (DeNicola & Tuveson 2009; Tuveson et al. 2004). This observation may explain why two batches of BPEC infected with the same set of genes behave differently. When the level of expression of HRAS is too high the cells undergo growth arrest and senescence, which would explain the difference observed in terms of proliferation rate (Figure 6.13), but they might still retain their oncogenic behaviour due to the presence of other oncogenes, therefore they are still able to form colonies in soft agar (Figure 6.14). However, western blot analysis showed that the level of HRAS expression in BPEC infected with BMI1/ER $\alpha$ /hTERT/HRAS\_2010 is only slightly higher compared to BMI1/ER $\alpha$ /hTERT/HRAS\_2009 and similar to HRAS level in BPEC infected with hTERT/HRAS (Figure 6.10). Due to the lack of cells, it was not possible to repeat the experiment and clarify whether the change in morphology observed in BPEC plus BMI1/ER $\alpha$ /hTERT/HRAS\_2010 were caused by the higher expression of

HRAS. More contradictory results were obtained when the cells were tested for anchorage-dependent growth and change in proliferation rate. Both batches of BPEC infected with BMI1/ER $\alpha$ /hTERT/HRAS were able to form colonies but only the 2009 batch showed an increase in proliferation rate (Figure 6.13 and Figure 6.14). However, western blot analysis showed that BPEC plus BMI1/ER $\alpha$ /hTERT/HRAS\_2010 had higher expression of BMI1, HRAS, ER $\alpha$  and hTERT, compared to the BPEC plus BMI1/ER $\alpha$ /hTERT/HRAS\_2009 batch (Figure 6.10 and 6.11). Based on these data it was not possible to draw any conclusion. If more cells were available the experiments should have been repeated, performing a western blot analysis before the invitro assay, in order to make sure that the cells express a similar level of all the transgenes used.

Duss et al. study showed that primary breast epithelial cells require ectopic expression of both BMI1 and ER $\alpha$  in order to bypass ER-dependent growth arrest (Duss et al. 2007). They also showed that primary breast epithelial cells required ectopic expression of both BMI1 and ER $\alpha$  in order to form colonies in soft agar. In BPEC it was not possible to evaluate whether BMI1/ER $\alpha$  would have same effects because no expression of BMI1 and ER $\alpha$  in BPEC plus BMI1/ER $\alpha$  was detected (Figure 6.10), therefore these cells can be considered as non infected BPEC. Studies conducted in fibroblasts and primary epithelial cells showed that BMI1 acts through a p16-dependent mechanism (Itahana et al. 2003). The level of p16 in the infected BPEC was checked, however the high variability in terms of expression of single proteins obtained in these set of experiments did not make possible to establish any correlation between BMI1 expression and p16 expression, it was not possible to evaluate the effect of BMI1 ectopic expression, along with other oncogenes, in BPEC. A limitation of the system used for this set of experiments was represented by



the short lifespan of the primary cells. After fifty days cells stopped growing, limiting the number of experiments.

After infection with lentiviral particles carrying CBX8/ER $\alpha$ , BPECs appeared to be much larger with irregular shape, and much flattened compared to other cells. These cells also did have small nuclei, large cytoplasmic portion, and multi-vacuoles started to appear in many of them (Figure 6.15) and the original shape of BPEC (Figure 6.2) was completely lost. The analysis of cytokeratin expression performed on the limited number of cells available showed positivity for both type of cytokeratins (epithelial/basal) in BPEC after infection with lentiviral particles carrying CBX8/ER $\alpha$  and CBX8/hTERT/HRAS (Figure 6.16 and 6.17). Western blot analysis showed that the levels of both CBX8 and ER $\alpha$  in BPEC plus CBX8/ER $\alpha$  were much higher compared to the batch of BPEC plus CBX8/hTERT/HRAS (Figure 6.18 and Table D.3 Appendix D). In fact, the level of CBX8 expression was 2.6 fold higher in BPEC plus CBX8/ER $\alpha$  compared to BPEC plus CBX8/hTERT/HRAS and to BPEC plus CBX8/ER $\alpha$ /hTERT/HRAS (Table D.3 Appendix D). The level of ER $\alpha$  expression was 13.5 fold higher in BPEC plus CBX8/ER $\alpha$  compared to BPEC plus CBX8/ER $\alpha$ /hTERT/HRAS (Table D.3 Appendix D). In order to establish a clear relationship between ectopic expression of CBX8/ER $\alpha$  and cytokeratin expression in BPEC, cells with similar level of expression of CBX8 and ER $\alpha$  would have been more informative. Due to lack of cells available it was not possible to test cytokeratin expression in BPEC plus CBX8/ER $\alpha$ /HRAS/hTERT, which expressed a level of CBX8 similar to BPEC plus CBX8/hTERT/HRAS and a much lower level of ER $\alpha$  expression (Figure 6.15 and Table D.3 Appendix D).

Ectopic expression of CBX8 and ER $\alpha$  did not confer any advantage in terms of proliferation (Figure 6.21). BPEC overexpressing CBX8/ER $\alpha$  showed a lower growth rate compared to non infected BPEC (late or early passage), and a slightly higher growth rate compared to BPEC plus BMI1/ER $\alpha$ /HRAS/hTERT (Figure 6.21). In addition, breast primary epithelial cells acquired the ability of anchorage-independent growth upon over-expression of CBX8/ER $\alpha$  (Figure 6.22), although when compared to BPEC plus BMI1/ER $\alpha$ /hTERT/HRAS, the number of colonies were lower. BPEC over-expressing CBX8 stopped growing and started to show signs of senescence (figure 6.6; see also appendix for more images), this effect might be due to fact that the cells were not immortalized properly. The level of hTERT expression detected in BPEC plus CBX8/hTERT/HRAS, in fact, was very low (Figure 6.20). The limited number of experiments performed and the unavailability of more BPEC did not make it possible to establish whether CBX8 and BMI1 act through different mechanism in breast primary epithelial cells. Upon CBX8 over-expression, very low or no expression of p16 was detected suggesting that CBX8 might act through a p16 independent mechanism, as reported in fibroblast studies (Dietrich et al. 2007). However, based only on the western blot analysis performed (Figure 6.20) it is not possible to make any hypothesis to this regard.

The system used for this first set of experiments showed too much variability and several technical problems, mainly due to lack of cells. Therefore a different system was chosen in order to elucidate the possible role of CBX8 ectopic expression in breast epithelial cells. A well established non tumourigenic epithelial breast cell line stably immortalized was chosen, B42CP (Unger et al., 2010) and some attributes of neoplastic transformation were tested, including proliferation rate, migration ability and anchorage dependent growth in soft agar. Infected B42CP cells

were tested for protein expression before and after invitro assays were performed (Figure 6.25 and 6.30) and western blot analysis showed expression of the correct proteins. The attention was focused only on CBX8 polycomb protein. The experiments were performed using independent batches of B42CP cells infected with different combination of genes: B42CP cells infected with lentiviral particles carrying GFP, B42CP cells infected with retroviral particles carrying HRAS and non infected B42CP cells were used as controls. For the two of the invitro assays (migration assay and colonies formation assays in soft agar) the GBM SNB19 (Welch et al. 1995) cell lines was used as control.

Even though cytokeratins are normally used for characterizing basal and luminal breast cancer cells they do not always give a clear answer in terms of myoepithelial/epithelial differentiation (Abd El-Rehim et al. 2004; Gusterson et al. 2005; Malzahn et al. 1998; van de Rijn et al. 2002; Yalcin-Ozuyisal et al. 2009). Within breast cancer tumour expressing luminal CKs, between 16% and 27% also express myoepithelial CKs (this group of cells is called mixed or bimodal), and cancer expressing purely myoepithelial CKs are extremely rare (Gusterson et al. 2005; Malzahn et al. 1998). Evidence that chemical addition to the cells growth media can cause transition of a cell subpopulation from luminal to myoepithelial has been reported (Sartorius et al. 2005). A clear CKs expression pattern, allowing distinguishing between pure epithelial and myoepithelial cells, has not been identified. In addition, several studies have shown that breast cancer cells are subjected to morphological transition over time and these changes are accompanied by switch in CKs expression. Luminal cells, for instance, can give rise to myoepithelial cells (Pechoux et al. 1999). Taking this into account, changes in

cytokeratin expression upon ectopic expression of CBX8 in B42CP cells was not investigated.

Dietrich et al. showed that inhibition of CBX8 expression in mouse and human fibroblasts results in growth arrest, and ectopic expression of CBX8 bypasses stress-induced senescence in mice, suggesting a cell growth promoting function for CBX8. In addition, they showed that both CBX8 and BMI1 associate with the *INK4A-ARF* locus in human and mouse fibroblasts, and that BMI1 is dependent on CBX8 and *viceversa* for binding *INK4A-ARF*, suggesting that the chromodomain of CBX8 alone is not sufficient for its binding to the *INK4A-ARF* locus, and that only when the two protein are bound together in a complex a correct conformation and stability is achieved. Upon the observation that downregulation of CBX8 leads to loss of proliferation and a decrease in cyclin A2 levels before a significant increase in p16<sup>INK4A</sup> levels, they suggested the possibility that CBX8 might regulate cell proliferation also through a pathway independent of *INK4A-ARF* (Dietrich et al. 2007).

To date the effect of ectopic expression of CBX8 polycomb protein in breast epithelial cells has not been investigated. Results obtained from experiments carried out in this thesis suggest that ectopic expression on polycomb protein CBX8 in mammary epithelial cells does not influence cell proliferation (Figure 6.26), and does not have any effect on other attributes of neoplastic transformation, including migration ability (Figure 6.27 and 6.28) and anchorage dependent growth in soft agar (Figure 6.29).

## **7 CHAPTER 7: CONCLUSIONS AND FUTURE WORK**

The association between increased PcG protein expression and breast cancer has been reported by several groups (Dietrich et al. 2007; Duss et al. 2007; Gonzalez et al. 2009; Pasini et al. 2004a; Pasini et al. 2004b; Raaphorst 2005; Widschwendter et al. 2007). However, exactly how PcG proteins participate in breast cancer formation is not fully understood. The work presented here investigated the effects of altering EZH2 and CBX8 in breast epithelial cells.

In chapters three and four I investigated the effect of EZH2 knockdown in several different types of breast cancer cells, in order to clarify whether different types of cells responded differently to EZH2 silencing and to identify which factors might induce a different response. Down regulation of EZH2 influenced all the cancer phenotypes tested, including anchorage-independent growth, cell migration and cell proliferation, suggesting that EZH2 may be a good therapeutic target for breast cancer. However, the effect of EZH2 knockdown varied between cell lines. In the presence of wild type BRCA1, down regulation of EZH2 induced a significant reduction of cell proliferation and cell migration, while a less significant effect was observed in the context of mutated BRCA1. These results support those by Gonzalez et al. and suggest that the presence of wild type BRCA1 is necessary in order to observe decreased cell proliferation, migration and anchorage-independent growth, upon EZH2 knockdown. There is no physical interaction reported between EZH2 and BRCA1 (Gonzalez et al. 2009), but it is possible there may be an indirect interaction via BRIT1. BRIT1/MCPH is a recently identified regulator of the DNA damage response, via the ATM/ATR pathway (Chaplet et al. 2006; Peng et al. 2009), and it is involved in chromatin state changes, (Wilson et al. 2010). It also regulates the expression of BRCA1 and Chk1 (Lin et al. 2005) and it is required for regulation

of G2/M cell cycle in response to ionizing radiation, since reduced levels of BRIT1 cause a reduction of BRCA1 and Chk1 expression levels and consequently loss of G2/M checkpoint control. Moreover, BRIT1 is reduced in several human cancers, including ovarian, and in breast cancer cell lines (Lin et al. 2010; Rai et al. 2006). EZH2 could be responsible for silencing BRIT1, which in turn cause reduction of BRCA1. Additional studies will be required in order to investigate this hypothesis, including analysis of level of expression of BRIT1 in breast cancer cell lines and tumours, and evaluation of any changes in the expression of BRIT1 upon EZH2 downregulation.

In chapter five I investigated the effect of ectopic expression of CBX8 in MCF10A cells. Ectopic expression of CBX8 in MCF10A cells did not exert any effect on cell migration and anchorage-independent growth, whereas there was a temporary increase in cellular proliferation. Studies conducted on human and mouse fibroblast have shown that CBX8 causes abnormal proliferation and neoplastic transformation acting through repression of p16(Ink4a)/Rb and the Arf/p53 pathways (Dietrich et al. 2007). The fact that MCF10A cells lack both copies of the p16 locus suggest that cells with an intact p16 locus are required for investigating the potential neoplastic transformation activity. Moreover, other oncogenic stimuli and genetic/epigenetic changes, along with CBX8 de-regulation, may be required in order to observe more definitive switch towards the neoplastic phenotype, e.g. H-RAS (Datta et al. 2007).

In Chapter six I further investigated the importance of CBX8 in breast cancer transformation using breast primary epithelial cells (BPEC) derived from reduction mammoplasty. The protocol used for growing primary cells was the protocol described by Ince et al. 2007. Using this protocol, a mixed population of cells was

observed, consisting of “epithelial-like” cells and “elongated” cells. Immunofluorescence analysis showed that the two distinct populations of cells expressed distinct CKs, “epithelial-like” cells were CK18 positive and “elongated” cells were CK14 positive. The use of this protocol presented a number of technical problems, including limited number of cells available and high variability in the expression of single proteins, therefore the data obtained cannot be used to shed light on the effect of ectopic expression of CBX8 in primary epithelial breast cells.

However, the choice of a different model, B42CP, suggests that CBX8 does not play a crucial role in neoplastic transformation of breast epithelial cells. Although additional experiments using different cells would be necessary to confirm these results.

In summary, data obtained in this thesis confirm the importance of de-regulation in EZH2 expression in breast cancer and further support the idea that EZH2 may represent a good therapeutic target candidate. Moreover, preliminary data about CBX8 suggest that not every PcG protein de-regulation may be linked to breast cancer. Understanding how different PcG participate in breast cancer formation and progression will help the identification of additional prognostic markers and therapeutic targets.

## References

- Abd El-Rehim DM, Pinder SE, Paish CE et al. Expression of luminal and basal cytokeratins in human breast carcinoma. *J Pathol* 2004; 203 (2):661-71.
- Adjei AA. Blocking oncogenic Ras signaling for cancer therapy. *J Natl Cancer Inst* 2001; 93 (14):1062-74.
- Aiyar SE, Sun JL, Blair AL et al. Attenuation of estrogen receptor alpha-mediated transcription through estrogen-stimulated recruitment of a negative elongation factor. *Genes Dev* 2004; 18 (17):2134-46.
- Al-Hajj M, Wicha MS, Benito-Hernandez A et al. Prospective identification of tumorigenic breast cancer cells. *Proc Natl Acad Sci U S A* 2003; 100 (7):3983-8.
- Albini A, Sporn MB. The tumour microenvironment as a target for chemoprevention. *Nat Rev Cancer* 2007; 7 (2):139-47.
- Allinen M, Beroukhi R, Cai L et al. Molecular characterization of the tumor microenvironment in breast cancer. *Cancer Cell* 2004; 6 (1):17-32.
- Alsaker MD, Opdahl S, Asvold BO et al. The association of reproductive factors and breastfeeding with long term survival from breast cancer. *Breast Cancer Res Treat* 2011.
- An HX, Beckmann MW, Reifenberger G et al. Gene amplification and overexpression of CDK4 in sporadic breast carcinomas is associated with high tumor cell proliferation. *Am J Pathol* 1999a; 154 (1):113-8.
- An J, Ribeiro RC, Webb P et al. Estradiol repression of tumor necrosis factor-alpha transcription requires estrogen receptor activation function-2 and is enhanced by coactivators. *Proc Natl Acad Sci U S A* 1999b; 96 (26):15161-6.
- Anderson E. The role of oestrogen and progesterone receptors in human mammary development and tumorigenesis. *Breast Cancer Res* 2002; 4 (5):197-201.
- Antoniou A, Pharoah PD, Narod S et al. Average risks of breast and ovarian cancer associated with BRCA1 or BRCA2 mutations detected in case Series unselected for family history: a combined analysis of 22 studies. *Am J Hum Genet* 2003; 72 (5):1117-30.
- Aoki R, Chiba T, Miyagi S et al. The polycomb group gene product Ezh2 regulates proliferation and differentiation of murine hepatic stem/progenitor cells. *J Hepatol* 2010; 52 (6):854-63.
- Aoto T, Saitoh N, Sakamoto Y et al. Polycomb group protein-associated chromatin is reproduced in post-mitotic G1 phase and is required for S phase progression. *J Biol Chem* 2008; 283 (27):18905-15.
- Aplin AE, Howe A, Alahari SK et al. Signal transduction and signal modulation by cell adhesion receptors: the role of integrins, cadherins, immunoglobulin-cell adhesion molecules, and selectins. *Pharmacol Rev* 1998; 50 (2):197-263.
- Arisan S, Buyuktuncer ED, Palavan-Unsal N et al. Increased expression of EZH2, a polycomb group protein, in bladder carcinoma. *Urol Int* 2005; 75 (3):252-7.
- Arnes JB, Collett K, Akslen LA. Independent prognostic value of the basal-like phenotype of breast cancer and associations with EGFR and candidate stem cell marker BMI-1. *Histopathology* 2008; 52 (3):370-80.
- Arpino G, Laucirica R, Elledge RM. Premalignant and in situ breast disease: biology and clinical implications. *Ann Intern Med* 2005; 143 (6):446-57.



Attardi LD, Reczek EE, Cosmas C et al. PERP, an apoptosis-associated target of p53, is a novel member of the PMP-22/gas3 family. *Genes Dev* 2000; 14 (6):704-18.

Azuara V, Perry P, Sauer S et al. Chromatin signatures of pluripotent cell lines. *Nat Cell Biol* 2006; 8 (5):532-8.

Bachmann IM, Halvorsen OJ, Collett K et al. EZH2 expression is associated with high proliferation rate and aggressive tumor subgroups in cutaneous melanoma and cancers of the endometrium, prostate, and breast. *J Clin Oncol* 2006; 24 (2):268-73.

Bae I, Rih JK, Kim HJ et al. BRCA1 regulates gene expression for orderly mitotic progression. *Cell Cycle* 2005; 4 (11):1641-66.

Baer R, Ludwig T. The BRCA1/BARD1 heterodimer, a tumor suppressor complex with ubiquitin E3 ligase activity. *Curr Opin Genet Dev* 2002; 12 (1):86-91.

Barbareschi M, Pelosio P, Caffo O et al. Cyclin-D1-gene amplification and expression in breast carcinoma: relation with clinicopathologic characteristics and with retinoblastoma gene product, p53 and p21WAF1 immunohistochemical expression. *Int J Cancer* 1997; 74 (2):171-4.

Bardos JI, Saurin AJ, Tissot C et al. HPC3 is a new human polycomb orthologue that interacts and associates with RING1 and Bmi1 and has transcriptional repression properties. *J Biol Chem* 2000; 275 (37):28785-92.

Barsky SH, Karlin NJ. Myoepithelial cells: autocrine and paracrine suppressors of breast cancer progression. *J Mammary Gland Biol Neoplasia* 2005; 10 (3):249-60.

Bartkova J, Lukas J, Muller H et al. Cyclin D1 protein expression and function in human breast cancer. *Int J Cancer* 1994; 57 (3):353-61.

Bauer KR, Brown M, Cress RD et al. Descriptive analysis of estrogen receptor (ER)-negative, progesterone receptor (PR)-negative, and HER2-negative invasive breast cancer, the so-called triple-negative phenotype: a population-based study from the California cancer Registry. *Cancer* 2007; 109 (9):1721-8.

Bea S, Tort F, Pinyol M et al. BMI-1 gene amplification and overexpression in hematological malignancies occur mainly in mantle cell lymphomas. *Cancer Res* 2001; 61 (6):2409-12.

Beausejour CM, Krtolica A, Galimi F et al. Reversal of human cellular senescence: roles of the p53 and p16 pathways. *Embo J* 2003; 22 (16):4212-22.

Benton G, Croke E, George J. Laminin-1 induces E-cadherin expression in 3-dimensional cultured breast cancer cells by inhibiting DNA methyltransferase 1 and reversing promoter methylation status. *Faseb J* 2009; 23 (11):3884-95.

Benusiglio PR, Lesueur F, Luccarini C et al. Common ERBB2 polymorphisms and risk of breast cancer in a white British population: a case-control study. *Breast Cancer Res* 2005; 7 (2):R204-9.

Berge EO, Knappskog S, Lillehaug JR et al. Alterations of the retinoblastoma gene in metastatic breast cancer. *Clin Exp Metastasis* 2010; 28 (3):319-26.

Berger SL, Kouzarides T, Shiekhatar R et al. An operational definition of epigenetics. *Genes Dev* 2009; 23 (7):781-3.

Bernard D, Martinez-Leal JF, Rizzo S et al. CBX7 controls the growth of normal and tumor-derived prostate cells by repressing the Ink4a/Arf locus. *Oncogene* 2005; 24 (36):5543-51.

Bernstein BE, Mikkelsen TS, Xie X et al. A bivalent chromatin structure marks key developmental genes in embryonic stem cells. *Cell* 2006a; 125 (2):315-26.

Bernstein E, Duncan EM, Masui O et al. Mouse polycomb proteins bind differentially to methylated histone H3 and RNA and are enriched in facultative heterochromatin. *Mol Cell Biol* 2006b; 26 (7):2560-9.

Berthon P, Pancino G, de Cremoux P et al. Characterization of normal breast epithelial cells in primary cultures: differentiation and growth factor receptors studies. *In Vitro Cell Dev Biol* 1992; 28A (11-12):716-24.

Bertucci F, Finetti P, Cervera N et al. How basal are triple-negative breast cancers? *Int J Cancer* 2008; 123 (1):236-40.

Bezsonova I, Walker JR, Bacik JP et al. Ring1B contains a ubiquitin-like docking module for interaction with Cbx proteins. *Biochemistry* 2009; 48 (44):10542-8.

Bhattacharyya A, Ear US, Koller BH et al. The breast cancer susceptibility gene BRCA1 is required for subnuclear assembly of Rad51 and survival following treatment with the DNA cross-linking agent cisplatin. *J Biol Chem* 2000; 275 (31):23899-903.

Biason-Lauber A, Konrad D, Meyer M et al. Ovaries and female phenotype in a girl with 46,XY karyotype and mutations in the CBX2 gene. *Am J Hum Genet* 2009; 84 (5):658-63.

Birgisdottir V, Stefansson OA, Bodvarsdottir SK et al. Epigenetic silencing and deletion of the BRCA1 gene in sporadic breast cancer. *Breast Cancer Res* 2006; 8 (4):R38.

Bocker W, Moll R, Poremba C et al. Common adult stem cells in the human breast give rise to glandular and myoepithelial cell lineages: a new cell biological concept. *Lab Invest* 2002; 82 (6):737-46.

Boehm JS, Hahn WC. Understanding transformation: progress and gaps. *Curr Opin Genet Dev* 2005; 15 (1):13-7.

Boiani M, Scholer HR. Regulatory networks in embryo-derived pluripotent stem cells. *Nat Rev Mol Cell Biol* 2005; 6 (11):872-84.

Bombonati A, Sgroi DC. The molecular pathology of breast cancer progression. *J Pathol* 2011; 223 (2):307-17.

Borresen-Dale AL. TP53 and breast cancer. *Hum Mutat* 2003; 21 (3):292-300.

Boulton SJ. BRCA1-mediated ubiquitylation. *Cell Cycle* 2006; 5 (14):1481-6.

Boyer LA, Plath K, Zeitlinger J et al. Polycomb complexes repress developmental regulators in murine embryonic stem cells. *Nature* 2006; 441 (7091):349-53.

Boyle JM, Mitchell EL, Greaves MJ et al. Chromosome instability is a predominant trait of fibroblasts from Li-Fraumeni families. *Br J Cancer* 1998; 77 (12):2181-92.

Bozzuto G, Ruggieri P, Molinari A. Molecular aspects of tumor cell migration and invasion. *Ann Ist Super Sanita* 2010; 46 (1):66-80.

Bracken AP, Dietrich N, Pasini D et al. Genome-wide mapping of Polycomb target genes unravels their roles in cell fate transitions. *Genes Dev* 2006; 20 (9):1123-36.

Bracken AP, Helin K. Polycomb group proteins: navigators of lineage pathways led astray in cancer. *Nat Rev Cancer* 2009; 9 (11):773-84.

Bracken AP, Kleine-Kohlbrecher D, Dietrich N et al. The Polycomb group proteins bind throughout the INK4A-ARF locus and are disassociated in senescent cells. *Genes Dev* 2007; 21 (5):525-30.

Bracken AP, Pasini D, Capra M et al. EZH2 is downstream of the pRB-E2F pathway, essential for proliferation and amplified in cancer. *Embo J* 2003; 22 (20):5323-35.

Brisken C, O'Malley B. Hormone action in the mammary gland. *Cold Spring Harb Perspect Biol* 2010; 2 (12):a003178.

Bryant HU, Glasebrook AL, Yang NN et al. An estrogen receptor basis for raloxifene action in bone. *J Steroid Biochem Mol Biol* 1999; 69 (1-6):37-44.

Bryant RJ, Cross NA, Eaton CL et al. EZH2 promotes proliferation and invasiveness of prostate cancer cells. *Prostate* 2007; 67 (5):547-56.

Brzozowski AM, Pike AC, Dauter Z et al. Molecular basis of agonism and antagonism in the oestrogen receptor. *Nature* 1997; 389 (6652):753-8.

Buerger H, Otterbach F, Simon R et al. Comparative genomic hybridization of ductal carcinoma in situ of the breast-evidence of multiple genetic pathways. *J Pathol* 1999; 187 (4):396-402.

Burdall SE, Hanby AM, Lansdown MR et al. Breast cancer cell lines: friend or foe? *Breast Cancer Res* 2003; 5 (2):89-95.

Cailleau R, Young R, Olive M et al. Breast tumor cell lines from pleural effusions. *J Natl Cancer Inst* 1974; 53 (3):661-74.

Caldarella A, Crocetti E, Bianchi S et al. Female Breast Cancer Status According to ER, PR and HER2 Expression: A Population Based Analysis. *Pathol Oncol Res* 2011.

Caldas C, Aparicio S. Cell memory and cancer--the story of the trithorax and Polycomb group genes. *Cancer Metastasis Rev* 1999; 18 (2):313-29.

Caldas C, Hahn SA, da Costa LT et al. Frequent somatic mutations and homozygous deletions of the p16 (MTS1) gene in pancreatic adenocarcinoma. *Nat Genet* 1994; 8 (1):27-32.

Cam H, Dynlacht BD. Emerging roles for E2F: beyond the G1/S transition and DNA replication. *Cancer Cell* 2003; 3 (4):311-6.

Campbell LL, Polyak K. Breast tumor heterogeneity: cancer stem cells or clonal evolution? *Cell Cycle* 2007; 6 (19):2332-8.

Campos EI, Reinberg D. Histones: annotating chromatin. *Annu Rev Genet* 2009; 43:559-99.

Cao L, Li W, Kim S et al. Senescence, aging, and malignant transformation mediated by p53 in mice lacking the Brcal full-length isoform. *Genes Dev* 2003; 17 (2):201-13.

Cao R, Tsukada Y, Zhang Y. Role of Bmi-1 and Ring1A in H2A ubiquitylation and Hox gene silencing. *Mol Cell* 2005; 20 (6):845-54.

Cao R, Wang L, Wang H et al. Role of histone H3 lysine 27 methylation in Polycomb-group silencing. *Science* 2002; 298 (5595):1039-43.

Cao R, Zhang Y. The functions of E(Z)/EZH2-mediated methylation of lysine 27 in histone H3. *Curr Opin Genet Dev* 2004; 14 (2):155-64.

Chano T, Ikebuchi K, Ochi Y et al. RB1CC1 activates RB1 pathway and inhibits proliferation and cologenic survival in human cancer. *PLoS One* 2010; 5 (6):e11404.

Chaplet M, Rai R, Jackson-Bernitsas D et al. BRIT1/MCPH1: a guardian of genome and an enemy of tumors. *Cell Cycle* 2006; 5 (22):2579-83.

Chase A, Cross NC. Aberrations of EZH2 in Cancer. *Clin Cancer Res* 2011; 17 (9):2613-8.

Cheang MC, Chia SK, Voduc D et al. Ki67 index, HER2 status, and prognosis of patients with luminal B breast cancer. *J Natl Cancer Inst* 2009; 101 (10):736-50.

Chen HC. Boyden chamber assay. *Methods Mol Biol* 2005; 294:15-22.

Chen JQ, Russo J. ERalpha-negative and triple negative breast cancer: molecular features and potential therapeutic approaches. *Biochim Biophys Acta* 2009; 1796 (2):162-75.

Chen S, Bohrer LR, Rai AN et al. Cyclin-dependent kinases regulate epigenetic gene silencing through phosphorylation of EZH2. *Nat Cell Biol* 2010; 12 (11):1108-14.

Cheng AS, Culhane AC, Chan MW et al. Epithelial progeny of estrogen-exposed breast progenitor cells display a cancer-like methylome. *Cancer Res* 2008; 68 (6):1786-96.

Cheng AS, Lau SS, Chen Y et al. EZH2-mediated concordant repression of Wnt antagonists promotes  $\beta$ -catenin-dependent hepatocarcinogenesis. *Cancer Res* 2010.

Choi YJ, Choi YL, Cho EY et al. Expression of Bmi-1 protein in tumor tissues is associated with favorable prognosis in breast cancer patients. *Breast Cancer Res Treat* 2009; 113 (1):83-93.

Cichon MA, Degnim AC, Visscher DW et al. Microenvironmental influences that drive progression from benign breast disease to invasive breast cancer. *J Mammary Gland Biol Neoplasia* 2010; 15 (4):389-97.

Clark GJ, Der CJ. Aberrant function of the Ras signal transduction pathway in human breast cancer. *Breast Cancer Res Treat* 1995; 35 (1):133-44.

Clark GM. Prognostic and Predictive Factors for Breast Cancer. *Breast Cancer* 1995; 2 (2):79-89.

Clarke RB, Howell A, Potten CS et al. Dissociation between steroid receptor expression and cell proliferation in the human breast. *Cancer Res* 1997; 57 (22):4987-91.

Coene ED, Gadelha C, White N et al. A novel role for BRCA1 in regulating breast cancer cell spreading and motility. *J Cell Biol* 2011; 192 (3):497-512.

Collett K, Eide GE, Arnes J et al. Expression of enhancer of zeste homologue 2 is significantly associated with increased tumor cell proliferation and is a marker of aggressive breast cancer. *Clin Cancer Res* 2006; 12 (4):1168-74.

Collins LC, Martyniak A, Kandel MJ et al. Basal cytokeratin and epidermal growth factor receptor expression are not predictive of BRCA1 mutation status in women with triple-negative breast cancers. *Am J Surg Pathol* 2009; 33 (7):1093-7.

Constantinidou A, Jones RL, Reis-Filho JS. Beyond triple-negative breast cancer: the need to define new subtypes. *Expert Rev Anticancer Ther* 2010; 10 (8):1197-213.

Core N, Joly F, Boned A et al. Disruption of E2F signaling suppresses the INK4a-induced proliferative defect in M33-deficient mice. *Oncogene* 2004; 23 (46):7660-8.

Cortez D, Wang Y, Qin J et al. Requirement of ATM-dependent phosphorylation of brca1 in the DNA damage response to double-strand breaks. *Science* 1999; 286 (5442):1162-6.

Cotter TG, Lennon SV, Glynn JG et al. Cell death via apoptosis and its relationship to growth, development and differentiation of both tumour and normal cells. *Anticancer Res* 1990; 10 (5A):1153-9.

Cowin & Wysolmerski J. Molecular mechanisms guiding embryonic mammary gland development. *Cold Spring Harb Perspect Biol* 2010; 2 (6):a003251.

Crea F, Hurt EM, Farrar WL. Clinical significance of Polycomb gene expression in brain tumors. *Mol Cancer* 2010; 9:265.

Cristofanilli M, Gonzalez-Angulo AM, Buzdar AU et al. Paclitaxel improves the prognosis in estrogen receptor negative inflammatory breast cancer: the M. D. Anderson Cancer Center experience. *Clin Breast Cancer* 2004; 4 (6):415-9.

Crook T, Brooks LA, Crossland S et al. p53 mutation with frequent novel condons but not a mutator phenotype in BRCA1- and BRCA2-associated breast tumours. *Oncogene* 1998; 17 (13):1681-9.

Czermin B, Melfi R, McCabe D et al. Drosophila enhancer of Zeste/ESC complexes have a histone H3 methyltransferase activity that marks chromosomal Polycomb sites. *Cell* 2002; 111 (2):185-96.

Datta S, Hoenerhoff MJ, Bommi P et al. Bmi-1 cooperates with H-Ras to transform human mammary epithelial cells via dysregulation of multiple growth-regulatory pathways. *Cancer Res* 2007; 67 (21):10286-95.

De Lorenzo C, Cozzolino R, Carpentieri A et al. Biological properties of a human compact anti-ErbB2 antibody. *Carcinogenesis* 2005; 26 (11):1890-5.

de Ruijter TC, Veeck J, de Hoon JP et al. Characteristics of triple-negative breast cancer. *J Cancer Res Clin Oncol* 2011; 137 (2):183-92.

Debnath J, Mills KR, Collins NL et al. The role of apoptosis in creating and maintaining luminal space within normal and oncogene-expressing mammary acini. *Cell* 2002; 111 (1):29-40.

Debnath J, Muthuswamy SK, Brugge JS. Morphogenesis and oncogenesis of MCF-10A mammary epithelial acini grown in three-dimensional basement membrane cultures. *Methods* 2003; 30 (3):256-68.

DeNicola GM, Tuveson DA. RAS in cellular transformation and senescence. *Eur J Cancer* 2009; 45 Suppl 1:211-6.

Dickson RB, Johnson MD, Bano M et al. Growth factors in breast cancer: mitogenesis to transformation. *J Steroid Biochem Mol Biol* 1992; 43 (1-3):69-78.

Dietrich N, Bracken AP, Trinh E et al. Bypass of senescence by the polycomb group protein CBX8 through direct binding to the INK4A-ARF locus. *Embo J* 2007; 26 (6):1637-48.

Dimri G, Band H, Band V. Mammary epithelial cell transformation: insights from cell culture and mouse models. *Breast Cancer Res* 2005; 7 (4):171-9.

Dimri GP, Martinez JL, Jacobs JJ et al. The Bmi-1 oncogene induces telomerase activity and immortalizes human mammary epithelial cells. *Cancer Res* 2002; 62 (16):4736-45.

Ding L, Erdmann C, Chinnaiyan AM et al. Identification of EZH2 as a molecular marker for a precancerous state in morphologically normal breast tissues. *Cancer Res* 2006a; 66 (8):4095-9.

Ding L, Klier CG. Enhancer of Zeste 2 as a marker of preneoplastic progression in the breast. *Cancer Res* 2006b; 66 (19):9352-5.

Dodds DC, Omeis IA, Cushman SJ et al. Neuronal pentraxin receptor, a novel putative integral membrane pentraxin that interacts with neuronal pentraxin 1 and 2 and taipoxin-associated calcium-binding protein 49. *J Biol Chem* 1997; 272 (34):21488-94.

Dontu G, Abdallah WM, Foley JM et al. In vitro propagation and transcriptional profiling of human mammary stem/progenitor cells. *Genes Dev* 2003a; 17 (10):1253-70.

Dontu G, Al-Hajj M, Abdallah WM et al. Stem cells in normal breast development and breast cancer. *Cell Prolif* 2003b; 36 Suppl 1:59-72.

Dontu G, Liu S, Wicha MS. Stem cells in mammary development and carcinogenesis: implications for prevention and treatment. *Stem Cell Rev* 2005; 1 (3):207-13.

Drabsch Y, Ten Dijke P. TGF-beta Signaling in Breast Cancer Cell Invasion and Bone Metastasis. *J Mammary Gland Biol Neoplasia* 2011; 16 (2):97-108.

Drayton S, Brookes S, Rowe J et al. The significance of p16INK4a in cell defenses against transformation. *Cell Cycle* 2004; 3 (5):611-5.

Dukers DF, van Galen JC, Giroth C et al. Unique polycomb gene expression pattern in Hodgkin's lymphoma and Hodgkin's lymphoma-derived cell lines. *Am J Pathol* 2004; 164 (3):873-81.

Duss S, Andre S, Nicoulaz AL et al. An oestrogen-dependent model of breast cancer created by transformation of normal human mammary epithelial cells. *Breast Cancer Res* 2007; 9 (3):R38.

Dworkin AM, Huang TH, Toland AE. Epigenetic alterations in the breast: Implications for breast cancer detection, prognosis and treatment. *Semin Cancer Biol* 2009; 19 (3):165-71.

Ehrlich M. DNA hypomethylation, cancer, the immunodeficiency, centromeric region instability, facial anomalies syndrome and chromosomal rearrangements. *J Nutr* 2002; 132 (8 Suppl):2424S-9S.

El-Tanani M, Platt-Higgins A, Rudland PS et al. Ets gene PEA3 cooperates with beta-catenin-Lef-1 and c-Jun in regulation of osteopontin transcription. *J Biol Chem* 2004; 279 (20):20794-806.

El-Tanani MK, Campbell FC, Crowe P et al. BRCA1 suppresses osteopontin-mediated breast cancer. *J Biol Chem* 2006; 281 (36):26587-601.

Elledge RM, Green S, Pugh R et al. Estrogen receptor (ER) and progesterone receptor (PgR), by ligand-binding assay compared with ER, PgR and pS2, by immuno-histochemistry in predicting response to tamoxifen in metastatic breast cancer: a Southwest Oncology Group Study. *Int J Cancer* 2000; 89 (2):111-7.

Elsheikh SE, Green AR, Rakha EA et al. Global histone modifications in breast cancer correlate with tumor phenotypes, prognostic factors, and patient outcome. *Cancer Res* 2009; 69 (9):3802-9.

Elston CW, Ellis IO. Pathological prognostic factors in breast cancer. I. The value of histological grade in breast cancer: experience from a large study with long-term follow-up. *Histopathology* 1991; 19 (5):403-10.

Emerman JT, Wilkinson DA. Routine culturing of normal, dysplastic and malignant human mammary epithelial cells from small tissue samples. *In Vitro Cell Dev Biol* 1990; 26 (12):1186-94.

Ethier SP. Human breast cancer cell lines as models of growth regulation and disease progression. *J Mammary Gland Biol Neoplasia* 1996; 1 (1):111-21.

Ethier SP, Summerfelt RM, Cundiff KC et al. The influence of growth factors on the proliferative potential of normal and primary breast cancer-derived human breast epithelial cells. *Breast Cancer Res Treat* 1991; 17 (3):221-30.

Fabbro M, Savage K, Hobson K et al. BRCA1-BARD1 complexes are required for p53Ser-15 phosphorylation and a G1/S arrest following ionizing radiation-induced DNA damage. *J Biol Chem* 2004; 279 (30):31251-8.

Fan S, Ma YX, Wang C et al. Role of direct interaction in BRCA1 inhibition of estrogen receptor activity. *Oncogene* 2001; 20 (1):77-87.

Fan S, Wang J, Yuan R et al. BRCA1 inhibition of estrogen receptor signaling in transfected cells. *Science* 1999; 284 (5418):1354-6.

Federico A, Pallante P, Bianco M et al. Chromobox protein homologue 7 protein, with decreased expression in human carcinomas, positively regulates E-cadherin expression by interacting with the histone deacetylase 2 protein. *Cancer Res* 2009; 69 (17):7079-87.

Feinberg AP, Ohlsson R, Henikoff S. The epigenetic progenitor origin of human cancer. *Nat Rev Genet* 2006; 7 (1):21-33.

Ferguson AT, Lapidus RG, Baylin SB et al. Demethylation of the estrogen receptor gene in estrogen receptor-negative breast cancer cells can reactivate estrogen receptor gene expression. *Cancer Res* 1995; 55 (11):2279-83.

Fischle W, Wang Y, Jacobs SA et al. Molecular basis for the discrimination of repressive methyl-lysine marks in histone H3 by Polycomb and HP1 chromodomains. *Genes Dev* 2003; 17 (15):1870-81.

Flanagan JF, Mi LZ, Chruszcz M et al. Double chromodomains cooperate to recognize the methylated histone H3 tail. *Nature* 2005; 438 (7071):1181-5.

Foray N, Marot D, Randrianarison V et al. Constitutive association of BRCA1 and c-Abl and its ATM-dependent disruption after irradiation. *Mol Cell Biol* 2002; 22 (12):4020-32.

Fowler AM, Alarid ET. Amping up estrogen receptors in breast cancer. *Breast Cancer Res* 2007; 9 (4):305.

Francis NJ, Kingston RE. Mechanisms of transcriptional memory. *Nat Rev Mol Cell Biol* 2001; 2 (6):409-21.

Friend SH, Bernards R, Rogelj S et al. A human DNA segment with properties of the gene that predisposes to retinoblastoma and osteosarcoma. *Nature* 1986; 323 (6089):643-6.

Gallagher DJ, Gaudet MM, Pal P et al. Germline BRCA mutations denote a clinicopathologic subset of prostate cancer. *Clin Cancer Res* 2010; 16 (7):2115-21.

Gao X, Nawaz Z. Progesterone receptors - animal models and cell signaling in breast cancer: Role of steroid receptor coactivators and corepressors of progesterone receptors in breast cancer. *Breast Cancer Res* 2002; 4 (5):182-6.

Garbe JC, Bhattacharya S, Merchant B et al. Molecular distinctions between stasis and telomere attrition senescence barriers shown by long-term culture of normal human mammary epithelial cells. *Cancer Res* 2009; 69 (19):7557-68.

Gatza ML, Lucas JE, Barry WT et al. A pathway-based classification of human breast cancer. *Proc Natl Acad Sci U S A* 2010; 107 (15):6994-9.

Gazdar AF, Kurvari V, Virmani A et al. Characterization of paired tumor and non-tumor cell lines established from patients with breast cancer. *Int J Cancer* 1998; 78 (6):766-74.

Gecz J, Gaunt SJ, Passage E et al. Assignment of a Polycomb-like chromobox gene (CBX2) to human chromosome 17q25. *Genomics* 1995; 26 (1):130-3.

Genovese C, Trani D, Caputi M et al. Cell cycle control and beyond: emerging roles for the retinoblastoma gene family. *Oncogene* 2006; 25 (38):5201-9.

Giacca AJ, Kastan MB. The complexity of p53 modulation: emerging patterns from divergent signals. *Genes Dev* 1998; 12 (19):2973-83.

Gil J, Bernard D, Martinez D et al. Polycomb CBX7 has a unifying role in cellular lifespan. *Nat Cell Biol* 2004; 6 (1):67-72.

Gillett CE, Miles DW, Ryder K et al. Retention of the expression of E-cadherin and catenins is associated with shorter survival in grade III ductal carcinoma of the breast. *J Pathol* 2001; 193 (4):433-41.

Glover JN. Insights into the molecular basis of human hereditary breast cancer from studies of the BRCA1 BRCT domain. *Fam Cancer* 2006; 5 (1):89-93.

Gluz O, Liedtke C, Gottschalk N et al. Triple-negative breast cancer--current status and future directions. *Ann Oncol* 2009; 20 (12):1913-27.

Gonzalez ME, Duprie ML, Krueger H et al. Histone Methyltransferase EZH2 Induces Akt-Dependent Genomic Instability and BRCA1 Inhibition in Breast Cancer. *Cancer Res* 2011; 71 (6):2360-70.

Gonzalez ME, Li X, Toy K et al. Downregulation of EZH2 decreases growth of estrogen receptor-negative invasive breast carcinoma and requires BRCA1. *Oncogene* 2009; 28 (6):843-53.

Graham JD, Roman SD, McGowan E et al. Preferential stimulation of human progesterone receptor B expression by estrogen in T-47D human breast cancer cells. *J Biol Chem* 1995; 270 (51):30693-700.

Graham JD, Yeates C, Balleine RL et al. Progesterone receptor A and B protein expression in human breast cancer. *J Steroid Biochem Mol Biol* 1996; 56 (1-6 Spec No):93-8.

Gudjonsson T, Adriance MC, Sternlicht MD et al. Myoepithelial cells: their origin and function in breast morphogenesis and neoplasia. *J Mammary Gland Biol Neoplasia* 2005; 10 (3):261-72.

Gunster MJ, Raaphorst FM, Hamer KM et al. Differential expression of human Polycomb group proteins in various tissues and cell types. *J Cell Biochem Suppl* 2001; Suppl 36:129-43.

Gustafsson JA. Estrogen receptor beta--a new dimension in estrogen mechanism of action. *J Endocrinol* 1999; 163 (3):379-83.

Gusterson BA, Ross DT, Heath VJ et al. Basal cytokeratins and their relationship to the cellular origin and functional classification of breast cancer. *Breast Cancer Res* 2005; 7 (4):143-8.

Hahn WC. Immortalization and transformation of human cells. *Mol Cells* 2002; 13 (3):351-61.

Hahn WC. Telomere and telomerase dynamics in human cells. *Curr Mol Med* 2005; 5 (2):227-31.

Hahn WC, Counter CM, Lundberg AS et al. Creation of human tumour cells with defined genetic elements. *Nature* 1999; 400 (6743):464-8.

Hall JM, McDonnell DP. The estrogen receptor beta-isoform (ERbeta) of the human estrogen receptor modulates ERalpha transcriptional activity and is a key regulator of the cellular response to estrogens and antiestrogens. *Endocrinology* 1999; 140 (12):5566-78.

Hallstrom TC, Mori S, Nevins JR. An E2F1-dependent gene expression program that determines the balance between proliferation and cell death. *Cancer Cell* 2008; 13 (1):11-22.

Hammond SL, Ham RG, Stampfer MR. Serum-free growth of human mammary epithelial cells: rapid clonal growth in defined medium and extended serial passage with pituitary extract. *Proc Natl Acad Sci U S A* 1984; 81 (17):5435-9.

Hanahan & Weinberg. The hallmarks of cancer. *Cell* 2000; 100 (1):57-70.

Hanahan & Weinberg. Hallmarks of cancer: the next generation. *Cell* 2011; 144 (5):646-74.

Hansen KH, Bracken AP, Pasini D et al. A model for transmission of the H3K27me3 epigenetic mark. *Nat Cell Biol* 2008; 10 (11):1291-300.

Harkin K SaDP. BRCA1 and BRCA2: Role in the DNA Damage Response, Cancer Formation and Treatment. *The DNA Damage Response: Implications on Cancer Formation and Treatment* 2009; 18:415-43.

Hartmann LC, Sellers TA, Frost MH et al. Benign breast disease and the risk of breast cancer. *N Engl J Med* 2005; 353 (3):229-37.

Haupt B, Ro JY, Schwartz MR. Basal-like breast carcinoma: a phenotypically distinct entity. *Arch Pathol Lab Med* 2010; 134 (1):130-3.

Haupt Y, Bath ML, Harris AW et al. bmi-1 transgene induces lymphomas and collaborates with myc in tumorigenesis. *Oncogene* 1993; 8 (11):3161-4.

Herranz N, Pasini D, Diaz VM et al. Polycomb complex 2 is required for E-cadherin repression by the Snail1 transcription factor. *Mol Cell Biol* 2008; 28 (15):4772-81.

Herschkowitz JI, He X, Fan C et al. The functional loss of the retinoblastoma tumour suppressor is a common event in basal-like and luminal B breast carcinomas. *Breast Cancer Res* 2008; 10 (5):R75.



Herschkowitz JI, Simin K, Weigman VJ et al. Identification of conserved gene expression features between murine mammary carcinoma models and human breast tumors. *Genome Biol* 2007; 8 (5):R76.

Hoenerhoff MJ, Chu I, Barkan D et al. BMI1 cooperates with H-RAS to induce an aggressive breast cancer phenotype with brain metastases. *Oncogene* 2009; 28 (34):3022-32.

Holst F, Stahl PR, Ruiz C et al. Estrogen receptor alpha (ESR1) gene amplification is frequent in breast cancer. *Nat Genet* 2007; 39 (5):655-60.

Hori M, Shimazaki J, Inagawa S et al. Overexpression of MDM2 oncoprotein correlates with possession of estrogen receptor alpha and lack of MDM2 mRNA splice variants in human breast cancer. *Breast Cancer Res Treat* 2002; 71 (1):77-83.

Hosey AM, Gorski JJ, Murray MM et al. Molecular basis for estrogen receptor alpha deficiency in BRCA1-linked breast cancer. *J Natl Cancer Inst* 2007; 99 (22):1683-94.

Hu M, Yao J, Carroll DK et al. Regulation of in situ to invasive breast carcinoma transition. *Cancer Cell* 2008; 13 (5):394-406.

Hu X, Stern HM, Ge L et al. Genetic alterations and oncogenic pathways associated with breast cancer subtypes. *Mol Cancer Res* 2009; 7 (4):511-22.

Hu Z, Fan C, Oh DS et al. The molecular portraits of breast tumors are conserved across microarray platforms. *BMC Genomics* 2006; 7:96.

Huang DP, Ng MH, Lo KW et al. Molecular basis of cancer. *Hong Kong Med J* 1997; 3 (2):186-94.

Huang KH, Liu JH, Li XX et al. [Association of Bmi-1 mRNA expression with differentiation, metastasis and prognosis of gastric carcinoma]. *Nan Fang Yi Ke Da Xue Xue Bao* 2007; 27 (7):973-5.

Hui L, Zheng Y, Yan Y et al. Mutant p53 in MDA-MB-231 breast cancer cells is stabilized by elevated phospholipase D activity and contributes to survival signals generated by phospholipase D. *Oncogene* 2006; 25 (55):7305-10.

Hulka BS, Moorman PG. Breast cancer: hormones and other risk factors. *Maturitas* 2001; 38 (1):103-13; discussion 13-6.

Hulka BS, Moorman PG. Breast cancer: hormones and other risk factors. *Maturitas* 2008; 61 (1-2):203-13; discussion 13.

Hurd C, Khattree N, Dinda S et al. Regulation of tumor suppressor proteins, p53 and retinoblastoma, by estrogen and antiestrogens in breast cancer cells. *Oncogene* 1997; 15 (8):991-5.

Imbalzano KM, Tatarkova I, Imbalzano AN et al. Increasingly transformed MCF-10A cells have a progressively tumor-like phenotype in three-dimensional basement membrane culture. *Cancer Cell Int* 2009; 9:7.

Ince TA, Richardson AL, Bell GW et al. Transformation of different human breast epithelial cell types leads to distinct tumor phenotypes. *Cancer Cell* 2007; 12 (2):160-70.

Itahana K, Zou Y, Itahana Y et al. Control of the replicative life span of human fibroblasts by p16 and the polycomb protein Bmi-1. *Mol Cell Biol* 2003; 23 (1):389-401.

Ivshina AV, George J, Senko O et al. Genetic reclassification of histologic grade delineates new clinical subtypes of breast cancer. *Cancer Res* 2006; 66 (21):10292-301.

Jacobs JJ, Kieboom K, Marino S et al. The oncogene and Polycomb-group gene bmi-1 regulates cell proliferation and senescence through the ink4a locus. *Nature* 1999; 397 (6715):164-8.

Jacobs SA, Khorasanizadeh S. Structure of HP1 chromodomain bound to a lysine 9-methylated histone H3 tail. *Science* 2002; 295 (5562):2080-3.

Jacobs SA, Taverna SD, Zhang Y et al. Specificity of the HP1 chromo domain for the methylated N-terminus of histone H3. *Embo J* 2001; 20 (18):5232-41.

Jahanzeb M. Adjuvant trastuzumab therapy for HER2-positive breast cancer. *Clin Breast Cancer* 2008; 8 (4):324-33.

Jeffers LJ, Coull BJ, Stack SJ et al. Distinct BRCT domains in Mcph1/Brit1 mediate ionizing radiation-induced focus formation and centrosomal localization. *Oncogene* 2008; 27 (1):139-44.

Jiang SY, Jordan VC. A molecular strategy to control tamoxifen resistant breast cancer. *Cancer Surv* 1992; 14:55-70.

Jordan VC. Selective estrogen receptor modulation: concept and consequences in cancer. *Cancer Cell* 2004; 5 (3):207-13.

Jovanovic J, Ronneberg JA, Tost J et al. The epigenetics of breast cancer. *Mol Oncol* 2010; 4 (3):242-54.

Kadar K, Kiraly M, Porcsalmy B et al. Differentiation potential of stem cells from human dental origin - promise for tissue engineering. *J Physiol Pharmacol* 2009; 60 Suppl 7:167-75.

Kamminga LM, Bystrykh LV, de Boer A et al. The Polycomb group gene Ezh2 prevents hematopoietic stem cell exhaustion. *Blood* 2006; 107 (5):2170-9.

Kang MK, Kim RH, Kim SJ et al. Elevated Bmi-1 expression is associated with dysplastic cell transformation during oral carcinogenesis and is required for cancer cell replication and survival. *Br J Cancer* 2007; 96 (1):126-33.

Kaustov L, Ouyang H, Amaya M et al. Recognition and specificity determinants of the human cbx chromodomains. *J Biol Chem* 2011; 286 (1):521-9.

Kaustov L, Ouyang H, Amaya M et al. Recognition and specificity determinants of the human cbx chromodomains. *J Biol Chem*; 286 (1):521-9.

Keen JC, Davidson NE. The biology of breast carcinoma. *Cancer* 2003; 97 (3 Suppl):825-33.

Keller PJ, Lin AF, Arendt LM et al. Mapping the cellular and molecular heterogeneity of normal and malignant breast tissues and cultured cell lines. *Breast Cancer Res* 2010; 12 (5):R87.

Kendrick H, Regan JL, Magnay FA et al. Transcriptome analysis of mammary epithelial subpopulations identifies novel determinants of lineage commitment and cell fate. *BMC Genomics* 2008; 9:591.

Kerlikowske K, Molinaro A, Cha I et al. Characteristics associated with recurrence among women with ductal carcinoma in situ treated by lumpectomy. *J Natl Cancer Inst* 2003; 95 (22):1692-702.

Kerppola TK. Polycomb group complexes--many combinations, many functions. *Trends Cell Biol* 2009; 19 (12):692-704.

Khalil AM, Guttman M, Huarte M et al. Many human large intergenic noncoding RNAs associate with chromatin-modifying complexes and affect gene expression. *Proc Natl Acad Sci U S A* 2009; 106 (28):11667-72.

Kheradmand Kia S, Solaimani Kartalaei P, Farahbakhshian E et al. EZH2-dependent chromatin looping controls INK4a and INK4b, but not ARF, during human progenitor cell differentiation and cellular senescence. *Epigenetics Chromatin* 2009; 2 (1):16.

Kim JH, Yoon SY, Jeong SH et al. Overexpression of Bmi-1 oncoprotein correlates with axillary lymph node metastases in invasive ductal breast cancer. *Breast* 2004a; 13 (5):383-8.

Kim JH, Yoon SY, Kim CN et al. The Bmi-1 oncoprotein is overexpressed in human colorectal cancer and correlates with the reduced p16INK4a/p14ARF proteins. *Cancer Lett* 2004b; 203 (2):217-24.

Kim MS, Kondo T, Takada I et al. DNA demethylation in hormone-induced transcriptional derepression. *Nature* 2009; 461 (7266):1007-12.

King MC, Marks JH, Mandell JB. Breast and ovarian cancer risks due to inherited mutations in BRCA1 and BRCA2. *Science* 2003; 302 (5645):643-6.

Kingston RE, Bunker CA, Imbalzano AN. Repression and activation by multiprotein complexes that alter chromatin structure. *Genes Dev* 1996; 10 (8):905-20.

Kirmizis A, Bartley SM, Farnham PJ. Identification of the polycomb group protein SU(Z)12 as a potential molecular target for human cancer therapy. *Mol Cancer Ther* 2003; 2 (1):113-21.

Kita Y, Tseng J, Horan T et al. ErbB receptor activation, cell morphology changes, and apoptosis induced by anti-Her2 monoclonal antibodies. *Biochem Biophys Res Commun* 1996; 226 (1):59-69.

Kleer CG, Cao Q, Varambally S et al. EZH2 is a marker of aggressive breast cancer and promotes neoplastic transformation of breast epithelial cells. *Proc Natl Acad Sci U S A* 2003; 100 (20):11606-11.

Knight WA, Livingston RB, Gregory EJ et al. Estrogen receptor as an independent prognostic factor for early recurrence in breast cancer. *Cancer Res* 1977; 37 (12):4669-71.

Kodach LL, Jacobs RJ, Heijmans J et al. The role of EZH2 and DNA methylation in the silencing of the tumour suppressor RUNX3 in colorectal cancer. *Carcinogenesis* 2010; 31 (9):1567-75.

Koeffler HP, McCormick F, Denny C. Molecular mechanisms of cancer. *West J Med* 1991; 155 (5):505-14.

Korber P, Becker PB. Nucleosome dynamics and epigenetic stability. *Essays Biochem* 2010; 48 (1):63-74.

Kotake Y, Cao R, Viatour P et al. pRB family proteins are required for H3K27 trimethylation and Polycomb repression complexes binding to and silencing p16INK4alpha tumor suppressor gene. *Genes Dev* 2007; 21 (1):49-54.

Kufe P, Weichselbaum. Cell proliferation. In, translator and editor *Cancer Medicine*. Vol. chapter 3: Holland-Frei 2003.

Kunisue H, Kurebayashi J, Otsuki T et al. Anti-HER2 antibody enhances the growth inhibitory effect of anti-oestrogen on breast cancer cells expressing both oestrogen receptors and HER2. *Br J Cancer* 2000; 82 (1):46-51.

Kunju LP, Cookingham C, Toy KA et al. EZH2 and ALDH-1 mark breast epithelium at risk for breast cancer development. *Mod Pathol* 2011.

Kuppumbatti YS, Rexer B, Nakajo S et al. CRBP suppresses breast cancer cell survival and anchorage-independent growth. *Oncogene* 2001; 20 (50):7413-9.

Kushner PJ, Agard D, Feng WJ et al. Oestrogen receptor function at classical and alternative response elements. *Novartis Found Symp* 2000a; 230:20-6; discussion 7-40.

Kushner PJ, Agard DA, Greene GL et al. Estrogen receptor pathways to AP-1. *J Steroid Biochem Mol Biol* 2000b; 74 (5):311-7.

Kuzmichev A, Margueron R, Vaquero A et al. Composition and histone substrates of polycomb repressive group complexes change during cellular differentiation. *Proc Natl Acad Sci U S A* 2005; 102 (6):1859-64.

Lachner M, O'Carroll D, Rea S et al. Methylation of histone H3 lysine 9 creates a binding site for HP1 proteins. *Nature* 2001; 410 (6824):116-20.

Lange CA, Gioeli D, Hammes SR et al. Integration of rapid signaling events with steroid hormone receptor action in breast and prostate cancer. *Annu Rev Physiol* 2007; 69:171-99.

Lapidus RG, Ferguson AT, Ottaviano YL et al. Methylation of estrogen and progesterone receptor gene 5' CpG islands correlates with lack of estrogen and progesterone receptor gene expression in breast tumors. *Clin Cancer Res* 1996; 2 (5):805-10.

Lee EY, Muller WJ. Oncogenes and tumor suppressor genes. *Cold Spring Harb Perspect Biol* 2010; 2 (10):a003236.

Lee EY, To H, Shew JY et al. Inactivation of the retinoblastoma susceptibility gene in human breast cancers. *Science* 1988; 241 (4862):218-21.

Lee TI, Jenner RG, Boyer LA et al. Control of developmental regulators by Polycomb in human embryonic stem cells. *Cell* 2006; 125 (2):301-13.

Leeb M, Pasini D, Novatchkova M et al. Polycomb complexes act redundantly to repress genomic repeats and genes. *Genes Dev*; 24 (3):265-76.

Lessard J, Schumacher A, Thorsteinsdottir U et al. Functional antagonism of the Polycomb-Group genes *eed* and *Bmi1* in hemopoietic cell proliferation. *Genes Dev* 1999; 13 (20):2691-703.

Levine SS, Weiss A, Erdjument-Bromage H et al. The core of the polycomb repressive complex is compositionally and functionally conserved in flies and humans. *Mol Cell Biol* 2002; 22 (17):6070-8.

Li B, Zhou J, Liu P et al. Polycomb protein Cbx4 promotes SUMO modification of de novo DNA methyltransferase Dnmt3a. *Biochem J* 2007; 405 (2):369-78.

Li X, Gonzalez ME, Toy K et al. Targeted overexpression of EZH2 in the mammary gland disrupts ductal morphogenesis and causes epithelial hyperplasia. *Am J Pathol* 2009; 175 (3):1246-54.

Li YH, Zhu C. A modified Boyden chamber assay for tumor cell transendothelial migration in vitro. *Clin Exp Metastasis* 1999; 17 (5):423-9.

Liang CC, Park AY, Guan JL. In vitro scratch assay: a convenient and inexpensive method for analysis of cell migration in vitro. *Nat Protoc* 2007; 2 (2):329-33.

Lim E, Vaillant F, Wu D et al. Aberrant luminal progenitors as the candidate target population for basal tumor development in BRCA1 mutation carriers. *Nat Med* 2009; 15 (8):907-13.

Lin SY, Liang Y, Li K. Multiple roles of BRIT1/MCPH1 in DNA damage response, DNA repair, and cancer suppression. *Yonsei Med J* 2010; 51 (3):295-301.

Lin SY, Rai R, Li K et al. BRIT1/MCPH1 is a DNA damage responsive protein that regulates the Brca1-Chk1 pathway, implicating checkpoint dysfunction in microcephaly. *Proc Natl Acad Sci U S A* 2005; 102 (42):15105-9.

Lindeman GJ, Visvader JE. Insights into the cell of origin in breast cancer and breast cancer stem cells. *Asia Pac J Clin Oncol* 2010; 6 (2):89-97.

Liu G, Schwartz JA, Brooks SC. Estrogen receptor protects p53 from deactivation by human double minute-2. *Cancer Res* 2000; 60 (7):1810-4.

Livasy CA, Perou CM, Karaca G et al. Identification of a basal-like subtype of breast ductal carcinoma in situ. *Hum Pathol* 2007; 38 (2):197-204.

Loeb LA, Loeb KR, Anderson JP. Multiple mutations and cancer. *Proc Natl Acad Sci U S A* 2003; 100 (3):776-81.

Lopez-Garcia MA, Geyer FC, Lacroix-Triki M et al. Breast cancer precursors revisited: molecular features and progression pathways. *Histopathology* 2010; 57 (2):171-92.

Ma XJ, Dahiya S, Richardson E et al. Gene expression profiling of the tumor microenvironment during breast cancer progression. *Breast Cancer Res* 2009; 11 (1):R7.

Ma XJ, Salunga R, Tuggle JT et al. Gene expression profiles of human breast cancer progression. *Proc Natl Acad Sci U S A* 2003; 100 (10):5974-9.

MacMahon B, Trichopoulos D, Brown J et al. Age at menarche, probability of ovulation and breast cancer risk. *Int J Cancer* 1982; 29 (1):13-6.

Maertens GN, El Messaoudi-Aubert S, Racek T et al. Several distinct polycomb complexes regulate and co-localize on the INK4a tumor suppressor locus. *PLoS One* 2009; 4 (7):e6380.

Mahmoudi T, Verrijzer CP. Chromatin silencing and activation by Polycomb and trithorax group proteins. *Oncogene* 2001; 20 (24):3055-66.

Mailand N, Bekker-Jensen S, Fastrup H et al. RNF8 ubiquitylates histones at DNA double-strand breaks and promotes assembly of repair proteins. *Cell* 2007; 131 (5):887-900.

Malkin D, Li FP, Strong LC et al. Germ line p53 mutations in a familial syndrome of breast cancer, sarcomas, and other neoplasms. *Science* 1990; 250 (4985):1233-8.

Malzahn K, Mitze M, Thoenes M et al. Biological and prognostic significance of stratified epithelial cytokeratins in infiltrating ductal breast carcinomas. *Virchows Arch* 1998; 433 (2):119-29.

Manke IA, Lowery DM, Nguyen A et al. BRCT repeats as phosphopeptide-binding modules involved in protein targeting. *Science* 2003; 302 (5645):636-9.

Marcus JN, Watson P, Page DL et al. Hereditary breast cancer: pathobiology, prognosis, and BRCA1 and BRCA2 gene linkage. *Cancer* 1996; 77 (4):697-709.

Martinez AM, Cavalli G. The role of polycomb group proteins in cell cycle regulation during development. *Cell Cycle* 2006a; 5 (11):1189-97.

Martinez AM, Colomb S, Dejardin J et al. Polycomb group-dependent Cyclin A repression in *Drosophila*. *Genes Dev* 2006b; 20 (4):501-13.

Matsukawa Y, Semba S, Kato H et al. Expression of the enhancer of zeste homolog 2 is correlated with poor prognosis in human gastric cancer. *Cancer Sci* 2006; 97 (6):484-91.

Mazo A, Hodgson JW, Petruk S et al. Transcriptional interference: an unexpected layer of complexity in gene regulation. *J Cell Sci* 2007; 120 (Pt 16):2755-61.

McKenna NJ, Lanz RB, O'Malley BW. Nuclear receptor coregulators: cellular and molecular biology. *Endocr Rev* 1999; 20 (3):321-44.

McKeon J, Slade E, Sinclair DA et al. Mutations in some Polycomb group genes of *Drosophila* interfere with regulation of segmentation genes. *Mol Gen Genet* 1994; 244 (5):474-83.

Mihic-Probst D, Kuster A, Kilgus S et al. Consistent expression of the stem cell renewal factor BMI-1 in primary and metastatic melanoma. *Int J Cancer* 2007; 121 (8):1764-70.

Min J, Zhang Y, Xu RM. Structural basis for specific binding of Polycomb chromodomain to histone H3 methylated at Lys 27. *Genes Dev* 2003; 17 (15):1823-8.

Miyakis S, Sourvinos G, Spandidos DA. Differential expression and mutation of the ras family genes in human breast cancer. *Biochem Biophys Res Commun* 1998; 251 (2):609-12.

Miyamoto K, Fukutomi T, Akashi-Tanaka S et al. Identification of 20 genes aberrantly methylated in human breast cancers. *Int J Cancer* 2005; 116 (3):407-14.

Mladkova J, Sanda M, Matouskova E et al. Phenotyping breast cancer cell lines EM-G3, HCC1937, MCF7 and MDA-MB-231 using 2-D electrophoresis and affinity chromatography for glutathione-binding proteins. *BMC Cancer* 2010; 10:449.

Moasser MM, Basso A, Averbuch SD et al. The tyrosine kinase inhibitor ZD1839 ("Iressa") inhibits HER2-driven signaling and suppresses the growth of HER2-overexpressing tumor cells. *Cancer Res* 2001; 61 (19):7184-8.

Mohammad HP, Cai Y, McGarvey KM et al. Polycomb CBX7 promotes initiation of heritable repression of genes frequently silenced with cancer-specific DNA hypermethylation. *Cancer Res* 2009; 69 (15):6322-30.

Mohsin SK, Weiss HL, Gutierrez MC et al. Neoadjuvant trastuzumab induces apoptosis in primary breast cancers. *J Clin Oncol* 2005; 23 (11):2460-8.

Molofsky AV, Pardal R, Iwashita T et al. Bmi-1 dependence distinguishes neural stem cell self-renewal from progenitor proliferation. *Nature* 2003; 425 (6961):962-7.

Mori S, Chang JT, Andrechek ER et al. Anchorage-independent cell growth signature identifies tumors with metastatic potential. *Oncogene* 2009; 28 (31):2796-805.

Morris GJ, Naidu S, Topham AK et al. Differences in breast carcinoma characteristics in newly diagnosed African-American and Caucasian patients: a single-institution compilation compared with the National Cancer Institute's Surveillance, Epidemiology, and End Results database. *Cancer* 2007; 110 (4):876-84.

Moudgil VK, Dinda S, Khattree N et al. Hormonal regulation of tumor suppressor proteins in breast cancer cells. *J Steroid Biochem Mol Biol* 2001; 76 (1-5):105-17.

Moulder SL, Yakes FM, Muthuswamy SK et al. Epidermal growth factor receptor (HER1) tyrosine kinase inhibitor ZD1839 (Iressa) inhibits HER2/neu (erbB2)-overexpressing breast cancer cells in vitro and in vivo. *Cancer Res* 2001; 61 (24):8887-95.

Mullan PB, Quinn JE, Harkin DP. The role of BRCA1 in transcriptional regulation and cell cycle control. *Oncogene* 2006; 25 (43):5854-63.

Muthuswamy SK, Li D, Lelievre S et al. ErbB2, but not ErbB1, reinitiates proliferation and induces luminal repopulation in epithelial acini. *Nat Cell Biol* 2001; 3 (9):785-92.

Nardone A, Corvigno S, Brescia A et al. Long-term cultures of stem/progenitor cells from lobular and ductal breast carcinomas under non-adherent conditions. *Cytotechnology*; 63 (1):67-80.

Neve RM, Chin K, Fridlyand J et al. A collection of breast cancer cell lines for the study of functionally distinct cancer subtypes. *Cancer Cell* 2006; 10 (6):515-27.

Nielsen PR, Nietlispach D, Mott HR et al. Structure of the HP1 chromodomain bound to histone H3 methylated at lysine 9. *Nature* 2002; 416 (6876):103-7.

Nowell PC. The clonal evolution of tumor cell populations. *Science* 1976; 194 (4260):23-8.

O'Carroll D, Erhardt S, Pagani M et al. The polycomb-group gene *Ezh2* is required for early mouse development. *Mol Cell Biol* 2001; 21 (13):4330-6.

Oates AJ, Barraclough R, Rudland PS. The identification of osteopontin as a metastasis-related gene product in a rodent mammary tumour model. *Oncogene* 1996; 13 (1):97-104.

Okorokov AL, Orlova EV. Structural biology of the p53 tumour suppressor. *Curr Opin Struct Biol* 2009; 19 (2):197-202.

Olivier M, Eeles R, Hollstein M et al. The IARC TP53 database: new online mutation analysis and recommendations to users. *Hum Mutat* 2002; 19 (6):607-14.

Orimo A, Gupta PB, Sgroi DC et al. Stromal fibroblasts present in invasive human breast carcinomas promote tumor growth and angiogenesis through elevated SDF-1/CXCL12 secretion. *Cell* 2005; 121 (3):335-48.

Orlando V, Paro R. Chromatin multiprotein complexes involved in the maintenance of transcription patterns. *Curr Opin Genet Dev* 1995; 5 (2):174-9.

Ottaviano YL, Issa JP, Parl FF et al. Methylation of the estrogen receptor gene CpG island marks loss of estrogen receptor expression in human breast cancer cells. *Cancer Res* 1994; 54 (10):2552-5.

Ou-Yang M, Liu HR, Zhang Y et al. ERM stable knockdown by siRNA reduced in vitro migration and invasion of human SGC-7901 cells. *Biochimie* 2011; 93 (5):954-61.

Palii SS, Robertson KD. Epigenetic control of tumor suppression. *Crit Rev Eukaryot Gene Expr* 2007; 17 (4):295-316.

Pallante P, Federico A, Berlingieri MT et al. Loss of the CBX7 gene expression correlates with a highly malignant phenotype in thyroid cancer. *Cancer Res* 2008; 68 (16):6770-8.

Park IK, Qian D, Kiel M et al. Bmi-1 is required for maintenance of adult self-renewing haematopoietic stem cells. *Nature* 2003; 423 (6937):302-5.

Pasini D, Bracken AP, Helin K. Polycomb group proteins in cell cycle progression and cancer. *Cell Cycle* 2004a; 3 (4):396-400.

Pasini D, Bracken AP, Jensen MR et al. Suz12 is essential for mouse development and for EZH2 histone methyltransferase activity. *Embo J* 2004b; 23 (20):4061-71.

Pechoux C, Gudjonsson T, Ronnov-Jessen L et al. Human mammary luminal epithelial cells contain progenitors to myoepithelial cells. *Dev Biol* 1999; 206 (1):88-99.

Pelegri F, Lehmann R. A role of polycomb group genes in the regulation of gap gene expression in *Drosophila*. *Genetics* 1994; 136 (4):1341-53.

Peng G, Lin SY. BRIT1/MCPH1 is a multifunctional DNA damage responsive protein mediating DNA repair-associated chromatin remodeling. *Cell Cycle* 2009; 8 (19):3071-2.

Perou CM, Sorlie T, Eisen MB et al. Molecular portraits of human breast tumours. *Nature* 2000; 406 (6797):747-52.

Petersen OW, Lind Nielsen H, Gudjonsson T et al. The plasticity of human breast carcinoma cells is more than epithelial to mesenchymal conversion. *Breast Cancer Res* 2001; 3 (4):213-7.

Petrucelli N, Daly MB, Feldman GL. BRCA1 and BRCA2 Hereditary Breast and Ovarian Cancer. 1993.

Pfeilschifter J, Koditz R, Pfohl M et al. Changes in proinflammatory cytokine activity after menopause. *Endocr Rev* 2002; 23 (1):90-119.

Pietersen AM, Horlings HM, Hauptmann M et al. EZH2 and BMI1 inversely correlate with prognosis and TP53 mutation in breast cancer. *Breast Cancer Res* 2008; 10 (6):R109.

Pirrotta V. Polycomb the genome: PcG, trxG, and chromatin silencing. *Cell* 1998; 93 (3):333-6.

Plo I, Laulier C, Gauthier L et al. AKT1 inhibits homologous recombination by inducing cytoplasmic retention of BRCA1 and RAD51. *Cancer Res* 2008; 68 (22):9404-12.

Polyak K. Breast cancer: origins and evolution. *J Clin Invest* 2007; 117 (11):3155-63.

Pownall ME, Gustafsson MK, Emerson CP, Jr. Myogenic regulatory factors and the specification of muscle progenitors in vertebrate embryos. *Annu Rev Cell Dev Biol* 2002; 18:747-83.

Prat A, Parker JS, Karginova O et al. Phenotypic and molecular characterization of the claudin-low intrinsic subtype of breast cancer. *Breast Cancer Res* 2010; 12 (5):R68.

Press MF, Jones LA, Godolphin W et al. HER-2/neu oncogene amplification and expression in breast and ovarian cancers. *Prog Clin Biol Res* 1990; 354A:209-21.

Pritchard K. Endocrinology and hormone therapy in breast cancer: endocrine therapy in premenopausal women. *Breast Cancer Res* 2005; 7 (2):70-6.

Promkan M, Liu G, Patmasiriwat P et al. BRCA1 modulates malignant cell behavior, the expression of survivin and chemosensitivity in human breast cancer cells. *Int J Cancer* 2009; 125 (12):2820-8.

Puppe J, Drost R, Liu X et al. BRCA1-deficient mammary tumor cells are dependent on EZH2 expression and sensitive to Polycomb Repressive Complex 2-inhibitor 3-deazaneplanocin A. *Breast Cancer Res* 2009; 11 (4):R63.

Quesnel B, Fenaux P, Philippe N et al. Analysis of p16 gene deletion and point mutation in breast carcinoma. *Br J Cancer* 1995; 72 (2):351-3.

Quinn JE, Kennedy RD, Mullan PB et al. BRCA1 functions as a differential modulator of chemotherapy-induced apoptosis. *Cancer Res* 2003; 63 (19):6221-8.

R. M. Elledge SAWF. Estrogen and progesterone receptors. *Diseases of the breast* 2000; 2:471-88.

Raaphorst FM. Deregulated expression of Polycomb-group oncogenes in human malignant lymphomas and epithelial tumors. *Hum Mol Genet* 2005; 14 Spec No 1:R93-R100.

Raaphorst FM, van Kemenade FJ, Blokzijl T et al. Coexpression of BMI-1 and EZH2 polycomb group genes in Reed-Sternberg cells of Hodgkin's disease. *Am J Pathol* 2000; 157 (3):709-15.

Rai R, Dai H, Multani AS et al. BRIT1 regulates early DNA damage response, chromosomal integrity, and cancer. *Cancer Cell* 2006; 10 (2):145-57.

Raica M, Jung I, Cimpean AM et al. From conventional pathologic diagnosis to the molecular classification of breast carcinoma: are we ready for the change? *Rom J Morphol Embryol* 2009; 50 (1):5-13.

Rakha EA, El-Sayed ME, Green AR et al. Prognostic markers in triple-negative breast cancer. *Cancer* 2007a; 109 (1):25-32.

Rakha EA, Ellis IO. Triple-negative/basal-like breast cancer: review. *Pathology* 2009a; 41 (1):40-7.

Rakha EA, Elsheikh SE, Aleskandarany MA et al. Triple-negative breast cancer: distinguishing between basal and nonbasal subtypes. *Clin Cancer Res* 2009b; 15 (7):2302-10.

Rakha EA, Tan DS, Foulkes WD et al. Are triple-negative tumours and basal-like breast cancer synonymous? *Breast Cancer Res* 2007b; 9 (6):404; author reply 5.

Ratsch SB, Gao Q, Srinivasan S et al. Multiple genetic changes are required for efficient immortalization of different subtypes of normal human mammary epithelial cells. *Radiat Res* 2001; 155 (1 Pt 2):143-50.

Reijm EA, Jansen MP, Ruigrok-Ritstier K et al. Decreased expression of EZH2 is associated with upregulation of ER and favorable outcome to tamoxifen in advanced breast cancer. *Breast Cancer Res Treat* 2010; 125 (2):387-94.



Ren X, Vincenz C, Kerppola TK. Changes in the distributions and dynamics of polycomb repressive complexes during embryonic stem cell differentiation. *Mol Cell Biol* 2008; 28 (9):2884-95.

Reynolds PA, Sigaroudinia M, Zardo G et al. Tumor suppressor p16INK4A regulates polycomb-mediated DNA hypermethylation in human mammary epithelial cells. *J Biol Chem* 2006; 281 (34):24790-802.

Richer JK, Jacobsen BM, Manning NG et al. Differential gene regulation by the two progesterone receptor isoforms in human breast cancer cells. *J Biol Chem* 2002; 277 (7):5209-18.

Richter GH, Plehm S, Fasan A et al. EZH2 is a mediator of EWS/FLI1 driven tumor growth and metastasis blocking endothelial and neuro-ectodermal differentiation. *Proc Natl Acad Sci U S A* 2009; 106 (13):5324-9.

Ringrose L, Paro R. Polycomb/Trithorax response elements and epigenetic memory of cell identity. *Development* 2007; 134 (2):223-32.

Rodriguez-Pinilla SM, Sarrio D, Honrado E et al. Vimentin and laminin expression is associated with basal-like phenotype in both sporadic and BRCA1-associated breast carcinomas. *J Clin Pathol* 2007; 60 (9):1006-12.

Romanov SR, Kozakiewicz BK, Holst CR et al. Normal human mammary epithelial cells spontaneously escape senescence and acquire genomic changes. *Nature* 2001; 409 (6820):633-7.

Rosen EM, Fan S, Pestell RG et al. BRCA1 gene in breast cancer. *J Cell Physiol* 2003; 196 (1):19-41.

Rosen JM, Zahnow C, Kazansky A et al. Composite response elements mediate hormonal and developmental regulation of milk protein gene expression. *Biochem Soc Symp* 1998; 63:101-13.

Rouzier R, Perou CM, Symmans WF et al. Breast cancer molecular subtypes respond differently to preoperative chemotherapy. *Clin Cancer Res* 2005; 11 (16):5678-85.

Rowan BG, O'Malley BW. Progesterone receptor coactivators. *Steroids* 2000; 65 (10-11):545-9.

Roylance R, Gorman P, Harris W et al. Comparative genomic hybridization of breast tumors stratified by histological grade reveals new insights into the biological progression of breast cancer. *Cancer Res* 1999; 59 (7):1433-6.

Rudland PS, Fernig DG, Smith JA. Growth factors and their receptors in neoplastic mammary glands. *Biomed Pharmacother* 1995; 49 (9):389-99.

Rush M, Appanah R, Lee S et al. Targeting of EZH2 to a defined genomic site is sufficient for recruitment of Dnmt3a but not de novo DNA methylation. *Epigenetics* 2009; 4 (6):404-14.

Sarma K, Margueron R, Ivanov A et al. Ezh2 requires PHF1 to efficiently catalyze H3 lysine 27 trimethylation in vivo. *Mol Cell Biol* 2008; 28 (8):2718-31.

Sartorius CA, Harvell DM, Shen T et al. Progestins initiate a luminal to myoepithelial switch in estrogen-dependent human breast tumors without altering growth. *Cancer Res* 2005; 65 (21):9779-88.

Satijn DP, Olson DJ, van der Vlag J et al. Interference with the expression of a novel human polycomb protein, hPc2, results in cellular transformation and apoptosis. *Mol Cell Biol* 1997; 17 (10):6076-86.

Savage H. BRCA1 and BRCA2: Role in the DNA Damage Response, Cancer Formation and Treatment. *The DNA Damage Response: Implications on Cancer Formation and Treatment* 2009; (chapter 18):415-43

Saville B, Wormke M, Wang F et al. Ligand-, cell-, and estrogen receptor subtype (alpha/beta)-dependent activation at GC-rich (Sp1) promoter elements. *J Biol Chem* 2000; 275 (8):5379-87.

Schneider R, Bannister AJ, Kouzarides T. Unsafe SETs: histone lysine methyltransferases and cancer. *Trends Biochem Sci* 2002; 27 (8):396-402.

Schumacher A, Magnuson T. Murine Polycomb- and trithorax-group genes regulate homeotic pathways and beyond. *Trends Genet* 1997; 13 (5):167-70.

Scott CL, Gil J, Hernando E et al. Role of the chromobox protein CBX7 in lymphomagenesis. *Proc Natl Acad Sci U S A* 2007; 104 (13):5389-94.

Seibold S, Rudroff C, Weber M et al. Identification of a new tumor suppressor gene located at chromosome 8p21.3-22. *Faseb J* 2003; 17 (9):1180-2.

Serrano M, Lin AW, McCurrach ME et al. Oncogenic ras provokes premature cell senescence associated with accumulation of p53 and p16INK4a. *Cell* 1997; 88 (5):593-602.

Shakhova O, Leung C, Marino S. Bmi1 in development and tumorigenesis of the central nervous system. *J Mol Med* 2005; 83 (8):596-600.

Shang Y, Brown M. Molecular determinants for the tissue specificity of SERMs. *Science* 2002; 295 (5564):2465-8.

Sharif J, Endoh M, Koseki H. Epigenetic memory meets G2/M: to remember or to forget? *Dev Cell* 2011; 20 (1):5-6.

Shaw RJ, Cantley LC. Ras, PI(3)K and mTOR signalling controls tumour cell growth. *Nature* 2006; 441 (7092):424-30.

Sherr CJ, McCormick F. The RB and p53 pathways in cancer. *Cancer Cell* 2002; 2 (2):103-12.

Sherr CJ, Roberts JM. CDK inhibitors: positive and negative regulators of G1-phase progression. *Genes Dev* 1999; 13 (12):1501-12.

Shi B, Liang J, Yang X et al. Integration of estrogen and Wnt signaling circuits by the polycomb group protein EZH2 in breast cancer cells. *Mol Cell Biol* 2007; 27 (14):5105-19.

Silva J, Silva JM, Dominguez G et al. Concomitant expression of p16INK4a and p14ARF in primary breast cancer and analysis of inactivation mechanisms. *J Pathol* 2003; 199 (3):289-97.

Simon JA. Polycomb group proteins. *Curr Biol* 2003; 13 (3):R79-80.

Simon JA, Lange CA. Roles of the EZH2 histone methyltransferase in cancer epigenetics. *Mutat Res* 2008; 647 (1-2):21-9.

Simon JA, Tamkun JW. Programming off and on states in chromatin: mechanisms of Polycomb and trithorax group complexes. *Curr Opin Genet Dev* 2002; 12 (2):210-8.

Slamon DJ, Clark GM, Wong SG et al. Human breast cancer: correlation of relapse and survival with amplification of the HER-2/neu oncogene. *Science* 1987; 235 (4785):177-82.

Smalley M, Ashworth A. Stem cells and breast cancer: A field in transit. *Nat Rev Cancer* 2003; 3 (11):832-44.

Smid M, Wang Y, Zhang Y et al. Subtypes of breast cancer show preferential site of relapse. *Cancer Res* 2008; 68 (9):3108-14.

Sneeringer CJ, Scott MP, Kuntz KW et al. Coordinated activities of wild-type plus mutant EZH2 drive tumor-associated hypertrimethylation of lysine 27 on histone H3 (H3K27) in human B-cell lymphomas. *Proc Natl Acad Sci U S A* 2010; 107 (49):20980-5.

Snouwaert JN, Gowen LC, Latour AM et al. BRCA1 deficient embryonic stem cells display a decreased homologous recombination frequency and an increased

frequency of non-homologous recombination that is corrected by expression of a brcal transgene. *Oncogene* 1999; 18 (55):7900-7.

Sorlie T, Perou CM, Tibshirani R et al. Gene expression patterns of breast carcinomas distinguish tumor subclasses with clinical implications. *Proc Natl Acad Sci U S A* 2001; 98 (19):10869-74.

Sorlie T, Tibshirani R, Parker J et al. Repeated observation of breast tumor subtypes in independent gene expression data sets. *Proc Natl Acad Sci U S A* 2003; 100 (14):8418-23.

Sotiriou C, Neo SY, McShane LM et al. Breast cancer classification and prognosis based on gene expression profiles from a population-based study. *Proc Natl Acad Sci U S A* 2003; 100 (18):10393-8.

Sparmann A, van Lohuizen M. Polycomb silencers control cell fate, development and cancer. *Nat Rev Cancer* 2006; 6 (11):846-56.

Speirs V, Green AR, Walton DS et al. Short-term primary culture of epithelial cells derived from human breast tumours. *Br J Cancer* 1998; 78 (11):1421-9.

Stampfer MR, Yaswen P. Culture models of human mammary epithelial cell transformation. *J Mammary Gland Biol Neoplasia* 2000; 5 (4):365-78.

Stampfer MR, Yaswen P. Human epithelial cell immortalization as a step in carcinogenesis. *Cancer Lett* 2003; 194 (2):199-208.

Starita LM, Horwitz AA, Keogh MC et al. BRCA1/BARD1 ubiquitinate phosphorylated RNA polymerase II. *J Biol Chem* 2005; 280 (26):24498-505.

Stingl J, Eaves CJ, Kuusk U et al. Phenotypic and functional characterization in vitro of a multipotent epithelial cell present in the normal adult human breast. *Differentiation* 1998; 63 (4):201-13.

Stingl J, Eaves CJ, Zandieh I et al. Characterization of bipotent mammary epithelial progenitor cells in normal adult human breast tissue. *Breast Cancer Res Treat* 2001; 67 (2):93-109.

Su IH, Dobenecker MW, Dickinson E et al. Polycomb group protein ezh2 controls actin polymerization and cell signaling. *Cell* 2005; 121 (3):425-36.

Sudo T, Utsunomiya T, Mimori K et al. Clinicopathological significance of EZH2 mRNA expression in patients with hepatocellular carcinoma. *Br J Cancer* 2005; 92 (9):1754-8.

Sun F, Chan E, Wu Z et al. Combinatorial pharmacologic approaches target EZH2-mediated gene repression in breast cancer cells. *Mol Cancer Ther* 2009; 8 (12):3191-202.

Swain SM, Wilson JW, Mamounas EP et al. Estrogen receptor status of primary breast cancer is predictive of estrogen receptor status of contralateral breast cancer. *J Natl Cancer Inst* 2004; 96 (7):516-23.

T'Ang A, Varley JM, Chakraborty S et al. Structural rearrangement of the retinoblastoma gene in human breast carcinoma. *Science* 1988; 242 (4876):263-6.

Takawa M, Masuda K, Kunizaki M et al. Validation of the histone methyltransferase EZH2 as a therapeutic target for various types of human cancer and as a prognostic marker. *Cancer Sci* 2010.

Tamimi RM, Rosner B, Colditz GA. Evaluation of a breast cancer risk prediction model expanded to include category of prior benign breast disease lesion. *Cancer* 2010; 116 (21):4944-53.

Tan J, Yang X, Zhuang L et al. Pharmacologic disruption of Polycomb-repressive complex 2-mediated gene repression selectively induces apoptosis in cancer cells. *Genes Dev* 2007; 21 (9):1050-63.

Tang X, Milyavsky M, Shats I et al. Activated p53 suppresses the histone methyltransferase EZH2 gene. *Oncogene* 2004; 23 (34):5759-69.

Tassone P, Tagliaferri P, Perricelli A et al. BRCA1 expression modulates chemosensitivity of BRCA1-defective HCC1937 human breast cancer cells. *Br J Cancer* 2003; 88 (8):1285-91.

Tavassoli FA, Norris HJ. A comparison of the results of long-term follow-up for atypical intraductal hyperplasia and intraductal hyperplasia of the breast. *Cancer* 1990; 65 (3):518-29.

Taylor-Papadimitriou J, Berdichevsky F, D'Souza B et al. Human models of breast cancer. *Cancer Surv* 1993; 16:59-78.

Thomas MJ, Seto E. Unlocking the mechanisms of transcription factor YY1: are chromatin modifying enzymes the key? *Gene* 1999; 236 (2):197-208.

Thor AD, Liu S, Edgerton S et al. Activation (tyrosine phosphorylation) of ErbB-2 (HER-2/neu): a study of incidence and correlation with outcome in breast cancer. *J Clin Oncol* 2000; 18 (18):3230-9.

Tischkowitz MD, Foulkes WD. The basal phenotype of BRCA1-related breast cancer: past, present and future. *Cell Cycle* 2006; 5 (9):963-7.

Tlsty TD, Crawford YG, Holst CR et al. Genetic and epigenetic changes in mammary epithelial cells may mimic early events in carcinogenesis. *J Mammary Gland Biol Neoplasia* 2004; 9 (3):263-74.

Tlsty TD, Romanov SR, Kozakiewicz BK et al. Loss of chromosomal integrity in human mammary epithelial cells subsequent to escape from senescence. *J Mammary Gland Biol Neoplasia* 2001; 6 (2):235-43.

Toll AD, Dasgupta A, Potoczek M et al. Implications of enhancer of zeste homologue 2 expression in pancreatic ductal adenocarcinoma. *Hum Pathol* 2010; 41 (9):1205-9.

Tomlinson GE, Chen TT, Stastny VA et al. Characterization of a breast cancer cell line derived from a germ-line BRCA1 mutation carrier. *Cancer Res* 1998; 58 (15):3237-42.

Tonini T, D'Andrilli G, Fucito A et al. Importance of Ezh2 polycomb protein in tumorigenesis process interfering with the pathway of growth suppressive key elements. *J Cell Physiol* 2008; 214 (2):295-300.

Tsutsui S, Yasuda K, Suzuki K et al. Macrophage infiltration and its prognostic implications in breast cancer: the relationship with VEGF expression and microvessel density. *Oncol Rep* 2005; 14 (2):425-31.

Turner NC, Reis-Filho JS, Russell AM et al. BRCA1 dysfunction in sporadic basal-like breast cancer. *Oncogene* 2007; 26 (14):2126-32.

Tuveson DA, Shaw AT, Willis NA et al. Endogenous oncogenic K-ras(G12D) stimulates proliferation and widespread neoplastic and developmental defects. *Cancer Cell* 2004; 5 (4):375-87.

Unger K, Wienberg J, Riches A, Hieber L, Walch A, Brown A, O'Brien PC, Briscoe C, Gray L, Rodriguez E, Jackl G, Knijnenburg J, Tallini G, Ferguson-Smith M, Zitzelsberger H. Novel gene rearrangements in transformed breast cells identified by high-resolution breakpoint analysis of chromosomal aberrations. *Endocr Relat Cancer*. 2010 Jan 29;17(1):87-98.

van de Rijn M, Perou CM, Tibshirani R et al. Expression of cytokeratins 17 and 5 identifies a group of breast carcinomas with poor clinical outcome. *Am J Pathol* 2002; 161 (6):1991-6.

van der Vlag J, Otte AP. Transcriptional repression mediated by the human polycomb-group protein EED involves histone deacetylation. *Nat Genet* 1999; 23 (4):474-8.

van Kemenade FJ, Raaphorst FM, Blokzijl T et al. Coexpression of BMI-1 and EZH2 polycomb-group proteins is associated with cycling cells and degree of malignancy in B-cell non-Hodgkin lymphoma. *Blood* 2001; 97 (12):3896-901.

van Lohuizen M, Verbeek S, Scheijen B et al. Identification of cooperating oncogenes in E mu-myc transgenic mice by provirus tagging. *Cell* 1991; 65 (5):737-52.

Vanaja DK, Ballman KV, Morlan BW et al. PDLIM4 repression by hypermethylation as a potential biomarker for prostate cancer. *Clin Cancer Res* 2006; 12 (4):1128-36.

Varambally S, Dhanasekaran SM, Zhou M et al. The polycomb group protein EZH2 is involved in progression of prostate cancer. *Nature* 2002; 419 (6907):624-9.

Vargo-Gogola T, Rosen JM. Modelling breast cancer: one size does not fit all. *Nat Rev Cancer* 2007; 7 (9):659-72.

Veneziani BM, Criniti V, Cavaliere C et al. In vitro expansion of human breast cancer epithelial and mesenchymal stromal cells: optimization of a coculture model for personalized therapy approaches. *Mol Cancer Ther* 2007; 6 (12 Pt 1):3091-100.

Venkitaraman AR. Cancer susceptibility and the functions of BRCA1 and BRCA2. *Cell* 2002; 108 (2):171-82.

Vincenz C, Kerppola TK. Different polycomb group CBX family proteins associate with distinct regions of chromatin using nonhomologous protein sequences. *Proc Natl Acad Sci U S A* 2008; 105 (43):16572-7.

Vire E, Brenner C, Deplus R et al. The Polycomb group protein EZH2 directly controls DNA methylation. *Nature* 2006; 439 (7078):871-4.

Visvanathan K, Sukumar S, Davidson NE. Epigenetic biomarkers and breast cancer: cause for optimism. *Clin Cancer Res* 2006; 12 (22):6591-3.

von Lintig FC, Dreilinger AD, Varki NM et al. Ras activation in human breast cancer. *Breast Cancer Res Treat* 2000; 62 (1):51-62.

Vonlanthen S, Heighway J, Altermatt HJ et al. The bmi-1 oncoprotein is differentially expressed in non-small cell lung cancer and correlates with INK4A-ARF locus expression. *Br J Cancer* 2001; 84 (10):1372-6.

Wang C, Fan S, Li Z et al. Cyclin D1 antagonizes BRCA1 repression of estrogen receptor alpha activity. *Cancer Res* 2005; 65 (15):6557-67.

Wang C, Navab R, Iakovlev V et al. Abelson interactor protein-1 positively regulates breast cancer cell proliferation, migration, and invasion. *Mol Cancer Res* 2007; 5 (10):1031-9.

Wang H, Wang L, Erdjument-Bromage H et al. Role of histone H2A ubiquitination in Polycomb silencing. *Nature* 2004; 431 (7010):873-8.

Wang Y, Cortez D, Yazdi P et al. BASC, a super complex of BRCA1-associated proteins involved in the recognition and repair of aberrant DNA structures. *Genes Dev* 2000; 14 (8):927-39.

Wang Z, Zang C, Cui K et al. Genome-wide mapping of HATs and HDACs reveals distinct functions in active and inactive genes. *Cell* 2009; 138 (5):1019-31.

Watanabe H, Soejima K, Yasuda H et al. Deregulation of histone lysine methyltransferases contributes to oncogenic transformation of human bronchoepithelial cells. *Cancer Cell Int* 2008; 8:15.

Watanabe Y, Maekawa M. Methylation of DNA in cancer. *Adv Clin Chem* 2010; 52:145-67.

Watson DM, Elton RA, Jack WJ et al. The H-ras oncogene product p21 and prognosis in human breast cancer. *Breast Cancer Res Treat* 1991; 17 (3):161-9.

Weikert S, Christoph F, Kollermann J et al. Expression levels of the EZH2 polycomb transcriptional repressor correlate with aggressiveness and invasive potential of bladder carcinomas. *Int J Mol Med* 2005; 16 (2):349-53.

Weinberg RA. The retinoblastoma protein and cell cycle control. *Cell* 1995; 81 (3):323-30.

Weiss RA. Multistage carcinogenesis. *Br J Cancer* 2004; 91 (12):1981-2.

Wellings SR, Jensen HM, Marcum RG. An atlas of subgross pathology of the human breast with special reference to possible precancerous lesions. *J Natl Cancer Inst* 1975; 55 (2):231-73.

Welm B, Behbod F, Goodell MA et al. Isolation and characterization of functional mammary gland stem cells. *Cell Prolif* 2003; 36 Suppl 1:17-32.

Welch WC, Morrison RS, Gross JL, Gollin SM, Kitson RB, Goldfarb RH, Giuliano KA, Bradley MK, Kornblith PL. Morphologic, immunologic, biochemical, and cytogenetic characteristics of the human glioblastoma-derived cell line, SNB-19. *In Vitro Cell Dev Biol Anim*. 1995 Sep;31(8):610-6.

Wenandy L, Kollgaard T, Letsch A et al. The 1170 A-P single-nucleotide polymorphism (SNP) in the Her-2/neu protein (HER2) as a minor histocompatibility antigen (mHag). *Leukemia* 2009; 23 (10):1926-9.

Whitcomb SJ, Basu A, Allis CD et al. Polycomb Group proteins: an evolutionary perspective. *Trends Genet* 2007; 23 (10):494-502.

Wicha MS. Development of 'synthetic lethal' strategies to target BRCA1-deficient breast cancer. *Breast Cancer Res* 2009; 11 (5):108.

Widschwendter M, Fiegl H, Egle D et al. Epigenetic stem cell signature in cancer. *Nat Genet* 2007; 39 (2):157-8.

Williams RR, Azuara V, Perry P et al. Neural induction promotes large-scale chromatin reorganisation of the Mash1 locus. *J Cell Sci* 2006; 119 (Pt 1):132-40.

Wilson BG, Wang X, Shen X et al. Epigenetic antagonism between polycomb and SWI/SNF complexes during oncogenic transformation. *Cancer Cell* 2010; 18 (4):316-28.

Wood JL, Liang Y, Li K et al. Microcephalin/MCPH1 associates with the Condensin II complex to function in homologous recombination repair. *J Biol Chem* 2008; 283 (43):29586-92.

Wu ZL, Zheng SS, Li ZM et al. Polycomb protein EZH2 regulates E2F1-dependent apoptosis through epigenetically modulating Bim expression. *Cell Death Differ* 2010; 17 (5):801-10.

Xiao Y. Enhancer of zeste homolog 2: A potential target for tumor therapy. *Int J Biochem Cell Biol* 2011; 43 (4):474-7.

Xu B, Kim S, Kastan MB. Involvement of Brcal in S-phase and G(2)-phase checkpoints after ionizing irradiation. *Mol Cell Biol* 2001; 21 (10):3445-50.

Xu J, Fan S, Rosen EM. Regulation of the estrogen-inducible gene expression profile by the breast cancer susceptibility gene BRCA1. *Endocrinology* 2005; 146 (4):2031-47.

Yalcin-Ozuysal O, Brisken C. From normal cell types to malignant phenotypes. *Breast Cancer Res* 2009; 11 (6):306.

Yan Y, Spieker RS, Kim M et al. BRCA1-mediated G2/M cell cycle arrest requires ERK1/2 kinase activation. *Oncogene* 2005; 24 (20):3285-96.

Yang X, Karuturi RK, Sun F et al. CDKN1C (p57) is a direct target of EZH2 and suppressed by multiple epigenetic mechanisms in breast cancer cells. *PLoS One* 2009; 4 (4):e5011.

Yang X, Phillips DL, Ferguson AT et al. Synergistic activation of functional estrogen receptor (ER)-alpha by DNA methyltransferase and histone deacetylase inhibition in human ER-alpha-negative breast cancer cells. *Cancer Res* 2001; 61 (19):7025-9.

Yao J, Weremowicz S, Feng B et al. Combined cDNA array comparative genomic hybridization and serial analysis of gene expression analysis of breast tumor progression. *Cancer Res* 2006; 66 (8):4065-78.

Yarden RI, Brody LC. BRCA1 interacts with components of the histone deacetylase complex. *Proc Natl Acad Sci U S A* 1999; 96 (9):4983-8.

Yarden Y, Ullrich A. Growth factor receptor tyrosine kinases. *Annu Rev Biochem* 1988; 57:443-78.

Yasmeen A, Liu W, Dekhil H et al. BRCA1 mutations contribute to cell motility and invasion by affecting its main regulators. *Cell Cycle* 2008; 7 (23):3781-3.

Yaswen P, Stampfer MR. Molecular changes accompanying senescence and immortalization of cultured human mammary epithelial cells. *Int J Biochem Cell Biol* 2002; 34 (11):1382-94.

Yerushalmi R, Gelmon KA, Leung S et al. Insulin-like growth factor receptor (IGF-1R) in breast cancer subtypes. *Breast Cancer Res Treat* 2010.

Yoshida K, Miki Y. Role of BRCA1 and BRCA2 as regulators of DNA repair, transcription, and cell cycle in response to DNA damage. *Cancer Sci* 2004; 95 (11):866-71.

Yu CL, Driggers P, Barrera-Hernandez G et al. The tumor suppressor p53 is a negative regulator of estrogen receptor signaling pathways. *Biochem Biophys Res Commun* 1997; 239 (2):617-20.

Yu K, Lee CH, Tan PH et al. Conservation of breast cancer molecular subtypes and transcriptional patterns of tumor progression across distinct ethnic populations. *Clin Cancer Res* 2004; 10 (16):5508-17.

Zeidler M, Kleer CG. The Polycomb group protein Enhancer of Zeste 2: its links to DNA repair and breast cancer. *J Mol Histol* 2006; 37 (5-7):219-23.

Zeidler M, Varambally S, Cao Q et al. The Polycomb group protein EZH2 impairs DNA repair in breast epithelial cells. *Neoplasia* 2005; 7 (11):1011-9.

Zhang RR, Man YG, Vang R et al. A subset of morphologically distinct mammary myoepithelial cells lacks corresponding immunophenotypic markers. *Breast Cancer Res* 2003; 5 (5):R151-6.

Zhang XW, Zhang L, Qin W et al. Oncogenic role of the chromobox protein CBX7 in gastric cancer. *J Exp Clin Cancer Res*; 29:114.

Zhang YB, Niu HT, Chang JW et al. EZH2 silencing by RNA interference inhibits proliferation in bladder cancer cell lines. *Eur J Cancer Care (Engl)* 2011; 20 (1):106-12.

Zhao Y, Tan J, Zhuang L et al. Inhibitors of histone deacetylases target the Rb-E2F1 pathway for apoptosis induction through activation of proapoptotic protein Bim. *Proc Natl Acad Sci U S A* 2005; 102 (44):16090-5.

Zheng L, Annab LA, Afshari CA et al. BRCA1 mediates ligand-independent transcriptional repression of the estrogen receptor. *Proc Natl Acad Sci U S A* 2001; 98 (17):9587-92.

Zhong Q, Chen CF, Chen PL et al. BRCA1 facilitates microhomology-mediated end joining of DNA double strand breaks. *J Biol Chem* 2002; 277 (32):28641-7.

Zhou BP, Hu MC, Miller SA et al. HER-2/neu blocks tumor necrosis factor-induced apoptosis via the Akt/NF-kappaB pathway. *J Biol Chem* 2000; 275 (11):8027-31.



## 8 APPENDICES

### 8.1 Appendix A: Raw data and additional tables of chapter 3

Cell Line	Gene Cluster	ER	PR	HER2	TP53	Tumor Type
600MPE	Lu	+	[-]		-	IDC
AU565	Lu	-	[-]	+	+ <sup>WT</sup>	AC
BT20	BaA	-	[-]		++ <sup>WT</sup>	IDC
BT474	Lu	+	[+]	+	+	IDC
BT483	Lu	+	[+]		-	IDC, pap
BT549	BaB	-	[-]		++ <sup>M</sup>	IDC, pap
CAMA1	Lu	+	[-]		+	AC
HBL100	BaB	-	[-]		++	N
HCC1007	Lu	+	[-]		[+/-]	Duc.Ca
HCC1143	BaA	-	[-]		++ <sup>M</sup>	Duc.Ca
HCC1187	BaA	-	[-]		++ <sup>M</sup>	Duc.Ca
HCC1428	Lu	+	[+]		[+]	AC
HCC1500	BaB	-	[-]		-	Duc.Ca
HCC1569	BaA	-	[-]	+	- <sup>M</sup>	MC
HCC1937	BaA	-	[-]		[-]	Duc.Ca
HCC1954	BaA	-	[-]	+	[+/-]	Duc.Ca
HCC202	Lu	-	[-]	+	[-]	Duc.Ca
HCC2157	BaA	-	[-]		[+]	Duc.Ca
HCC2185	Lu	-	[-]		[+]	MLCa
HCC3153	BaA	-	[-]		[-]	
HCC38	BaB	-	[-]		++ <sup>M</sup>	Duc.Ca
HCC70	BaA	-	[-]		++ <sup>M</sup>	Duc.Ca
HS578T	BaB	-	[-]		+ <sup>M</sup>	IDC
LY2	Lu	+	[-]		+/-	IDC
MCF10A	BaB	-	[-]		+/- <sup>WT</sup>	F
MCF12A	BaB	-	[-]		+	F
MCF7	Lu	+	[+]		+/- <sup>WT</sup>	IDC
MDAMB134VI	Lu	+	[-]		+/- <sup>WT</sup>	IDC
MDAMB157	BaB	-	[-]		-	MC
MDAMB175VII	Lu	+	[-]		+/- <sup>WT</sup>	IDC
MDAMB231	BaB	-	[-]		++ <sup>M</sup>	AC
MDAMB361	Lu	+	[-]	+	- <sup>WT</sup>	AC
MDAMB415	Lu	+	[-]		+	AC
MDAMB435	BaB	-	[-]		+ <sup>M</sup>	IDC
MDAMB436	BaB	[-]	[-]		[-]	IDC
MDAMB453	Lu	-	[-]		- <sup>WT</sup>	AC
MDAMB468	BaA	[-]	[-]		[+]	AC
SKBR3	Lu	-	[-]	+	+	AC
SUM1315MO2	BaB	-	[-]		[+]	IDC
SUM149PT	BaB	[-]	[-]		[+]	Inf Duc.Ca
SUM159PT	BaB	[-]	[-]		[-]	AnCar
SUM185PE	Lu	[-]	[-]		[-]	Duc.Ca
SUM190PT	BaA	-	[-]	+	[+/-]	Inf
SUM225CWN	BaA	-	[-]	+	++	IDC
SUM44PE	Lu	[+]	[-]		[-]	Ca
SUM52PE	Lu	[+]	[-]		[-]	Ca
T47D	Lu	+	[+]		++ <sup>M</sup>	IDC
UACC812	Lu	+	[-]	+	- <sup>WT</sup>	IDC
ZR751	Lu	+	[-]		-	IDC
ZR7530	Lu	+	[-]	+	- <sup>WT</sup>	IDC
ZR75B	Lu	+	[-]		+/-	

**Table A.1:** Features of breast cancer cell lines adapted from Neve et al., (2006). ER/PR/HER2/TP53 status: ER/PR positivity, HER2 overexpression and TP53 protein levels and mutational status are reported. Gene cluster and tumour type: Lu luminal, BaA basal A, BaB basal B, AC, Adenocarcinoma; AnCar, Anaplastic Carcinoma; Duc.Ca, Ductal Carcinoma; F, fibrocystic disease; IDC, Invasive Ductal Carcinoma; MC, metaplastic carcinoma; MLCa, Metastatic lobular carcinoma; N, Normal. Cells lines highlighted in yellow were used in the experiments in chapter 3.

	Day 0	Day 1	Day 2	Day3	Day4	Day 5	Day 6
Number of cells							
MDA-MB-231	40000	324622.2	1390370	4060089	5006133	5871585	6473807
MDA-MB-231 GIPZ	40000	341392.6	1579881	4385067	4885185	5602015	6649393
MDA-MB-231 17507	40000	252800	1000711	2441393	3620474	4764889	4839111
Standard error of the mean							
MDA-MB-231	1	316800	9443.63	186911	30446.1	93267.76	7812.17
MDA-MB-231 GIPZ	1	6143.92	2250.1	11244.71	27919.24	31809.16	6356.3
MDA-MB-231 17507	1	1495.34	6276.8	4410.64	67299.6	19412	6695.05

**Table A.2.** Raw data of figure 3.4. Cells were counted every 24 hours. The experiment was performed in triplicate and for each replica cells were counted three times. Values represent the mean of 9 counts (n=9). The error bars are calculated using the standard error of the mean.

	MDA-MB-231	MDA-MB-231 GIPZ	MDA-MD-231 17507
Replica 1	125	106	38
Replica 2	113	107	27
Replica 3	99	132	31
Mean	112.33	115	32
Standard error of the mean	7.51	8.50	3.21

**Table A.3** Raw data of figure 3.5. The experiment was performed in triplicate (replica 1, 2 and 3) and for each replica colonies were counted three times. Values represent the mean of 9 counts (n=9). The error bars are calculated using the standard error of the mean.

	MDA-MB-231	MDA-MB-231 GIPZ	MDA-MB-231 17507
Replica 1	101.6	94.6	12.6
Replica 2	150	74.6	115.6
Replica 3	94.6	160	41
Mean	115.44	109.78	56.44
Standard error of the mean	9.14	13.37	15.52

**Table A.4.** Raw data of figure 3.6. The experiment was performed in triplicate (replica 1, 2 and 3) and for each replica migrating cells from three randomly selected fields in the central part of the chamber were counted. Values represent the mean of 9 counts (n=9). The error bars are calculated using the standard error of the mean.

	Day 0 (AU)	Day 1 (AU)	Cell migration (%)
MDA-MB-231	47.45	10.03	78.87
MDA-MB-231 GIPZ	42.86	8.30	80.63
MDA-MB-231 17507	31.97	19.08	40.32

**Table A.5.** Raw data of figure 3.7. The area of the scratch free of cells was measured at day 0 and day 1 using the image j software. Values of the scratch at day 0 and day1 are reported in arbitrary units (AU). Cell migration is presented as percent closure using the formula: (Pre-migration area – Migration area)/Pre-migration area X 100.

	Day 0	Day 1	Day 2	Day 3	Day 4	Day 5	Day 6
Number of cells							
HCC1937	200000	192266.6	263911.1	307733.3	378755.5	368355.5	233155.5
HCC1937 GIPZ	200000	235555.5	272177.7	350488.8	346755.5	393422.2	300355.5
HCC1937 17507	200000	266666.6	258133.3	262844.4	301333.3	287555.5	255200.0
Standard error of the mean							
HCC1937	1.00	18400	13851.56	5019.665	15139.32	4871.89	1001.73
HCC1937 GIPZ	1.00	8738.28	12629.73	13819.01	33717.37	19831.79	18476.06
HCC193717507	1.00	25333.33	28310.66	13040.64	15279.33	25858.57	15172.69

**Table A.6.** Raw data of figure 3.9. Cells were counted every 24 hours. The experiment was performed in triplicate and for each replica cells were counted three times. Values represent the mean of 9 counts (n=9). The error bars are calculated using the standard error of the mean.

	HCC1937	HCC1937 GIPZ	HCC1937 17507
Replica 1	81	55	18
Replica 2	82	84	26
Replica 3	78	58	22
Mean	80.33	65.67	22
Standard error of the mean	1.20	9.21	2.31

**Table A.7.** Raw data of figure 3.10. The experiment was performed in triplicate (replica 1, 2 and 3) and for each replica colonies were counted three times. Values represent the mean of 9 counts (n=9). The error bars are calculated using the standard error of the mean.

	HCC1937	HCC1937 GIPZ	HCC1937 17507
Replica 1	77	25.5	74.67
Replica 2	62	24.5	80.5
Replica 3	87	24	75.6
Mean	75.33	24,67	77.58
Standard error of the mean	7.27	3.75	1.81

**Table A.8.** Raw data of figure 3.11. The experiment was performed in triplicate (replica 1, 2 and 3) and for each replica migrating cells from three randomly selected fields in the central part of the chamber were counted. Values represent the mean of 9 counts (n=9). The error bars are calculated using the standard error of the mean.

	Day 0 (AU)	Day 1 (AU)	Cell migration (%)
HCC1937	48.46	8.77	81.9
HCC1937 GIPZ	48.29	9.21	80.92
HCC1937 17507	51.04	13.31	73.94

**Table A.11.** Raw data of figure 3.12. The area of the scratch free of cells was measured at day 0 and day 1 using the image j software. Values of the scratch at day 0 and day1 are reported in arbitrary units (AU). Cell migration is presented as percent closure using the formula:  $(\text{Pre-migration area} - \text{Migration area}) / \text{Pre-migration area} \times 100$ .

## 8.2 Appendix B: Raw data and additional tables of chapter 4

	Day 0	Day 1	Day 2	Day 3	Day 4	Day 5	Day 6
HCC1937 BR69	200000.00	323022.22	513866.67	661866.67	661866.67	846133.33	788977.78
HCC1937 BR69 GIPZ	200000.00	376088.89	470044.44	638577.78	665688.89	606400.00	602488.89
HCC1937 BR69 17507	200000.00	271822.22	234488.89	248355.56	256088.89	362844.44	316133.33
Standard error of the mean							
HCC1937 BR69		6711.553	43725.47	36214.01	42729.12	23688.35	29164.90
HCC1937 BR69 GIPZ		43739.11	42722.28	24516.1	8483.65	11749.48	25749.72
HCC1937 BR69 17507		25789.27	28673.94	23644.44	5426.59	18387.97	18171.69

**Table B.1.** Raw data of figure 4.7 A. Cells were counted every 24 hours. The experiment was performed in triplicate and for each replica cells were counted three times. Values represent the mean of 9 counts (n=9). The error bars are calculated using the standard error of the mean.

	Day 0	Day 1	Day 2	Day 3	Day 4	Day 5	Day 6
HCC1937 EV28	200000	192266.67	263911.11	307733.33	378755.56	368355.56	233155.56
HCC1937 EV28 GIPZ	200000	235555.56	272177.78	350488.89	346755.56	393422.22	300355.56
HCC1937 EV28 17507	200000	266666.67	258133.33	262844.44	301333.33	287555.56	255200.00
Standard error of the mean							
EV28		18400	13851.56	5019.66	15139.32	4871.89	1001.72
EV28GIPZ		8738.28	12629.73	13819.01	33717.37	19831.79	18476.06
EV2817507		25333.33	28310.66	13040.64	15279.33	25858.57	15172.69

**Table B.2:** Raw data of figure 4.7 B. Cells were counted every 24 hours. The experiment was performed in triplicate and for each replica cells were counted three times. Values represent the mean of 9 counts (n=9). The error bars are calculated using the standard error of the mean.

	HCC1937 BR69	HCC1937 BR69 GIPZ	HCC1937 BR69 17507
Replica 1	9	3	5
Replica 2	4	5	4
Replica 3	3	4	1
Mean	5.33	4	3.33
Standard error of the mean	1.86	0.58	1.20

**Table B.3:** Raw data of figure 4.3. A. The experiment was performed in triplicate (replica 1, 2 and 3) and for each replica colonies were counted three times. Values represent the mean of 9 counts (n=9). The error bars are calculated using the standard error of the mean.

	HCC1937 EV28	HCC1937 EV28 GIPZ	HCC1937 EV28 17507
Replica 1	81	55	18
Replica 2	82	84	26
Replica 3	78	58	22
Mean	80.33	65.67	22
Standard error of the mean	1.20	9.21	2.31

**Table B.4:** Raw data of figure 4.3.B. The experiment was performed in triplicate (replica 1, 2 and 3) and for each replica colonies were counted three times. Values represent the mean of 9 counts (n=9). The error bars are calculated using the standard error of the mean.

	HCC1937 BR69	HCC1937 BR69 GIPZ	HCC1937 BR69 17507
Replica 1	136	104	46
Replica 2	70	101	60
Replica 3	133	124	57
Mean	113	109.67	54.33
Standard error of the mean	21.52	7.22	4.26

**Table B.5.** Raw data of figure 4.6.A. The experiment was performed in triplicate (replica 1, 2 and 3) and for each replica migrating cells from three randomly selected fields in the central part of the chamber were counted. Values represent the mean of 9 counts (n=9). The error bars are calculated using the standard error of the mean.

	HCC1937	HCC1937 EV28 GIPZ	HCC1937 EV28 17507
Replica 1	77	25.5	74.67
Replica 2	62	14.5	80.5
Replica 3	87	14	75.6
Mean	75.33	18	77.58
Standard error of the mean	7.27	3.75	1.81

**Table B.6:** Raw data of figure 4.6.B. The experiment was performed in triplicate (replica 1, 2 and 3) and for each replica migrating cells from three randomly selected fields in the central part of the chamber were counted. Values represent the mean of 9 counts (n=9). The error bars are calculated using the standard error of the mean.

	Day 0 (AU)	Day 1 (AU)	Cell migration (%)
HCC1937 BR69	60.82	8.56	85.92
HCC1937 BR69-GIPZ	56.94	8.23	85.54
HCC1937 BR69 - 17507	54.60	18.25	66.56

**Table B.7:** Raw data of figure 4.4. The area of the scratch free of cells was measured at day 0 and day 1 using the image j software. Values of the scratch at day 0 and day1 are reported in arbitrary units (AU). Cell migration is presented as percent closure using the formula:  $(\text{Pre-migration area} - \text{Migration area}) / \text{Pre-migration area} \times 100$ .

	Day 0 (AU)	Day 1 (AU)	Cell migration (%)
HCC1937EV28	48.46	8.77	81.9
HCC1937EV28 GIPZ	48.29	9.21	80.92
HCC1937EV28 17507	51.04	13.31	73.94

**Table B.8:** Raw data of figure 4.5. The area of the scratch free of cells was measured at day 0 and day 1 using the image j software. Values of the scratch at day 0 and day1 are reported in arbitrary units (AU). Cell migration is presented as percent closure using the formula:  $(\text{Pre-migration area} - \text{Migration area}) / \text{Pre-migration area} \times 100$ .



### 8.3 Appendix C: Raw data and additional tables of chapter 5

	Day 0	Day 1	Day 2	Day 3	Day 4
Number of cells					
MCF10A	71925.00	42866.67	182666.67	274066.67	142666.67
MCF10A + CBX6	37050.00	25466.67	135800.00	195333.33	114933.33
Standard error of the mean					
MCF10A	1.00	1841.50	3653.92	7603.80	4000.56
MCF10A + CBX6	1.00	569.60	3407.83	8473.75	2520.14

**Table C.1:** Raw data of Figure 5.4 A. Cells were counted every 48 hours. The experiment was performed in triplicate and for each replica cells were counted three times. Values represent the mean of 9 counts (n=9). The error bars are calculated using the standard error of the mean.

	Day1	Day2	Day3	Day4
MCF10A	16900	57900	226000	457000
MCF10A+CBX7	11000	48500	143000	329000
MCF10A+CBX8	17700	75600	354000	809000
Standard error of the mean				
MCF10A	1.00E+00	4684.13	3859.19	1489.22
MCF10A+CBX7	1.00E+00	2979.01	3075.35	1507.02
MCF10A+CBX8	1.00E+00	2458.32	7266.67	14722.47

**Table C.2:** Raw data of figure 5.4.B. Cells were counted every 48 hours. The experiment was performed in triplicate and for each replica cells were counted three times. Values represent the mean of 9 counts (n=9). The error bars are calculated using the standard error of the mean.

	Day 0	Day 1	Day 2	Day 3	Day 4
Number of cells					
MCF10A	70000	288600	257500	1188000	2370000
MCF10A + GFP	70000	99900	287700	565500	2235500
MCF10A + CBX8	70000	329600	1210000	3640000	3377500
Standard error of the mean					
MCF10A	1	29796.42	55132.42	22978.25	112101.1
MCF10A + GFP	1	29554.19	30056.56	22588.71	735712.4
MCF10A + CBX8	1	25026.92	103037.2	214320.6	209617.7

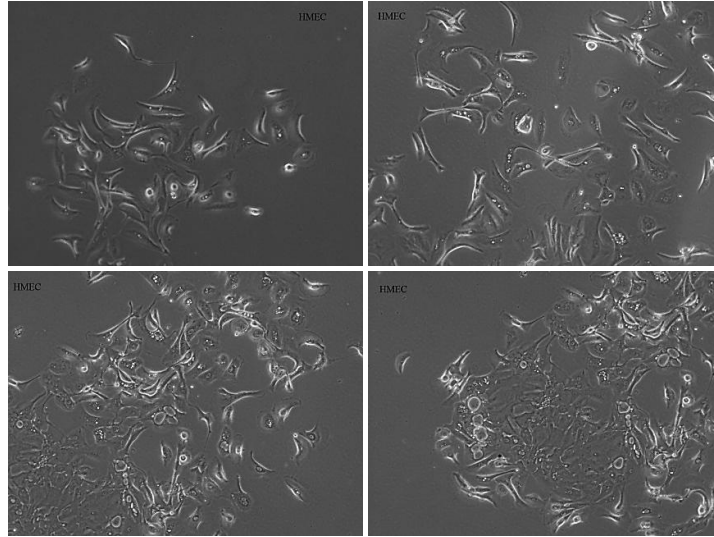
	Day 5	Day 6	Day 7	Day 8
Number of cells				
MCF10A	2588000	5765000	6840000	6735000
MCF10A + GFP	3225000	6253333	6168000	6058000
MCF10A + CBX8	3036000	6453333	7530666	7019256
Standard error of the mean				
MCF10A	196326.2	500824.3	248000	238700
MCF10A + GFP	167549.7	408982.5	399493.0	299893.0
MCF10A + CBX8	62780.03	448060.6	358406.3	337446.3

**Table C.3:** Raw data of figure 5.6. Cells were counted every 48 hours. The experiment was performed in triplicate and for each replica cells were counted three times. Values represent the mean of 9 counts (n=9). The error bars are calculated using the standard error of the mean.

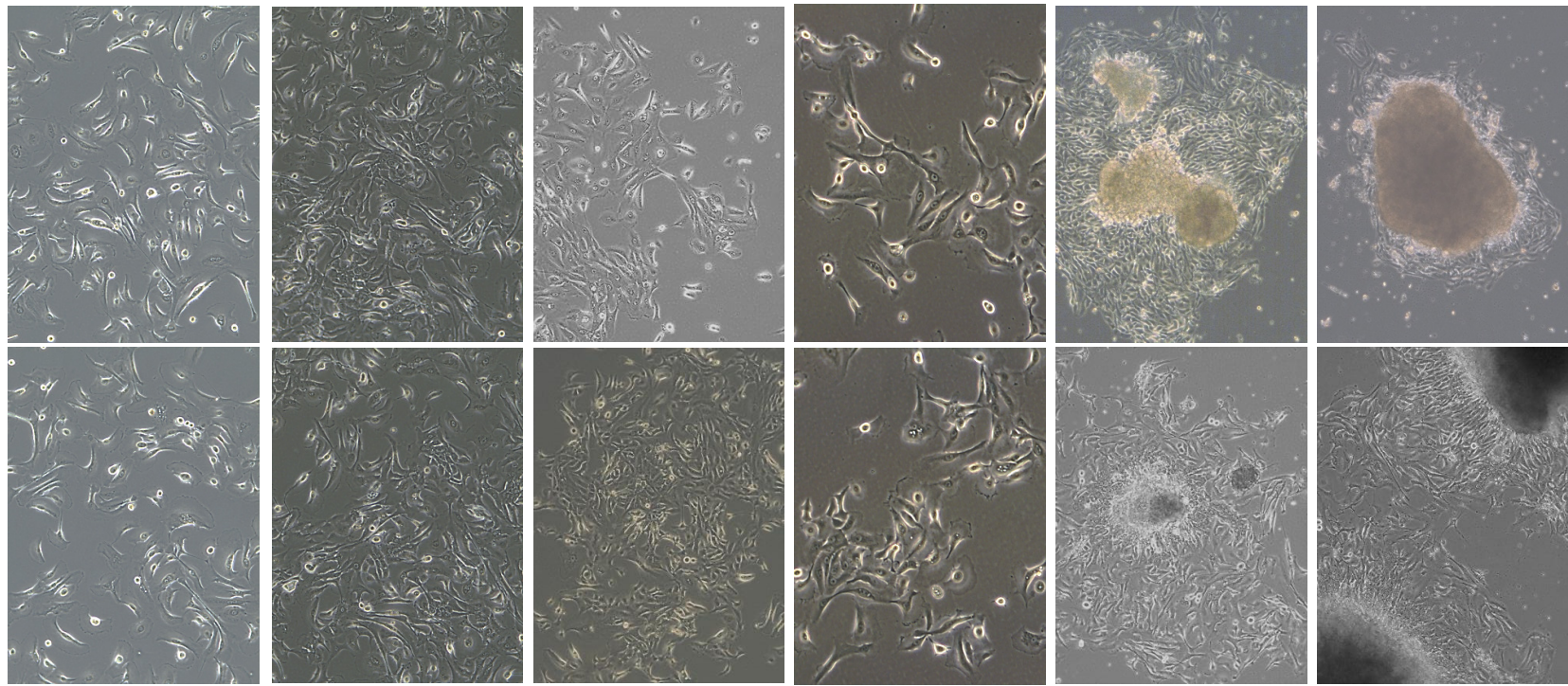
	MCF10A	MCF10A_GFP	MCF10A_CBX8
Count 1	25	44	49
Count 2	28	35	48
Count 3	17	49	38
Count 4	36	33	16
Count 5	30	30	37
Count 6	44	35	32
Count 7	23	44	20
Count 8	32	31	35
Count 9	27	23	55
Avarage	29.11	36	36.67
Standard error of the mean	2.6	2.73	4.33

**Table C4:** Raw data of Figure 5.7. The experiment was performed in triplicate (replica 1, 2 and 3) and for each replica migrating cells from three randomly selected fields in the central part of the chamber were counted. Values represent the mean of 9 counts (n=9). The error bars are calculated using the standard error of the mean.

**8.4 Appendix D:** Raw data and additional images of cultured primary cells of chapter 6



**Figure D.1:** Image of Human Mammary Epithelial Cells (HMEC). Cells were grown according to Duss et al. protocol. Photos were taken using the using the Axiovision imaging System. Objective magnification 10X.



Day 18

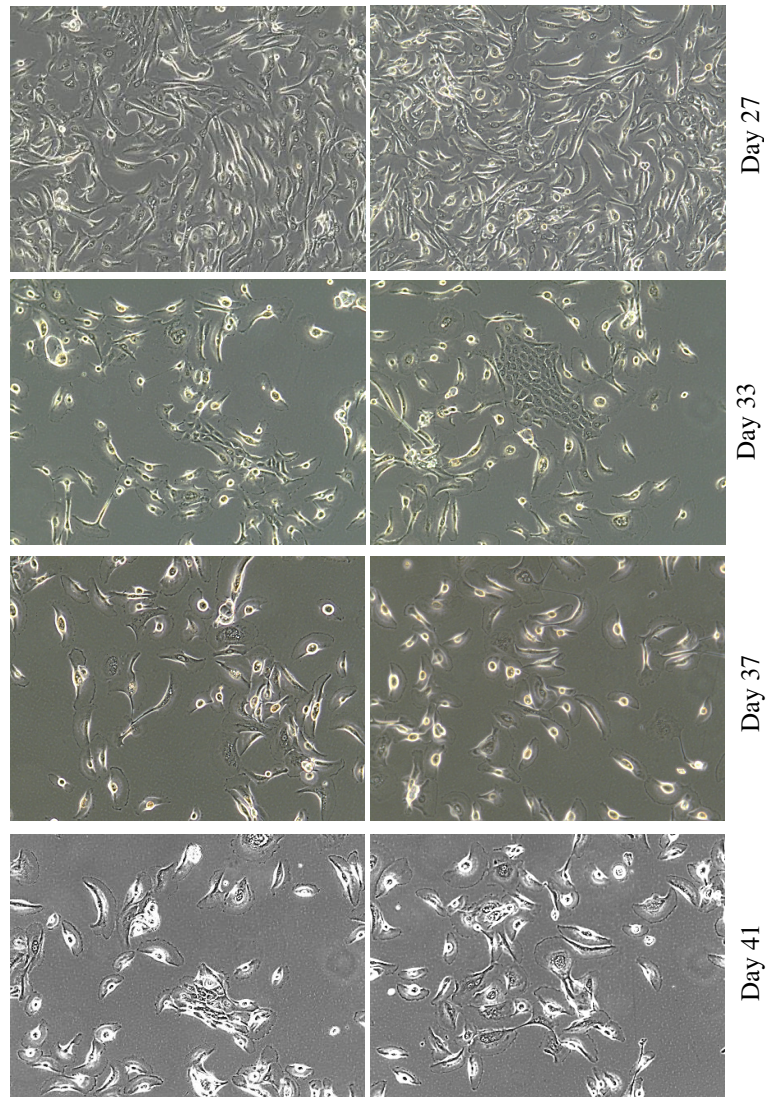
Day 15

Day 10

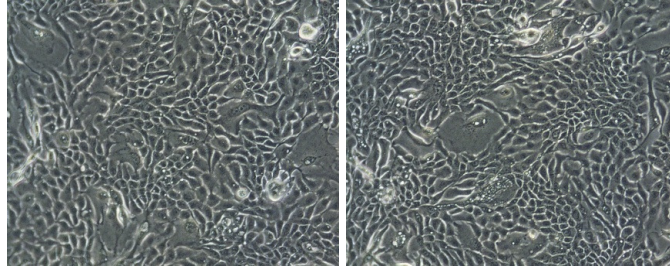
Day 9

Day 4

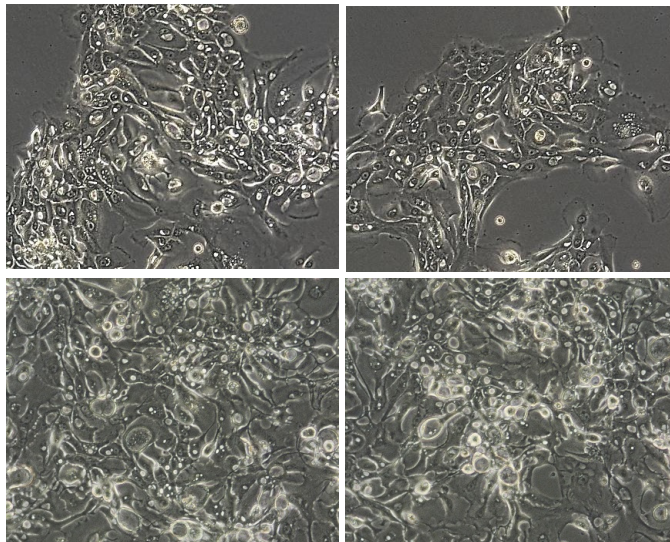
Day 1



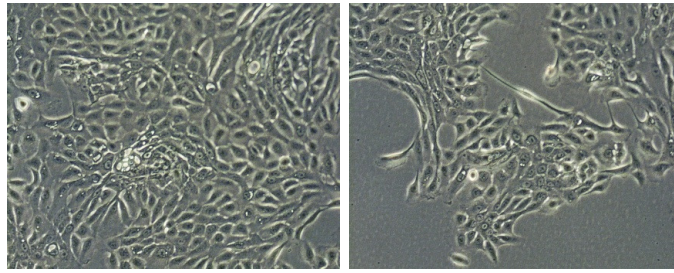
**Figure D.2:** Images of breast primary epithelial cells (BPEC). Representative images of cells grown according to Ince et al. protocol. Photos were taken using the using the Axiovision imaging System. Objective magnification 10X.



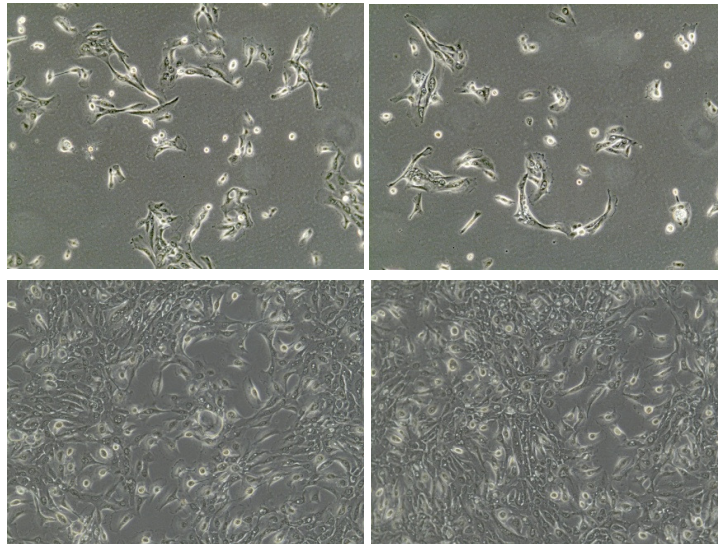
**Figure D.3:** Images of BPEC after ectopic over-expression of BMI1/ER $\alpha$ . Photos were taken using the using the Axiovision imaging System. Objective magnification 10X.



**Figure D.4:** Images of BPEC after ectopic expression of BMI1/ER $\alpha$ /hTERT/HRas\_2009. Photos were taken using the using the Axiovision imaging System. Objective magnification 10X.

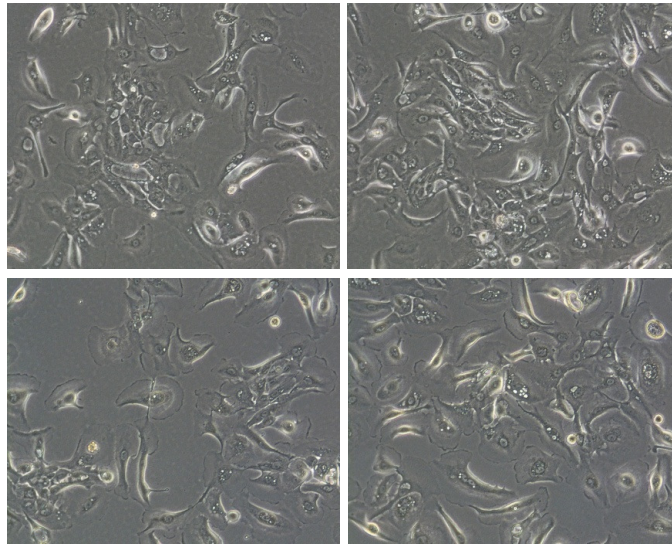


**Figure D.5:** Images of BPEC after ectopic expression of BMI1/ER $\alpha$ /hTERT/HRas\_2010. Photos were taken using the using the Axiovision imaging System. Objective magnification 10X.

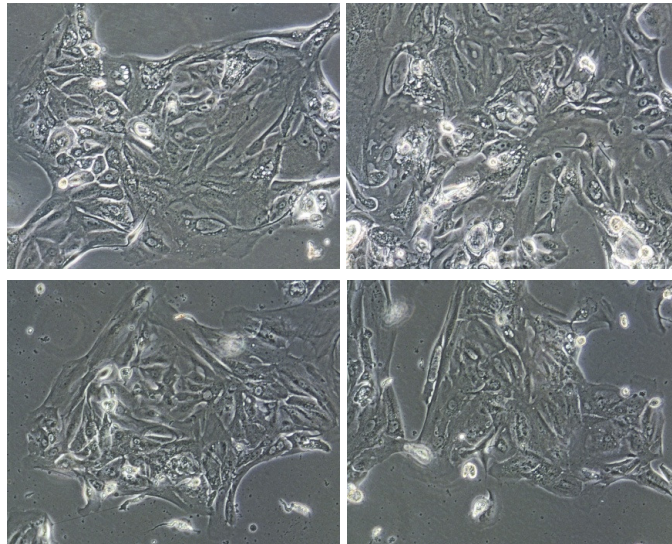


**Figure D.6:** Images of BPEC after ectopic expression of CBX8. Photos were taken using the using the Axiovision imaging System. Objective magnification 10X.

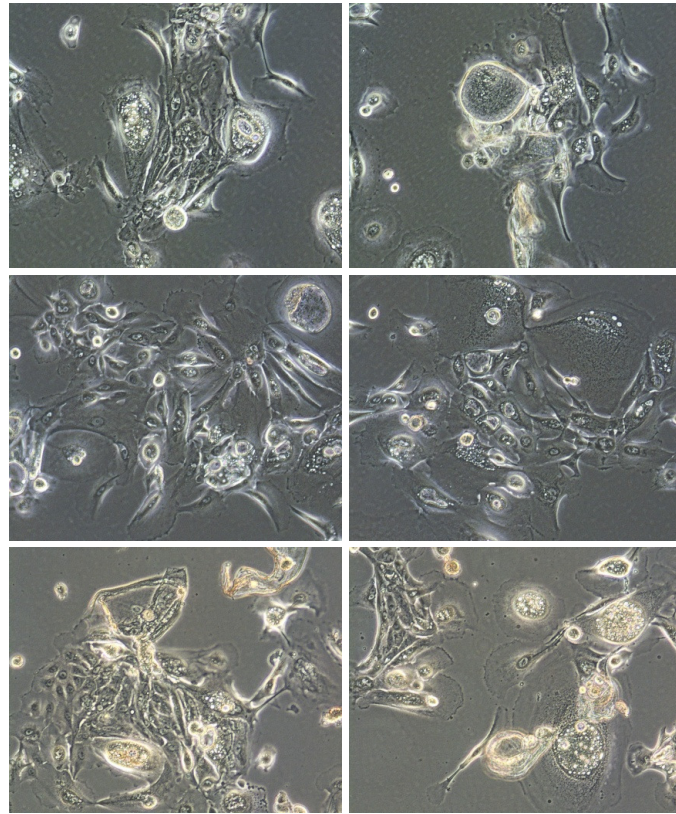




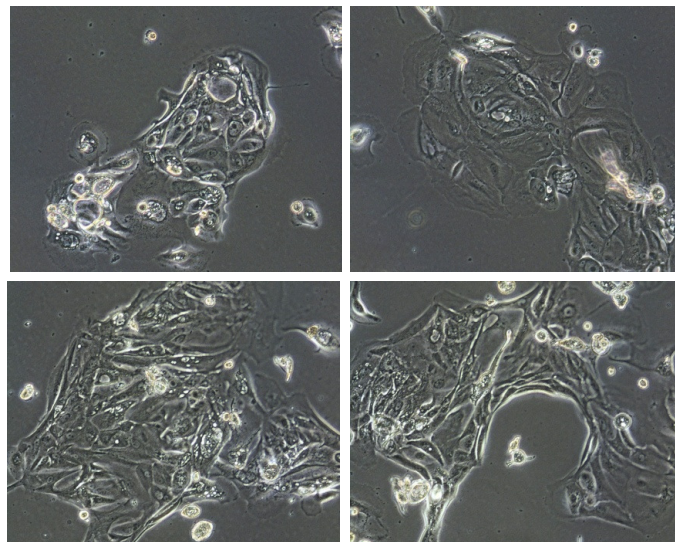
**Figure D.7:** Images of BPEC after ectopic expression of CBX8/ER $\alpha$ . Photos were taken using the Axiovision imaging System. Objective magnification 10X.



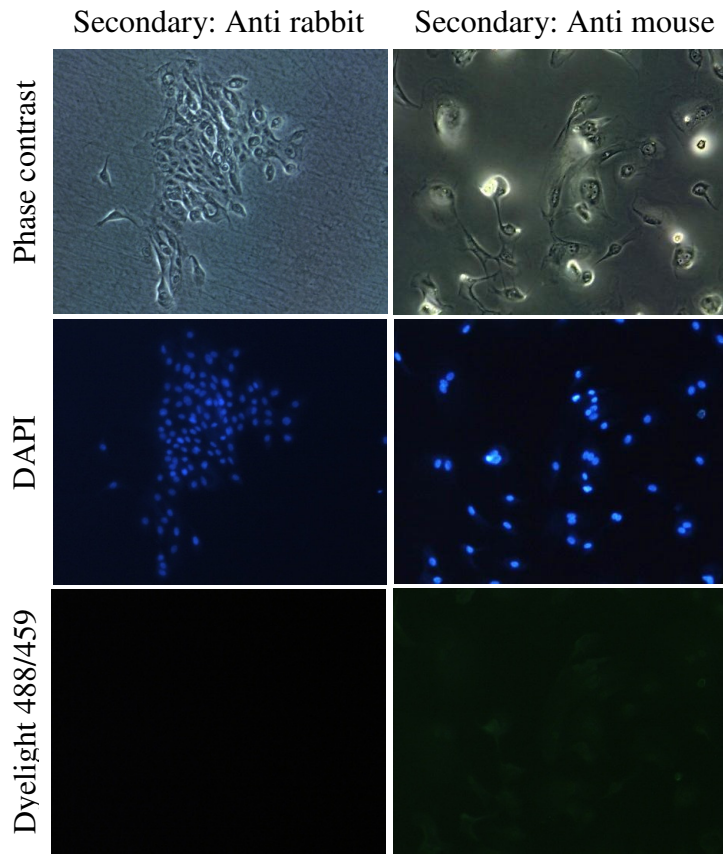
**Figure D.8:** Images of BPEC after ectopic expression of CBX8/ER/hTERT/HRas. Photos were taken using the Axiovision imaging System. Objective magnification 10X.



**Figure D.9:** Images of BPEC after ectopic expression of CBX8/hTERT/Hras. Photos were taken using the Axiovision imaging System. Objective magnification 10X.



**Figure D.10:** Images of BPEC after ectopic expression of hTERT/Hras. Photos were taken using the Axiovision imaging System. Objective magnification 10X.



**Figure D.11:** Immunofluorescence secondary antibody controls. Cells were visualized using an inverted microscope (Zeiss, Axiovert 40 CFL) and digital images were acquired using Axiovision imaging System. Objective magnification 10X.

	BMI1	ER $\alpha$	p16	HRAS
BPEC + BMI1/ER $\alpha$	0.83	1.19	1.1	0.75
BPEC + hTERT/HRAS			0,43	1,35
BPEC + BMI1/ER $\alpha$ /hTERT/HRAS_2010	36.43	28.96	1.94	1.57
BPEC + BMI1/ER $\alpha$ /hTERT/HRAS_2009	2.78	18.34	1.69	1.36
BPEC+GFP			0.69	0.71
BPEC	0.77	0.77	1	1

**Table D.1:** Quantification of western blot analysis Figure 6.10 and 6.12. the quantification was performed using the imageJ software.

	hTERT	a-SMA
BPEC+GFP	0	0.81
BPEC + BMI1/ER $\alpha$ /hTERT/HRAS_2009	0.95	0.56
BPEC + BMI1/ER $\alpha$ /hTERT/HRAS_2010	2.86	0.69
BPEC + hTERT/HRAS	9.17	1.20
BPEC + BMI1/ER $\alpha$	0	0.49
BPEC	0	0.69

**Table D2:** Quantification of western blot analysis Figure 6.11. the quantification was performed using the imageJ software.

	CBX8	Hras	p16	ER $\alpha$
BPEC + CBX8/ER $\alpha$	8.59	0.92	0.76	41.52
BPEC + hTERT/Hras	0.41	1.55	0.43	
BPEC + CBX8/ER $\alpha$ hTERT/Hras	3.33	0.42	0	3.73
BPEC + CBX8/hTERT/Hras	3.11	1.40	1.27	
BPEC+GFP	0.75	0.82	0.89	
BPEC	0.26	1	1	0.77

**Table D.3:** Quantification of western blot analysis Figure 6.18 and 6.20. the quantification was performed using the imageJ software.

	hTERT	a-SMA
BPEC+GFP	0	0.81
BPEC + CBX8/hTERT/HRAS	1.4	0.67
BPEC + hTERT/HRAS	9.17	1.20
BPEC + CBX8/ER $\alpha$	0	0.67
BPEC	0	0.69

**Table D.4:** Quantification of western blot analysis Figure 6.19. the quantification was performed using the imageJ software.

	Day 0	Day 1	Day 2	Day 3	Day 4	Day 5
Growth media	0.02	0.02	0.02	0.02	0.03	0.03
B42CP wt	0.07	0.25	0.38	1.04	1.44	0.64
B42CP GFP	0.07	0.27	0.39	1.07	1.36	0.58
B42CP HRAS	0.06	0.20	0.28	0.76	1.35	0.59
B42CP CBX8/HRAS	0.06	0.25	0.39	0.92	1.38	0.68
B42CP ER $\alpha$ /CBX8/HRAS	0.07	0.22	0.29	0.65	1.15	0.56

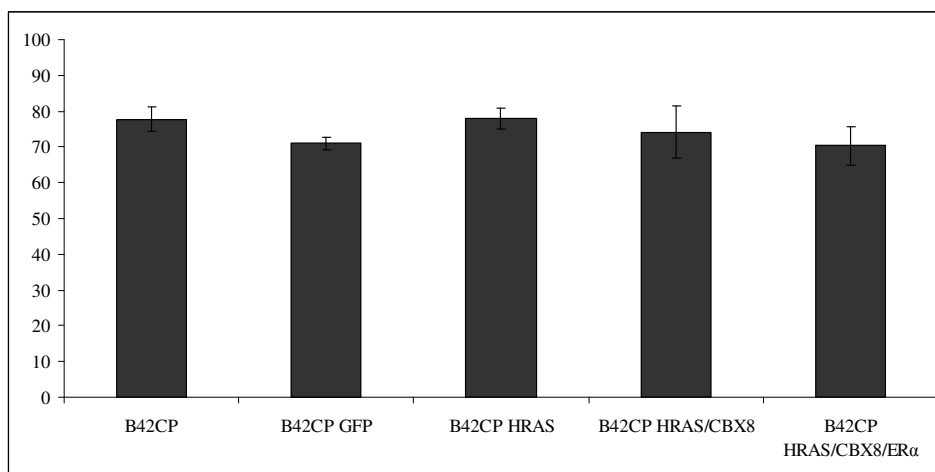
**Table D.5:** Raw data of figure 6.26. For each cell type 12 replica were performed. Values represent the mean of 12 counts (n=12). The error bars are calculated using the standard error of the mean.

	Time 0	14 Hours	Cell migration (%)
B42CP	39.76	8.02	79.84
B42CP GFP	42.20	12.63	70.07
B42CP HRAS	40.07	10.03	74.97
B42CP HRAS/CBX8	39.01	12.99	66.69
B42CP HRAS/CBX8/ER $\alpha$	42.68	15.18	64.35

**Table D.6:** Raw data of figure 6.27. The area of the scratch free of cells was measured at time 0 and at 14hours using the imageJ software. Values of the scratch at day 0 and day1 are reported in arbitrary units (AU). Cell migration is presented as percent closure using the formula: (Pre-migration area – Migration area)/Pre-migration area X 100.

Time 0 Scratch size (AU)					
	B42CP	B42CP GFP	B42CP HRAS	B42CP HRAS/CBX8	B42CP HRAS/CBX8/ER $\alpha$
Scratch 1	53.66	34.00	59.37	48.57	44.13
Scratch 2	39.76	42.20	40.07	39.01	42.68
Scratch 3	34.56	38.00	49.37	32.17	34.88
14 hours Scratch size (AU)					
Scratch 1	11.03	10.21	13.00	9.03	12.25
Scratch 2	8.02	12.63	10.03	12.99	15.18
Scratch 3	9.03	10.21	9.46	8.26	8.87
Cell migration (%)					
Scratch 1	79.45	69.95	78.10	81.41	72.24
Scratch 2	79.84	70.07	74.97	66.69	64.35
Scratch 3	73.96	73.12	80.84	74.33	74.56

**Table D.7:** Measurements relative to additional scratch performed with B42CP cells. The area of 3 different scratches free of cells was measured at time0 and at 14hours using the imageJ software. Values of the scratch at day0 and day1 are reported in arbitrary units (AU). Cell migration is presented as percent closure using the formula: (Pre-migration area – Migration area)/Pre-migration area X 100.



**Figure D.1:** Scratch measurements in table D.7 are represented in a graph. The size of the scratch was measured at time 0 and at 14 hours, using the software imageJ. Cell migration was expressed in percent closure and was calculated using the formula (Pre-migration area – Migration area)/Pre-migration area X 100 (see section 2.2.16 for more details).

	Replica 1	Replica 2	Replica 3	Average migrating cells	Standard error of the mean
SNB19	856	864	889	869.67	17.21
B42CP	0	0	0	0	0
B42CP GFP	0	0	0	0	0
B42CP HRAS	0	0	0	0	0
B42CP HRAS/CBX8	0	0	0	0	0
B42CP HRAS/CBX8/ER $\alpha$	0	0	0	0	0

**Table D.8:** Raw data of figure 6.28. The experiment was performed in triplicate and for each replica the whole chamber was analyzed. The error bars are calculated using the standard error of the mean.

	Replica1	Replica 2	Replica 3	Average colonies	Standard error of the mean
SNB19	25	28	23	25.33	2.52
B42CP	0	0	0	0	0
B42CP GFP	0	0	0	0	0
B42CP HRAS	0	0	0	0	0
B42CP HRAS/CBX8	0	0	0	0	0
B42CP HRAS/CBX8/ER $\alpha$	0	0	0	0	0

**Table D.9:** raw data of figure 6.29. The experiment was performed in triplicate (replica 1, 2 and 3) and for each replica colonies were counted three times. Values represent the mean of 9 counts (n=9). The error bars are calculated using the standard error of the mean.





## **8.5 Appendix E: Ethical approval**

MED27-08

APPROVED BY

UTREC Ethical Application Form (Human) 28.02.08

RECEIVED BY  
 PROF G HUMPHREYS  
 Approval Code: MD4357  
 28/3/08

UNIVERSITY OF ST ANDREWS TEACHING AND RESEARCH  
 ETHICS COMMITTEE (UTREC)

ETHICAL APPLICATION FORM

Researchers Name(s):

School/Unit:  Email(s):

Please Tick: Staff  Postgraduate  Undergraduate  (Module Code):   
 (double click on the box then click 'Checked' for a cross to appear in the box)

Project Title:

Supervisor(s):

Date:   
~~19/03/08~~ RA

Applications should be submitted electronically to either the Secretary or Convenor of the School Ethics Committee as *one single file* containing all relevant documents. The email containing the application must have the Researcher(s)' name in the 'subject' box. E.g. 'Ethics Application - Smith'  
 One original hard copy must also be submitted with the signatures of all applicants and supervisors.

**Rationale:** Please detail the project in 'lay language' *This summary will be reviewed by UTREC and may be published as part of its reporting procedures.*

Human breast tissue that is usually discarded after a reduction mammoplasty will be taken and used in experiments in the laboratory in order to model the origins of human breast cancer. Genes will be added to the breast cells to convert these normal cells into tumour cells. These tumour cells will then be compared with established cancer cell lines and tumour tissue microarrays to understand the causal initiating events in breast cancer progression.

**Ethical Considerations:** Please detail the main ethical considerations raised by the project, concentrating on any issues raised specifically in the red sections, and addressing, where appropriate, the issue of whether basic ethical criteria has been met in all supporting documentation and if not why not. *This summary will be reviewed by UTREC and may be published as part of its reporting procedures.*

Since there are no physical risks to the patient, confidentiality issue are the main consideration. Tissue will be given specific numerical identifiers and there are no personal identifiers associated with the tissue. The benefits of this research far outweigh any risks, which, due to the nature of the tissue acquisition and the goals of this study are negligible for the patient.

If ethical approval has been obtained from the University of St Andrews for research so similar to this project that a new review process may not be required, please give details of the application and the date of its approval:

**Approval Code:**

**Date Approved:**

**Project Title:**

**Researchers Name(s):**

**RESEARCH INFORMATION**

1. Estimated Start Date:

2. Estimated Duration of Project:

3. Is this research funded by an external sponsor or agency? **Yes**  **No**

If YES please give details:

For projects funded by ESRC please be aware of the Ethical and Legal Considerations found at <http://www.esds.ac.uk/aandp/create/ethical.asp>

4. Does this research entail collaboration with other researchers? **Yes**  **No**

If YES state names and institutions of collaborators:

5. If the research is collaborative has a framework been devised to ensure that all participants are given appropriate recognition in any outputs? **N/A**  **Yes**  **No**

6. Where projects raise ethical considerations to do with roles in research, intellectual property, publication strategies/authorship, responsibilities to funders, research with policy or other implications etc, have you taken appropriate steps to address these issues? **N/A**  **Yes**  **No**

7. Location of Research/Fieldwork to be conducted:

8. Is this research solely concerned with  
a. Published secondary data sources? **Yes**  **No**

b. Unpublished data but with appropriate permission, e.g. an archive curator?

Yes  No

If you have answered yes to Q8a or 8b but the project has other ethical considerations please go to Q12, Q30 & Q 31. If there are no other ethical considerations please sign and submit the form.

9. Who are the Intended Participants (*e.g. students*) and how will you recruit them?

N/A

10. Estimated duration of Participant Involvement

N/A

### ETHICAL CHECKLIST

11. Have you obtained permission to access the site of research?

N/A  Yes  No

If YES state agency /authority etc... & provide documentation

Tayside tissue bank (Dundee)

If NO please indicate why.

	N/A	Yes	No
12. Has ethical approval been sought and obtained from an external body e.g. NRES/LREC or other UK Universities? If YES, please attach a copy of the external application and approval.	<input type="checkbox"/>	<input checked="" type="checkbox"/>	<input type="checkbox"/>
13. Will you tell participants that their participation is voluntary?		<input checked="" type="checkbox"/>	<input type="checkbox"/>
14. Will you describe the main project/experimental procedures to participants in advance so that they can make an informed decision about whether or not to participate?		<input checked="" type="checkbox"/>	<input type="checkbox"/>
15. Will you tell participants that they may withdraw from the research at any time and for any reason, without having to give an explanation?	X	<input type="checkbox"/>	<input type="checkbox"/>
16. Please answer either a. or b.			
a. Will you obtain written consent from participants?		<input type="checkbox"/>	<input checked="" type="checkbox"/>
b. <i>(Social Anthropology Geography/Geosciences &amp; Biology only)</i> Will you obtain written consent from participants, in those cases where it is appropriate?		<input type="checkbox"/>	<input type="checkbox"/>
17. Please answer either a. or b.			
a. If the research is photographed or videoed or taped or observational, will you ask participants for their consent to being photographed or videoed or taped or observed?	<input checked="" type="checkbox"/>	<input type="checkbox"/>	<input type="checkbox"/>
b. <i>(Social Anthropology &amp; Biology only)</i> Will participants be free to reject the use of intrusive research methods such as audio-visual recorders and photography?	<input type="checkbox"/>	<input type="checkbox"/>	<input type="checkbox"/>
18. Will you tell participants that their data will be treated with full confidentiality and that if published, it will not be identifiable as theirs?		<input checked="" type="checkbox"/>	<input type="checkbox"/>
19. Will participants be clearly informed of how the data will be stored, who will have access to it, and when the data will be destroyed?		<input checked="" type="checkbox"/>	<input type="checkbox"/>
20. Will you debrief participants at the end of their participation, i.e. give them a brief explanation in writing of the study?		<input type="checkbox"/>	<input checked="" type="checkbox"/>
21. With questionnaires and/or interviews, will you give participants the option of omitting questions they do not want to answer?	<input checked="" type="checkbox"/>	<input type="checkbox"/>	<input type="checkbox"/>

If you have answered NO to any question 11 - 21, please give a brief explanation in the statement of Ethical Considerations on Page. 1, and expand in Q31 if necessary. If you answer YES, it must be clearly illustrated in the relevant paperwork which must be attached i.e. Participant Information Sheet, Consent Form, Debriefing Form, Questionnaires, Advertisement, etc...

**WORKING WITH CHILDREN/VULNERABLE PEOPLE**

Do participants fall into any of the following special groups? If they do, please tick the appropriate answer, refer to the relevant guidelines and complete Q31.

	Yes	No
22. a. Children (under 18 years of age)	<input type="checkbox"/>	<input checked="" type="checkbox"/>
b. People with learning or communication difficulties	<input type="checkbox"/>	<input checked="" type="checkbox"/>
c. Patients (including carers of NHS patients)	<input type="checkbox"/>	<input checked="" type="checkbox"/>
d. People in custody	<input type="checkbox"/>	<input checked="" type="checkbox"/>
e. Institutionalised persons	<input type="checkbox"/>	<input checked="" type="checkbox"/>

- |  |                          |                                     |
|--|--------------------------|-------------------------------------|
| f. People engaged in illegal activities e.g. drug-taking | <input type="checkbox"/> | <input checked="" type="checkbox"/> |
| g. Other vulnerable groups                               | <input type="checkbox"/> | <input checked="" type="checkbox"/> |

If you have answered YES to Q22 you may need to obtain satisfactory Enhanced Disclosure Scotland, Education Authority, Police, LREC (NHS) clearance.

- |  | Yes                      | No                       |
|--|--------------------------|--------------------------|
| 23. If working with children, institutionalised person(s) or vulnerable people, do you have:   |                          |                          |
| 1. Your Enhanced Disclosure Scotland Certificate?  | <input type="checkbox"/> | <input type="checkbox"/> |
| 2. If you have been in the UK for less than a year, equivalent documentation from the countries you have resided in? Information on what is required can be obtained from UTREC. | <input type="checkbox"/> | <input type="checkbox"/> |
| If YES a copy (or copies) must be submitted with this application to be retained by the School. If NO please explain in Q31.   |                          |                          |
| 24. If working with children or vulnerable people, have you constructed appropriate letters to, e.g. parents, children, headteachers, carers, institutions, police, etc.         | <input type="checkbox"/> | <input type="checkbox"/> |

**RISK AND SAFETY**

- |   | N/A                      | Yes                                 | No                                  |
|---|--------------------------|-------------------------------------|-------------------------------------|
| 25. Are any of the participants in a dependent relationship with the investigator e.g. lecturer/student? If YES, please give full explanation in Q31.   | <input type="checkbox"/> |                                     | <input checked="" type="checkbox"/> |
| 26. Will your project involve deliberately misleading participants in any way? If YES, give details in Q31 and state why it is necessary and explain how debriefing will occur.   | <input type="checkbox"/> |                                     | <input checked="" type="checkbox"/> |
| 27. Is there any realistic risk to any paid or unpaid participant(s), field assistant(s), helper(s) or student(s), involved in the project, experiencing either physical or psychological distress or discomfort? If YES, give details in Q31 and state what you will do if they should experience any problems e.g. who to contact for help. | <input type="checkbox"/> |                                     | <input checked="" type="checkbox"/> |
| 28. Is there any realistic risk to the investigator? If YES, have the appropriate risk assessment forms been submitted to the appropriate Safety Committee(s)?  | <input type="checkbox"/> |                                     | <input checked="" type="checkbox"/> |
| 29. <i>(Bute Medical School &amp; Biology only)</i> Have appropriate chemical, radiation and biological (including GMAG) risk assessments been submitted to the appropriate Safety Committee for approval?  | <input type="checkbox"/> | <input checked="" type="checkbox"/> | <input type="checkbox"/>            |
| 30. Do you think the processes, including any results of your research have the potential to cause any damage, harm or other problems for people in your study area? If YES please explain in Q31 and indicate how you will seek to obviate the effects.  | <input type="checkbox"/> |                                     | <input checked="" type="checkbox"/> |

There is an obligation on the Lead Researcher & Supervisor to bring to the attention of the School Ethics Committee (SEC) any issues with ethical implications not clearly covered by the above checklist.

**ETHICAL STATEMENT**

31. Write a clear but concise statement of the ethical considerations raised by the project and how you intend to deal with them. It may be that in order to do this you need to expand on the Ethical Considerations on page.1.

The breast tissue will be freshly acquired but no additional tissue will be taken for research other than what would be removed as part of the usual surgical procedure. Subjects will be recruited after they have been seen by a plastic surgeon and scheduled for reduction mammoplasty. Informed consent is obtained by the research nurse (Dundee) after full disclosure of the planned research. Written documentation of consent is kept under the authority of and administered by the Tayside Tissue bank. There are no associated risks for the patient since the research tissue will have already been excised as part of the patient’s reduction mammoplasty; the tissue will only be taken for research if there will be no impact on the patient’s pathologic diagnosis. By definition, we will only use reduction mammoplasty tissue that is free of any breast pathologic lesions. We have requested tissue from pre-menopausal women (age range 20-40), but there are no ethical implications in this selection that are additional to those described above. We do not collect any personal data.

Since there are no physical risks to the patient, confidentiality issues are the main consideration. Tissue will be given specific numerical identifiers and there are no personal identifiers associated with the tissue. The benefits of this research far outweigh any risks, which, due to the nature of the tissue acquisition and the goals of this study are negligible for the patient. It is hoped that the donation of normal breast tissue that would otherwise be stored or discarded would have a significant benefit for women in the future if this research proves fruitful and a test for early diagnosis of malignancy is developed.

There are no ethical issues related to the use of cancer cell lines obtained from recognised sources (e.g. ATCC). They are laboratory reagents regulated by biological risk assessments.

Tumour tissue microarrays (TMAs) have numerical identifiers and are anonymised for use in this study, so are not associated with personal information. They have external ethical approval (04/S1103/13 – University of Edinburgh).

**DOCUMENTATION CHECKLIST**

*Please tick as appropriate:*

	N/A	Yes	No
1. Ethical Application Form		<input checked="" type="checkbox"/>	<input type="checkbox"/>
2. Participant Information Sheet	<input checked="" type="checkbox"/>	<input type="checkbox"/>	<input type="checkbox"/>
3. Consent Form	<input checked="" type="checkbox"/>	<input type="checkbox"/>	<input type="checkbox"/>
4. Debriefing Form	<input checked="" type="checkbox"/>	<input type="checkbox"/>	<input type="checkbox"/>
5. External Permissions	<input type="checkbox"/>	<input checked="" type="checkbox"/>	<input type="checkbox"/>
6. Letters to Parents/Children/Headteacher etc...	<input checked="" type="checkbox"/>	<input type="checkbox"/>	<input type="checkbox"/>
7. Enhanced Disclosure Scotland and Equivalent ( <i>as necessary</i> )	<input checked="" type="checkbox"/>	<input type="checkbox"/>	<input type="checkbox"/>

8. Other  
*please list:*

**DECLARATION**

I am familiar with the UTREC Guidelines for Ethical Research (<http://www.st-andrews.ac.uk/utrec/guidelines.shtml>) and \*BPS, \*ESRC, \*MRC and \*ASA (\*please delete the guidelines not appropriate to your discipline) Guidelines for Research practices, and have discussed them with the other researchers involved in the project.

*(Students only)*

My supervisor has seen all relevant paperwork linked to this project. **Yes**  **No**

**Researcher(s)**

Print Name

Signature

Date

**Supervisor(s)**

The supervisor must ensure they have read both the application and the guidelines before signing below.

Print Name

Signature

Date

**OFFICIAL USE ONLY**

**STATEMENT OF ETHICAL APPROVAL**

This project has been considered using agreed University Procedures and has been:

- Approved
- Not Approved
  - More Clarification Required
  - New Submission Recommended
- Referred to UTREC

Conveners Name

Signature

Date:





# Tayside Tissue Bank - Request for Tissue Specimens

Request No: TR000083

Request Date: 28/01/2008

## Personal details

### Researcher

Paul Reynolds

### Institution

University of St Andrews

### Department

Medicine

### Co-workers

Co-researcher:

Prof. Richard Iggo

Clinician:

Mr Howard Stevenson

Pathologist:

Dr Lee Jordan

## Project Title

Analysis of mammary tumour models

## Precis of Project

Human reduction mammoplasty tissue will be used to prepare cell cultures of mammary epithelial cells and fibroblasts. These normal human cells will be infected with lentiviral vectors to introduce cDNAs encoding putative oncogenes and miRNAs targeting putative tumour suppressor genes. With current techniques, up to three lentiviruses can be used to infect the cells at one time with near 100% efficiency. The infection is done within 24 hours of resection of the tissue. The transduced cells will be tested in vitro and in mice for transformation/tumorigenicity and response to drugs. A typical experiment would be to introduce the oestrogen receptor gene (ESR1), BMI1 oncogene, MYC oncogene and ERBB2 oncogene into epithelial cells to produce transformed cells that are dependent on oestradiol for proliferation or to introduce the androgen receptor gene (AR), FOXA1 transcription factor, p53 miRNA and ERBB2 oncogene to produce transformed cells that are dependent on testosterone for proliferation. These transformed cells would act as models for the luminal and molecular apocrine classes of tumours identified using breast cancer microarrays. Similar lentiviral vectors will be used to modify human mammary fibroblasts to produce paracrine factors postulated to modify the response of tumour cells to drugs. For example, introduction of Wnt2 or CXCL12 will be used to modify the response to anthracyclines. This work builds on microarray results obtained from a clinical trial (EORTC 10994), in which Dundee participates (Prof AM Thompson). The microarray results feed directly back into the design of clinical trials by the EORTC Breast Cancer Group, for example to develop trials testing the use of antiandrogens in combination with Herceptin in molecular apocrine tumours or the use anti-stromal agents in combination with FEC in ER-negative tumours. The in vitro work was originated

in Switzerland by a student (Mr Stephan Duss) who was jointly supervised by Prof Richard Iggo and Dr Cathrin Brisken at the Swiss Institute for Experimental Cancer Research. It is being continued by Xenia Schmidt (iggo lab) and upon approval of this request by Vita Fedele (Reynolds lab). I have obtained HSE approval for the viral work and am obtaining Home Office approval for the animal work in the UK.

***This work has not been approved by the ethics committee***

### Specimens requested

Quantity	Tumour Site	In Form
50	Breast reduction	

### Services requested

Samples should not be frozen. Please arrange for samples to be collected from the operating theatre, and for a pathologist to perform gross dissection to identify tissue containing ducts. I will arrange for a person from my lab to go to Dundee to be ready to collect the tissue as soon as the pathologist has completed the dissection. It is important to process the samples quickly to maintain viability of the cells (eg <1 hour). Please take samples from pre-menopausal women (age range 20-40) and take samples preferably from patients without malignant disease.

### Funding

Name of funder	Grant number
University of St Andrews	CREYXX

### Additional comments

I am requesting my own authorization as a new PI. The Iggo lab has been receiving breast reductions and is successfully using them in the analysis of mammary tumour models.

As soon as you have approved the project, I will present it to the St Andrews ethics committee.



Tayside Tissue/Tumour Bank  
Level 6  
Ninewells Hospital & Medical School  
Dundee DD1 9SY  
Tel: 01382 496432

2008-03-10

Dr Paul A Reynolds  
Medicine  
University of St Andrews

Dear Paul,

**Re: Analysis of mammary tumour models**

The Tissue Bank Committee has approved your recent application for the above project.

The committee were fully supportive of the project. However you might wish to consider comments made by two of the members.

"A good project but patient selection and the mechanism for getting specimens to Pathology quickly requires detailed discussion and will have to involve members of the research team."

"I wonder if a one hour turn round time is a realistic prospect from excision to collection, including analysis by the pathologist and subsequent transport to St Andrews."

The continuance of the Tissue Bank facility is dependent on the financial support of the MRC, Cancer Research UK and NTRAC. Approval of projects, subsequent release and use of tissue samples from the bank is on condition that the Tayside Tissue Bank is acknowledged in any presentation, abstract or publication resulting from the use of the tissue. The Tayside Tissue Bank must also be informed when any paper or abstract resulting from a study is published.

Regards,

A handwritten signature in black ink, appearing to read 'D Kellock', written over a horizontal line.

David Kellock  
Tissue Bank Co-ordinator

# UNIVERSITY OF ST ANDREWS TEACHING AND RESEARCH ETHICS COMMITTEE (UTREC)

## ETHICAL AMENDMENT FORM

<b>Researchers Name(s):</b>	Dr. Paul Reynolds Ms. Vita Fedele Mrs. Mary Wilson	<b>Email(s):</b>	par10@st-and.ac.uk vf27@st-and.ac.uk mlw4@st-and.ac.uk
-----------------------------	--	------------------	--

<b>School/Unit:</b> <i>Please indicate</i>	Bute Medical School
---	---------------------

**Please Tick:** Staff  Postgraduate  Undergraduate  (Module Code):   
*(double click on the box then click 'Checked' for a cross to appear in the box)*

**Approval Code:**

**Original Title:**

**Amended Title:**  
*(If applicable)*

**Researchers Name(s):**

**Supervisor(s):**

**Date:**

**Amended Rationale:** Please give a BRIEF description of the amendments made to your project in 'lay language'. (NOTE; Where substantial amendments, in rationale or ethical considerations, are to be made please fill in a complete new Ethical Application Form rather than this form). *This will be reviewed by UTREC and may be published as part of its reporting procedures.*

*Do NOT exceed 75 words - approx 5 lines (for database reasons).*

**Additional named researchers**

**Amended Ethical Considerations:** Please indicate any 'new' ethical considerations brought about by the amendment of your project. *This summary will be reviewed by UTREC and may be published as part of its reporting procedures.*

*Do NOT exceed 75 words - approx 5 lines (for database reasons).*

**None**

**ETHICAL STATEMENT**

Write a clear but concise statement of the ethical considerations raised by the project and how you intend to deal with them. It may be that in order to do this you need to expand on the Ethical Considerations on page.1.

Since there are no physical risks to the patient, confidentiality issues are the main consideration. Tissue will be given specific numerical identifiers and there are no personal identifiers associated with the tissue. The benefits of this research far outweigh any risks, which, due to the nature of the tissue acquisition and the goals of this study are negligible for the patient.


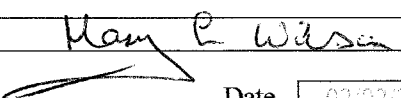
**DECLARATION**

I am familiar with the UTREC Guidelines for Ethical Research (<http://www.st-andrews.ac.uk/utrec/guidelines.shtml>) and \*BPS, \*ESRC, \*MRC and \*ASA (\*please delete the guidelines not appropriate to your discipline) Guidelines for Research practices, and have discussed them with the other researchers involved in the project.

*(Students only)*

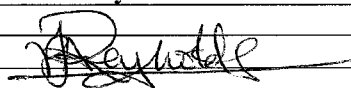
My supervisor has seen all relevant paperwork linked to this project. Yes  No

**Researcher(s)**

Print Name	Vita Fedele	Mary Wilson
Signature		
		Date <span style="float: right;">02/02/2009</span>

**Supervisor(s)**

The supervisor must ensure they have read both the application and the guidelines before signing below.

Print Name	Dr. Paul Reynolds
Signature	
	Date <span style="float: right;">02/02/2009</span>